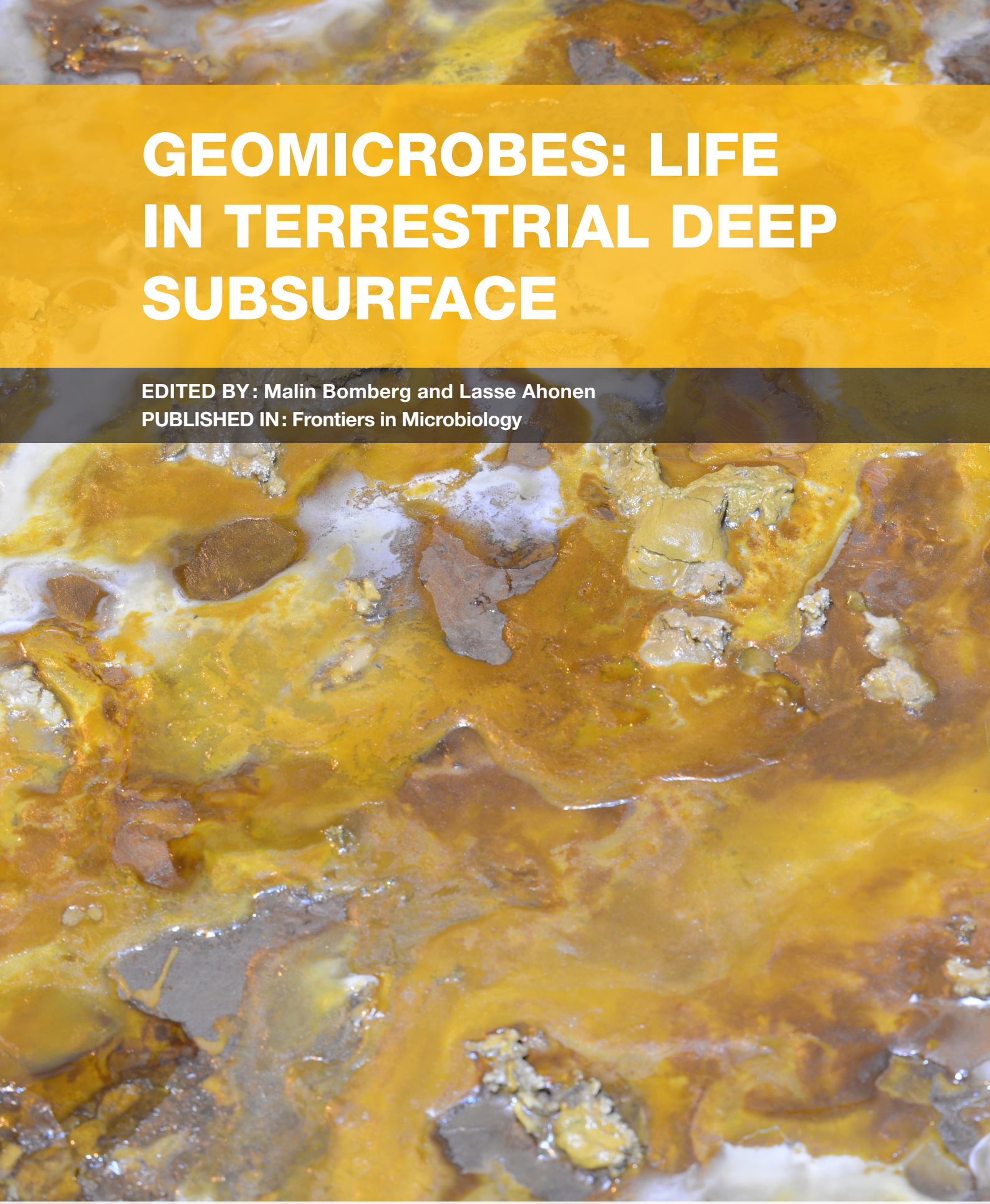

GEOMICROBES: LIFE IN TERRESTRIAL DEEP SUBSURFACE

EDITED BY: Malin Bomberg and Lasse Ahonen
PUBLISHED IN: Frontiers in Microbiology

frontiers Research Topics

frontiers

ISSN 1664-8714
ISBN 978-2-88945-179-1
DOI 10.3389/978-2-88945-179-1

About Frontiers

Frontiers is more than just an open-access publisher of scholarly articles: it is a pioneering approach to the world of academia, radically improving the way scholarly research is managed. The grand vision of Frontiers is a world where all people have an equal opportunity to seek, share and generate knowledge. Frontiers provides immediate and permanent online open access to all its publications, but this alone is not enough to realize our grand goals.

Frontiers Journal Series

The Frontiers Journal Series is a multi-tier and interdisciplinary set of open-access, online journals, promising a paradigm shift from the current review, selection and dissemination processes in academic publishing. All Frontiers journals are driven by researchers for researchers; therefore, they constitute a service to the scholarly community. At the same time, the Frontiers Journal Series operates on a revolutionary invention, the tiered publishing system, initially addressing specific communities of scholars, and gradually climbing up to broader public understanding, thus serving the interests of the lay society, too.

Dedication to Quality

Each Frontiers article is a landmark of the highest quality, thanks to genuinely collaborative interactions between authors and review editors, who include some of the world's best academicians. Research must be certified by peers before entering a stream of knowledge that may eventually reach the public - and shape society; therefore, Frontiers only applies the most rigorous and unbiased reviews.
Frontiers revolutionizes research publishing by freely delivering the most outstanding research, evaluated with no bias from both the academic and social point of view.
By applying the most advanced information technologies, Frontiers is catapulting scholarly publishing into a new generation.

What are Frontiers Research Topics?

Frontiers Research Topics are very popular trademarks of the Frontiers Journals Series: they are collections of at least ten articles, all centered on a particular subject. With their unique mix of varied contributions from Original Research to Review Articles, Frontiers Research Topics unify the most influential researchers, the latest key findings and historical advances in a hot research area! Find out more on how to host your own Frontiers Research Topic or contribute to one as an author by contacting the Frontiers Editorial Office: **researchtopics@frontiersin.org**

GEOMICROBES: LIFE IN TERRESTRIAL DEEP SUBSURFACE

Topic Editors:
Malin Bomberg, VTT Technical Research Centre of Finland, Finland
Lasse Ahonen, Geological Survey of Finland, Finland

Biofilm on rock surface in the Pyhäsalmi Mine, Finland (photo Mikko Numminen)

The deep subsurface is, in addition to space, one of the last unknown frontiers to human kind. A significant part of life on Earth resides in the deep subsurface, hiding great potential of microbial life of which we know only little. The conditions in the deep terrestrial subsurface are thought to resemble those of early Earth, which makes this environment an analog for studying early life in addition to possible extraterrestrial life in ultra-extreme conditions.

Early microorganisms played a great role in shaping the conditions on the young Earth. Even today deep subsurface microorganisms interact with their geological environment transforming the conditions in the groundwater and on rock surfaces. Essential elements for life are richly present but in difficultly accessible form. The elements driving the microbial deep life is still not completely identified. Most of the microorganisms detected by novel molecular techniques still lack cultured representatives. Nevertheless, using modern sequencing techniques and bioinformatics the functional roles of these microorganisms are being revealed. We are starting to see the differences and similarities between the life in the deep subsurface and surface domains. We may even begin to see the function of evolution by comparing deep life to life closer to the surface of Earth. Deep life consists of organisms from all known domains of life. This Research Topic reveals some of the rich diversity and functional properties of the great biomass residing in the deep dark subsurface.

Citation: Bomberg, M., Ahonen, L., eds. (2017). Geomicrobes: Life in Terrestrial Deep Subsurface. Lausanne: Frontiers Media. doi: 10.3389/978-2-88945-179-1

Table of Contents

Eukaryotes

frontiers in Microbiology

EDITORIAL
published: 31 January 2017
doi: 10.3389/fmicb.2017.00103

Editorial: Geomicrobes: Life in Terrestrial Deep Subsurface

Malin Bomberg[1]* *and Lasse Ahonen*[2]

[1] VTT Technical Research Centre of Finland Ltd., Espoo, Finland, [2] Geological Survey of Finland, Espoo, Finland

Keywords: deep biosphere, iron oxidation, heavy metal resistance, bedrock aquifer, limestone cave, mine microbiology, biogeological methane cycling

Editorial on the Research Topic

Geomicrobes: Life in Terrestrial Deep Subsurface

INTRODUCTION

The deep terrestrial biosphere is an intriguing research field linking to astrobiology and evolution of life on early Earth (Grosch and Hazen, 2015). Living in the deep, dark, anoxic, oligotrophic, saline, highly pressurized and often hot subsurface requires some striking characteristics of the inhabitants (Kieft, 2016). We still know only little about the biochemical processes actually taking place deep in the Earth's crust, or about the interactions within microbial communities residing in the isolated aquifers. Nevertheless, the deep subsurface is planned to serve as geological repository for e.g., nuclear and other hazardous wastes and carbon dioxide (De Coninck and Benson, 2014; Russell et al., 2015). We still do not know how the long isolated deep bedrock environments will respond to these intrusions, or what the fate of the repositories will be. With this Research Topic we aimed to collect new knowledge about the roles and functions of microbial communities in the undisturbed or disturbed subsurface and called upon our colleagues to step up to the task. The deep subsurface is of interest worldwide and we received contributions from Asia, Australia, Africa, North America, and Europe!

WHAT DID WE LEARN?

The deep terrestrial subsurface is difficult to access, but can be reached through drillholes in the rock that reach the aquifers (Sohlberg et al.), cave streams (Brannen-Donnely and Engel), water seeping through mine walls (Borgonie et al.), drillholes in mines and caves (Miettinen et al.; Rajala et al.; Bonis and Gralnick; Kutvonen et al.) and by collecting rock material and scrapings from caves (Wu et al.) and mines (Dziewit et al.). The deep subsurface microbial communities are very diverse, spanning all domains of life (Borgonie et al.; Miettinen et al.; Sohlberg et al.).

Metals are important factors driving deep subsurface life (e.g., Parnell et al., 2016). Iron, one of the most common compounds in the Earth's crust, plays an important role and is part of many biomolecules. Reduced iron may serve as electron source for iron-oxidizing microorganisms, such as *Marinobacter subterrani* (Bonis and Gralnick) living in the iron-rich calcium chloride brine in the Soudan iron mine at more than 700 m depth. Iron redox reactions may support vast microbial communities in various environments. Iron oxidation occurs in many microbial species, which may affect the corrosion of e.g., carbon steel in deep geological repositories for radioactive waste. Radioactive metallic wastes originate from decommissioning activities in nuclear power plants. In Olkiluoto nuclear power plant, Finland, the decommissioning wastes are stored in an underground bedrock repository at 60–100 m depth. The temperature of the surrounding groundwater affects the communities causing microbially induced corrosion of carbon steel.

OPEN ACCESS

Edited by:
Paul Bodelier, Nederlands Instituut voor Ecologie (KNAW), Netherlands

Reviewed by:
Tillmann Lueders, Helmholtz Zentrum München, Germany

***Correspondence:**
Malin Bomberg
malin.bomberg@vtt.fi

Specialty section:
This article was submitted to Terrestrial Microbiology, a section of the journal Frontiers in Microbiology

Received: *14 November 2016*
Accepted: *13 January 2017*
Published: *31 January 2017*

Citation:
Bomberg M and Ahonen L (2017) Editorial: Geomicrobes: Life in Terrestrial Deep Subsurface. Front. Microbiol. 8:103. doi: 10.3389/fmicb.2017.00103

In the Lubin copper mine, Poland, microorganisms are exposed to high levels of heavy metals (HM) and diverse resistance strategies are employed. Dziewit et al. isolated HM resistant bacteria from the mine and found several plasmids and broad-host-range transposons carrying various HM resistance markers. HM tolerance genes located on extra chromosomal elements can play a key role in the adaptation of microbial communities to HM stress, due to possible horizontal gene transfer.

Pyhäsalmi mine in Finland, one of Europe's deepest mines, provides an opportunity for sampling deep groundwater fractions through underground drillholes reaching more than 2 km below ground. Only low numbers of microbial cells were found in these deep, saline and high-pressure fluids (Miettinen et al.). However, the microbial diversity was surprisingly high, including bacteria, archaea and fungi. Borgonie et al. managed to reach even deeper, down to 3.4 km depth, in the South African Tona Tau gold mine. Sampled stalactites revealed life forms, even nematodes, trapped in the stalactite since its formation, displaying a signature for the origin of the deep groundwater and earlier conditions on Earth.

In an epigenic carst stream with fast turnover rates and seasonal variations in water volumes and nutrient flow, Brannen-Donnelly and Engel showed microbial lineages that were specific to the different stream habitats but did not appear between the habitats (running water or static sediment). Rajala et al. reported similar results as biofilm on carbon steel surfaces differed distinctly from the planktonic community in Fennoscandian groundwater. Wu et al. showed that the bacterial community colonizing the walls of the limestone Jinjia Cave, China, changed with growing distance from the cave mouth. The authors suggested that the deepest end of the cave was inhabited by obligate cave-colonizing Gammaproteobacteria often detected from caves world-wide.

Nitrogen compounds, such as nitrate and ammonia, are generally in short supply in deep groundwater, but may enter the depths through explosives used in the bedrock or through infiltration from the surface. The bacterial numbers increased significantly when these compounds were available and radically changed the microbial community structure (Kutvonen et al.). The bacteria that used these compounds as energy source were distinct from those using them as nitrogen source. Many of the bacteria detected were methylotrophs, which may be able to utilize nitrate for the oxidation of methane. Methane is one of the most common carbon sources in the Fennoscandian deep subsurface. It is synthesized both biotically and abiotically, and distinguishing between the two is difficult in deep subsurface environments (Kietäväinen and Purkamo). The versatility of ways for biological methanogenesis in deep subsurface and the syntrophic/co-existing networks of unusual metabolisms involved in this process is fascinating. Ancient carbon stored in the bedrock may be recycled by fermenters in to building blocks for methane or other compounds, which makes the isotopic determination of methane as biotic or abiotic challenging.

CONCLUSIONS

The deep biosphere has the potential to reveal novel factors about the evolution of life on Earth. There is still much to learn about the size of the microbial communities, the genetic variation and metabolic functions in the deepest part of the biosphere. For example, microorganisms tend to attach to surfaces forming biofilms, thus altering the impact of the microorganisms in deep subsurface environments, and these biofilms with their impact on the whole microbial community are yet near impossible to replicate in the laboratory. We also get a good idea only of the microorganisms resembling already known ones, leaving much of our obtained sequence data as part of the dark matter. In order to find out how the deep subsurface microbial communities really work and interact with their biotic and abiotic environment and their impact on globally important phenomena, such as climate change, we need to be able to study them *in situ* as well as improve the databases against which we compare our sequence data. These are some of the biggest challenges the deep biosphere research community faces to date.

AUTHOR CONTRIBUTIONS

MB (lead editor) compiled the editorial and wrote the paper with assistance from LA.

REFERENCES

De Coninck, H., and Benson, S. M. (2014). Carbon dioxide capture and storage: issues and prospects. *Annu. Rev. Environ. Resour.* 39, 243–270. doi: 10.1146/annurev-environ-032112-095222

Grosch, E. G., and Hazen, R. M. (2015). Microbes, mineral evolution, and the rise of microcontinents—origin and coevolution of life with early earth. *Astrobiology* 15, 922–939. doi: 10.1089/ast.2015.1302

Kieft, T. L. (2016). "Microbiology of the deep continental biosphere," in *Their World: A Diversity of Microbial Environments*; *Advances in Environmental Microbiology*, ed C. J. Hurst (Cham: Springer International Publishing), 225–249.

Parnell, J., Brolly, C., Spinks, S., and Bowden, S. (2016). Metalliferous biosignatures for deep subsurface microbial activity. *Origins Life Evol. Biospher.* 46, 107–118. doi: 10.1007/s11084-015-9466-x

Russell, A. W., Reijonen, H. M., and McKinley, I. G. (2015). Natural analogues: studies of geological processes relevant to radioactive waste disposal in deep geological repositories. *Swiss J. Geosci.* 108, 75–100. doi: 10.1007/s00015-015-0187-y

Conflict of Interest Statement: The authors declare that the research was conducted in the absence of any commercial or financial relationships that could be construed as a potential conflict of interest.

frontiers in Microbiology

ORIGINAL RESEARCH
published: 30 March 2015
doi: 10.3389/fmicb.2015.00244

Profiling bacterial diversity in a limestone cave of the western Loess Plateau of China

Yucheng Wu[1]†, Liangcheng Tan[2,3]*†, Wuxing Liu[4], Baozhan Wang[1], Jianjun Wang[5], Yanjun Cai[2] and Xiangui Lin[1]*

[1] State Key Laboratory of Soil and Sustainable Agriculture, Institute of Soil Science – Chinese Academy of Sciences, Nanjing, China, [2] State Key Laboratory of Loess and Quaternary Geology, Institute of Earth Environment – Chinese Academy of Sciences, Xi'an, China, [3] Joint Center for Global Change Studies, Beijing, China, [4] Key Laboratory of Soil Environment and Pollution Remediation, Institute of Soil Science – Chinese Academy of Sciences, Nanjing, China, [5] State Key Laboratory of Lake Science and Environment, Nanjing Institute of Geography and Limnology – Chinese Academy of Sciences, Nanjing, China

OPEN ACCESS

Edited by:
Malin Bomberg,
VTT Technical Research Centre of Finland, Finland

Reviewed by:
Neil Duncan Gray,
University of Newcastle, UK
Francesca Cappitelli,
Università degli Studi di Milano, Italy

***Correspondence:**
Yucheng Wu,
State Key Laboratory of Soil and Sustainable Agriculture, Institute of Soil Science – Chinese Academy of Sciences, 71 East Beijing Road, Nanjing 210008, China
ycwu@issas.ac.cn;

Liangcheng Tan,
State Key Laboratory of Loess and Quaternary Geology, Institute of Earth Environment – Chinese Academy of Sciences, 97 Yanxiang Road, Xi'an 710061, China
tanlch@ieecas.cn

† These authors have contributed equally to this work.

Specialty section:
This article was submitted to Terrestrial Microbiology, a section of the journal Frontiers in Microbiology

Received: 12 December 2014
Accepted: 12 March 2015
Published: 30 March 2015

Citation:
Wu Y, Tan L, Liu W, Wang B, Wang J, Cai Y and Lin X (2015) Profiling bacterial diversity in a limestone cave of the western Loess Plateau of China.
Front. Microbiol. 6:244.
doi: 10.3389/fmicb.2015.00244

Bacteria and archaea sustain subsurface cave ecosystems by dominating primary production and fueling biogeochemical cyclings, despite the permanent darkness and shortage of nutrients. However, the heterogeneity and underlying mechanism of microbial diversity in caves, in particular those well connect to surface environment are largely unexplored. In this study, we examined the bacterial abundance and composition in Jinjia Cave, a small and shallow limestone cave located on the western Loess Plateau of China, by enumerating and pyrosequencing small subunit rRNA genes. The results clearly reveal the contrasting bacterial community compositions in relation to cave habitat types, i.e., rock wall deposit, aquatic sediment, and sinkhole soil, which are differentially connected to the surface environment. The deposits on the cave walls were dominated by putative cave-specific bacterial lineages within the γ-Proteobacteria or Actinobacteria that are routinely found on cave rocks around the world. In addition, sequence identity with known functional groups suggests enrichments of chemolithotrophic bacteria potentially involved in autotrophic C fixation and inorganic N transformation on rock surfaces. By contrast, bacterial communities in aquatic sediments were more closely related to those in the overlying soils. This is consistent with the similarity in elemental composition between the cave sediment and the overlying soil, implicating the influence of mineral chemistry on cave microhabitat and bacterial composition. These findings provide compelling molecular evidence of the bacterial community heterogeneity in an East Asian cave, which might be controlled by both subsurface and surface environments.

Keywords: bacterial diversity, cave, rock surface, pyrosequencing, elemental composition, 16S rRNA

Introduction

Most biological communities are dependent on the energy and carbon fixation of photosynthesis. However, perpetual darkness prevents the colonization of phototrophs in subterranean cave environments. Limited energy and nutrients can enter caves via entrance, sinkholes, underground

hydrology, and drip waters (Barton and Jurado, 2007), and the aphotic and oligotrophic environments only allow for the survival and functioning of species adapted to the oligotrophic conditions. This is clarified by the dominance of microbial chemoautotrophic production in some cave ecosystems (Sarbu et al., 1996; Chen et al., 2009), which fixes carbon and imports energy into cave food web.

Bacteria and archaea constitute the vast majority of biodiversity in caves and are ubiquitous in various cave habitats such as soils, sediments, stream waters, and rock surfaces (Engel et al., 2004; Barton and Jurado, 2007). Many known bacterial phyla have been detected in cave environments by sequencing of 16S rRNA genes (Engel et al., 2004; Barton et al., 2007; Ortiz et al., 2013b), greatly advancing our understanding of bacterial diversity since its introduction to microbial ecology (Roesch et al., 2007). For example, the dominant taxa on cave walls are largely affiliated with a few phyla such as Proteobacteria, Acidobacteria, and Actinobacteria (Barton et al., 2007; Pašić et al., 2010; Cuezva et al., 2012). Bacterial richness in cave sediments could be comparable to that in overlying soils (Ortiz et al., 2013b), but the rock surfaces are normally colonized by the lowest diversity natural microbial communities (Macalady et al., 2007; Yang et al., 2011). By comparison of geographically distinct caves, which mostly locate in Europe and America, it was supposed that rock surfaces could be colonized by common phylotypes that were rarely found in other habitats (Porca et al., 2012), suggesting the presence of specific cave bacterial lineages. However, whether they are present in caves in other area, e.g., East Asia merits further study.

Mounting evidence indicates that microbes may sustain cave ecosystems by dominating primary production and fueling biogeochemical cyclings. This has been revealed in some deep caves that are well isolated from the surface environment, including the Movile cave (Romania; Sarbu et al., 1996), the Frasassi cave (Italy; Desai et al., 2013), and the Kartchner Caverns (US; Ortiz et al., 2013a). In these caves, chemoautotrophic microbes are largely responsible for CO_2 fixation and potentially participate in inorganic nitrogen (Desai et al., 2013; Tetu et al., 2013) and sulfur transformation (Chen et al., 2009). Moreover, interactions between microorganisms and rock may contribute to speleogenesis, the process of cave development that was previously viewed as abiotic and often attributed to the erosion of bedrock by water containing dissolved CO_2 (Engel et al., 2004). For example, in sulfidic caves, the microbial oxidation of H_2S produces sulfuric acid, which reacts with carbonate and causes rock dissolution (Engel et al., 2004; Macalady et al., 2007). Bacteria are able to modify rock surfaces through the oxidation of some metal elements [e.g., Fe(II) and Mn(II)], which causes ferromanganese depositing on cave walls (Carmichael et al., 2013).

Cave microbial communities are often highly variable dependent on the microhabitats. Significantly different bacterial diversity and composition were observed on rock walls within one single cave, possibly related to the host rock geochemistry (Barton et al., 2007). Nutrient inputs and disturbances may also contribute to cave microbial diversity. Organic matter and microbes could be carried into caves by air current, seepage water (Shabarova et al., 2013) and animal and human activities. The latter is a serious issue especially for caves open for tourism, which may introduce unwanted species and cause deterioration of paleolithic paintings (Ikner et al., 2007; Diaz-Herraiz et al., 2013). As such, cave bacterial diversity could be shaped by both interior (e.g., the rock geochemistry) and exterior (natural or anthropogenic) environments, and the influence of the latter is likely dependent on the cave's connectivity to outside world. However, the heterogeneity and mechanism of microbial diversity inside of caves, in particular in those easily exposed to the surface are still poorly understood.

In this study, we focused on the bacterial communities in Jinjia Cave, a limestone cave in the semi-humid western Loess Plateau of China. The cave is short and shallow in contrasting to those studied previously, and was supposed to be influenced by the surface due to the limited depth. By using next generation sequencing of 16S rRNA genes, we profiled the bacterial communities colonizing different habitats including rock wall deposits, sediments in small pool and sinkhole, and overlying soils. Meanwhile, the microhabitat characteristics were examined by a detailed analysis of the elemental composition of the sample. The aims of the study were therefore to explore the bacterial heterogeneity within a single cave in relation to habitat type and to evaluate the linkage between inside and outside bacterial communities.

Materials and Methods

Cave Description and Sampling

Jinjia Cave (34°35.80′N, 104°30.05′E, 2443 m a.s.l.) is located approximately 25 km southeast of Zhang County, east Gansu Province, China (**Figure 1A**). This area is in the western Loess Plateau, with an annual precipitation of ∼440 mm and average temperature of ∼7.4°C. Most of the rainfall (>80%) occurred in the monsoon season. Modern vegetation overlying the cave was composed of temperate scrub and grass (Tan, 2008).

The cave, formed of Permian limestone, has an entrance of ∼6 m × 7 m with ∼200 m in length and 40 m-thick ceiling rock. The underground river was dry upon sampling, but a few small and shallow pools with a water depth of ∼5–10 cm were present (**Figure 1B**). The cave was not open for tourism, and hence was less exposed to human activity. When sampling from the entrance to the end of the cave in January 2013, the temperature increased from −5.5°C at the entrance to 7°C at the deepest passage.

To avoid the possible anthropogenic influence at the entrance and twilight zones, seven samples from the dark zone of the cave were collected, including four deposits on cave wall and two sediments in pools and in the soil at the bottom of a sinkhole. Among them, two cave wall deposits (E/F) and one sediment (G) were collected in the chamber ∼60 m from the main entrance (outer chamber), and the other two deposits (A/B) were obtained from the accessible deepest part of the cave (inner passage, **Figure 1B**). During sampling, the loose minerals were collected by scraping the rock surface with a sterile spatula. Two sediment samples (C/D) were collected from pools in the outer chamber and a passage approximately 3/4 of the way into the cave, respectively. In addition, three overlying soils (H/I/J) were also collected. It

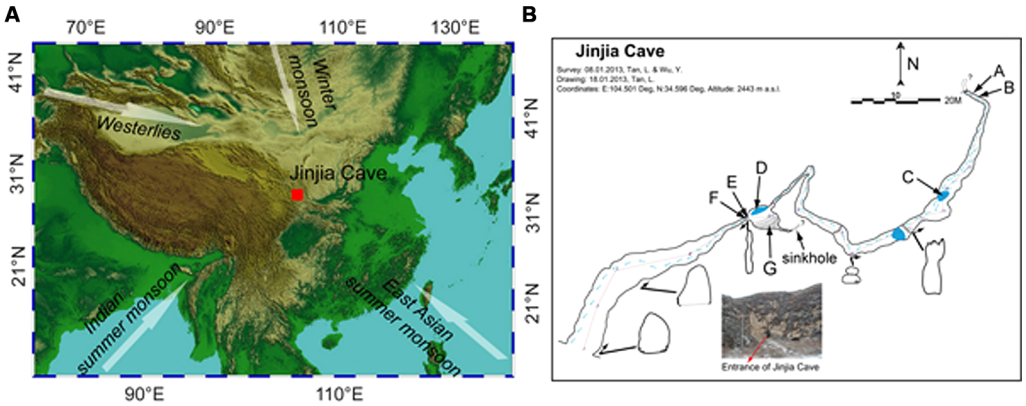

FIGURE 1 | Location (A) and plan view (B) of Jinjia Cave. Arrows in **(A)** indicate the directions of the east Asian summer monsoon, Indian summer monsoon, east Asian winter monsoon, and westerlies. The letters A and B (cave wall deposit), C and D (pool sediment), E and F (cave wall deposit), and G (sediment) in **(B)** mark the sampling sites inside the cave. Samples H, I, and J were from soils overlying the cave and were not shown in **(B)**.

should be noted that sample G and H were located on the bottom and the top of a small sinkhole, respectively. All the samples were put in sterile tubes, transported under the refrigeration to the laboratory and stored at −20°C until use.

Elemental Analysis

The samples were freeze-dried, finely ground to 200 mesh size (<74 μm) and homogenized in an agate mortar. Five grams of the powdered sample was compressed into a thin compact disk. Concentrations of major (e.g., Si, Al, and Ca) and trace elements (e.g., Rb, Sr, and Ba) were analyzed using a Philips PW4400 X-ray fluorescence (XRF) spectrometer at the Institute of Earth Environment – Chinese Academy of Sciences (Sun et al., 2008). Calibration was performed with Chinese national soil reference samples. Analytical precision was better than 1% for major elements and better than 5% for trace elements. The Student's *t*-test and principal component analysis (PCA) were carried out with SPSS 13.0 to inform the difference between rock deposit and soil/sediment samples and the similarity in sample elemental composition, respectively.

DNA Extraction and Quantitative PCR (q-PCR) of Bacterial 16S rRNA Genes

DNA was extracted from approximately 0.5 g samples (fresh weight) with the FastDNA SPIN Kit for Soil (MP Biomedicals) following the manufacturer's instructions. Ten-fold diluted DNA did not significantly inhibit the PCR reaction by calculating the q-PCR amplification efficiency of bacterial 16S rRNA gene with serial dilutions of extracts, therefore was used in all downstream molecular analysis.

Quantitative-PCR was performed on an iCycler instrument (Bio-Rad). The primer sets of 515f and 907r (Stahl and Amann, 1991; Muyzer et al., 1995) were used for the quantification of bacterial 16S rRNA genes with the SYBR green-based reactions performed in triplicate for each sample. The 20-μL reaction mixture contained 10-μL TransStart Green qPCR SuperMix (Transgen, Beijing, China), 0.2 μmol L^{-1} of each primer, and 2-μL template DNA. Reactions were run with 3 min at 95°C, 40 cycles of 15 s at 95°C, 30 s at 55°C, 30 s at 72°C, following by a plate read. The amplification specificity was checked by melting curve analysis and electrophoresis. The q-PCR standards were generated using plasmid DNA from one clone containing bacterial 16S rRNA gene. A dilution series of the standard template across seven orders of magnitude (10^1–10^7) was used per assay. The control was run with water as the template instead of DNA extract. The q-PCR amplification efficiency for the standards was 97.7% with r^2-value of 0.997.

454 Pyrosequencing

Pyrosequencing of 16S rRNA genes was performed on a Roche 454 GS FLX Titanium sequencer (Roche Diagnostics Corporation, Branford, CT, USA) as previously described (Wu et al., 2013). Briefly, the V4 region of the 16S rRNA gene was amplified from all samples with the tagged 515f and 907r primers. The triplicate PCR amplicons for each sample were pooled, gel purified, and combined in equimolar ratios into a single tube for pyrosequencing analysis. Sample information and sequences were deposited in the Sequence Read Archive of NCBI under accession number PRJNA268982.

Sequence Analysis and Community Comparison

Analysis of 454 pyrosequencing data was conducted using the Mothur software v1.30.2[1] (Schloss et al., 2009) combined with RDP II[2] for taxonomic identification. All reads obtained were processed by removing tags and primer, with only reads with an average quality score above 30 and read lengths above 250 nt deemed acceptable. The trimmed sequences were aligned against the SILVA bacterial 16S rRNA gene databases using the Needleman algorithm. Chimeric sequences were identified and removed using the implementation of Chimera-uchime (Edgar

[1]http://www.mothur.org/
[2]http://rdp.cme.msu.edu/

et al., 2011). Potential chloroplasts and mitochondria sequences were identified and discarded by an assignment against respective sequence references. The high quality sequences were aligned to generate a distance matrix and clustering with the average neighbor algorithm. Representative sequences for each operational taxonomic unit (OTU), as defined by a 97% sequence identity, were obtained for further taxonomic analysis. Taxonomic placement of each OTU was carried out with RDP Classifier (Wang et al., 2007) with a confidence threshold of >80% selected.

Operational taxonomic unit richness and Shannon and Simpson diversity of each library were calculated at the cut-off of 0.03. Principal coordinate analysis (PCoA) was performed based on Bray–Curtis dissimilarity distances between the libraries with Mothur. Maximum likelihood (M-L) trees were calculated based on the Jukes–Cantor correction with Mega version 5.2 (Tamura et al., 2011) with representative cave sequences and the closest relatives deposited in the Genbank database. Bootstrap support was calculated (1000 replications).

Results

Elemental Compositions

The major and trace element concentrations of cave wall deposits, sinkhole and surface soils, and one limestone bedrock sample are shown in **Table 1**. PCA analysis indicates that the elemental compositions of deposits on the cave wall (A/B/E/F) showed broad similarities with that of the limestone bedrock (Figure S1). In contrast, the elemental composition of sinkhole soil (G) was highly similar to that of the soil overlying the cave (H). Significant enrichments ($P < 0.05$ or 0.01, *t*-test) of Ca and deficits of Na, Al, Si, K, Ti, and Rb in deposits from the cave walls and limestone bedrock were in contrast to those of the sinkhole soil. Notably, Mn and Fe in some deposits were especially enriched. For example, Fe in sample A was by far the most abundant element (51.9%) and was more than 5-fold higher than in limestone bedrock (9.06%), while Mn in B/F (>15%) was approximately three times higher than in bedrock (4.16%).

q-PCR of Bacterial 16S rRNA Genes

Bacterial 16S rRNA genes were recovered from all samples with q-PCR (**Figure 2A**), with a high variation in copy number across two orders of magnitude observed. In the surface soils, 16S rRNA gene copies ranged from 3.18×10^8 to 8.34×10^8 g^{-1} *d.w.*, which were 1–2 orders of magnitude more than for samples inside in the cave. The highest 16S rRNA gene abundance in sample E inside the cave was 7.82×10^7 copies g^{-1} *d.w.*, approximately 12.6 times higher than the lowest copy number (6.21×10^6 g^{-1}) found in sample F. No sample type or location-associated abundance pattern was observed.

Bacterial Diversity

After quality filtering and removal of chimera, chloroplasts, and mitochondria sequences, 76532 reads (representing 50.5% of the original dataset) with an average length of 368.5-bp were extracted. The library size for each sample ranged from 6265 to 10481 reads (**Table 2**), and a total of 8127 OTUs at a 97% cut-off for sequence identity were observed. Observed OTU number and diversity index calculations for each sample were based upon randomly subsampling down to the lowest reads number (i.e., 6265) to avoid bias associated with library size (Gihring et al., 2012).

TABLE 1 | Major and trace element concentrations of samples collected inside in and outside Jinjia Cave.

Sample type	Sample ID	Na* (%)	Mg (%)	Al** (%)	Si** (%)	P (‰)	K** (%)	Ca** (%)	Sc (ppm)	Ti* (‰)	V (ppm)	Cr (ppm)	Mn (%)	Fe (%)	Co (ppm)
Cave wall deposits	A	0.30	0.50	0.62	1.68	9.21	0.07	6.56	104	0.36	79.7	24.2	0.30	51.9	49.1
	B	0.61	0.77	1.62	6.16	1.67	0.45	5.02	0.79	0.20	185	22.1	15.0	17.0	67.6
	E	0.99	1.25	3.60	9.84	2.16	1.09	6.91	6.51	2.97	218	66.5	10.9	12.0	75.7
	F	0.59	0.70	1.53	2.96	4.46	0.30	6.24	4.74	0.33	172	59.3	15.4	32.1	16.6
Sediment	G	1.36	1.06	5.84	28.4	0.74	1.85	0.97	11.9	4.06	138	75.5	0.09	3.79	19.9
Surface soil	H	1.24	1.09	6.06	28.5	0.60	1.97	0.76	12.4	3.97	136	71.9	0.08	3.74	15.9
Limestone bedrock	–	0.23	0.35	1.00	2.15	1.44	0.20	28.7	9.33	0.52	139	14.8	4.16	9.06	29.4

Sample type	Sample ID	Ni (ppm)	Cu (ppm)	Zn (ppm)	Ga** (ppm)	As (ppm)	Rb** (ppm)	Sr (ppm)	Y (ppm)	Zr* (ppm)	Nb* (ppm)	Ba (‰)	Hf* (ppm)	Pb (ppm)	CO_3^- (%)
Cave wall deposits	A	<10	<10	<10	2.80	622	10.0	300	7.44	26.1	2.03	0.18	0.73	12.4	36.8
	B	181	76.2	85.2	0.42	117	15.0	990	32.1	83.8	7.49	11.6	3.95	29.7	51.7
	E	141	70.5	149	6.89	105	45.3	330	48.6	189	11.7	5.59	5.78	36.1	51.8
	F	223	<10	17.9	3.30	430	15.5	262	36.1	67.6	6.68	4.29	0.24	30.6	39.6
Sediment	G	35.5	31.6	89.9	17.0	19.0	110	144	30.6	316	16.4	0.48	9.68	39.8	55.9
Surface soil	H	34.9	30.5	90.6	17.6	15.9	119	133	27.5	240	15.8	0.50	7.71	27.9	55.9
Limestone bedrock	–	35.6	<10	9.97	3.47	139	10.9	250	11.2	55.5	4.28	1.68	0.60	11.6	53.6

** and ** represents the values for cave wall deposits and sediment/soil that are significantly different (P < 0.05 or 0.01, respectively). A bedrock sample was not included in the t-test.*

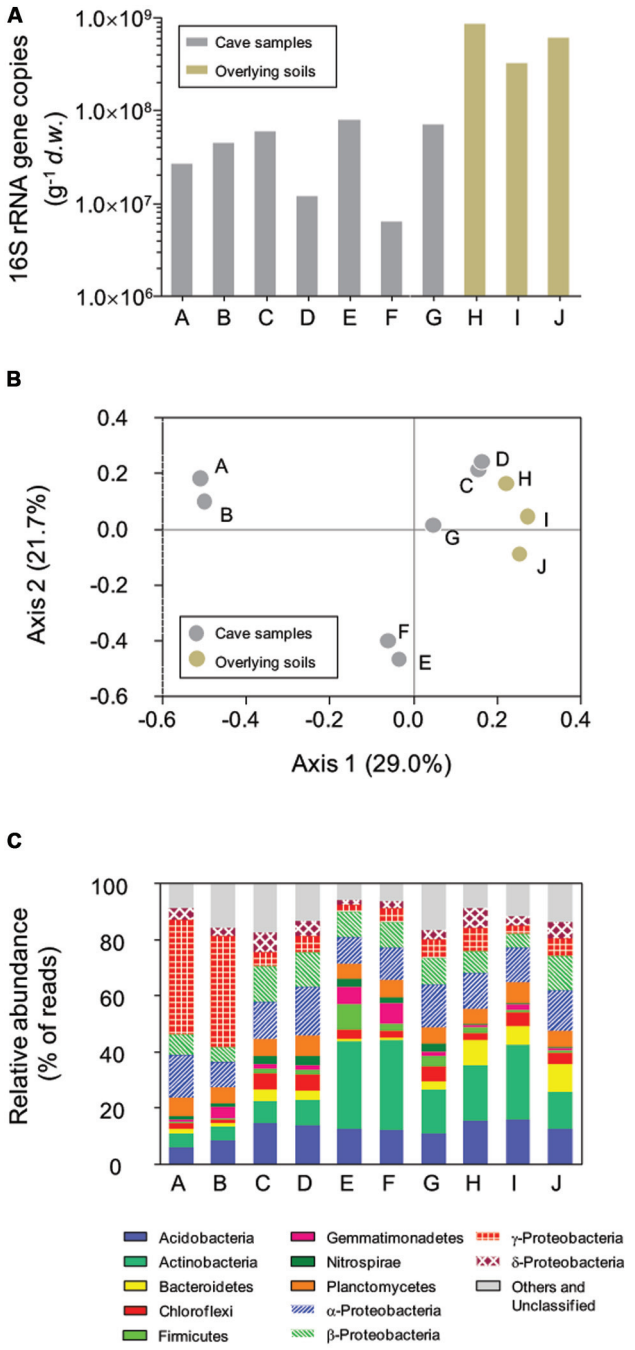

FIGURE 2 | Abundance of bacterial 16S rRNA genes (A), principal coordinate analysis (PCoA) plot based on Bray–Curtis distances (0.03 cutoff) between samples (B), and the relative abundance of dominant phyla in Jinjia Cave and related surface soils (C). Samples A, B, E, and F are from cave wall deposits, C and D are from pool sediments, G is a sinkhole soil and H–J are overlying soils.

A large variability in OTU richness among the samples was observed, with comparable values in relation to sample type or collection location. The lowest OTU number was observed on deposits on the cave wall in the inner passage (A/B, with a mean of 759.5), followed by the deposits in the outer chamber (E/F, 992.5). The sinkhole sample G was located a few meters away from sample E and F, but the OTU number was about two times higher than the latter. Despite the low bacterial abundance, the two sediment samples from the pools (C/D) had the most diverse bacterial communities, with a mean OTU number of 2602.5, which was close to surface soils (H/I/J, 2241.3) and approximately threefold higher than deposit samples A and B. Such a diversity pattern was confirmed by the Shannon and Inverse Simpson Indices calculation (**Table 2**). Overall, the diversity in soil and sediments was significantly higher than in rock deposits ($P < 0.01$, t-test).

TABLE 2 | Summary of 454 pyrosequencing and calculated diversity indices for each sample[a].

Sample type	Sample	No. of qualified reads	Observed OTUs	Shannon (H′)	Inverse Simpson (1/D)
Cave wall deposits	A	8750	687	4.10	9.43
	B	7848	832	4.19	7.99
	E	6280	1067	5.24	48.7
	F	10481	918	5.05	30.1
Pool sediment	C	7084	2706	7.08	407
	D	9096	2499	6.85	357
Sinkhole soil	G	7476	2120	6.46	172
	H	6854	2620	7.01	378
Surface soil	I	6410	1972	6.54	226
	J	6265	2132	6.74	284

[a]*Operational taxonomic units (OTUs), Shannon and Simpson indices are calculated at 97% sequence identity. Random subsampling down to the lowest reads number (6265) was performed to avoid bias associated with library size.*

Pairwise Bray–Curtis distance between samples was calculated based on OTU classification. PCoA analysis was performed to reveal the relatedness among bacterial communities (**Figure 2B**). The first two axes of the Bray–Curtis PCoA biplot together explained 50.7% of the total variance in the communities. All communities clustered into three major groups, with deposits on cave wall forming two independent groups by their location. The third group consisted of sediments and sinkhole soil, as well as the three surface soil samples, suggesting more similar bacterial compositions in these samples.

Taxonomic Patterns

All 454 reads were aligned against the SILVA bacterial ribosomal RNA reference database to derive the phyla-level community taxonomic profiles (**Figure 2C**). In total, 21 phyla and 11 candidate divisions were identified from 69921 out of 76532 reads, with varied dominant phyla observed in relation to the sample type and collection site. For example, deposit samples A and B from the outer chamber were highly dominated by γ-Proteobacteria, of which the relative reads abundance was almost 40% of the libraries, while the actinobacterial reads accounted for a third of the libraries of deposit samples from inner chamber (E and

Group	Taxa	A	B	C	D	E	F	G	H	I	J
OTU_01	Proteobacteria: γ-Proteobacteria	30,78	34,61	0,30	0,23	0,02	0,39	0,33	0,00	0,02	0,00
OTU_02	Actinobacteria: Actinomycetales	0,02	0,51	0,00	0,19	6,07	15,61	4,17	0,00	0,02	0,03
OTU_03	Acidobacteria: Gp4	1,82	2,34	0,35	0,32	5,05	5,25	0,16	0,34	0,25	0,69
OTU_04	Firmicutes: Bacillus	0,59	0,13	0,32	0,43	8,54	1,76	1,86	0,10	1,53	0,40
OTU_05	Unclassified bacteria	0,30	2,19	0,27	0,27	3,41	4,64	0,46	0,12	0,05	0,51
OTU_06	Proteobacteria: γ-Proteobacteria	1,12	3,95	0,79	1,09	0,05	0,84	2,44	0,23	0,80	0,05
OTU_07	Acidobacteria: Gp6	0,19	0,11	2,26	1,51	0,37	0,70	0,83	1,63	2,71	1,31
OTU_08	Proteobacteria: Rhizobiales	8,19	0,73	0,03	0,00	0,00	0,08	0,07	0,00	0,00	0,00
OTU_09	Proteobacteria: Burkholderiales	0,27	0,33	0,71	1,12	0,80	1,00	1,70	1,27	1,05	0,70
OTU_10	Acidobacteria: Gp6	0,21	0,61	0,71	0,68	0,78	0,70	0,94	0,89	1,72	0,56
OTU_11	Nitrospira: Nitrospira	0,26	0,45	0,82	1,20	0,99	1,64	1,31	0,22	0,05	0,00
OTU_12	Actinobacteria: Arthrobacter	0,05	0,00	0,38	0,76	0,64	0,75	2,12	0,93	0,84	1,10
OTU_13	Proteobacteria: Rhizobiales	1,18	1,04	0,75	0,69	0,18	1,38	0,56	0,35	0,20	0,16
OTU_14	Actinobacteria: Pseudonocardia	0,13	0,08	0,06	0,05	4,09	1,29	0,92	0,03	0,23	0,19
OTU_15	Acidobacteria: Gp6	0,15	0,74	0,66	0,76	0,57	0,45	0,28	0,79	1,08	0,93
OTU_16	Proteobacteria: Sulfuritalea	0,88	1,02	0,72	0,76	0,00	0,32	0,88	1,21	0,05	0,00
OTU_17	Actinobacteria: Blastococcus	0,00	0,00	0,14	0,24	0,64	0,47	0,29	0,29	1,47	3,26
OTU_18	Unclassified bacteria	0,33	0,34	0,82	1,30	0,41	0,27	0,59	0,51	0,27	1,02
OTU_19	Proteobacteria: γ-Proteobacteria	2,21	2,70	0,03	0,02	0,00	0,28	0,09	0,00	0,00	0,00
OTU_20	Proteobacteria: β-Proteobacteria	0,47	0,65	0,40	0,34	0,84	1,62	0,17	0,48	0,09	0,22
OTU_21	Proteobacteria: Variovorax	0,08	0,01	0,44	0,51	0,84	0,53	0,42	0,82	1,47	0,78
OTU_22	Acidobacteria: Gp6	0,11	0,18	1,45	1,18	0,08	0,12	0,48	0,66	0,73	0,67
OTU_23	Proteobacteria: Bradyrhizobiaceae	0,06	0,03	0,44	0,35	0,22	1,08	0,19	0,89	1,31	0,91
OTU_24	Proteobacteria: β-Proteobacteria	2,18	0,71	0,16	0,04	0,57	0,70	0,07	0,26	0,19	0,05
OTU_25	Nitrospira: Nitrospira	0,56	0,32	1,02	1,00	0,38	0,22	1,03	0,13	0,00	0,00
OTU_27	Gemmatimonadetes: Gemmatimonas	0,01	1,36	0,06	0,03	1,16	1,44	0,00	0,00	0,00	0,19
OTU_28	Proteobacteria: Rhodospirillaceae	0,79	1,71	0,30	0,21	0,02	0,10	0,39	0,61	0,28	0,10
OTU_29	Actinobacteria: Solirubrobacter	0,00	0,06	0,28	0,19	0,75	0,94	0,08	0,55	0,89	0,91
OTU_30	Actinobacteria: Acidimicrobineae	0,05	0,37	0,01	0,01	1,93	1,35	0,28	0,04	0,02	0,30
OTU_31	Proteobacteria: γ-Proteobacteria	3,69	0,17	0,00	0,01	0,00	0,02	0,00	0,00	0,00	0,02
OTU_32	Proteobacteria: Rhizobiales	0,03	0,10	0,16	0,54	0,68	1,17	1,21	0,04	0,05	0,02
OTU_33	Proteobacteria: β-Proteobacteria	0,00	0,04	0,97	0,75	0,13	0,13	0,48	0,83	0,61	0,56
OTU_35	Acidobacteria: Gp7	0,08	0,10	0,14	0,33	0,38	0,18	1,50	0,32	0,30	1,17
OTU_36	Actinobacteria: Rubrobacteridae	0,00	0,01	0,01	0,01	2,90	0,75	0,07	0,00	0,16	0,40
OTU_37	Actinobacteria: Solirubrobacterales	0,00	0,00	0,00	0,01	2,52	0,48	0,60	0,04	0,09	0,40
OTU_40	Bacteroidetes: Flavobacterium	0,15	0,03	0,34	0,74	0,00	0,00	0,24	1,11	1,01	0,21
OTU_41	Proteobacteria: β-Proteobacteria	0,33	0,19	0,92	0,99	0,00	0,00	0,82	0,10	0,05	0,02
OTU_43	Acidobacteria: Gp6	0,00	0,00	0,83	0,88	0,00	0,00	0,62	0,57	0,72	0,00
OTU_44	Proteobacteria: Steroidobacter	0,00	0,00	0,14	0,09	0,00	0,01	0,01	0,79	2,43	0,40
OTU_45	Proteobacteria: Rhizobiales	0,06	0,06	0,44	0,91	0,19	0,31	0,47	0,28	0,25	0,16
OTU_46	Actinobacteria: Micrococcineae	0,00	0,03	0,48	0,37	0,00	0,00	0,03	2,13	0,37	0,10
OTU_49	Proteobacteria: β-Proteobacteria	0,02	0,24	1,06	0,90	0,00	0,00	0,32	0,47	0,02	0,00
OTU_50	Proteobacteria: Nitrosospira	0,43	0,01	0,03	0,09	2,07	0,18	0,28	0,03	0,05	0,02
OTU_55	Proteobacteria: Massilia	0,01	1,06	0,01	0,08	0,30	0,20	0,16	0,53	0,14	0,16
OTU_56	Actinobacteria: Nocardioides	0,00	0,01	0,07	0,10	0,11	0,01	0,01	0,57	1,08	0,89
OTU_57	Proteobacteria: Lysobacter	1,29	0,54	0,04	0,01	0,02	0,10	0,03	0,10	0,08	0,05
OTU_58	Proteobacteria: Microvirga	0,00	0,00	0,18	0,16	0,06	0,00	0,19	0,23	0,58	1,39
OTU_63	Proteobacteria: β-Proteobacteria	0,00	0,00	0,00	0,00	0,33	1,40	0,00	0,00	0,00	0,00
OTU_75	Proteobacteria: Rhodospirillaceae	0,51	1,13	0,00	0,00	0,00	0,00	0,00	0,00	0,00	0,00
OTU_78	Proteobacteria: δ-Proteobacteria	1,29	0,11	0,00	0,00	0,00	0,00	0,00	0,03	0,00	0,00
OTU_79	Proteobacteria: Polaromonas	0,09	0,01	0,06	0,10	0,00	0,00	1,14	0,19	0,05	0,00
Sum of top 10 OTUs		53,75	52,10	10,94	11,19	37,72	36,08	18,48	11,72	15,83	12,88

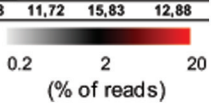

FIGURE 3 | Distribution matrix with the 10 most abundant taxa in each sample. Abundances are based on DNA amplicons. Taxa were defined by using Classifier of RDP with 80% selected as a threshold. Numbers show the relative abundance (% of the reads) of individual operational taxonomic unit (OTU). Sequences were deposited in the NCBI Sequence Read Archive under accession number PRJNA268982.

F). In contrast, the relative abundances of the most dominant phyla in the other samples were low, and there were apparent differences in specific phylum between cave and surface communities. For instance, the relative abundance of phylum *Nitrospira* in the surface soils (average 0.32 ± 0.18%, $n = 3$) was much lower than in subterranean samples (2.39 ± 0.82%, $n = 7$).

Representative sequences from the top 10 most abundant OTUs of each library were further classified with RDP (**Figure 3**). For deposit samples A and B, one OTU affiliated with γ-Proteobacteria (OTU_01) constituted 30.8 and 34.6% of the libraries, respectively. Together with the closely related OTU_19, OTU_01 represented the most dominant bacterial clade on the rock surface in the inner cave. The closest relatives in the Genbank database (96–100% sequence identity) to OTU_01 and OTU_19 were almost exclusively recovered from geographically distinct caves, constituting the cave bacterial lineage I (**Figure 4A**). The closest pure culture to OTU_01 is a chemolithoautotrophic sulfur oxidizer (*Thioprofundum hispidum*, 95% sequence identity). Surprisingly, however, the relative abundance of this clade in other two deposit samples (E/F) was minimal (<0.4%). The second most abundant OTU in deposit A (OTU_08, 8.2% of the library; **Figure 3**) was associated with environmental sequences mostly recovered from cold terrestrial habitats. The closest pure culture to OTU_08 is *Methylocella tundrae* of α-Proteobacteria (98% identity). Deposit samples E and F were predominated by Actinobacteria, Acidobacteria, and Proteobacteria (**Figure 2C**). Two Actinobacterial OTUs (OTU_02 and OTU_14) together constituted 10.2 and 16.9% of the communities, respectively,

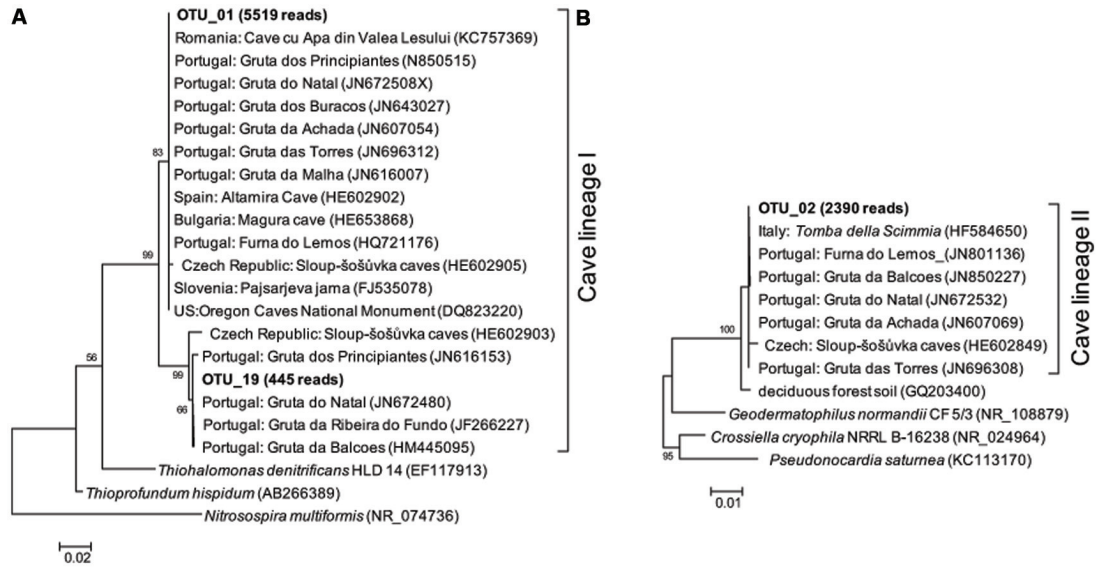

FIGURE 4 | Maximum likelihood (M-L) tree of two cave bacterial lineages, respectively, dominant in cave wall deposits A/B (A) and E/F (B). Sequences retrieved from the present study are shown in bold, with the number in parentheses indicating the total reads. Bootstrap values >50% are shown in the trees.

with OTU_02 routinely recovered from cave environments (cave lineage II, **Figure 4B**). Acidobacteria (OTU_03) and one unclassified phylotype (OTU_05) were also abundant in samples E and F. In addition, *Bacillus*-related sequences were only dominant in sample E (OTU_04, 8.54%).

The dominance of abundant OTUs in sinkhole soil, pool sediments, and surface soils was found to be much less than in deposits on the cave wall, as indicated by the accumulated relative abundances of the top 10 OTUs, which ranged from 10.94 to 18.48% (**Figure 3**). The most abundant taxa in pool sediments included those within subgroup 6 (Gp6) of Acidobacteria, which was relatively rare in rock deposits but constituted a major fraction in overlying soil communities (OTU_07, OTU_22, and OTU_43, **Figure 3**). Moreover, as has been revealed at the phylum level, *Nitrospira*-related OTUs (OTU_11 and 25) were relatively rare in the surface soils.

Discussion

Jinjia Cave, like other subterranean ecosystems, is ubiquitously colonized by bacteria as indicated by the recovery of 16S rRNA genes from all samples. Assuming most bacterial genomes possess 1–7 ribosomal RNA operons (Větrovský and Baldrian, 2013), this equates to 10^6–10^7 bacterial cells per gram of sample, much less than that in the overlying soil but still typical of cave environments (Barton and Jurado, 2007). The low abundance of bacteria might be related to the aphotic conditions and the limited input of nutrients, which limits the proliferation of phototrophs or copiotrophs. In contrast, the bacterial richness inside the cave was more comparable to that in the surface soils, although the rock deposits had much lower OTU numbers than the cave sediments (**Table 2**). This and the diversity indices indicate the distinctness of bacterial communities on rock walls.

The rock surface might be one of the most distinct habitats in caves. The similarities in elemental compositions between the four rock wall deposits and the limestone, in particular the significant enrichment of Ca, indicates their origin from bedrock. The supplies of energy and nutrients on the rock surface are exclusively dependent on the inputs through air currents or seepage water, implying the extreme starvation, and predicting the species sorting under these conditions. Mineral chemistry may also impact the microbial community inhabiting the rock surface (Hutchens et al., 2010). Consistently, all of the four rock deposits were dominated by a few phylotypes that have been identified in geographically distinct European and American caves and may represent cave-adapted bacterial lineages. The cave lineage I within γ-Proteobacteria (**Figure 4A**) found in inner cave deposit samples A and B (32.99 and 37.31% of the reads, respectively) is likely an obligate cave clade, because the more similar sequences (>96% identity) in Genbank were exclusively recovered from caves. The OTU_01-related phylotypes have been found to be a major component of yellow mats attached to rock surfaces and was proposed as a core OTU in several caves (Porca et al., 2012). To our knowledge, this is the first evidence of the presence of cave-specific bacterial lineages in an East Asian cave. Currently there is no cultivated representative of the lineage, and the distantly related pure cultures include chemolithoautotrophic sulfur oxidizers *T. hispidum* (Mori et al., 2011) and *Thiohalomonas denitrificans* (Sorokin et al., 2007). Whether this lineage lives an obligate autotrophic and sulfur-transforming life and what the mechanism of their adaptation to oligotrophic rock surface may be both merit further study.

Rocks of the outer chamber shared less overlap with those in the inner passage, suggesting different habitat traits from the

innermost passage rock walls, despite their similarity in elemental components. The most abundant bacteria in deposit samples E and F were closely related to Pseudonocardiaceae of Actinobacteria (OTU_02), which are common on subterranean rocks (Porca et al., 2012) but also present in soils. It has been suggested that organic carbon exposure may contribute to the enrichment of Pseudonocardiaceae on rock surfaces (Diaz-Herraiz et al., 2013). Consistent with this idea and in contrast to the deeper cave, the outer chamber is more easily accessible, and thus the availability of organic C might have been high due to the inputs through the main entrance or other connections such as the nearby sinkhole (**Figure 1**). Nonetheless, because of the low sequence identity of OTU_02, as well as the other abundant phylotypes to known strains, its functional traits on the rock surfaces of the inner cave are still unclear.

In addition to the enrichment of putative cave lineages, there were abundant putative chemolithoautotrophic taxa inside Jinjia Cave, such as *Nitrospira* and *Nitrosospira*, for which all cultivated representative are capable of autotrophic C fixation (Koops et al., 2006; Lücker et al., 2010). *Nitrospira* and *Nitrosospira* are involved in the two-step autotrophic nitrification, suggesting the presence of the CO_2-fixation-coupled ammonia oxidation process, which has been supposed to sustain the primary production of some cave ecosystems (Sarbu et al., 1996; Ortiz et al., 2013a). Chen et al. (2009) also identified the activity of ammonia and sulfur-oxidizing bacteria in the chemolithotrophic Movile Cave using a stable isotope approach. As such, it is very likely that lithochemotrophy is one of the dominant bacterial life strategies in the darkness of Jinjia Cave.

Previous studies have suggested microbial roles in the formation of Mn- and Fe-rich deposits on the cave rock walls (Spilde et al., 2005; Carmichael et al., 2013). Mn-oxidizing bacteria mostly fall within Firmicutes, Proteobacteria, and Actinobacteria (Tebo et al., 2005), among which *Bacillus* has been well studied as a model Mn oxidizer (Francis and Tebo, 2002). By contrast, most iron-oxidizing bacteria are affiliated with Proteobacteria (Hedrich et al., 2011). Some *Methylocella* of α-Proteobacteria possess the capability of Fe(II) oxidation (Lu et al., 2010). Interestingly, *Bacillus*- (OTU_04) and *Methylocella*-related phylotypes (OTU_08) dominated two deposit samples in Jinjia Cave, while iron-reducing *Aciditerrimonas*-related sequences (OTU_30; Itoh et al., 2011) were also enriched in all deposit samples, implicating bacterial involvement in the ferromanganese deposit formation in Jinjia Cave. Further cultivation and metabolism analysis will be helpful for revealing the geochemical roles of these abundant and many other relatively rare bacteria.

The spatial heterogeneity in bacterial communities inside Jinjia Cave, as revealed by the broad variability of richness, composition, and dominant phylotypes, might be related to the substantial difference in cave habitats. This heterogeneity was even obvious for the same sample type (e.g., deposits A/B versus E/F; Ortiz et al., 2013b). In other cases, however, samples share common dominant phylotypes despite their considerable spatial distance. For instance, in this study, both pool sediments that are connected by underground hydrology revealed nearly identical dominant OTUs. Elemental analysis provided some clues of species sorting by microhabitats. The highly similar elemental compositions of samples G and H are not surprising (**Table 1**), because the sediment sample G very likely originated from the surface materials that could be carried into the cave via the sinkhole. This partially explains why sample G had a distinct bacterial community from the nearby rock wall deposits (E/F).

In contrast, the community overlaps between cave sediments and surface soils suggests an influence from surface environments. Due to the limited depth and length of Jinjia Cave, nutrients, energy, and microbes can constantly enter through the entrance, sinkholes, underground streams, and drip water and can thus modify microhabitat and shape microbial community. This is highlighted by the similarities in elemental and bacterial compositions between samples G and H that were associated with a small sinkhole, whereas bacterial communities in pool sediments were very likely partly controlled by underground stream and seepage waters carrying dissolved organic carbon and nutrients from the surface. Mass effect could be another factor affecting the bacterial communities in Jinjia Cave (Shabarova et al., 2013), because microbes on the surface may disperse via seepage water into the subterranean environments. This is partly supported by the fact that the pool and sinkhole sediments had more chloroplasts contamination (0.11–0.25% of each library) than rock deposits (0–0.04%), which was very likely imported from the overlying soils (0.92–1.35%). Seasonal variation in temperature within the cave might contribute to the bacterial heterogeneity too, as suggested by the difference of 12.5°C from the entrance to the deepest passage on the sampling. Overall, the external influence on cave bacterial community structure seems not to be negligible and requires further study.

Conclusion

In this study, we profiled the bacterial communities in a short and shallow limestone cave, Jinjia Cave from western Loess Plateau of China by ribo-tag pyrosequencing. Highly heterogeneous bacterial diversity in Jinjia Cave could be related to the habitat type and might be affected by interconnection between subsurface and surface environments. The rock wall deposit communities were less diverse and dominated by possible indigenous cave bacteria, which is likely controlled by the rock surface geochemistry. Based on comparison with known functional guilds, we speculate that the bacteria on cave walls are potentially involved in CO_2 fixation, N transformation, and speleogenesis. However, due to the absence of more biogeochemical and microbial activity information, the functions of the dominant cave bacterial lineage are still an open question.

Acknowledgments

We thank Professor Feng Wu and Mr. Hao Zheng for the help in sample and data analysis. This study was supported by the National Natural Science Foundation of China

(41371310; 41372192), State Key Laboratory of Soil and Sustainable Agriculture (Y212000014), and Key Program of the Chinese Academy of Sciences (KZZD-EW-04-01). YW and LT acknowledges the fellowships from Youth Innovation Promotion Association, Chinese Academy of Sciences.

Supplementary Material

The Supplementary Material for this article can be found online at: http://www.frontiersin.org/journal/10.3389/fmicb.2015.00244/abstract

References

Barton, H. A., and Jurado, V. (2007). What's up down there? Microbial diversity in caves. *Microbe* 2, 132–138.

Barton, H. A., Taylor, N. M., Kreate, M. P., Springer, A. C., Oehrle, S. A., and Bertog., J. L. (2007). The impact of host rock geochemistry on bacterial community structure in oligotrophic cave environments. *Int. J. Speleol.* 36, 93–104. doi: 10.5038/1827-806X.36.2.5

Carmichael, M. J., Carmichael, S. K., Santelli, C. M., Strom, A., and Bräuer, S. L. (2013). Mn(II)-oxidizing bacteria are abundant and environmentally relevant members of ferromanganese deposits in caves of the Upper Tennessee river basin. *Geomicrobiol. J.* 30, 779–800. doi: 10.1080/01490451.2013.769651

Chen, Y., Wu, L., Boden, R., Hillebrand, A., Kumaresan, D., Moussard, H., et al. (2009). Life without light: microbial diversity and evidence of sulfur- and ammonium-based chemolithotrophy in Movile Cave. *ISME J.* 3, 1093–1104. doi: 10.1038/ismej.2009.57

Cuezva, S., Fernandez-Cortes, A., Porca, E., Pašić, L., Jurado, V., Hernandez-Marine, M., et al. (2012). The biogeochemical role of actinobacteria in Altamira cave, Spain. *FEMS Microbiol. Ecol.* 81, 281–290. doi: 10.1111/j.1574-6941.2012.01391.x

Desai, M. S., Assig, K., and Dattagupta, S. (2013). Nitrogen fixation in distinct microbial niches within a chemoautotrophy-driven cave ecosystem. *ISME J.* 7, 2411–2423. doi: 10.1038/ismej.2013.126

Diaz-Herraiz, M., Jurado, V., Cuezva, S., Laiz, L., Pallecchi, P., Tiano, P., et al. (2013). The actinobacterial colonization of Etruscan paintings. *Sci. Rep.* 3, 1440. doi: 10.1038/srep01440

Edgar, R. C., Haas, B. J., Clemente, J. C., Quince, C., and Knight, R. (2011). UCHIME improves sensitivity and speed of chimera detection. *Bioinformatics* 27, 2194–2200. doi: 10.1093/bioinformatics/btr381

Engel, A. S., Stern, L. A., and Bennett, P. C. (2004). Microbial contributions to cave formation: new insights into sulfuric acid speleogenesis. *Geology* 32, 369–372. doi: 10.1130/G20288.1

Francis, C. A., and Tebo, B. M. (2002). Enzymatic manganese(II) oxidation by metabolically dormant spores of diverse *Bacillus* species. *Appl. Environ. Microbiol.* 68, 874–880. doi: 10.1128/AEM.68.2.874-880.2002

Gihring, T. M., Green, S. J., and Schadt, C. W. (2012). Massively parallel rRNA gene sequencing exacerbates the potential for biased community diversity comparisons due to variable library sizes. *Environ. Microbiol.* 14, 285–290. doi: 10.1111/j.1462-2920.2011.02550.x

Hedrich, S., Schlömann, M., and Johnson, D. B. (2011). The iron-oxidizing proteobacteria. *Microbiology* 157, 1551–1564. doi: 10.1099/mic.0.045344-0

Hutchens, E., Gleeson, D., Mcdermott, F., Miranda-Casoluengo, R., and Clipson, N. (2010). Meter-scale diversity of microbial communities on a weathered pegmatite granite outcrop in the Wicklow Mountains, Ireland; evidence for mineral induced selection? *Geomicrobiol. J.* 27, 1–14. doi: 10.1080/01490450903232157

Ikner, L., Toomey, R., Nolan, G., Neilson, J., Pryor, B., and Maier, R. (2007). Culturable microbial diversity and the impact of tourism in Kartchner Caverns, Arizona. *Microb. Ecol.* 53, 30–42. doi: 10.1007/s00248-006-9135-8

Itoh, T., Yamanoi, K., Kudo, T., Ohkuma, M., and Takashina, T. (2011). *Aciditerrimonas ferrireducens* gen. nov., sp nov., an iron-reducing thermoacidophilic actinobacterium isolated from a solfataric field. *Int. J. Syst. Evol. Microbiol.* 61, 1281–1285. doi: 10.1099/ijs.0.023044-0

Koops, H.-P., Purkhold, U., Pommerening-Röser, A., Timmermann, G., and Wagner, M. (2006). "The lithoautotrophic ammonia-oxidizing bacteria," in *The Prokaryotes*, eds M. Dworkin, S. Falkow, E. Rosenberg, K.-H. Schleifer, and E. Stackebrandt (New York, NY: Springer), 778–811.

Lu, S., Gischkat, S., Reiche, M., Akob, D. M., Hallberg, K. B., and Küsel, K. (2010). Ecophysiology of Fe-cycling bacteria in acidic sediments. *Appl. Environ. Microbiol.* 76, 8174–8183. doi: 10.1128/AEM.01931-10

Lücker, S., Wagner, M., Maixner, F., Pelletier, E., Koch, H., Vacherie, B., et al. (2010). A *Nitrospira* metagenome illuminates the physiology and evolution of globally important nitrite-oxidizing bacteria. *Proc. Natl. Acad. Sci. U.S.A.* 107, 13479–13484. doi: 10.1073/pnas.1003860107

Macalady, J. L., Jones, D. S., and Lyon, E. H. (2007). Extremely acidic, pendulous cave wall biofilms from the Frasassi cave system, Italy. *Environ. Microbiol.* 9, 1402–1414. doi: 10.1111/j.1462-2920.2007.01256.x

Mori, K., Suzuki, K.-I., Urabe, T., Sugihara, M., Tanaka, K., Hamada, M., et al. (2011). *Thioprofundum hispidum* sp. nov., an obligately chemolithoautotrophic sulfur-oxidizing gammaproteobacterium isolated from the hydrothermal field on Suiyo Seamount, and proposal of *Thioalkalispiraceae* fam. nov. in the order Chromatiales. *Int. J. Syst. Evol. Microbiol.* 61, 2412–2418. doi: 10.1099/ijs.0.026963-0

Muyzer, G., Teske, A., Wirsen, C., and Jannasch, H. (1995). Phylogenetic relationships of *Thiomicrospira* species and their identification in deep-sea hydrothermal vent samples by denaturing gradient gel electrophoresis of 16S rDNA fragments. *Arch. Microbiol.* 164, 165–172. doi: 10.1007/BF02529967

Ortiz, M., Legatzki, A., Neilson, J. W., Fryslie, B., Nelson, W. M., Wing, R. A., et al. (2013a). Making a living while starving in the dark: metagenomic insights into the energy dynamics of a carbonate cave. *ISME J.* 8, 478–491. doi: 10.1038/ismej.2013.159

Ortiz, M., Neilson, J., Nelson, W., Legatzki, A., Byrne, A., Yu, Y., et al. (2013b). Profiling bacterial diversity and taxonomic composition on speleothem surfaces in Kartchner Caverns, AZ. *Microb. Ecol.* 65, 371–383. doi: 10.1007/s00248-012-0143-6

Pašić, L., Kovće, B., Sket, B., and Herzog-Velikonja, B. (2010). Diversity of microbial communities colonizing the walls of a Karstic cave in Slovenia. *FEMS Microbiol. Ecol.* 71, 50–60. doi: 10.1111/j.1574-6941.2009.00789.x

Porca, E., Jurado, V., Žgur-Bertok, D., Saiz-Jimenez, C., and Pašić, L. (2012). Comparative analysis of yellow microbial communities growing on the walls of geographically distinct caves indicates a common core of microorganisms involved in their formation. *FEMS Microbiol. Ecol.* 81, 255–266. doi: 10.1111/j.1574-6941.2012.01383.x

Roesch, L. F., Fulthorpe, R. R., Riva, A., Casella, G., Hadwin, A. K. M., Kent, A. D., et al. (2007). Pyrosequencing enumerates and contrasts soil microbial diversity. *ISME J.* 1, 283–290.

Sarbu, S. M., Dane, T. C., and Kinkle, B. K. (1996). A chemoautotrophically based cave ecosystems. *Science* 272, 1953–1955. doi: 10.1126/science.272.5270.1953

Schloss, P. D., Westcott, S. L., Ryabin, T., Hall, J. R., Hartmann, M., Hollister, E. B., et al. (2009). Introducing mothur: open-source, platform-independent, community-supported software for describing and comparing microbial communities. *Appl. Environ. Microbiol.* 75, 7537–7541. doi: 10.1128/AEM.01541-09

Shabarova, T., Widmer, F., and Pernthaler, J. (2013). Mass effects meet species sorting: transformations of microbial assemblages in epiphreatic subsurface karst water pools. *Environ. Microbiol.* 15, 2476–2488. doi: 10.1111/1462-2920.12124

Sorokin, D. Y., Tourova, T. P., Braker, G., and Muyzer, G. (2007). *Thiohalomonas denitrificans* gen. nov., sp. nov. and *Thiohalomonas nitratireducens* sp. nov., novel obligately chemolithoautotrophic, moderately halophilic, thiodenitrifying Gammaproteobacteria from hypersaline habitats. *Int. J. Syst. Evol. Microbiol.* 57, 1582–1589. doi: 10.1099/ijs.0.65112-0

Spilde, M. N., Northup, D. E., Boston, P. J., Schelble, R. T., Dano, K. E., Crossey, L. J., et al. (2005). Geomicrobiology of cave ferromanganese deposits: a field and laboratory investigation. *Geomicrobiol. J.* 22, 99–116. doi: 10.1080/01490450590945889

Stahl, D. A., and Amann, R. (1991). "Development and application of nucleic acid probes," in *Nucleic Acid Techniques in Bacterial Systematics*, eds E. Stackebrandt and M. Goodfellow (New York: Wiley), 205–248.

Sun, Y., Wu, F., Clemens, S. C., and Oppo, D. W. (2008). Processes controlling the geochemical composition of the South China Sea sediments during the last climatic cycle. *Chem. Geol.* 257, 240–246. doi: 10.1016/j.chemgeo.2008.10.002

Tamura, K., Peterson, D., Peterson, N., Stecher, G., Nei, M., and Kumar, S. (2011). MEGA5: molecular evolutionary genetics analysis using maximum likelihood, evolutionary distance, and maximum parsimony methods. *Mol. Biol. Evol.* 28, 2731–2739. doi: 10.1093/molbev/msr121

Tan, L. (2008). *High-Resolution Monsoon Precipitation Variations in China during the Last 2000 Years*. Ph.D. thesis, Chinese Academy of Sciences, Beijing.

Tebo, B. M., Johnson, H. A., Mccarthy, J. K., and Templeton, A. S. (2005). Geomicrobiology of manganese(II) oxidation. *Trends Microbiol.* 13, 421–428. doi: 10.1016/j.tim.2005.07.009

Tetu, S. G., Breakwell, K., Elbourne, L. D., Holmes, A. J., Gillings, M. R., and Paulsen, I. T. (2013). Life in the dark: metagenomic evidence that a microbial slime community is driven by inorganic nitrogen metabolism. *ISME J.* 7, 1227–1236. doi: 10.1038/ismej.2013.14

Větrovský, T., and Baldrian, P. (2013). The variability of the 16S rRNA gene in bacterial genomes and its consequences for bacterial community analyses. *PLoS ONE* 8:e57923. doi: 10.1371/journal.pone.0057923

Wang, Q., Garrity, G. M., Tiedje, J. M., and Cole, J. R. (2007). Naïve Bayesian classifier for rapid assignment of rRNA sequences into the new bacterial taxonomy. *Appl. Environ. Microbiol.* 73, 5261–5267. doi: 10.1128/AEM.00062-07

Wu, Y., Ke, X., Hernández, M., Wang, B., Dumont, M. G., Jia, Z., et al. (2013). Autotrophic growth of bacterial and archaeal ammonia oxidizers in freshwater sediment microcosms incubated at different temperatures. *Appl. Environ. Microbiol.* 79, 3076–3084. doi: 10.1128/AEM.00061-13

Yang, H., Ding, W., Zhang, C. L., Wu, X., Ma, X., He, G., et al. (2011). Occurrence of tetraether lipids in stalagmites: implications for sources and GDGT-based proxies. *Org. Geochem.* 42, 108–115. doi: 10.1016/j.orggeochem.2010.11.006

Conflict of Interest Statement: The authors declare that the research was conducted in the absence of any commercial or financial relationships that could be construed as a potential conflict of interest.

frontiers in Microbiology

ORIGINAL RESEARCH
published: 21 July 2015
doi: 10.3389/fmicb.2015.00729

Bacterial diversity differences along an epigenic cave stream reveal evidence of community dynamics, succession, and stability

OPEN ACCESS

Edited by:
Malin Bomberg, VTT Technical Research Centre of Finland, Finland

Reviewed by:
Christian Griebler, Helmholtz Zentrum München - Institute of Groundwater Ecology, Germany
Jack A. Stanford, Flathead Lake Biological Station University of Montana, USA

***Correspondence:**
Kathleen Brannen-Donnelly, Department of Earth and Planetary Sciences, University of Tennessee, 1412 Circle Drive, Knoxville, TN 37996, USA
kbrannen@vols.utk.edu

Specialty section:
This article was submitted to Terrestrial Microbiology, a section of the journal Frontiers in Microbiology

Received: *06 April 2015*
Accepted: *03 July 2015*
Published: *21 July 2015*

Citation:
Brannen-Donnelly K and Engel AS (2015) Bacterial diversity differences along an epigenic cave stream reveal evidence of community dynamics, succession, and stability. Front. Microbiol. 6:729. doi: 10.3389/fmicb.2015.00729

Kathleen Brannen-Donnelly* and Annette S. Engel

Department of Earth and Planetary Sciences, University of Tennessee, Knoxville, TN, USA

Unchanging physicochemical conditions and nutrient sources over long periods of time in cave and karst subsurface habitats, particularly aquifers, can support stable ecosystems, termed autochthonous microbial endokarst communities (AMEC). AMEC existence is unknown for other karst settings, such as epigenic cave streams. Conceptually, AMEC should not form in streams due to faster turnover rates and seasonal disturbances that have the capacity to transport large quantities of water and sediment and to change allochthonous nutrient and organic matter sources. Our goal was to investigate whether AMEC could form and persist in hydrologically active, epigenic cave streams. We analyzed bacterial diversity from cave water, sediments, and artificial substrates (Bio-Traps®) placed in the cave at upstream and downstream locations. Distinct communities existed for the water, sediments, and Bio-Trap® samplers. Throughout the study period, a subset of community members persisted in the water, regardless of hydrological disturbances. Stable habitat conditions based on flow regimes resulted in more than one contemporaneous, stable community throughout the epigenic cave stream. However, evidence for AMEC was insufficient for the cave water or sediments. Community succession, specifically as predictable exogenous heterotrophic microbial community succession, was evident from decreases in community richness from the Bio-Traps®, a peak in Bio-Trap® community biomass, and from changes in the composition of Bio-Trap® communities. The planktonic community was compositionally similar to Bio-Trap® initial colonizers, but the downstream Bio-Trap® community became more similar to the sediment community at the same location. These results can help in understanding the diversity of planktonic and attached microbial communities from karst, as well as microbial community dynamics, stability, and succession during disturbance or contamination responses over time.

Keywords: community assembly, stream, cave, microorganisms, succession, community dynamics, Bio-Traps®

Introduction

Caves are diagnostic dissolutional features in karst landscapes underlain by soluble rock (e.g., limestone or dolomite) where surface water sinks into the subsurface and flows in a network of self-evolving underground stream passages (Ford and Williams, 2013). Although hydrological flow regimes, watershed geometry, aqueous geochemistry, and bedrock geology differ between karst systems (Nico et al., 2006; Simon et al., 2007; Bonacci et al., 2008), many have similar, stable environmental conditions and components that contribute to habitability and ecosystem development (Hahn and Fuchs, 2009; Griebler et al., 2010). Microbes are important components of all subterranean ecosystems (Chapelle, 2000) and of every type of karst habitat (Griebler and Lueders, 2009). Although the compositions of microbial communities (from the aspect of alpha-diversity) have been widely evaluated from karst (Griebler and Lueders, 2009), much still remains to be explored, including microbial diversity trends over time (Engel, 2010). Microbes regulate chemical reactions that cause mineral dissolution and precipitation (Engel et al., 2004; Engel and Randall, 2011; Lian et al., 2011) and affect contaminant remediation (Thomas and Ward, 1992). As such, interest in microbial communities in various karst settings has increased (Griebler et al., 2010), and attempts have been made to understand whether microbial diversity differs throughout distinct types of karst systems and what ecosystem conditions control or regulate community composition. For instance, in karst aquifers and cave pools where water residence times are exceedingly long, from months to years, autochthonous microbial endokarst communities (AMEC) develop (Farnleitner et al., 2005; Pronk et al., 2008). Understanding AMEC is important to groundwater ecology, biogeochemistry of karst aquifers, and water resource management and conservation (Farnleitner et al., 2005; Pronk et al., 2008; Griebler and Lueders, 2009; Zhou et al., 2012).

Previously described AMEC have been sampled as planktonic phenomena from annual and monthly sample events of karst springs (Farnleitner et al., 2005; Pronk et al., 2008). A uniform definition for AMEC has not been applied, despite other types of groundwater systems having taxonomic and functionally distinct attached and planktonic communities (Hazen et al., 1991; Alfreider et al., 1997; Lehman, 2007; Flynn et al., 2008; Zhou et al., 2012). Conceptually AMEC should be homogenized communities of planktonic and attached microbial cells from within a karst aquifer setting. Under elevated flow conditions during recharge events, high flow velocities would mobilize sediment (Dogwiler and Wicks, 2004) and cause high shear stress on sediment-attached cells (Rehmann and Soupir, 2009; Ghimire and Deng, 2013). Biofilm development on sediments and aquifer surfaces would be limited and attached cells would become entrained into the water column and become part of the planktonic community (Rehmann and Soupir, 2009). A prescribed minimum time limit for AMEC formation in karst has not been described, but this is not surprising because the stability and potential AMEC successional patterns over time in most groundwater systems are also not well understood (Farnleitner et al., 2005). Typical AMEC bacterial compositions are apparently comprised of Acidobacteria, Nitrospira, Gammaproteobacteria, and Deltaproteobacteria, and AMEC comprise the majority of the overall community abundances (Farnleitner et al., 2005; Pronk et al., 2008). The major taxonomic groups in AMEC are phylogenetically related to surface-derived groups, but not identical, thereby highlighting the importance of being sourced from within a subsurface system. Although no truly endemic karst microorganisms have been identified (Griebler and Lueders, 2009), arguably enhanced genetic divergences between surface communities and AMEC could result from long flow path travel distances and longer periods of isolation between the surface and subsurface.

As such, it is unclear whether AMEC are present or can persist in systems where turnover rates are expected to be high, such as in cave streams. Cave streams are dynamic, usually turbulent underground features that form from sinking surface water. Water is sourced from the surface and may reemerge from a conduit some distance later as a spring. Cave stream habitats that become established based on prevailing physicochemical gradients may only last for hours to weeks, according to the hydrological connection (i.e., continuous, flashy, etc.) with the surface. Sediment suspension and deposition events caused by recharge flooding or flushing of the system could compositionally homogenize water and sediment microbial communities (at the level of beta-diversity), which would hamper the ability to detect AMEC from transported allochthonous communities. In this study, we investigated the diversity and prevalence of microorganisms from 16S rRNA gene sequences in stream water and cave sediments along a continuously flowing cave stream of fixed length but having different flow rates due to storm events over a 6 month period. In addition to documenting novel bacterial diversity for an epigenic cave stream, we compared water-transported (i.e., planktonic) and sediment (i.e., attached) bacterial diversity to test the hypothesis that an AMEC exists, despite storm water and sediment disturbances and differential contribution of surface-derived bacterial groups into the subsurface. We expected water and sediment communities to be similar to each other after high flow events, but that sediment communities would represent AMEC in between high flow events that would resuspend some or all of the cave sediments.

We also hypothesized that disturbance events reveal successional patterns between upstream and downstream communities. Studying microbial community successional patterns has proven difficult in many ecological systems (Shade et al., 2013). For this study, we used the definition of succession from Fierer et al. (2010), as the "orderly and predictable manner by which communities change over time following the colonization of a new environment." During 4 months, we seeded bacterial communities on artificial substrates (Bio-Trap® samplers) that were fixed in one upstream and one downstream location in the cave system. The Bio-Traps® were subsampled every month so that only a portion of material was removed and the rest remained in a sampler. This experimentally contrasted cave stream sediment samples, which had the potential to be redistributed and mobilized during the study. The newly formed Bio-Trap® communities every month were compared

to preexisting water and sediment communities to test the hypothesis that Bio-Trap® communities would resemble sediment communities over time, despite being colonized initially by planktonic microbes. Combined, these results provide evidence for cave stream community assembly and community succession. Underlying drivers that could explain spatial and temporal changes in bacterial diversity were statistically evaluated against stream discharge, rainfall, and geochemistry, including fluorescence spectral data for chromophoric dissolved organic matter (CDOM) that highlighted organic matter seasonal changes.

Materials and Methods

Site Characterization

We conducted the study from July through December, 2013, in the Cascade Cave system within Carter Caves State Resort Park (CCSRP) in Carter County, Kentucky (**Figure 1**). The system is comprised of at least three surveyed caves that formed within the carbonate Slade Formation (Mississippian) (Engel and Engel, 2009). The caves are situated in the James Branch stream watershed, which flows into Tygart's Creek at local base-level (Dougherty, 1985; Engel and Engel, 2009). The entire watershed is approximately 4 km^2. The surface stream flows over Pennsylvanian and Mississippian interbedded sandstone and shale units before it sinks underground at a waterfall called Fort Falls (herein referred to as the surface sampling location). The cave system has flowing water year-round. Jones Cave is the first access point to the cave stream (herein referred to as the upstream sampling location). There is a karst window 500 m downstream from Jones Cave where surface water enters the subsurface from a small surface stream. The entrance to another cave, Sandy Cave, is located at the window. Cascade Cave has several entrances, and one is reached downstream of the karst window and Sandy Cave. Where the cave stream emerges at the surface as a karst spring and another entrance to Cascade Cave, we sampled at the Lake Room (herein referred to as the downstream sampling location). The total estimated distance of the underground cave stream from the top of the water fall to resurgence is approximately 1.5 km. Preliminary (i.e., unpublished) tracer tests from Fort Falls to the Lake Room indicate a base flow travel time of about 12 h. All of the sampling was done in less than 3 h to evaluate contemporaneous microbial communities that could be present or established at each location, specifically planktonic communities from water, attached communities from sediment, and newly formed communities from the Bio-Trap® devices.

At each sample location and time, water flow rates were calculated by an average of three flow readings using a Geopacks Basic Flowmeter. Passage or channel cross-sectional area and water depth were measured to calculate discharge (Q) as the product of velocity, depth of the water, and channel width. Sediment particle transport was calculated by comparing stream velocity to the Stokes Settling Velocity for all the grain sizes present in the sediment samples (methods describes below), according to Ferguson and Church (2004). With no automated meteorological station data from CCSRP, daily precipitation data are measured and recorded at the Fort Falls location by a citizen scientist who works in CCSRP (Supplemental Figure 1).

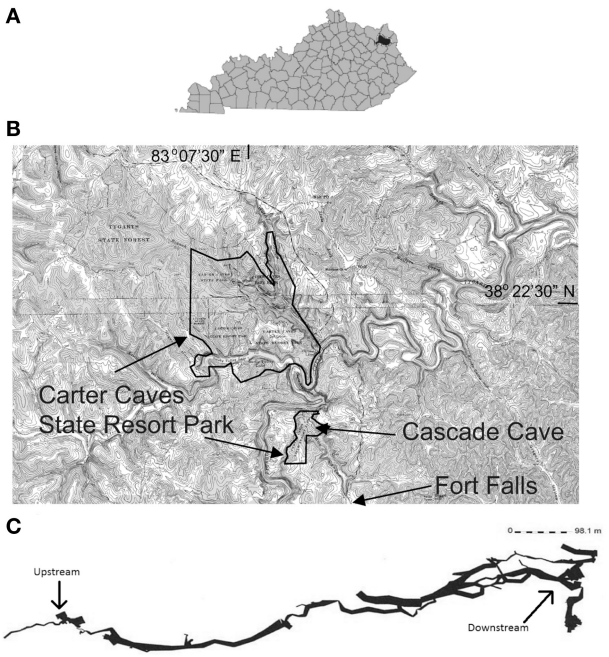

FIGURE 1 | (A) Black area denotes Carter County, Kentucky. **(B)** Spliced topographic maps from the United States Geological Survey showing the location of Carter Caves State Resort Park boundaries, relative location of Cascade Cave and Fort Falls, modified from Engel and Engel (2009). Specific location details are withheld at the request of the park. **(C)** A generalized line-plot map of the Cascade Cave system, including Cascade Cave (downstream), Sandy Cave, and Jones Cave (upstream). Map provided by Dr. Horton H. Hobbs, III, and the Wittenberg University Speleological Society, Springfield, Ohio (USA).

Water and Sediment Sampling and Analyses

At each sampling location, physicochemical properties were measured using standard electrode methods (American Public Health et al., 2005), including pH, temperature, dissolved oxygen, total dissolved solids, and conductivity. At least 500 mL of cave stream water were manually filtered through duplicate 0.22 μm Sterivex™ (PVDF, EMD Millipore) filters. Filters were frozen at −20°C until use. The filtered water was collected for anion (using clean HDPE bottles), cation (using acid-washed HDPE bottles), and total organic carbon (TOC) and total nitrogen (TN) analyses (using baked glass VOA vials). Cations were preserved with trace metal grade nitric acid. Samples were put on ice for transport and stored at 4°C until analysis. Alkalinity, representing bicarbonate concentration, was measured from 0.2 μm-filtered water in the field by manual titration to an end-point of pH 4.3 with 0.1 N H_2SO_4 (American Public Health et al., 2005). Major dissolved ions were measured on a Dionex ICS-2000 ion chromatograph, with standards checks accurate within two standard deviations. Total inorganic carbon (TIC) and dissolved organic carbon (DOC) concentrations were analyzed for filtered water with a

Shimadzu Model TOC-V Total Carbon Analyzer. DOC was reported as the difference between dissolved non-purgable organic carbon and TIC (American Public Health et al., 2005). The standard used for minimum detection limit was $C_8H_5KO_4$, and the precision between replicate sample injections was 2% of the relative percent difference (RPD) for DOC > 4 mg/L and 5% RPD for DOC < 4 mg/L. TN content were measured by a high temperature catalytic oxidation with chemiluminescence minimum detection level of 0.01 mg/L (ASTM, 2008).

During some sampling times, only bare carbonate rock was exposed at a sample location in the cave where sediment had been present previously. If sediments were available to collect at a sampling location, then at least 25 g were aseptically collected from 0 to 2 cm deep and placed into sterile Falcon tubes; as such, any one particle had to be <20 mm to fit in the tube. Sediment was stored at −20°C until use. Sediment grain size was analyzed in triplicate for each sample from sieving air-dried material through sieves for >2, 1 mm, 500, 250, 150, and <150 μm. Weights of each sieved aliquot were measured to ±0.0001 g at least three times.

Fluorescence Spectroscopy

Qualitative information about organic matter sources, composition, bioavailability, and the differences between allochthonous and autochthonous DOM can be determined from the natural concentration of CDOM (Coble, 1996; McKnight et al., 2001). The relative contributions of different CDOM sources in the filtered stream water were evaluated from excitation emission matrices (EEMs) produced by a Horiba Scientific Fluoromax4 spectrofluorometer with a Xenon lamp. A total of 43 emission scans were completed for each sample with setting of λEM = 250–550-nm, 2.5-nm steps; λEX = 240–550-nm, and 5-nm steps. Instrument settings were PMT voltage 800 V, EX/EM slits 5-nm each, and an integration time 0.1 s. Spectral corrections for primary and secondary inner filter effects of EEMs were made using absorbance spectra collected using a Thermo Scientific Evolution 200 series spectrophotometer in a 1-cm cuvette over the 200–700 nm wavelength range with pyrogen-free deionized (DI) (>18.1 MΩ) water as the reference. Raman scattering was removed from EEMs by subtracting a DI water blank spectrum collected from each sample spectrum. Rayleigh scattering effects were edited from each spectrum, following correction and blank subtraction (Lakowicz, 2007).

Fluorescence data were interpreted from index analyses from individual emission scans or extracted from EEMs using methods previously described (Birdwell and Engel, 2010). We used the Fluorescence Index (FI) to assess terrestrial and microbial contributions to CDOM fluorescence (McKnight et al., 2001), the Humification Index (HIX) to estimate the degree of DOM humification (Ohno, 2002), and the Biological or Freshness Index (BIX) to evaluate the contribution of biological or microbial processes to CDOM fluorescence (Huguet et al., 2009).

Microbial Succession Experiment

Standard Bio-Trap® samplers baited with 30 g of 2-mm diameter Bio-Sep® beads made of Nomex® composite and powdered activated carbon were obtained from Microbial Insights, Inc. (Knoxville, TN, USA) (www.microbe.com). Slits on the samplers were 0.4 mm wide, and the inside of the samplers was wrapped with 0.011 mm mesh screen to reduce sediment and macrofauna intrusion. Bio-Traps® were suspended in triplicate (overall weight 1.3 kg) via ropes attached to the cave wall by using non-destructive, spring-loaded camming devices at Jones Cave (upstream location) and in the Lake Room (downstream location) (Supplemental Figure 1). At base-flow (i.e., low flow) conditions, Bio-Traps® were in contact with sediment or bare rock at the bottom of the stream channel, but were not buried in the sediment. The samplers were also weighted by using 0.2 kg weights so that they would become suspended in the water column only during exceptionally high flow events (i.e., in excess of 0.5 m/s). The Bio-Traps® were sampled every month for 4 months. From each Bio-Trap®, 2.5 g beads were separated out and frozen until extraction. During the study period, no fine-grained or sand particles were observed in the Bio-Traps®. At the time of deployment (August 2013), the water column and sediment microbial communities were sampled at Fort Falls (surface location) and at both Bio-Trap® sample locations. Over the next 4 months at both Bio-Trap® locations, water column, surface sediment, and Bio-Trap® microbial communities were sampled. Only the water column and sediment microbial communities were sampled at the Fort Falls location at those times.

DNA Extraction and Pyrosequencing

Total environmental nucleic acids were extracted from two Sterivex™ filters collected at each sampling location using a method modified from Riemann et al. (2008). Briefly, sucrose lysis buffer (0.75 M sucrose, 0.5 M Tris-HCl, 0.4 M EDTA) and 5 mg/mL lysozyme (Fisher BioReagents) were added to each filter prior to incubation at 37°C for 30 min. Proteinase K (100-μg/mL final concentration; Fisher BioReagents) and 10% SDS were added, and digestion continued at 55°C overnight. The lysate was drawn from the filter and combined with a 1X TE buffer wash of the filter prior to adding 0.3 M sodium acetate and molecular grade 100% isopropanol. Lysates were centrifuged and pellets were separated from the supernatants and resuspended in TE buffer. Nucleic acids were precipitated from the suspensions using 25:24:1 phenol:chloroform:isoamyl alcohol (pH 8) twice, and 24:1 chloroform:isoamyl alcohol once, prior to pelleting by centrifugation. Pellets were washed with 100% molecular grade ethanol twice and then resuspended in 1X TE buffer.

MoBio PowerSoil® Extraction kits, following manufacturer instructions (MoBio Laboratories, Inc., Carlsbad, CA, USA), were used to extract total nucleic acids from 0.25 g of beads collected from each Bio-Trap® and separately from 0.25 g of sediments at each sampling location. Extractions for each sample type per sample period and location were done in triplicate.

The quality and quantity of extracted DNA were verified by examining products on TBE agarose gels with ethidium bromide staining after electrophoresis and by measuring the ratio of absorbance maxima at 260 and 280 nm, and 260 and 230 nm, with a Thermo Scientific Nanodrop 2000c Spectrophotometer. Duplicate (for water) or triplicate (for Bio-sep® beads or sediment) extractions at a sampling

location and month were homogenized prior to purification, barcoding, and amplicon pyrosequencing using a Roche 454 FLX Titanium instrument and reagents, as described in Dowd et al. (2008), at the Molecular Research LP (MrDNA) laboratory (www.mrdnalab.com; Shallowater, Texas, USA). The V1-V3 region of 16S rRNA genes was amplified using 27F-534R primers (Dowd et al., 2008).

qPCR Analyses

Bacterial biomass was estimated for all samples by quantitative PCR (qPCR) using a CFX96 Real-Time PCR System (Bio-Rad Laboratories, Hercules, CA, USA), according to the approach described by Ortiz et al. (2014). Briefly, for a 10-ml qPCR reaction with a 2x SensiFAST™ SYBR® No-ROX Kit (Bioline Meridian Life Science Company, Tauton, MA), 400 mg/mL bovine serum albumin solution, 400 nM of each primer, and 400 pg DNA extract were used. Primers used for bacterial 16S rRNA amplification were 338F and 518R (Ortiz et al., 2014). A standard curve was used to calculate the number of 16S rRNA amplicons (Zhu et al., 2005):

$$N = [(A/B) \times d] \times (V/C)$$

N is the total number of cells in the initial sample; A is the number of 16S rRNA amplicons per PCR tube, as calculated from the standard curve; B is the number of μL of cell lysate in the PCR tube, and d the lysate dilution factor; V is the initial lysate volume expressed in μL, and C is the average number of 16S rRNA copies per bacterial cell. Based on the retrieved bacterial diversity from our samples, and specifically of the predominance of Proteobacteria, we used the value 4.2 based on the genome assessment work of Vetrovsky and Baldrian (2013). N was divided by the amount of water filtered for each sample, or the amount of sediment or Bio-Trap® beads used during the extractions, to find the number of cells per mL of water, or the number of cells per gram of sediment or Bio-Traps®, respectively.

Sequence Analyses

Amplicon sequence data were quality screened and chimera checked prior to clustering into operational taxonomic units (OTUs) based on 95% sequence similarity using QIIME (Crawford et al., 2009; Caporaso et al., 2010; Edgar et al., 2011). A 95% cut-off was used to cluster OTUs at the genus level because of the short length of the pyrosequences (Kunin et al., 2010). The greengenes 13_8 database (Desantis et al., 2006) was used as the reference for the usearch61 method for chimera checking (Edgar et al., 2011) and for picking OTUs using the open reference method (Desantis et al., 2006). From the 18,177 OTUs generated for the full dataset (397,144 amplicons; Supplemental Table 1), representative sequences were chosen for classification by the RDP Classifier at 80% confidence intervals using QIIME (Wang et al., 2007). Alpha-diversity was calculated in QIIME to generate rarefaction curves (Supplemental Figure 3) (Crawford et al., 2009; Caporaso et al., 2010) and Shannon diversity (H') and Chao1 indices were calculated in the computer program R using the package phyloseq (version 1.10.0) (McMurdie and Holmes, 2013). Higher numbers for both indices indicate greater OTU-level richness. All OTUs shared between samples were compared for presence/absence. Details regarding data processing are provided in the Supplemental Materials and Methods in R markdown format.

All raw amplicons obtained from this study were submitted to the NCBI Sequence Read Archive (SRA) under the Bioproject PRJNA283038, with the accession numbers SAMN03451533–SAMN03451581 (http://www.ncbi.nlm.nih.gov). Summaries for the amplicon data, including SRA Accession Numbers for each sample, are included in Supplemental Table 1.

Statistical Analyses

The significance of changes in geochemical variables over time and between sampling months, as well as in microbial diversity data, were analyzed statistically using several approaches. Analysis of variance (ANOVA), reported as the F-test value with significance evaluated from a p-value of < 0.05, was done with geochemical data between month, season, and location using the car package in R (Fox and Weisberg, 2011). Summary code completed in R is included in the Supplemental Materials and Methods. Sediment grain size comparisons were done using the G2Sd package for sediment size analysis (Gallon and Fournier, 2013). Permutational multivariate analysis of variance (PERMANOVA), calculated with the Adonis function in the vegan package for R, was used to detect similarities in the means of multivariate groups described by material type (i.e., water, sediment, Bio-Trap®), location (i.e., surface, upstream, and downstream), and month, such that community OTU representation would be equivalent for all groups. PERMANOVA was also used to detect similarities in the composition and/or relative abundances of different OTUs based on geochemical variable (i.e., Cl, Ca, HIX, etc.). PERMANOVA was performed with the Adonis function from the vegan package for community ecology on a Bray-Curtis dissimilarity matrix and significance was assessed with 9999 permutations (Oksanen et al., 2013). Non-metric multidimensional scaling (NMDS) was used on a Bray-Curtis dissimilarity matrix to represent the pairwise dissimilarity graphically between OTUs in each sample. Statistically significant environmental variables (p-value < 0.05) were plotted as vectors representing the average of factor levels using envfit, from the vegan package (Oksanen et al., 2013).

To investigate any linear relationships between the distribution of OTUs among samples and any redundant geochemical gradients, a redundancy analysis (RDA) was performed. The significance of RDA axes was calculated by the PCAsignificance function in the BiodiversityR package (Kindt, 2014). To evaluate the relationship between OTU distribution among sediment samples and sediment size, another RDA was performed on only sediment samples. RDAs were performed with the RDA function from the vegan package on a Bray-Curtis dissimilarity matrix (Oksanen et al., 2013), which was produced using a culled dataset of only OTUs present more than three times in at least 20% of the samples (McMurdie and Holmes, 2013). Only 313 of the original 18,177 OTUs remained and application of a 2.0 CV cutoff resulted in 178 OTUs.

TABLE 1 | Geochemical and hydrological data from each sample.

Sample month	Sample location	Sample name	Temp °C	pH	Alkalinity mg/L	DOC[a] mg/L	Total N[b] mg/L	Cl mg/L	SO_4^{2-} mg/L	NO_3^- mg/L	Na mg/L	Mg mg/L	Ca mg/L	Flow rate m/s[c]	Discharge m3/s[d]	FI[e]	HIX[f]	BIX[g]
July	Surface	CCRW.13JB1	17.1	7.1	56.85	3.08	0.46	10.1	30.1	BDL	5.99	2.71	9.23	BDL	NC	1.97	6.97	0.63
July	Downstream	CCRW.13JA1	21.5	7.4	58.07	6.62	0.46	5.61	19.09	BDL	5.23	4.81	17.45	BDL	NC	2.0	10.33	0.58
July	Surface	CCRW.13JB3	21.5	7.5	84.66	NM	NM	25.58	33.34	BDL	12.24	10.25	8.34	0.78	0.21	2.01	11.08	0.61
July	Downstream	CCRW.13JA3	17.3	7.3	84.42	NM	NM	18.68	27.05	1.09	8.93	7.66	20.67	2.23	0.6	2.0	10.33	0.58
August	Surface	CCRW.13A3	24	7.2	84.42	3.0	0.77	17.84	31.03	1.41	8.11	8.50	10.22	5.25	0.82	2.01	8.51	0.65
August	Upstream	CCRW.13A2	20.3	7.3	93.6	5.2	0.99	11.6	24.31	1.28	7.74	6.89	14.78	4.4	0.69	1.99	8.29	0.64
August	Downstream	CCRW.13A1	18.3	7.3	87.84	NM	NM	10.59	17.01	1.03	6.69	5.56	15.3	6.23	1.68	1.96	8.88	0.64
September	Surface	CCRW.13SF3	22	7.4	107.36	3.0	0.31	24.23	28.62	0.27	12.53	10.46	41.48	BDL	NC	2.1	0.93	0.68
September	Upstream	CCRW.13S3	17.9	7.5	110.28	2.85	0.55	34.66	32.61	BDL	10.4	8.93	40.79	BDL	NC	2.14	0.93	0.66
September	Downstream	CCRW.13SL3	18	7.4	127.36	1.79	0.65	19.07	21.69	1.55	9.52	7.39	47.09	BDL	NC	2.11	0.91	0.66
October	Surface	CCRW.13O3	16.9	7.7	125.41	0.27	0.28	30.12	29.37	BDL	11.34	10.24	38.62	BDL	NC	2.11	0.92	0.69
October	Upstream	CCRW.13O2	15.2	7.7	152.01	2.54	0.33	23.78	30.94	BDL	10.22	10.19	41.5	BDL	NC	2.12	0.93	0.69
October	Downstream	CCRW.13O1	13.7	7.8	133.95	3.81	0.57	22.59	20.37	1.05	7.64	7.05	46.21	BDL	NC	2.12	0.93	0.69
November	Surface	CCRW.13N3	10.1	7.5	105.65	1.48	0.32	23.49	38.44	BDL	11.73	9.93	32.02	0.76	0.2	2.13	0.91	0.67
November	Upstream	CCRW.13N2	8.7	7.5	88.57	2.48	0.40	20.09	34.61	BDL	9.68	9.16	35.66	3.2	0.05	2.19	0.91	0.69
November	Downstream	CCRW.13N1	10	7.5	130.05	3.99	0.42	22.28	29.44	0.82	9.64	7.73	40.22	1.67	0.14	2.16	0.9	0.7
December	Surface	CCRW.13D3	4.3	7.1	93.2	1.7	0.93	17.9	35.23	BDL	9.44	6.09	9.00	3.7	10.18	2.04	0.9	0.59
December	Upstream	CCRW.13D2	3.8	7.3	62.46	1.67	0.98	19.45	33.77	BDL	14.59	7.35	13.16	4.95	0.7	2.12	0.9	0.66
December	Downstream	CCRW.13D1	4.9	7.5	93.2	1.69	0.56	18.33	28.32	BDL	9.29	6.52	15.63	2.95	1.32	2.2	0.9	0.66

NM, not measured.

[a] *DOC, dissolved organic carbon measured as the difference between dissolved non-purgable organic carbon and total inorganic carbon.*

[b] *Total N, total dissolved nitrogen measured as all N compounds present in sample, including nitrogen compounds in DOM.*

[c] *Water flow rate; BDL, below detection limit for the flow meter measurement.*

[d] *NC, not calculated because velocity measurements were below detection.*

[e] *FI, Fluorescence index, see text for description.*

[f] *HIX, Humification index, see text for description.*

[g] *BIX, Biological index, see text for description.*

Results

Stream Dynamics, Sediment Characteristics, and Aqueous Geochemistry

Several major rainfall events occurred during the study within the watershed (Supplemental Figure 2). Stream discharge fluctuated from unperceivable by flow meter to as high as 1.36 m^3/s at the downstream location (**Table 1**). At these flow rates during the study period, sediment particles up to 2 mm in diameter may have been mobilized during four different precipitation events based on Stokes calculations. Excluding the largest particles (i.e., cobbles), coarse to very coarse sand (0.5–2 mm diameter) was sampled from the upstream location at Jones Cave. The average particle sizes downstream in the Lake Room were fine-medium sand (0.125–0.5 mm) (Supplemental Figure 4). There was <1% contribution of silt- or clay-sized particles at both sampling locations. After a large storm event in December (Supplemental Figure 2), sediment remobilization and redistribution was evident and finer particles were deposited at the downstream location (Supplemental Figure 4).

Geochemical parameters for all of the stream water pH, ranging from 7.1 to 7.8, at each location significantly varied by month (ANOVA F-test = 33; p-value < 0.001), as did stream temperature, ranging from 21°C (July) to 4°C (December) (p-value < 0.001) (**Table 1**). Other geochemical parameters, including alkalinity, also significantly differed by month (ANOVA F-test = 8.7; p-values for all analyses < 0.05). The amount of DOC (ranging from 0.27 to 6.6 mg/L) and total dissolved N (ranging from 0.33 to 1 mg/L) did not significantly differ for any analysis by month or between locations. However, the quality of the carbon, as assessed by using fluorescence indices FI and HIX (**Table 1**), did significantly differ by month (Supplemental Table 2). In July and August, CDOM fluorescence was dominated by humic acids derived from terrigenous material and less proteinaceous CDOM than later months in the Fall and Winter seasons.

Controls on Bacterial Biomass and Diversity

The number of 16S rRNA gene copies qPCR reaction ranged from 1×10^5 to 1×10^2 copies/sample, which was used to calculate biomass per gram of sediment or Bio-Trap® beads, or per mL water. Bio-Trap® samples had higher biomass (up to 2.6×10^6 cells/gram) than the other sample types; water had the least biomass at only 1×10^4 cells/mL (**Figure 2**). Sediment biomass was greatest in August and decreased through the winter months, but biomass in the cave stream was relatively stable throughout the study period. Biomass in the Bio-Trap® samplers for both sampling locations were nearly the same, with the least biomass at the beginning of the experiment and the highest biomass in November.

The 18,177 OTUs were affiliated with 402 classified genera. The most abundant classes for all the OTUs included Betaproteobacteria (35% of all sequences), Gammaproteobacteria (16% of all sequences), Alphaproteobacteria (15% of all sequences), and Opitutae (4% of all sequences). The planktonic community throughout the cave stream was dominated by Betaproteobacteria (48%), Alphaproteobacteria (8%), and Opitutae (6%). The sediment samples throughout the cave were dominated by Gammaproteobacteria (34%), followed by Alphaproteobacteria (16%) and Betaproteobacteria (12%). The Bio-Trap® communities from both locations had nearly equal distributions of Betaproteobacteria (26%), Alphaproteobacteria (24%), and Gammaproteobacteria (23%). Over time, observed Bio-trap® community OTU abundances decreased (**Figure 3A**), but calculated richness and evenness were unchanged (according to H' and Chao1, **Figures 3B,C**, respectively).

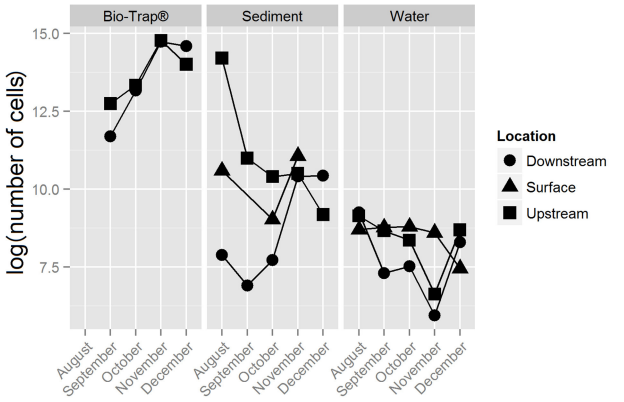

FIGURE 2 | Bio-Trap®, sediment, and water biomass estimates from qPCR results, displayed as log (number of cells) over time for each type of sample at the surface, upstream, and downstream locations.

Prior to testing hypotheses related to AMEC existence and community succession, changes in bacterial diversity based on environmental gradients over time were evaluated. Each sample's taxonomic profile was compared temporally and spatially. Overall OTU taxonomic distribution between locations was significantly distinct from each other (i.e., upstream vs. downstream) (PERMANOVA p-value < 0.05, r^2 = 6%), and taxonomy differed significantly by month (PERMANOVA p-value < 0.001, r^2 = 18%). OTU taxonomy clustered significantly by sample type (i.e., water, sediment, Bio-Traps®), according to both ordination in NMDS space (**Figure 4**) and a RDA (**Figure 5**) that tested potential multidimensional and linear relationships among environment gradients and taxonomy, respectively. Changes in seasonal CDOM quality from FI and HIX fluorescence indices accounted for observed bacterial diversity variation for water and Bio-Trap® samples, but not the sediment samples (RDA axis 2, 14.9%; **Figure 5**). Instead, diversity from the sediment samples clustered by location and according to sediment size (**Figure 6**), which also differed over time.

Shared Community Membership and Potential Succession

The number of shared OTUs was evaluated based on sample location, type (sediment, water, Bio-Traps®), and month to assess community stability, which could potentially provide evidence for AMEC. A shared OTU was identified if amplicons from more than one sample type, location, or month were present. Overall, the number of shared OTUs for any location or

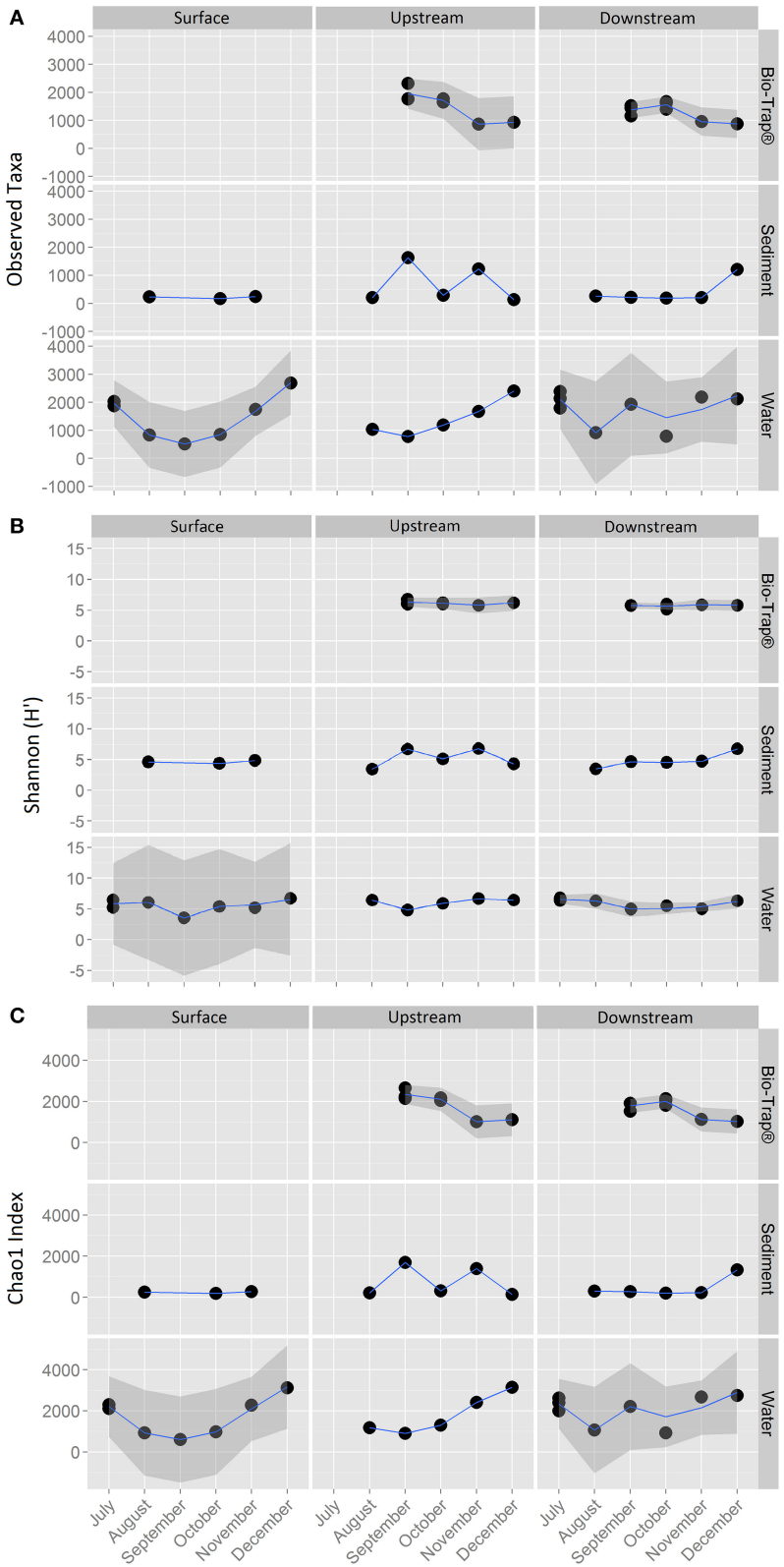

FIGURE 3 | Alpha-diversity richness and evenness indices for (A) Observed, (B) Shannon, and (C) Chao1, values by sample type and location over a 6 month period.

sample month was low, between 0.1 and 4% (**Table 2**), in contrast to the total number of OTUs retrieved during the 6 months. No OTUs comprised amplicons from all sediment, water, and Bio-Trap® samples from any location and any month (**Table 2**). But, there were shared OTUs from the sediments, water, and Bio-Traps® at each location over the 6 month study period (**Table 3**; **Figure 7**), although the total number of shared OTUs was different for each material. Specifically, shared OTUs for sediment samples were comparatively lower (0.01–4% of the total) than the water and Bio-Trap® samples, which shared 20–65% of the OTUs when binned by sample type. The shared and prevalent OTUs over time showed sequence abundance changes (**Figure 7**). Some of the most prevalent OTUs had a similar trend over time in both upstream and downstream locations (**Figure 7**).

To assess community succession, comparisons among shared OTUs from sediment, water, and Bio-Traps® were made. Evidence for community succession was indicated if OTUs were comprised of amplicons from Bio-Traps® and either water or sediment over time. Upstream and downstream Bio-Trap® samples had more shared OTUs with water (20 OTUs upstream and 13 downstream) than with sediment (0 OTUs upstream and 1 downstream). Downstream, the number of shared OTUs between Bio-Traps® and sediments increased by the end of the study (**Table 3**). This trend was not observed upstream, as the number of shared OTUs between Bio-Traps® and sediments remained low (**Table 3**).

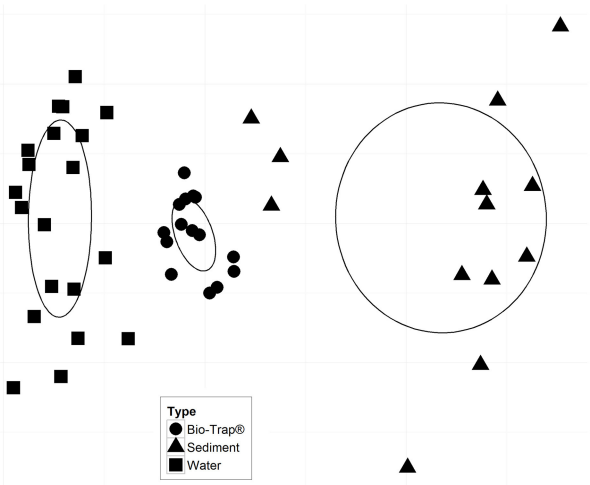

FIGURE 4 | Non-metric multidimensional scaling (NMDS) plot based on a Bray-Curtis dissimilarity matrix; stress = 0.082. Ellipses represent the standard error of the weighted average of scores of samples, and the direction of the principal axis of the ellipse is defined by the weighted correlation of samples. There were no statistically significant environmental vectors (p-value < 0.05).

Discussion

Originally described from karst spring water, AMEC represent stable communities that develop over months to years and that form from a mix of planktonic and biofilm (i.e., attached) communities within a karst aquifer (Farnleitner et al., 2005; Pronk et al., 2008). Karst aquifers have interconnected networks

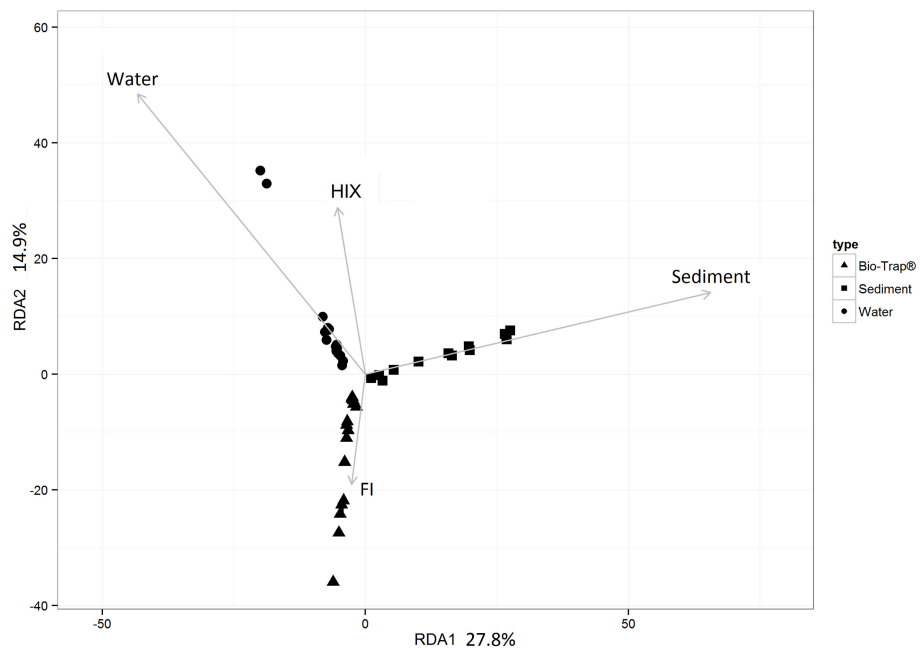

FIGURE 5 | Redundancy analysis (RDA) of the culled OTU dataset as a function of the fluorescence indices HIX and FI. Significance of each RDA axis was calculated with the RDAsignificance function from the BiodiversityR package for R (Kindt, 2014).

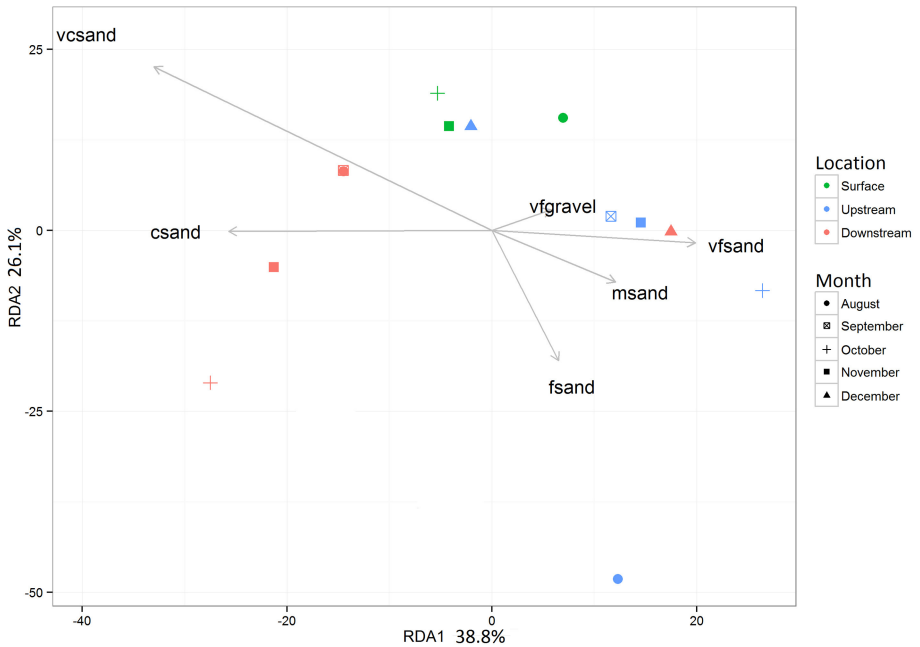

FIGURE 6 | Redundancy analysis (RDA) of the culled OTU dataset as a function of the grain size analysis from the G2SD package gran_stat function output (Gallon and Fournier, 2013). Significance of each RDA axis was calculated with the RDAsignificance function from the BiodiversityR package for R (Kindt, 2014).

of solutionally-enlarged conduits and voids, solutionally-enlarged fractures and bedding partings, and bedrock matrix. Each component has its own flow regime, ranging from fast and potentially turbulent flow in conduits to Darcian or diffusive flow in fractures and the matrix (Ford and Williams, 2013). AMEC have previously been found within saturated conduits and voids and along fractures in the subsurface, where flow may be fast but residence times are long so environmental conditions remain stable, particularly pH and temperature (Farnleitner et al., 2005; Pronk et al., 2008). When AMEC were originally described, attached communities were not analyzed, presumably due to difficulties sampling karst bedrock surfaces from wells (Engel and Northup, 2008). Well boreholes completed in karst aquifers usually intercept fractures, conduits, and voids, and nothing but water can usually be physically sampled when voids are encountered. Moreover, these zones are cased off during well completion and inhibit future access to aquifer bedrock surfaces. Karst well construction and sampling contrasts other groundwater systems, such as porous sand and gravel aquifers, because aquifer sediment and/or rock material can be physically sampled from cores during well construction. From these other types of groundwater systems, planktonic and attached microbial communities can be distinct based on taxonomic (Hazen et al., 1991; Alfreider et al., 1997; Lehman, 2007; Flynn et al., 2008; Zhou et al., 2012) and functional diversity (Wilhartitz et al., 2009). Moreover, planktonic microbial communities in porous sand and gravel aquifers can be seasonally dynamic while sediment-attached communities are unchanging (Zhou et al., 2012). Understanding how AMEC form and evolve is important because karst systems are highly susceptible to contamination (Vesper et al., 2001) and AMEC may play an important role the stability of microbial communities during ecosystem biogeochemical cycling or contaminant response.

Caves allow for direct entry into karst aquifer systems (Yagi et al., 2010; Morasch, 2013). Prior to this study, knowledge about cave stream bacterial diversity was limited and understanding how environmental parameters impact cave stream bacteria was poor (Engel, 2010). The hydrology of cave streams is different from that of the original AMEC habitats because residence times can be much shorter, on the order of hours to days, and environmental conditions can vary daily (Farnleitner et al., 2005; Pronk et al., 2008). Cave streams are hydrologically comparable to surface streams, and stable communities comparable to AMEC have not yet been identified from surface streams (Lyautey et al., 2005; Besemer et al., 2007, 2012; Lear et al., 2008; Wey et al., 2012). However, in surface streams, sediment-attached microbial communities have been shown to express seasonal diversity trends (Feris et al., 2003; Hullar et al., 2006; Wey et al., 2012) and the distribution of planktonic bacteria and bacteria attached to fine benthic organic matter also correlates to surface stream pH (Fierer et al., 2007). As such, because cave streams are hydrologically connected to the surface, seasonal trends linked to physicochemistry may be observed from cave stream microbial communities. We found that, although there were significant differences for some environmental parameters over time, there were no significant differences in bacterial diversity over time at any one location along the cave stream. The duration of study

TABLE 2 | Number of shared OTUs by taxonomic Phylum and Class for each sample type upstream and downstream, as well as shared among both locations (represented by the "shared" column), over time.

Phylum	Class	Bio-Trap®			Sediment				Water			
		Upstream	Downstream	Shared	Surface	Upstream	Downstream	Shared	Surface	Up-stream	Down-stream	Shared
Acidobacteria	Acidobacteria-6	8 (1.3)	4 (1.1)	4 (1.3)	1 (4.2)	1 (0.2)	1 (0.4)	–	–	–	–	–
Acidobacteria	[Chloracidobacteria]	3 (0.2)	1 (0)	1 (0.1)	–	–	–	–	–	–	–	–
Actinobacteria	Acidimicrobiia	–	–	–	2 (2.8)	–	–	–	–	–	–	–
Actinobacteria	Thermoleophilia	–	–	–	5 (3.8)	–	3 (4.1)	–	–	–	–	–
Actinobacteria	Actinobacteria	–	–	–	–	–	–	–	1 (0.1)	3 (1.1)	4 (1.6)	2 (0.4)
Chloroflexi	Ellin6529	–	–	–	1 (1.3)	–	1 (0.2)	–	–	–	–	–
Chloroflexi	P2-11E	–	–	–	2 (0.5)	–	–	–	–	–	–	–
Chloroflexi	Anaerolineae	3 (0.3)	–	–	–	–	–	–	–	–	–	–
Chloroflexi	Chloroflexi	1 (0)	–	–	–	–	–	–	–	–	–	–
Proteobacteria	Alphaproteobacteria	88 (14.9)	61 (12.8)	48 (12.0)	3 (3.1)	–	8 (5)	–	–	9 (1.3)	2 (2)	2 (1.7)
Proteobacteria	Betaproteobacteria	52 (12.8)	55 (14.2)	38 (13.3)	4 (1.6)	1 (0)	3 (2.6)	–	53 (20.2)	39 (14.6)	41 (18.2)	19 (13.1)
Proteobacteria	Deltaproteobacteria	1 (0)	1 (0)	11 (17.3)	–	–	–	–	–	–	–	–
Proteobacteria	Gammaproteobacteria	18 (16.6)	24 (18.6)	–	–	–	–	–	–	3 (0.3)	2 (0)	–
Proteobacteria	Epsilonproteobacteria	–	–	–	–	–	–	–	1 (0.2)	–	–	–
Proteobacteria	NA	–	2 (0.8)	–	–	–	–	–	–	–	–	–
[Thermi]	Deinococci	1 (0)	–	–	–	–	–	–	–	–	–	–
Bacteroidetes	[Saprospirae]	3 (0.6)	5 (0.7)	1 (0.5)	–	–	–	–	–	–	1 (0.1)	–
Bacteroidetes	Cytophagia	5 (0.9)	7 (1.5)	5 (1.3)	–	–	–	–	1 (1.3)	4 (3.2)	2 (4)	1 (3.6)
Bacteroidetes	Sphingobacteriia	1 (0)	4 (0.4)	–	–	–	–	–	–	–	–	1 (1.0)
Bacteroidetes	Flavobacteriia	–	–	–	–	–	–	–	1 (0.7)	4 (1.5)	1 (0.8)	–
Gemmatimonadetes	Gemmatimonadetes	1 (0)	2 (0.1)	–	–	–	–	–	–	–	–	–
Nitrospirae	Nitrospira	5 (2.6)	6 (8.6)	5 (6.4)	–	–	–	–	–	1 (0.1)	–	–
Planctomycetes	OM190	1 (0)	1 (0)	–	–	–	–	–	–	–	–	–
Planctomycetes	Planctomycetia	9 (0.9)	6 (1.1)	1 (0.7)	–	–	–	–	–	–	–	–
Planctomycetes	vadinHA49	–	–	–	–	–	–	–	1 (0)	–	–	–
Verrucomicrobia	Opitutae	2 (0.2)	3 (0.3)	2 (0.3)	–	–	–	–	1 (0)	7 (0.6)	3 (5.1)	2 (0.2)
Armatimonadetes	Armatimonadia	–	1 (0)	–	–	–	–	–	–	–	–	–
Elusimicrobia	Elusimicrobia	–	1 (0)	–	–	–	–	–	–	–	–	–
Cyanobacteria	Chloroplast	–	–	–	–	–	–	–	2 (0.6)	–	–	–
OP3	PBS-25	–	–	–	–	–	–	–	1 (0.1)	1 (0.1)	–	–
Fibrobacteres	Fibrobacteria	–	–	–	–	–	–	–	–	1 (0)	–	–
NA	NA	1 (0)	–	–	–	–	–	–	–	–	–	–
Totals												
#OTUs shared in group		203 (4)	184 (4.2)	116 (2.2)	18 (3.4)	2 (0.1)	16 (0.9)	–	62 (1)	72 (1.5)	56 (0.7)	27 (0.3)
# OTUs in group		5107	4342	5107	528	2527	1697	–	6495	4875	8025	8025
# Of sequences in group		63683	76729	140412	6029	34942	13172	–	74936	17472	35245	127653

Numbers in parentheses represent the percent abundance, determined to be the number of sequences in shared OTUs normalized by the shared group total.

TABLE 3 | Number of OTUs shared between Bio-Trap® samples and Water/Sediment environment types in both August and December for both locations inside the cave.

	Bio-Trap®			
	Upstream August	Upstream December	Downstream August	Downstream December
Water	153	216	110	199
Sediment	12	26	13	212

may have been too short to observe potential lasting effects of seasonality on community assembly.

Conceptually, there is a low probability of AMEC development in cave streams because of more rapid removal or redistribution of material of all sizes (from clay particles to large logs), including microbial communities. In contrast to the original AMEC studies of planktonic communities (Farnleitner et al., 2005; Pronk et al., 2008), we hypothesized that sediment communities would be compositionally stable over time and provide evidence for AMEC formation because planktonic communities would likely be dominated by transient populations from the surface and stream water residence times would be too short for autochthonous communities to develop, in contrast to cave pools (Shabarova and Pernthaler, 2010; Shabarova et al., 2013, 2014). There were shared OTUs among the water samples throughout the entire study (**Table 2**), and the shared OTUs between the surface water and cave water indicated that some of the planktonic bacteria were ubiquitously distributed throughout the cave system (**Table 2**). This may be due to their survival throughout the duration of the flowpath, not that they are AMEC. In prior studies, to indicate a unique habitat consistent with microorganisms sourced autochthonously from within a system, >30% of total sequences should be considered unclassified (<50% sequence similarity) past the domain level (Farnleitner et al., 2005; Pronk et al., 2008). From alpine systems, AMEC consist of Acidobacteria, Nitrospira, Gammaproteobacteria, and Deltaproteobacteria (Farnleitner et al., 2005; Pronk et al., 2008). In our study, the diversity of shared OTUs from the cave stream was different than previously described AMEC. Compared to the full bacterial diversity, the shared communities represented very little of the total diversity retrieved for all sample types (<4%; **Table 2**). Consequently, we do not believe there is sufficient evidence that AMEC developed in the cave stream water. Also, as was originally described, AMEC should represent common bacterial groups that occur both in the water and from attached biofilms on sediments and aquifer surfaces (Farnleitner et al., 2005; Pronk et al., 2008). Sediment remobilization would cause similarity in planktonic and sediment-attached communities. However, our results do not support this because there were few OTUs shared between water and sediment communities over time (**Table 2**). But, as separate habitats, water and sediments each shared OTUs throughout the entire study period (**Table 2**). Sediments at each location had distinct bacterial community compositions (**Figure 5**) that correlated to sediment size. At the upstream location, only two OTUs were shared (representing 0.1% of the overall community) over time, perhaps because sediment upstream may be more transient than downstream. Downstream, 16 OTUs, or 0.9% of the total diversity, were shared over time, and were comprised of Alpha- and Betaproteobacteria, Chloroflexi, Actinobacteria, and Acidobacteria. There were no OTUs shared between the surface sediments and upstream cave sediments, but four OTUs were shared between the surface sediments and downstream cave sediments. This may provide evidence that the cave sediment communities are not endemic to the karst system, but more work needs to be done in the future and over longer periods of time to verify this result.

One reason why there is limited evidence for AMEC in the cave stream may be linked to the frequency of flooding. Significant rainfall events have the capacity to mobilize sediments of certain sizes. Based on calculated volume estimates for the different areas of the cave, flooding frequency, and particle size distribution, the smaller sediment upstream in the cave was probably only in place at most 8 weeks during the study period. For AMEC to form in cave sediments, we would expect that the sediments should remain in place, or that attached communities are able to colonize newly (re)deposited sediments after an extended period of time. This would also increase the ability to readily distinguish AMEC from transient microbial communities. The monthly sampling intervals during the study period may have been too long to capture a stable community in the sediments because AMEC diversity was not easily distinguished from the sediments. Collectively from these results, it is unclear that AMEC, as defined originally (Farnleitner et al., 2005), formed in the cave stream sediments that were sampled in this study. We should point out that our sampling was biased toward smaller sediment sizes, and AMEC may develop on larger cobbles and boulders that are not mobilized as frequently as the smaller sediment sizes. Future work should sample the large sediment particles and the submerged cave wall and stream bottom surfaces because AMEC may be present on more stable surfaces in the stream.

Lastly, we examined the potential for successional patterns in cave stream communities by using artificial substrates (i.e., Bio-Trap® samplers). Knowledge about community succession in cave stream systems has been completely lacking. We hypothesized that Bio-Trap® communities would resemble sediment communities over time and we compared the community compositions among the planktonic and sediment-attached communities with those of the Bio-Traps®. Initially, even though the upstream and downstream planktonic communities differed, the Bio-Traps® at the upstream and downstream locations were dominated by OTUs shared with water at each location. Differences between the upstream and downstream communities were likely due to stochastic effects and dispersal potential (Fierer et al., 2010), but it is clear from the data that the planktonic microorganisms were the pioneering community for the Bio-Traps®. From a succession perspective, the downstream Bio-Traps® had more OTUs comprised of sediment amplicons at the end of the study (**Table 3**), but the upstream Bio-Traps® had the same small number of sediment-shared amplicons throughout the study. These results

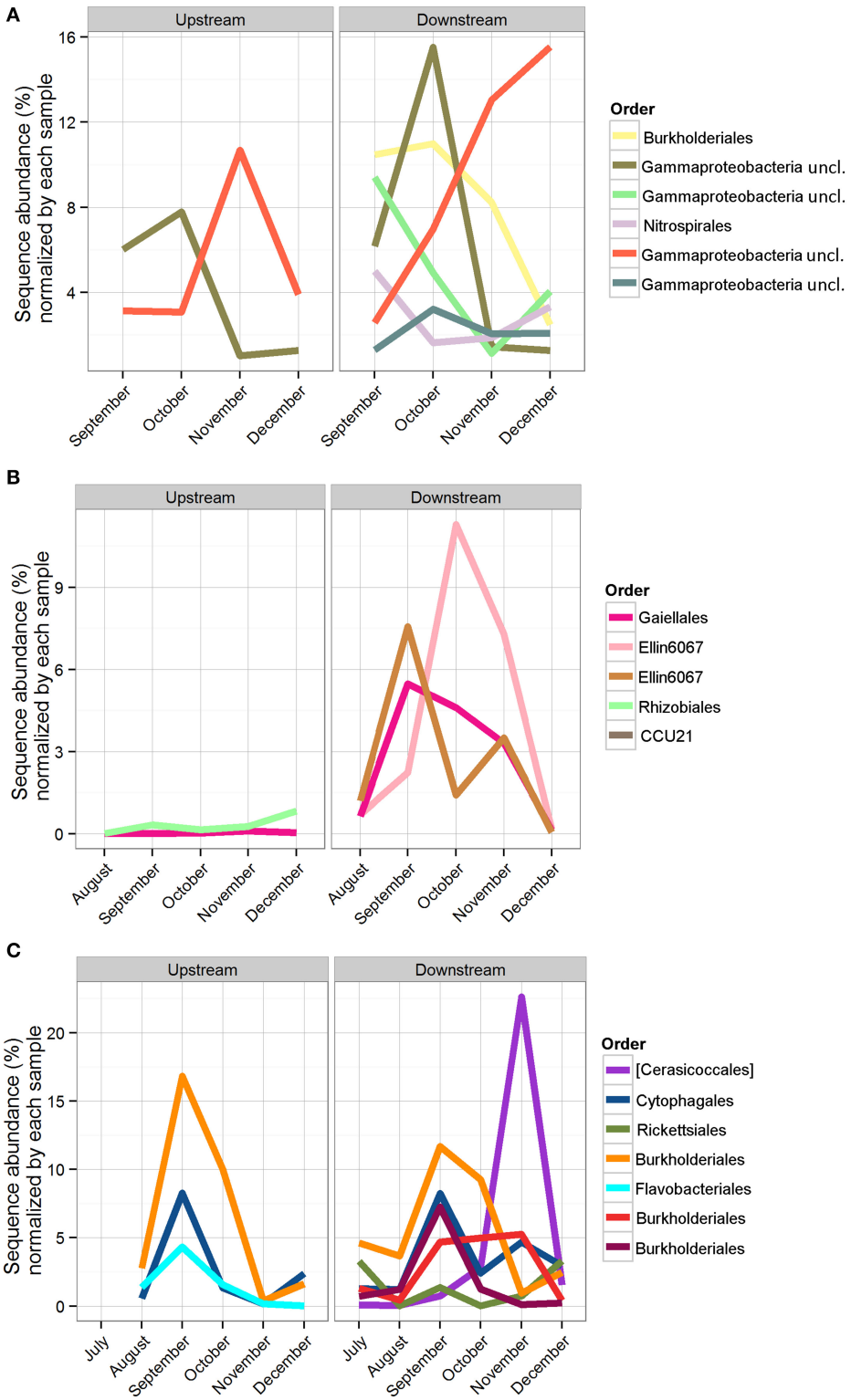

FIGURE 7 | Sequence abundance of OTUs present for the duration of the study, normalized by the total abundance of sequences in the sample. Each OTU is colored by its taxonomic order, and the same color represents the same OTU across locations. **(A)** Bio-Trap® samples, triplicates were averaged for the sequence abundances; **(B)** Sediment samples; **(C)** Water samples.

imply that the rate at which sediment-attached microorganisms colonize new surfaces differs depending on the location along the cave stream flowpath. At the end of the study, the relative abundances of several shared OTUs decreased at the upstream location but increased at the downstream location, suggesting that distinct Bio-Trap® communities formed according to the environmental conditions at each location (Fierer et al., 2010).

Variance among Bio-Trap® and water bacterial community compositions was positively correlated with CDOM quality along the cave stream flowpath, but CDOM quality did not correlate to sediment microbial community diversity. Bio-Trap® communities were likely utilizing CDOM in the water and not the sediments. This distinction is consistent with surface stream studies (Hullar et al., 2006), as well as karst aquifers (Simon et al., 2010), and the differences may be due to organic matter in the streambed being partitioned differently from the water column (Simon et al., 2010). Although the effect of temperature on the nature of CDOM in surface streams has been shown to play an important role in planktonic bacterial community structure and function (Van Der Gucht et al., 2005; Hullar et al., 2006), it is still unclear how environmental conditions affect CDOM in the cave streams and subsequent microbial community composition and assembly. Cave streams lack CDOM photodegradation, as well as the active photosynthesis that occurs in surface streams, which means that CDOM transported into the cave from the surface has the potential to retain its original properties. But, as CDOM is cycled along the flowpath, upstream CDOM is transformed and transported downstream or into the sediments for additional processing. The potential for CDOM quality to diminish with increasing travel time downstream may impact the composition and assembly of heterotrophic communities along the flowpath. The type of heterotrophic community that developed in the cave stream over time is consistent with exogenous (vs. endogenous) communities because these commonly form aquatic biofilms under reduced light conditions and reach a diversity plateau with only small shifts in biomass once the community reaches the plateau phase (Fierer et al., 2010). This is observed from the Bio-Trap® samplers with a biomass peak in November (**Figure 3**) (Fierer et al., 2010). Future research should address if specific differences exist regarding the nature and behavior of water vs. sediment organic matter and how those changes affect exogenous community composition and assembly over time.

In conclusion, microbes are essential for organic carbon and nutrient cycling in karst systems (Gibert et al., 1994; Simon et al., 2007). We found several distinct shared planktonic and attached bacterial communities in the cave stream, which is a novel outcome. However, although we found shared OTUs that were stable for the duration of our study, there were no OTUs shared between the planktonic and attached microbial communities. Therefore, we found limited evidence for AMEC in this cave stream. Nevertheless, the definition of AMEC should be updated, as we struggled during our data analysis to find a set of ubiquitous requirements that could be used for comparison. The Bio-Trap® bacterial communities that stabilized over time in both upstream and downstream locations along a cave stream provide evidence that succession following a large-scale (perhaps sterilizing) environmental disturbance does occur in cave streams (Fierer et al., 2010). Despite the many flooding events during this study period, the community richness trend was predictable over time for all the Bio-Trap® samples, even though the pioneering microbial community was not the same. Sediment size and mobilization play key roles in the sediment-attached karst microbial community structure. Organic carbon quality governs the planktonic karst microbial community structure in a cave stream. These findings also indicate that cave stream communities with short water residence times can follow successional patterns in response to disturbances, like flooding or contamination events, although community stability only exists for short periods of time between disturbances.

Acknowledgments

Funding for this research was provided in part by a National Science Foundation Graduate Research Fellowship and the Cave Conservancy Foundation Karst Studies Scholarship to K.M.B.-D., and the Jones Endowment for Aqueous Geochemistry at the University of Tennessee. T. Hazen provided Bio-Traps® for the research, and B. Donnelly, C. Dietz, and A. Campion assisted in field sample collection. Thanks to S. Plummer for the rainfall data, as well as the staff at Carter Cave State Resort Park for granting permission to conduct the study. Thanks to H. H. Hobbs, III, for providing the cave map. A. Steen and J. Price provided R assistance. We also thank the reviewers for improving the manuscript.

Supplementary Material

The Supplementary Material for this article can be found online at: http://journal.frontiersin.org/article/10.3389/fmicb.2015.00729

References

Alfreider, A., Krossbacher, M., and Psenner, R. (1997). Groundwater samples do not reflect bacterial densities and activity in subsurface systems. *Water Res.* 31, 832–840.

American Public Health, A., Eaton, A. D., American Water Works, A., and Water Environment, F. (2005). *Standard Methods for the Examination of Water and Wastewater*. Washington, DC: APHA-AWWA-WEF.

ASTM. (2008). "D5373-08. Standard test methods for instrumental determination of carbon, hydrogen, and nitrogen in laboratory samples of coal," in *Annual Book of ASTM Standards* (West Conshohocken, PA), 19428–12959.

Besemer, K., Peter, H., Logue, J. B., Langenheder, S., Lindstrom, E. S., Tranvik, L. J., et al. (2012). Unraveling assembly of stream biofilm communities. *ISME J.* 6, 1459–1468. doi: 10.1038/ismej.2011.205

Besemer, K., Singer, G., Limberger, R., Chlup, A. K., Hochedlinger, G., Hodl, I., et al. (2007). Biophysical controls on community succession in stream biofilms. *Appl. Environ. Microbiol.* 73, 4966–4974. doi: 10.1128/AEM.00588-07

Birdwell, J. E., and Engel, A. S. (2010). Characterization of dissolved organic matter in cave and spring waters using UV–Vis absorbance

and fluorescence spectroscopy. *Org. Geochem.* 41, 270–280. doi: 10.1016/j.orggeochem.2009.11.002

Bonacci, O., Pipan, T., and Culver, D. C. (2008). A framework for karst ecohydrology. *Environ. Geol.* 56, 891–900. doi: 10.1007/s00254-008-1189-0

Caporaso, J. G., Kuczynski, J., Stombaugh, J., Bittinger, K., Bushman, F. D., Costello, E. K., et al. (2010). QIIME allows analysis of high-throughput community sequencing data. *Nat. Methods* 7, 335–336. doi: 10.1038/nmeth.f.303

Chapelle, F. H. (2000). The significance of microbial processes in hydrogeology and geochemistry. *Hydrogeol. J.* 8, 41–46. doi: 10.1007/PL00010973

Coble, P. (1996). Characterization of marine and terrestrial DOM in seawater using excitation-emission spectroscopy. *Mar. Chem.* 51, 325–346.

Crawford, P. A., Crowley, J. R., Sambandam, N., Muegge, B. D., Costello, E. K., Hamady, M., et al. (2009). Regulation of myocardial ketone body metabolism by the gut microbiota during nutrient deprivation. *Proc. Natl. Acad. Sci. U.S.A.* 106, 11276–11281. doi: 10.1073/pnas.0902366106

Desantis, T. Z., Hugenholtz, P., Larsen, N., Rojas, M., Brodie, E. L., Keller, K., et al. (2006). Greengenes, a chimera-checked 16S rRNA gene database and workbench compatible with ARB. *Appl. Environ. Microbiol.* 72, 5069–5072. doi: 10.1128/AEM.03006-05

Dogwiler, T., and Wicks, C. M. (2004). Sediment entrainment and transport in fluviokarst systems. *J. Hydrol.* 295, 163–172. doi: 10.1016/j.jhydrol.2004.03.002

Dougherty, P. H. (1985). "An overview of the geology and physical geography of Kentucky," in *Caves and Karst of Kentucky*, ed H. Percy (Dougherty, KY: Geol. Survey Special Publication XI), 79–80.

Dowd, S. E., Callaway, T. R., Wolcott, R. D., Sun, Y., McKeehan, T., Hagevoort, R. G., et al. (2008). Evaluation of the bacterial diversity in the feces of cattle using 16S rDNA bacterial tag-encoded FLX amplicon pyrosequencing (bTEFAP). *BMC Microbiol.* 8:125. doi: 10.1186/1471-2180-8-125

Edgar, R. C., Haas, B. J., Clemente, J. C., Quince, C., and Knight, R. (2011). UCHIME improves sensitivity and speed of chimera detection. *Bioinformatics* 27, 2194–2200. doi: 10.1093/bioinformatics/btr381

Engel, A. S. (2010). "Microbial diversity of cave ecosystems," in *Geomicrobiology: Molecular and Environmental Perspective*, eds L. L. Barton, M. Mandl, and A. Loy (Springer), 219–238. doi: 10.1007/978-90-481-9204-5_10

Engel, A. S., and Engel, S. A. (eds.). (2009). "A field guide for the karst of Carter Caves State Resort Park and the surrounding area, northeastern Kentucky," in *Select Field Guides to Cave and Karst Lands of the United States*, Vol. 15 (Leesburg, VA: Karst Waters Institute Special Publication), 87–106.

Engel, A. S., and Northup, D. E. (2008). "Caves and karst as model systems for advancing the microbial sciences," in *Frontiers of Karst Research*, eds J. B. Martin and W. W. White (Leesburg: Karst Waters Institute Special Publication), 37–48.

Engel, A. S., and Randall, K. W. (2011). Experimental evidence for microbially mediated carbonate dissolution from the saline water zone of the Edwards Aquifer, Central Texas. *Geomicrobiol. J.* 28, 313–327. doi: 10.1080/01490451.2010.500197

Engel, A. S., Stern, L. A., and Bennett, P. C. (2004). Microbial contributions to cave formation: new insights into sulfuric acid speleogenesis. *Geology* 32, 369. doi: 10.1130/g20288.1

Farnleitner, A. H., Wilhartitz, I., Ryzinska, G., Kirschner, A. K., Stadler, H., Burtscher, M. M., et al. (2005). Bacterial dynamics in spring water of alpine karst aquifers indicates the presence of stable autochthonous microbial endokarst communities. *Environ. Microbiol.* 7, 1248–1259. doi: 10.1111/j.1462-2920.2005.00810.x

Ferguson, R. I., and Church, M. (2004). A simple universal equation for grain settling velocity. *J. Sediment. Res.* 74, 933–937.

Feris, K., Ramsey, P., Frazar, C., Rillig, M., Gannon, J., and Holben, W. (2003). Structure and seasonal dynamics of hyporheic zone microbial communities in free-stone rivers of the estern United States. *Microb. Ecol.* 46, 200–215. doi: 10.1007/BF03036883

Fierer, N., Morse, J. L., Berthrong, S. T., Bernhardt, E. S., and Jackson, R. B. (2007). Environmental controls on the landscape-scale biogeography of stream bacterial communities. *Ecology* 88, 2162–2173. doi: 10.1890/06-1746.1

Fierer, N., Nemergut, D., Knight, R., and Craine, J. M. (2010). Changes through time: integrating microorganisms into the study of succession. *Res. Microbiol.* 161, 635–642. doi: 10.1016/j.resmic.2010.06.002

Flynn, T. M., Sanford, R. A., and Bethke, C. M. (2008). Attached and suspended microbial communities in a pristine confined aquifer. *Water Resour. Res.* 44, W07425–W07432. doi: 10.1029/2007wr006633

Ford, D., and Williams, P. D. (2013). *Karst Hydrogeology and Geomorphology.* Chichester: John Wiley & Sons.

Fox, J., and Weisberg, S. (2011). *An {R} Companion to Applied Regression*. Thousand Oaks, CA: Sage.

Gallon, R. K., and Fournier, J. (2013). *G2Sd: Grain-size Statistics and Description of Sediment, 2.0 Edn.*

Ghimire, B., and Deng, Z. (2013). Hydrograph-based approach to modeling bacterial fate and transport in rivers. *Water Res.* 47, 1329–1343. doi: 10.1016/j.watres.2012.11.051

Gibert, J., Danielopol, D., and Stanford, J. A. (1994). *Groundwater Ecology.* San Diego, CA: Academic Press.

Griebler, C., and Lueders, T. (2009). Microbial biodiversity in groundwater ecosystems. *Freshwat. Biol.* 54, 649–677. doi: 10.1111/j.1365-2427.2008.02013.x

Griebler, C., Stein, H., Kellermann, C., Berkhoff, S., Brielmann, H., Schmidt, S., et al. (2010). Ecological assessment of groundwater ecosystems – Vision or illusion? *Ecol. Eng.* 36, 1174–1190. doi: 10.1016/j.ecoleng.2010.01.010

Hahn, H. J., and Fuchs, A. (2009). Distribution patterns of groundwater communities across aquifer types in south-western Germany. *Freshwat. Biol.* 54, 848–860. doi: 10.1111/j.1365-2427.2008.02132.x

Hazen, T. C., Jimenes, L., Lopez De Victoria, G., and Fliermans, C. B. (1991). Comparison of bacteria from deep subsurface sediment and adjacent groundwater. *Microb. Ecol.* 22, 293–304.

Huguet, A., Vacher, L., Relexans, S., Saubusse, S., Froidefond, J. M., and Parlanti, E. (2009). Properties of fluorescent dissolved organic matter in the Gironde Estuary. *Org. Geochem.* 40, 706–719. doi: 10.1016/j.orggeochem.2009.03.002

Hullar, M. A., Kaplan, L. A., and Stahl, D. A. (2006). Recurring seasonal dynamics of microbial communities in stream habitats. *Appl. Environ. Microbiol.* 72, 713–722. doi: 10.1128/AEM.72.1.713-722.2006

Kindt, R. (2014). *BiodiversityR: GUI for Biodiversity, Suitability and Community Ecology Analysis*.

Kunin, V., Engelbrektson, A., Ochman, H., and Hugenholtz, P. (2010). Wrinkles in the rare biosphere: pyrosequencing errors can lead to artificial inflation of diversity estimates. *Environ. Microbiol.* 12, 118–123. doi: 10.1111/j.1462-2920.2009.02051.x

Lakowicz, J. R. (2007). *Principles of Fluorescence Spectroscopy*. New York, NY: Springer Science & Business Media.

Lear, G., Anderson, M. J., Smith, J. P., Boxen, K., and Lewis, G. D. (2008). Spatial and temporal heterogeneity of the bacterial communities in stream epilithic biofilms. *FEMS Microbiol. Ecol.* 65, 463–473. doi: 10.1111/j.1574-6941.2008.00548.x

Lehman, R. M. (2007). Understanding of aquifer microbiology is tightly linked to sampling approaches. *Geomicrobiol. J.* 24, 331–341. doi: 10.1080/01490450701456941

Lian, B., Yuan, D., and Liu, Z. (2011). Effect of microbes on karstification in karst ecosystems. *Chin. Sci. Bull.* 56, 3743–3747. doi: 10.1007/s11434-011-4648-z

Lyautey, E., Jackson, C. R., Cayrou, J., Rols, J. L., and Garabetian, F. (2005). Bacterial community succession in natural river biofilm assemblages. *Microb. Ecol.* 50, 589–601. doi: 10.1007/s00248-005-5032-9

McKnight, D. M., Boyer, E. W., Westerhoff, P. K., Doran, P. T., Kulbe, T., and Anderson, D. T. (2001). Spectrofluorometric characterization of dissolved organic matter for indication of precursor organic material and aromaticity. *Limnol. Oceanogr.* 46, 38–48. doi: 10.4319/lo.2001.46.1.0038

McMurdie, P. J., and Holmes, S. (2013). phyloseq: an R package for reproducible interactive analysis and graphics of microbiome census data. *PLoS ONE* 8:e61217. doi: 10.1371/journal.pone.0061217

Morasch, B. (2013). Occurrence and dynamics of micropollutants in a karst aquifer. *Environ. Pollut.* 173, 133–137. doi: 10.1016/j.envpol.2012.10.014

Nico, G., Daniel, H., and Rossi, P. (2006). Review: Microbial biocenoses in pristine aquifers and an assessment of investigative methods. *Hydrogeol. J.* 14, 926–941. doi: 10.1007/s10040-005-0009-9

Ohno, T. (2002). Fluorescence inner-filtering correction for determining the humification index of dissolved organic matter. *Envion. Sci. Technol.* 38, 742–746. doi: 10.1021/es0155276

Oksanen, J., Blanchet, F., Kindt, R., Legendre, P., O'hara, R., Simpson, G., et al. (2013). *Vegan: Community Ecology Package*.

Ortiz, M., Legatzki, A., Neilson, J. W., Fryslie, B., Nelson, W. M., Wing, R. A., et al. (2014). Making a living while starving in the dark: metagenomic insights into the energy dynamics of a carbonate cave. *ISME J.* 8, 478–491. doi: 10.1038/ismej.2013.159

Pronk, M., Goldscheider, N., and Zopfi, J. (2008). Microbial communities in karst groundwater and their potential use for biomonitoring. *Hydrogeol. J.* 17, 37–48. doi: 10.1007/s10040-008-0350-x

Rehmann, C. R., and Soupir, M. L. (2009). Importance of interactions between the water column and the sediment for microbial concentrations in streams. *Water Res.* 43, 4579–4589. doi: 10.1016/j.watres.2009.06.049

Riemann, L., Leitet, C., Pommier, T., Simu, K., Holmfeldt, K., Larsson, U., et al. (2008). The native bacterioplankton community in the central baltic sea is influenced by freshwater bacterial species. *Appl. Environ. Microbiol.* 74, 503–515. doi: 10.1128/AEM.01983-07

Shabarova, T., and Pernthaler, J. (2010). Karst pools in subsurface environments: collectors of microbial diversity or temporary residence between habitat types. *Environ. Microbiol.* 12, 1061–1074. doi: 10.1111/j.1462-2920.2009.02151.x

Shabarova, T., Villiger, J., Morenkov, O., Niggemann, J., Dittmar, T., and Pernthaler, J. (2014). Bacterial community structure and dissolved organic matter in repeatedly flooded subsurface karst water pools. *FEMS Microbiol. Ecol.* 89, 111–126. doi: 10.1111/1574-6941.12339

Shabarova, T., Widmer, F., and Pernthaler, J. (2013). Mass effects meet species sorting: transformations of microbial assemblages in epiphreatic subsurface karst water pools. *Environ. Microbiol.* 15, 2476–2488. doi: 10.1111/1462-2920.12124

Shade, A., Caporaso, J. G., Handelsman, J., Knight, R., and Fierer, N. (2013). A meta-analysis of changes in bacterial and archaeal communities with time. *ISME J.* 7, 1493–1506. doi: 10.1038/ismej.2013.54

Simon, K. S., Pipan, T., and Culver, D. C. (2007). A conceptual model of the flow and distribution of organic carbon in caves. *J. Cave Karst Stud.* 69, 279–284.

Simon, K. S., Pipan, T., Ohno, T., and Culver, D. C. (2010). Spatial and temporal patterns in abundance and character of dissolved organic matter in two karst aquifers. *Fundam. Appl. Limnol.* 177, 81–92. doi: 10.1127/1863-9135/2010/0177-0081

Thomas, J. M., and Ward, C. H. (1992). Subsurface microbial ecology and bioremediation. *J. Hazard. Mater.* 32, 179–194.

Van Der Gucht, K., Vandekerckhove, T., Vloemans, N., Cousin, S., Muylaert, K., Sabbe, K., et al. (2005). Characterization of bacterial communities in four freshwater lakes differing in nutrient load and food web structure. *FEMS Microbiol. Ecol.* 53, 205–220. doi: 10.1016/j.femsec.2004.12.006

Vesper, D. J., Loop, C. M., and White, W. B. (2001). Contaminant transport in karst aquifers. *Theor. Appl. Karstol.* 13, 101–111. doi: 10.1007/s10040-003-0299-8

Vetrovsky, T., and Baldrian, P. (2013). The variability of the 16S rRNA gene in bacterial genomes and its consequences for bacterial community analyses. *PLoS ONE* 8:e57923. doi: 10.1371/journal.pone.0057923

Wang, Q., Garrity, G. M., Tiedje, J. M., and Cole, J. R. (2007). Naive Bayesian classifier for rapid assignment of rRNA sequences into the new bacterial taxonomy. *Appl. Environ. Microbiol.* 73, 5261–5267. doi: 10.1128/AEM.00062-07

Wey, J. K., Jurgens, K., and Weitere, M. (2012). Seasonal and successional influences on bacterial community composition exceed that of protozoan grazing in river biofilms. *Appl. Environ. Microbiol.* 78, 2013–2024. doi: 10.1128/AEM.06517-11

Wilhartitz, I. C., Kirschner, A. K., Stadler, H., Herndl, G. J., Dietzel, M., Latal, C., et al. (2009). Heterotrophic prokaryotic production in ultraoligotrophic alpine karst aquifers and ecological implications. *FEMS Microbiol. Ecol.* 68, 287–299. doi: 10.1111/j.1574-6941.2009.00679.x

Yagi, J. M., Neuhauser, E. F., Ripp, J. A., Mauro, D. M., and Madsen, E. L. (2010). Subsurface ecosystem resilience: long-term attenuation of subsurface contaminants supports a dynamic microbial community. *ISME J.* 4, 131–143. doi: 10.1038/ismej.2009.101

Zhou, Y., Kellermann, C., and Griebler, C. (2012). Spatio-temporal patterns of microbial communities in a hydrologically dynamic pristine aquifer. *FEMS Microbiol. Ecol.* 81, 230–242. doi: 10.1111/j.1574-6941.2012.01371.x

Zhu, F., Massana, R., Not, F., Marie, D., and Vaulot, D. (2005). Mapping of picoeucaryotes in marine ecosystems with quantitative PCR of the 18S rRNA gene. *FEMS Microbiol. Ecol.* 52, 79–92. doi: 10.1016/j.femsec.2004.10.006

Conflict of Interest Statement: The authors declare that the research was conducted in the absence of any commercial or financial relationships that could be construed as a potential conflict of interest.

frontiers in Microbiology

ORIGINAL RESEARCH
published: 15 October 2015
doi: 10.3389/fmicb.2015.01079

Nitrate and ammonia as nitrogen sources for deep subsurface microorganisms

Heini Kutvonen[1†], Pauliina Rajala[2], Leena Carpén[2] and Malin Bomberg[1]*

[1] Material Recycling and Geotechnology, VTT Technical Research Centre of Finland, Espoo, Finland, [2] Materials Performance, VTT Technical Research Centre of Finland, Espoo, Finland

We investigated the N-utilizing bacterial community in anoxic brackish groundwater of the low and intermediate level nuclear waste repository cave in Olkiluoto, Finland, at 100 m depth using ^{15}N-based stable isotope probing (SIP) and enrichment with $^{14/15}$N-ammonium or $^{14/15}$N-nitrate complemented with methane. Twenty-eight days of incubation at 12°C increased the concentration of bacterial 16S rRNA and nitrate reductase (*nar*G) gene copies in the substrate amended microcosms simultaneously with a radical drop in the overall bacterial diversity and OTU richness. *Hydrogenophaga/Malikia* were enriched in all substrate amended microcosms and *Methylobacter* in the ammonium and ammonium+methane supplemented microcosms. *Sulfuricurvum* was especially abundant in the nitrate+methane treatment and the unamended incubation control. Membrane-bound nitrate reductase genes (*nar*G) from *Polarimonas* sp. were detected in the original groundwater, while *Burkholderia*, *Methylibium,* and *Pseudomonas narG* genes were enriched due to substrate supplements. Identified *amo*A genes belonged to *Nitrosomonas* sp. ^{15}N-SIP revealed that Burkholderiales and Rhizobiales clades belonging to the minority groups in the original groundwater used ^{15}N from ammonium and nitrate as N source indicating an important ecological function of these bacteria, despite their low number, in the groundwater N cycle in Olkiluoto bedrock system.

Keywords: nitrate reducer, ammonia oxidizer, stable isotope probing, nitrogen cycle, terrestrial deep biosphere, groundwater, crystalline bedrock, nitrogen assimilation

OPEN ACCESS

Edited by:
Lisa Y. Stein,
University of Alberta, Canada

Reviewed by:
Jennifer F. Biddle,
University of Delaware, USA
Richard S. Winder,
Natural Resources Canada, Canada

****Correspondence:***
Malin Bomberg,
VTT Technical Research Centre of Finland, PO Box 1000, Tietotie 2, FI-02044 VTT Espoo, Finland
malin.bomberg@vtt.fi

†Present Address:
Heini Kutvonen,
United Medix Laboratories Ltd., Espoo, Finland

Specialty section:
This article was submitted to Terrestrial Microbiology, a section of the journal Frontiers in Microbiology

Received: *03 August 2015*
Accepted: *21 September 2015*
Published: *15 October 2015*

Citation:
Kutvonen H, Rajala P, Carpén L and Bomberg M (2015) Nitrate and ammonia as nitrogen sources for deep subsurface microorganisms. Front. Microbiol. 6:1079. doi: 10.3389/fmicb.2015.01079

Introduction

Nitrogen (N) is one of the basic elements of all life forms and is essential for the production of amino and nucleic acids (Bothe et al., 2007). N depletion may be a growth-limiting factor in many environments, such as deep bedrock groundwater. However, use of explosives in e.g., construction into bedrock environments and mining may increase the concentration of N compounds in these environments, due to under detonated explosives (Beller et al., 2004). Use of pesticides, such as atrazine, has also been shown to be a source of N pollution in karst aquifers that are in connection to agricultural sites (Iker et al., 2010). Despite the generally low metabolic activity of deep groundwater microorganisms (e.g., D'Hondt et al., 2002; Rajala et al., 2015a) these N compounds may affect the activity and growth of deep bedrock microbial communities.

Nitrate is generally present only at low concentrations in pristine anoxic crystalline bedrock groundwater because it has been used as an alternative electron acceptor to oxygen and reduced to

N_2 in anaerobic redox processes (Bothe et al., 2007; Posiva, 2009). Dissimilatory nitrate reduction is a process where the oxidative force of nitrate is used as energy source in the oxidation of organic substrates by denitrifying bacteria. Denitrifying bacteria are mostly heterotrophic and often facultatively anaerobic with the ability to switch between oxygen and nitrate respiration depending on the environmental conditions (Luque-Almagro et al., 2011). Nitrate-reducing bacteria (NRB) have been shown by MPN enrichment studies to colonize groundwater in Olkiluoto, Finland at least to a depth of 300 m (Pedersen, 2008). The same study showed that the distribution and abundance of NRB correlated with that of the cultivable heterotrophic aerobic bacteria, indicating that nitrate as an optional terminal electron acceptor if oxygen is not available. However, depending on depth of the groundwater and location of the study site, denitrification and nitrate respiration in deep crystalline bedrock groundwater have been predicted to be low based on studies focusing on detection of essential genes for denitrification in deep crystalline bedrock environments (Nyyssönen et al., 2014; Purkamo et al., 2015). Nevertheless, NRB otherwise below the detection limit have been shown to significantly increase the transcription of *nar*G genes in response to increased concentration of methane together with sulfate under N_2 atmosphere in deep groundwater (Rajala et al., 2015a). In addition, it has been shown that certain ε-proteobacterial lineages couple reduction of nitrate to simultaneous oxidation of sulfide (reviewed in Campbell et al., 2006).

Ammonia/ammonium is an essential nutrient and energy source in both oceanic and terrestrial hydrothermal environments, where genes involved in ammonia oxidation have been found (Wang et al., 2009). However, little is known about the microbial community metabolizing ammonia or ammonium in pristine deep and cold crystalline bedrock groundwater. In the nitrification process ammonia is oxidized via nitrite to nitrate by the ammonia monooxygenase (AMO) enzyme. In pristine groundwater the concentration of ammonia is low. However, ammonia may be produced during fermentation of biomass, such as dead biofilm and ancient organic material trapped in the rock. In addition, under-detonated explosives may serve as an ultimate source for the production of ammonia by the DNRA process. Nevertheless, ammonia-oxidizing bacteria (AOB) have been found to be scarce in Fennoscandian Shield groundwater (Purkamo et al., 2015).

In addition to functioning as energy sources both nitrate and ammonia are N sources for microorganisms. Nyyssönen et al. (2014) showed by analysing metagenomic data from the Outokumpu deep borehole, that ammonia was the main source of N in the deep groundwater.

The N cycle in deep crystalline bedrock groundwater environments have not yet been extensively studied. In karst-bedrock environment the aerobic and anaerobic oxidation of ammonia has been shown to be slow (Ray et al., 2010) and the microbial communities changed as a result of N contamination by atrazine (Iker et al., 2010). In deep geological repositories for spent nuclear fuel, introduced N compounds may have great implications for the long-term safety of the stored nuclear waste. In Finland, low and intermediate level radioactive waste is stored in a repository at 100 m depth in the bedrock of Olkiluoto Island since 1992. This waste consists of metallic and organic materials from maintenance and decommissioning activities in the nuclear power plant. N compounds, such as ammonium and nitrate may increase microbial activity in this environment, which may cause microbially induced corrosion of the steel and cause release of radionuclides (Rajala et al., 2015b). Here we aimed to gain more insight to both the energy-producing and assimilatory aspects of the N cycle, which could affect the stability of the low and intermediate level radioactive waste repository. We focused especially on nitrate and ammonium in the deep groundwater, since these compounds may be introduced in to the groundwater system at the repository site through construction of the repository. In microcosm experiments we followed the consumption on these N compounds as well as the change in the general bacterial as well as NRB and AOB communities influenced by these compounds. In addition, we aimed to identify the nitrate and ammonium assimilating bacterial community by Stable Isotope Probing (SIP) with ^{15}N labeled substrates.

Materials and Methods

Chemistry

The chemical composition of groundwater in the beginning of the experiment was analyzed at the ALS Finland. Dissolved metals were analyzed by ICP-OES and N compounds spectrophotometrically according to the CSN ISO 11732 and CSN ISO 13395. pH, redox-potential, oxygen content and temperature of the water were measured inside an anaerobic glove bag with a HACH Sension 156 m (Hach Lange Gmbh, Germany) and electrical conductivity with a CDM92 conductivity meter (Radiometer-analytical, France) on site.

Experimental Setup

Groundwater samples were collected in May 2013 from drill hole VLJ-KR9 in the low and intermediate level nuclear waste repository tunnel situated in the crystalline bedrock at the site of the Olkiluoto nuclear power plant, Finland. The drill hole VLJ-KR9 was drilled in 1995 in to the wall of the VLJ-tunnel at approximately 95 m depth from the ground surface. The total length of the drill hole is 20.04 m and it bears slightly downwards reaching a depth of 95.249 m from the ground surface. The first 66 mm of the drill hole is cased and the opening is sealed with a welded flange plug equipped with a pressure sensor and tap for sampling. The drill hole is regularly purged. Before the sampling a sterile, gas tight polyacetate tube was connected to the sampling tap of the borehole and groundwater was run for 30 min before the start of the sample collection in order to remove excess air from the tube.

Altogether 30 groundwater samples of 2.4 L each were collected in sterile borosilicate glass bottles previously rendered anaerobic under constant N_2 flow. The groundwater was introduced to the bottles through the sterile polyacetate tube directly from the borehole located in the wall of the tunnel. In order to reduce exposure to oxygen in the microcosm bottles a volume of 50% overflow was allowed before each bottle was sealed with a tight-fitting butyl rubber septum

and open-top screw-cap. The water samples were transported in a cooling-box with ice to the laboratory within 1d of sampling. The sample bottles were divided into 10 treatment groups with three replicates per treatment. The treatments were; (1) baseline sample, biomass was captured on 0.2 μm pore-size cellulose acetate membranes (Corning, MA, USA) by filtering 2.4 L groundwater on-site immediately after sampling and immediately frozen on dry ice, (2) $Na^{15}NO_3$ addition, (3) $^{15}NH_4Cl$ addition, (4) $Na^{15}NO_3$+CH_4addition, (5)$^{15}NH_4Cl$+CH_4addition, (6) $Na^{14}NO_3$addition, (7)$^{14}NH_4Cl$ addition, (8) $Na^{14}NO_3$+CH_4addition, (9)$^{14}NH_4Cl$+CH_4 addition, and (10) no substrate additions (incubation control). N substrates and methane were added at the beginning of the experiment and again after 14 days of incubation. The N substrates (sodium nitrate and ammonium chloride, atom 98% ^{15}N, Sigma-Aldrich) were sterilized using a 0.2 μm pore size syringe filter and rendered anaerobic by sterile N_2 gas flow for 30 min. Five milliliters N substrates (62.5 mM stock solution) were added to a final concentration of 0.13 mM. The N substrates and 5 mL sterile methane (treatments 4, 5, 8, and 9), i.e., approximately 2 mL L^{-1} sample water, were added aseptically to the 2.4 L microcosms through the butyl rubber stoppers using a sterile syringe and needle. The microcosms were incubated at a temperature of +12°C, which was as close to that of the drill hole at 95 m depth from ground surface as possible for 28 d.

The biomass of each sample was collected by vacuum suction on 0.2 μm-pore-size cellulose acetate membranes (Corning, MA, USA) at the end of the incubation period. The filter membranes were cut out of the filter funnels using sterile scalpels, inserted into sterile 50 mL screw cap tubes (Corning, MA, USA) and frozen at −80°C until use.

The consumption or production of nitrate and ammonium was monitored by subsamples retrieved at the beginning of the experiment before and after addition of substrates, after 14 days incubation before and after addition of substrates and at the end of the incubation period. At each sampling time, 5 mL subsamples were retrieved using a sterile syringe and needle pushed through the butyl rubber septum of each bottle. The concentration of nitrate and ammonium of each subsample was measured spectrophotometrically using the Hach–Lange DR 2800 spectrophotometer (Hach–Lange, UK) and the LCK304 kit for ammonium and LCK339 kit for nitrate according to the manufacturer's instructions. The consumption and production of nitrate and ammonium was determined by comparing the concentration of N compounds after 14 and 28d of incubation to the concentrations immediately after substrate addition. The balance of N substrates in the different incubations was normalized to relative abundances of the measured N compounds in each different incubation type for better comparison between different treatments.

DNA Extraction

Filters with the collected biomass were carefully thawed on ice. Microbial DNA was extracted using the Metagenomic isolation kit for water (Epicentre, USA). The DNA was extracted according to the manufacturer's protocol and eluted in 50 μL elution buffer.

Quantification of the Number of Bacteria and Nitrate Reducers by qPCR

The bacterial population in the original groundwater and in the water samples after incubation with or without substrates was determined by 16S rRNA gene targeted qPCR using universal bacterial 16S rRNA gene-targeting primers fD1 (Weisburg et al., 1991) and P2 (Muyzer et al., 1993). In addition, the concentration of *nar*G genes of the nitrate reducers was tested with primers narG1960m2f/narG2050M2F (López-Gutiérrez et al., 2004).

The qPCR reactions were performed in 10 μL reaction volumes using the KAPA 2 × Syrb® FAST qPCR-kit on a LightCycler480 qPCR machine (Roche Applied Science, Germany). Each reaction contained 2.5 μM of relevant forward and reverse primer and 1 μL DNA extract. Each reaction was run in triplicate and no-template control reactions were used to determine background fluorescence in the reactions.

The qPCR conditions consisted of an initial denaturation at 95°C for 10 min followed by 45 amplification cycles of 15 s at 95°C, 30 s at 55°C, and 30 s at 72°C with a quantification measurement at the end of each elongation. A final extension step of 3 min at 72°C was performed prior to a melting curve analysis. This consisted of a denaturation step for 10 s at 95°C followed by an annealing step at 65°C for 1 min prior to a gradual temperature rise to 95°C at a rate of 0.11°C s^{-1} during which the fluorescence was continuously measured. The number of bacterial 16S rRNA genes and *nar*G genes was determined by comparing the amplification result (Cp) to that of a 10-fold dilution series (10^1–10^7 copies μL^{-1}) of *Escherichia coli* (ATCC 31608) 16S rRNA genes and *Pseudomonas aeruginosa* (ATCC 15692) *nar*G, respectively, in plasmid. A qPCR assay for the *amo*A genes was not conducted due to low specificity of the used primers to the *amo*A gene (see Section Ammonia Oxidizers).

PCR

PCR reactions for denaturing gradient gel electrophoresis (DGGE) analysis of the bacterial 16S rRNA genes, *nar*G and *amo*A gene profiles in the original groundwater and after the incubation period were performed in 50 μL reactions. The reactions contained 1 u KAPA Hifi—polymerase in 1 × KAPA HF-buffer, 0.6 mM dNTP, 0.4 μM of each relevant primer and 1 μL DNA extract. The PCR program consisted of a 5 min initial denaturation step at 98°C followed by 40 cycles of denaturation at 98°C for 20 s, annealing at 55°C (16S rRNA genes) or 57°C (*amo*A and *nar*G) for 15 s and elongation at 72°C for 30 s, and a final extension at 72°C for 5 min. For the bacterial 16S rRNA genes, primers U968fGC /U1401r (Nübel et al., 1996) were used; the *nar*G and *amo*A DGGE PCR products were obtained with primers *nar*G2179F/*nar*G2488R-GC (Pastorelli et al., 2013) and *amo*A1F/*amo*A2RGC (Nicolaisen and Ramsing, 2002), respectively.

DGGE

Profiles of bacterial communities having 16S rRNA gene, *nar*G and *amo*A genes were resolved vs. different treatments using DGGE. The DGGE was performed on a Bio-Rad DCode TM Universal Mutation Detection System (Bio-Rad, USA). For the 16S rRNA gene fragments, a denaturing gradient of 35–65% was

used and the electrophoresis was run for 20 h at 85 V at 60°C as described in Nübel et al. (1996). The denaturants used was urea (42 g/100 mL in 100% denaturing solution) and formamide (40% formamide in 100% denaturing solution). The denaturing gradient used for the *amo*A-gene fragments was 30–70% and the electrophoresis was run for run 6 h with 200 V at 60°C according to Nicolaisen and Ramsing (2002). The *nar*G-gene fragments were subjected to DGGE using a denaturing gradient of 40–70% for 17 h with 70 V at 60°C according to Pastorelli et al. (2013). All gels were made of 8% polyacrylamide.

DGGE bands were detected using SYRB-green I nucleic acid stain (Fisher Scientific, UK) according to the manufacturers protocol and imaged under UV light using a GEL DOC XR+2000 transilluminator (Bio Rad, USA). Prominent DGGE fragments were extracted from the gels using sterile plastic Pasteur pipettes. DNA from the gel plugs was extracted into 20 μL of molecular grade water overnight at 4°C and the DGGE band was reamplified with the relevant primer pair without the GC-clamp, as described above using 2 μL extracted DNA as template. The reamplified DGGE bands were shipped to Macrogen Inc, South Korea on ice packs, for sequencing.

Phylogenetic analyses were performed on the sequences of the DGGE bands with GENEIOUS PRO (Biomatters Ltd, New Zealand). All sequences were imported into GENEIOUS PRO, and aligned to reference sequences and most closely matching sequences in the NCBI nucleotides database (http://blast.ncbi.nlm.nih.gov/) determined with the blastn tool in GENEIOUS PRO. The alignments were performed with the MAFFT tool in GENEIOUS PRO with default settings and the alignments were edited manually. Phylogenetic analyses were performed on the alignments of the 16S rRNA gene sequences using PhyML (Guidon and Gascuel, 2003) with the Jukes-Cantor69 substitution model (Jukes and Cantor, 1969). The *nar*G and *amo*A gene sequences were translated in to amino acid sequences using translation table 11 prior to alignment with MAFFT and a phylogenetic analysis with PhyML using the WAG substitution model (Whelan and Goldman, 2001). Bootstrap support for nodes were calculated based on 1000 random repeats for all phylogenetic analyses.

Isopycnic Centrifugation and Gradient Fractionation

In order to separate the ^{15}N-containing DNA fraction of the microbial community that had consumed the N substrates from the rest of the community DNA density gradient centrifugation was performed using 5 ml Quick-seal polyallomer tubes (BeckmanCoulter, Brea, CA, USA) in a Beckman ultracentrifuge with a VTI 65.2 vertical tube rotor. Each tube contained a fixed volume of 35 μL extracted DNA suspended in 4.9 mL of CsCl in gradient buffer (5 mL 1 M Tris-HCl, 0.375 g KCl, 0.15 mL EDTA) with a density of 1.725. The DNA was centrifuged for 62 h at 44,100 g at 22°C.

After centrifugation the gradients were apportioned, starting at tube bottoms, into 22 equal fractions of approximately 200 μL. The centrifugation tube was first pierced with hypodermic needles at the top and bottom and the fractions were pushed out through the bottom needle by pushing sterile water mixed with dye at a rate of 200 μL min^{-1} in to the top of the centrifuge tube using a syringe pump (New Era Pump Systems, Inc., Farmingdale, NY, USA). Gradient formation in the centrifugation was determined by including a control tube without DNA in each run and fractioning the gradient as for the DNA samples. The nd value of each of the control fractions was determined using a refractometer (DR301-95, A. Krüss Optitronic, Germany). In addition, the nd value of the first and last fraction of the DNA sample tubes was also measured in order to ensure that a gradient has been formed during the centrifugation.

Due to the potential for low separation efficiency when there is low concentration of N in the DNA and the high density of GC-rich DNA, fractions with densities 1.725–1.733 were recentrifuged as before, but with the addition of 8 μL (10 mg mL^{-1}) bis-Benzimide in each sample to improve buoyancy of GC-rich DNA as described in Buckley et al. (2007). This was performed according to gradient formation in controls during the first centrifugation. After centrifugation, gradients were apportioned as before directly onto MultiScreenf® Filter Plates (Merck Millipore Ltd., Cork, Ireland) and purified from CsCl salt using a 96-well Vacuum Manifold (Merck Millipore Ltd., Cork, Ireland) with 5 volumes (200 μL) sterile water.

Fractions containing heavy and light DNA were determined by qPCR as described above for the bacterial 16S rRNA gene. DNA from fractions having density of 1.72 and 1.735 were determined to contain DNA fractions of interest and subjected to high throughput (HTP) amplicon sequencing.

High Throughput Amplicon Sequencing and Sequence Analysis

Libraries for 454 HTP amplicon sequencing were prepared by PCR of DNA from the original groundwater used in the experiment, the supplemented incubations and incubation control, and also the heavy-fraction DNA of the $Na^{15}NO_3$,$^{15}NH_4Cl$, $Na^{15}NO_3$+CH_4, and$^{15}NH_4Cl$+CH_4 treatments. For HTP sequencing, amplicon libraries from the three replicates of each treatment were combined due to the low amount of DNA in the heavy fraction DNA extracts.

Bacterial 16S rRNA fragments covering the V1–V3 variable regions were amplified with primers 8F (Edwards et al., 1998) and P2 (Muyzer et al., 1993) equipped with adapter and MID sequences (tags) at their 5' end in a single round PCR as described in Bomberg et al. (2015). PCRs were performed with KAPA HiFi polymerase (Kapa Biosystems, Inc., Boston, MA, USA) in 1 × HF buffer. Each 50 μL reaction contained 0.5 mM dNTP and 1 μM primer mix. PCR conditions consisted of an initial denaturation step of 30 s at 98°C, followed by 35 cycles of 10 s at 98°C, 15 s at 55°C, and 15 s at 72°C, and a final extension step at 72°C for 5 min. Sequencing of the PCR products was performed at BeckmanCoulters Genomics using the FLX 454 Titanium (454 Life Sciences, Branford, CT, USA).

Sequence reads were analyzed using Mothur (v 1.33.1, Schloss et al., 2009) where the flow-grams were denoised using the default parameters of the sff.multiple workflow in Mothur, trimmed to remove adapter, barcode, and primer sequences, and to exclude sequences that did not meet the quality criteria (i.e., no barcode and primer mismatches, no ambiguous nucleotides,

maximum eight-nucleotide-long homopolymer stretches and defined minimum length of 200 bp). The bacterial 16S rRNA sequences were aligned to the Silva v_119 reference alignment (Pruesse et al., 2007) and the alignments were screened to include sequences with defined start positions and minimum end position. The aligned sequences were preclustered prior to chimera detection with the Chimera.slayer command in Mothur and possible chimeric sequences were removed. A distance matrix was calculated for the chimera-filtered sequences using a cut-off of 0.05 without penalty for end gaps. The sequences were clustered into Operational Taxonomic Units (OTUs) according to the distance matrix using the nearest-neighbor method. The representative sequences of the OTUs sharing 97% sequence similarity within each OTU were classified using the Silva v_119 reference database (Pruesse et al., 2007). Alpha diversity analyses were performed on data normalized to 448 sequence reads per sample and rarefaction analyses were performed on the total number of sequence reads per sample.

Accession Numbers

The sequences of the DGGE bands will be deposited in the European Nucleotide Archives (ENA; https://www.ebi.ac.uk/ena) under accession numbers LN866782-LN866813 for 16S rRNA genes, LN866814-LN866821 for *amo*A genes and LN866822-LN866841 for *nar*G genes. The HTP sequence reads were submitted to ENA under accession numbers ERS739681-ERS739690.

Results

Groundwater Chemistry

At the time of sampling the groundwater contained 0.178 mg L^{-1} ammonium-N, 0.229 mg L^{-1} ammonium, <0.040 mg L^{-1} nitrate, and <0.150 mg L^{-1} nitrite at pH 8.06. The pH, temperature (T), reduction potential (Eh) and electric conductivity (Ec) of the groundwater was 8.09, 10.3°C, 58 mV vs. Standard Hydrogen Electrode (SHE) and 2.26 mS cm^{-1}, respectively. Other physicochemical parameters are presented in **Table 1**.

TABLE 1 | The physicochemical composition of the groundwater at the time of sampling.

Measurement	Value		
T	10.3°C		
O_2	0.09 mg L^{-1}		
Alkalinity	5.28 mmol L^{-1}		
Eh	58 mV vs. SHE		
Ec	2.26 mS cm^{-1}		
Sulfide	0.061 mg L^{-1}		
Phosphate	0.223 mg L^{-1}		
CO_{2free}	3.68 mg L^{-1}		
CO_{2total}	236 mg L^{-1}		
F_{total}	0.378 mg L^{-1}		
Br_{total}	1.93 mg L^{-1}		
Cl_{total}	513 mg L^{-1}		
Ca $_{total}$	76.3 mg L^{-1}	Ca $_{soluble}$	74 mg L^{-1}
Mg $_{total}$	20.3 mg L^{-1}	Mg $_{soluble}$	21.6 mg L^{-1}
Na $_{total}$	421 mg L^{-1}	Na $_{soluble}$	420 mg L^{-1}
Fe $_{total}$	0.109 mg L^{-1}	Fe $_{soluble}$	0.0624 mg L^{-1}
Mn $_{total}$	0.161 mg L^{-1}	Mn $_{soluble}$	0.153 mg L^{-1}
S $_{total}$	40.4 mg L^{-1}	S $_{soluble}$	48.7 mg L^{-1}

For the metals Ca, Mg, Na, Fe, Mn, and S both the total ($_{total}$) and the soluble ($_{soluble}$) forms were measured.

Consumption of Ammonium and Nitrate

The original concentrations of ammonium and nitrate were low (**Figures 1A,C**). During 4 weeks of incubation at 12°C the amount of ammonium decreased almost 20% from the original concentration at the time of sampling (**Figure 1B**). The concentration of nitrate, on the other hand increased 22.5% over the same time period (**Figure 1D**). After addition of the N substrates, the concentration of ammonia decreased 34.5% in the microcosms that had received ammonium and methane (NH_4+CH_4) and 51.5% those only receiving ammonium (NH_4). However, the ammonium concentration ceased to decrease after 2 weeks of incubation (**Figure 1**). In the nitrate-supplemented microcosms, the relative concentration of nitrate increased in all treatments after the first addition of nitrate (**Figure 1D**). However, after 4 weeks of incubation 21.2% of the added nitrate had been consumed in microcosms supplemented with nitrate (NO_3) only, while the nitrate concentration in the nitrate+methane (NO_3+CH_4) remained high.

Over the time of incubation the concentration of nitrate increased with approximately 25% in the unamended control microcosms, while the concentration of ammonium decreased by the same magnitude (**Figure 1**). The concentration of ammonium in the nitrate-supplemented microcosms increased slightly toward the end of the incubation period in the NO_3-supplemented microcosms, and during the first 14 days in the NO_3+CH_4-supplemented microcosms, but was not extensively produced from the added ammonium (**Figure 1B**). In the NH_4+CH_4-supplemented microcosms, on the other hand, the NO_3 concentration increased noticeably with approximately 230% during the first 14 days of incubation where after the NO_3 was consumed to about 40% of the original NO_3 concentration by the end of the incubation period, indicating that NO_3 was initially produced from the added NH_4 (**Figure 1D**).

Quantitative Analysis of Microbial Community

There were 7.8×10^4 copies mL^{-1} of the bacterial 16S rRNA gene in the original groundwater. The addition of NH_4+CH_4 and NO_3 had the greatest effect on the bacterial community and increased the concentration of bacterial 16S rRNA gene copies 12-fold over the 28d incubation period to 9.5×10^5 mL^{-1} and 9.7×10^5 mL^{-1}, respectively (**Figure 2A**). In the other treatments the number of bacteria also increased, including the control (unamended) microcosms, by three to five fold.

There were 2.2×10^2 *nar*G gene copies mL^{-1} corresponding to the population of NRB in the original groundwater (**Figure 2B**). The NH_4+CH_4 treatment had the greatest effect on the NRB

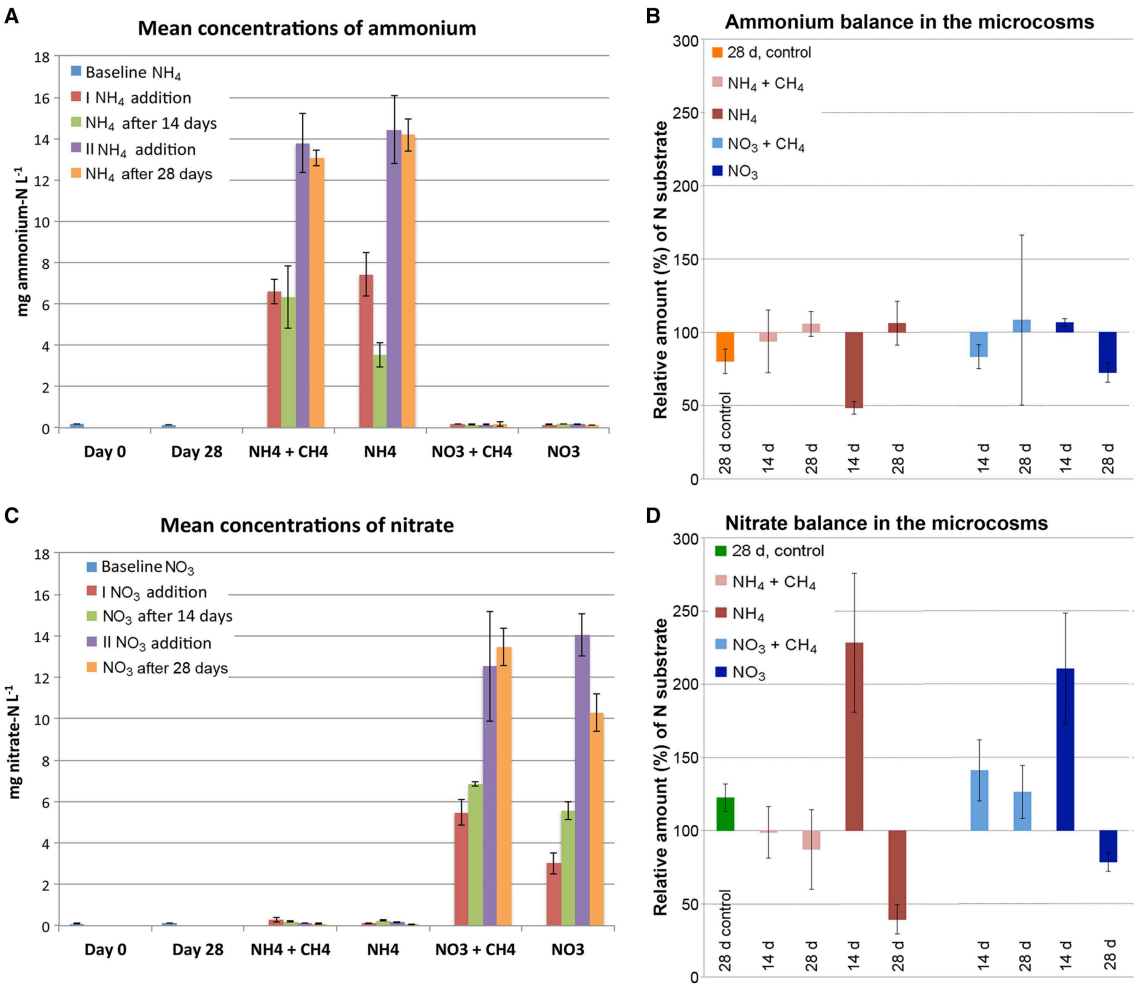

FIGURE 1 | The average concentration (A,C) and relative balance (B,D) of ammonium and nitrate in the microcosms. In **(A,C)** the average concentration of ammonia or nitrate (mg L^{-1}) is measured from the original groundwater and the 28d controls (blue), directly after the first addition of N-substrate (red), 14d after the first addition of N-substrate (green), directly after the second addition of N-substrate (purple), and at the end of the experiment (orange). In **(B,D)** the relative change in the concentration of ammonium and nitrate is illustrated for incubations with NH_4+CH_4 (pink), NH_4 (red), NO_3+CH_4 (light blue) and NO_3 (dark blue) after 14 and 28d of incubation. The change in ammonium concentration over 28 days in **(B)** is shown in orange and the change in nitrate concentration in **(D)** in green. The relative amount of N substrates in **(B,D)** above 100% are considered produced and below 100% consumed compared to the amount of N substrates measured directly after addition of substrates.

increasing the concentration of *nar*G genes to 3.9×10^3 copies mL^{-1} over the course of incubation. In nitrate-treated microcosms the increase in *nar*G genes was 2.7×10^3 copies mL^{-1}. Without substrate additions, the concentration of *nar*G genes did not increase during the incubation time.

Bacterial Community Composition

The number of sequence reads obtained from 454 pyro sequencing ranged from 448 to 5772 sequence reads per sample from the original groundwater and the different microcosms (**Table 2**). The bacterial community in the original groundwater was diverse (H' = 3.07) according to the 454 amplicon sequence profiles, which showed 125 OTUs belonging to 61 different bacterial genera (**Figure 3**, **Table 2**, Table S1). The richness estimates (chao and ace) indicated that only between 21 and 41% of the OTU richness in the original groundwater was captured. Over 28d the microbial OTU diversity increased (H' = 3.51) to altogether 146 OTUs, but the number of identified genera decreased to 43 and according to the richness estimates only 19.2–35.5% of the total OTU richness was obtained. In the substrate amended microcosms the diversity was significantly lower, H' = 0.04–0.70, than that of the original groundwater and the 28d incubation controls. The number of observed OTUs ranged from 2 to 19 and according to the richness estimates between 60.8 and 100% of the total diversity of the bacterial communities was captured (**Table 2**). The low number of OTUs obtained as well as the low diversity and richness indices indicates that the addition of N substrates enriched a specific population of bacteria involved in N cycling during the incubation.

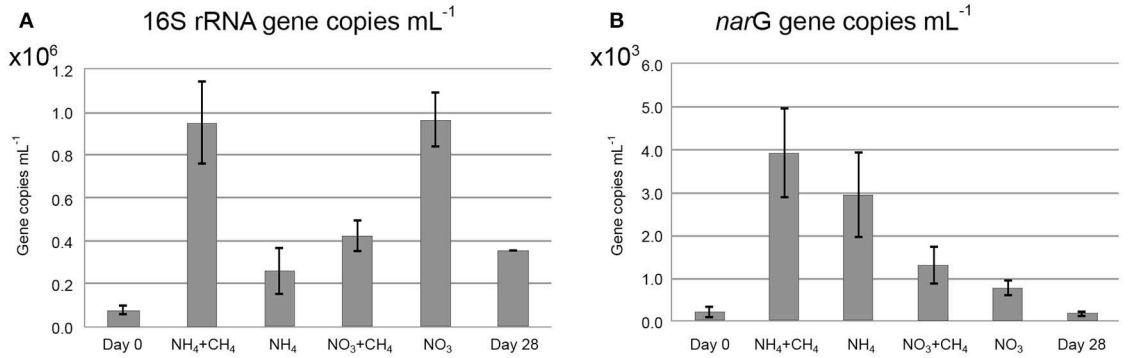

FIGURE 2 | The concentrations of (A) bacterial 16S rRNA gene copies, (B) *nar*G gene copies mL^{-1} in the original groundwater (Day 0), the incubations with substrates (NH_4+CH_4, NH_4, NO_3+CH_3, NO_3) and without substrates (Day 28).

TABLE 2 | Alpha diversity estimates of the original groundwater (Day 0) and after 28 days of incubation in the control microcosms (Day 28) and the microcosms supplemented with NH_4+CH_4, NH_4, NO_3+CH_4, NO_3.

Sample	Number of sequences	Number of observed OTUs	Estimation of OTU richness*		% richness captured		Diversity index*	
			Chao	ace	chao	ace	Shannon H'	Simpson
Day 0	610	125	303.14	575.37	41.23	21.73	3.07	0.21
NH4+CH4	527	2	2	2	100	100	0.04	0.99
NH4	5772	19	30.25	31.25	62.81	60.80	0.50	0.85
NO3+CH4	5072	7	7.5	8.79	93.33	79.67	0.70	0.65
NO3	1296	8	8.33	11.89	96.00	67.30	0.55	0.77
Day 28	448	146	411	760.30	35.52	19.20	3.51	0.11

The calculations are based on 454 pyro sequencing reads and the data was normalized to 448 reads per sample.
**Calculated on data normalized to 448 random reads per sample.*

Based on pyro sequencing data 12 bacterial genera were present at over 1% relative abundance in the original groundwater. The most abundant bacteria belonged to an unassigned group of *Parcubacteria* (Rinke et al., 2012) [formerly Candidate division (Cd) OD1], the β-proteobacterial genus *Gallionella* and the *Microgenomates* (Rinke et al., 2012; formerly Cd OP11, **Figure 3**, Table S1). Interestingly, in the 28d incubation controls the relative abundance of *Sulfuricurvum* increased from 0 to 41.5%, the *Parcubacteria* group from 16.9 to 27.5% and the Comamonadaceae genus *Malikia* from 0 to 5.6%. In the NH_4 and NH_4+CH_4 incubations *Malikia* contributed with 48.7% and 41.6% of the sequence reads, respectively, being the most abundant bacterial group enriched in these microcosms. *Methylobacter* was the second most abundant bacterial genus contributing with 35.9 and 43.8% of the sequence reads, respectively. In addition, *Hydrogenophaga* had become enriched (11.2% of the sequence reads) in the NH_4+CH_4 incubations but was present at below 1% in the NH_4 microcosms. The NO_3- and NO_3+CH_4 amendments enriched the *Malikia* most and 86.5% and 69.2% of the sequence reads belonged to this genus, respectively. In addition, 5.0% and 20.5% of the sequence reads belonged to *Sulfuricurvum* and 4.4% and 2.6% belonged to *Sulfuricella*, respectively. *Methylobacter* contributed with 2.4% of the sequence reads in the NO_3+CH_4—amended microcosms, but were not found in the microcosms with only NO_3. Instead, the NO_3—amended microcosms contained *Acetobacterium* sequences, 2.8%, which were additionally only detected in the original groundwater samples.

The DGGE profiles showing the most abundant taxa in the bacterial communities were similar to the pyro sequencing profiles. The DGGE profiles of the bacterial taxa enriched during incubation were also similar between the different treatments, but specific phylotypes were more clearly detected in comparison to the ones seen in the original groundwater (**Figure 4**). The genera detected by DGGE affiliated with the β-proteobacterial *Hydrogenophaga/Malikia* cluster and ε-proteobacterial *Sulfuricurvum* (**Figures 5**, **6**). The most common bacteria detected by DGGE in all substrate-amended microcosms belonged to ε-proteobacterial *Sulfuricurvum* and β-proteobacterial *Hydrogenophaga/Malikia* (**Figures 5**, **6**), although the 454-pyrosequencing detected *Sulfuricurvum* enriched only in NO_3+CH_4—amended microcosms and in the 28d controls, and at low abundance in the NH_4- and NO_3-amended microcosms. DGGE bands belonging to γ-proteobacterial *Methylobacter* were found in the original groundwater and in the microcosms amended with NH_4 and NH_4+CH_4 in the DGGE analysis (**Figures 5**, **6**). In addition, δ-proteobacterial *Desulfocapsa* were detected by DGGE in

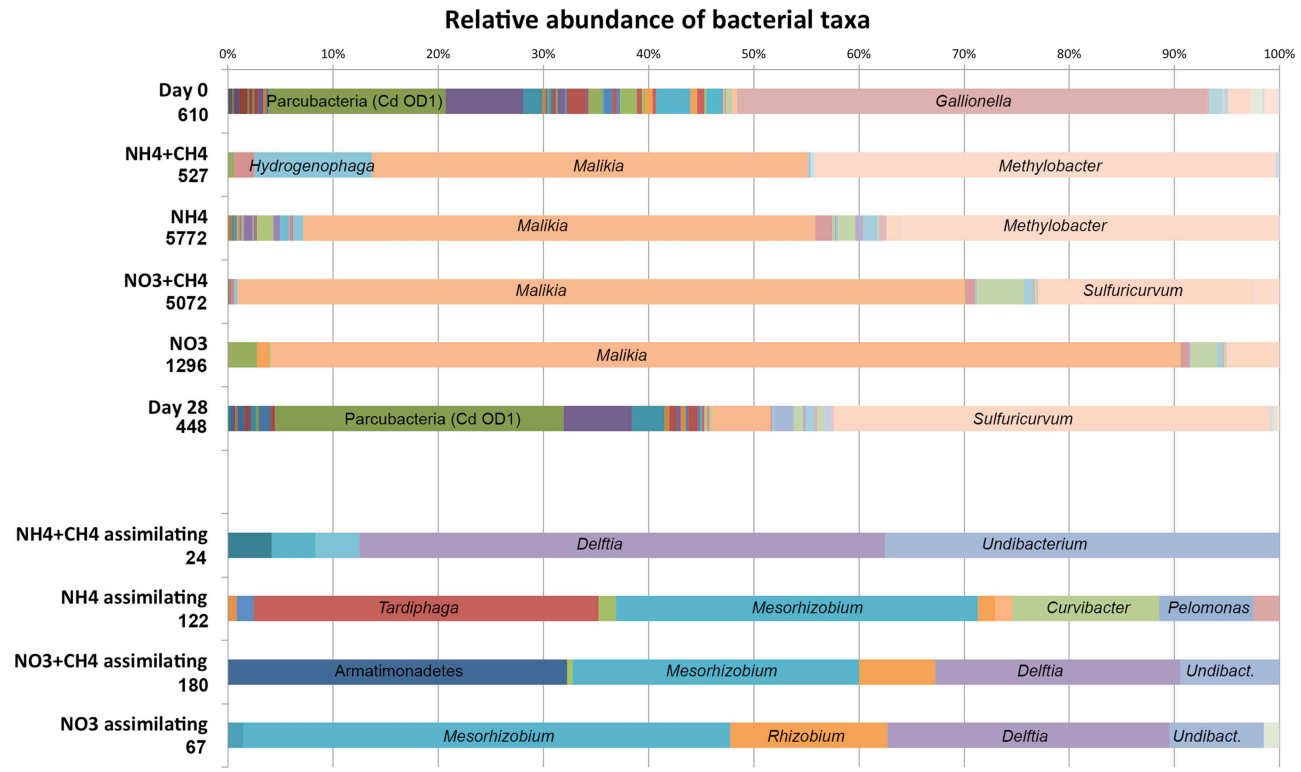

FIGURE 3 | The relative abundance of bacterial genera detected by high throughput amplicon sequencing from the original groundwater (Day 0), N- and C-supplemented microcosms and the non-supplemented control (Day 28). The lower part of the figure shows the relative abundance of nitrogen assimilating bacteria detected from the ^{15}N fractions. The number in by each category indicates the number of sequence reads. The names of the most prominent genera are indicated in the bar graph. More detailed information of the relative abundance of different bacterial taxa detected in the study can be found in Table S1.

all microcosms although they were not detected by 454 pyro sequencing.

Ammonia Oxidizers

The *amo*A genes of ammonia oxidizing bacteria were detected by DGGE but of a total of 46 sequenced DGGE bands 8 bands provided a correct *amo*A sequence (**Figure 7**). Of these sequences, 7 were obtained from NO_3-amended microcosms and one from unamended (control) microcosms. All detected *amo*A gene fragments were similar to β-proteobacterial *Nitrosomonas*-type *amo*A genes (**Figure 8**).

Nitrate Reducers

*nar*G genes of NRB were detected by DGGE (**Figure 9**). Altogether 20 bands were successfully sequenced and identified to be *nar*G gene fragments. *nar*G gene sequences belonging to four different taxonomical groups were found (**Figure 10**). These sequences were similar to *narG* genes of *Pseudomonas* (bands 1, 2, 9, 10, 13, 14, 15, 17, 18), *Methylibium* (bands 3, 6, 8, 11, 19), *Alicycliphilus* (band 16), *Polaromonas* (bands 4, 5, 20), *Herminiimonas* (band 7), and to an uncultured group of bacteria (band 12). *Pseudomonas* and *Methylibium nar*G genes were frequently detected in all substrate-amended microcosms, while *Polaromonas nar*G was found in microcosms amended with NH_4+CH_4 or NH_4 and in the untreated controls. *Alicycliphilus narG* was detected only in microcosms supplemented with NO_3 and only in one band. *nar*G band 12 was obtained from NH_4 supplemented microcosms only, but the position of the DGGE band was similar to many others in the other treatments, which were not successfully sequenced; this indicated that the particular *nar*G type was common in the microcosms.

Nitrogen Assimilating Bacteria

The bacterial communities corresponding to different treatments changed over time due to the different substrates added to the microcosms. After double isopycnic centrifugation was applied in order to separate first the heavy DNA fraction from the light DNA fraction and then the ^{15}N-enriched heavy DNA from the GC-rich heavy DNA, the amount of DNA left was not adequate to obtain DGGE bands of detectable density. However, 454 amplicon sequencing provided a low number of sequence reads from the ^{15}N-enriched DNA, after pooling the three replicate microcosms within each treatment. Several genera belonging to α-proteobacterial Rhizobiales (*Rhizobium*, *Mesorhizobium*, *Tardiphaga*) and β-proteobacterial Burkholderiales (*Delftia*, *Undibacterium, Curvibacter, Pelomonas*) were detected in the ^{15}N-enriched heavy DNA fraction from all amended microcosms (**Figure 3**; Table S1). In addition, sparse Nitrospirales 16S rRNA gene reads were found in the $^{15}NH_4$-amended samples,

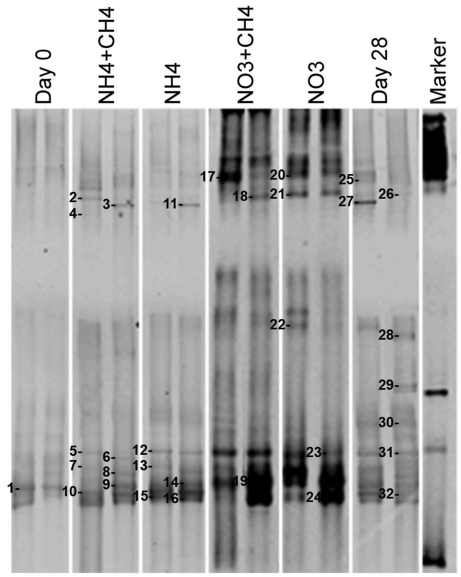

FIGURE 4 | Bacterial community profiles from PCR-DGGE of DNA extracted from original groundwater (Day 0) and supplemented vs. control microcosms (Day 28). The supplemented treatments are shown as described in **Figure 2**.

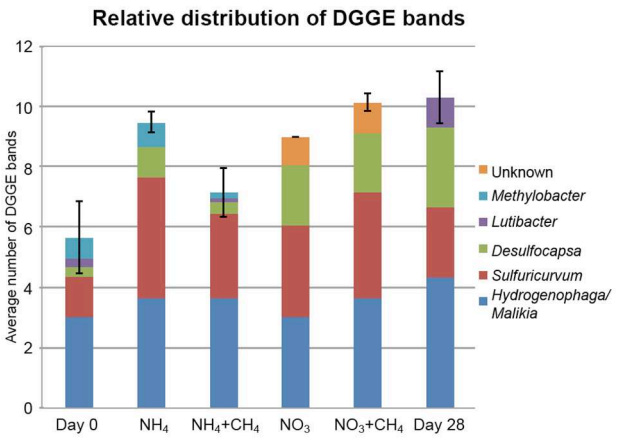

FIGURE 5 | Average number of DGGE bands per replicate treatment (X axis) and the distribution of bacterial taxa identified from the DGGE profiles of the different treatments (Y axis). The number of replicates was 3 (Day 0 and 28) or 6 per treatment (substrate supplemented microcosms). The error bars show standard error of mean (SEM). The supplemented treatments are shown as described in **Figure 2**.

along actinobacterial *Propionibacterium* from the $^{15}NH_4$+CH_4-amended microcosms (Table S1). In the $^{15}NO_3$-amended samples, a few reads resembling cyanobacterial sequences were detected, and in the $^{15}NO_3$+CH_4-amended microcosms, an unassigned group of Armatimonadetes constituted the single most abundant 16S rRNA gene type detected in this treatment (**Figure 3**; Table S1). The corresponding fractions of the ^{14}N substrate-amended microcosms were also tested by PCR, but no PCR fragments were obtained.

Discussion

Nitrogenous compounds, such as nitrate and ammonia may have great effect on the microbial activities in the deep geological repository for low and intermediate level radioactive waste that has been constructed in to the crystalline bedrock of Olkiluoto, Finland. Enhanced microbial activity may cause microbially induced corrosion of the metallic waste, as shown by Rajala et al. (2015b) and affect the long-term safety of the repository. In oligotrophic crystalline bedrock environments methane may be an important component of gases dissolved in the groundwater and may serve as carbon source for the microbial communities and thus increase microbial activity. Nitrate-reducing microbial communities have been found in Olkiluoto deep groundwater by Most Probable Number analysis to depths greater than 300 m (Pedersen, 2008). Olkiluoto groundwater has in general large amounts of dissolved N_2 and the amount of CH_4 increases with depth from 1 to 1000 $\mu L\ L^{-1}$ groundwater to a depth of 300 m, but increases 100-fold after this depth from where it may diffuse in to more shallow groundwater (e.g., Pedersen, 2008). Different N compounds may be introduced to the repository environment from explosives that have been incompletely detonated during construction of the repository.

In this study, we showed that added nitrate and ammonium had a great effect on the bacterial community in brackish groundwater in Olkiluoto at the depth of ca. 100 m. The bacterial community increased during the 28d incubation as a result amendment with N substrates and methane with the highest increase in the NH_4+CH_4 and NO_3 treatments. The microbial community consumed NH_4 during the first 2 weeks of incubation, both with and without CH_4, but the consumption decreased toward the end of the incubation period. NO_3 consumption was detected at the end of the incubation period, but not together with CH_4. This indicates that the NH_4- and NO_3-consuming populations were not in general affected by CH_4. However, the CH_4-consuming community despite their intrinsic differences may affect the N-cycling community. The N substrates also decreased the number of detected OTUs, the estimated OTU richness and diversity indices of the microbial communities in the microcosms, while in the unamended 28d control microcosms these factors increased (**Table 2**). It is thus possible that introduction of N substrates in the repository area may have significant effect on the corrosion rate of the metallic radioactive waste by explicitly increasing specific types of microorganisms.

ε-proteobacteria belonging to the *Sulfuricurvum* sp. were found to be a main constituent of the bacterial communities in all microcosms according to the DGGE (**Figure 5**) and the pyro sequencing assay showed that their relative abundance clearly increased in the NO_3- and NO_3+CH_4-amended microcosms and in the 28d controls (**Figure 3**; Table S1). These bacteria are common inhabitants of groundwater environments (Kodama and Watanabe, 2004; Bomberg et al., 2015) and it has recently been shown that *Sulfuricurvum denitrificans* use nitrate as electron acceptor. However, some species lack the common cytoplasmic membrane bound *Nar* nitrate reductase (Handley et al., 2014). In addition, Sievert et al. (2008) speculated that

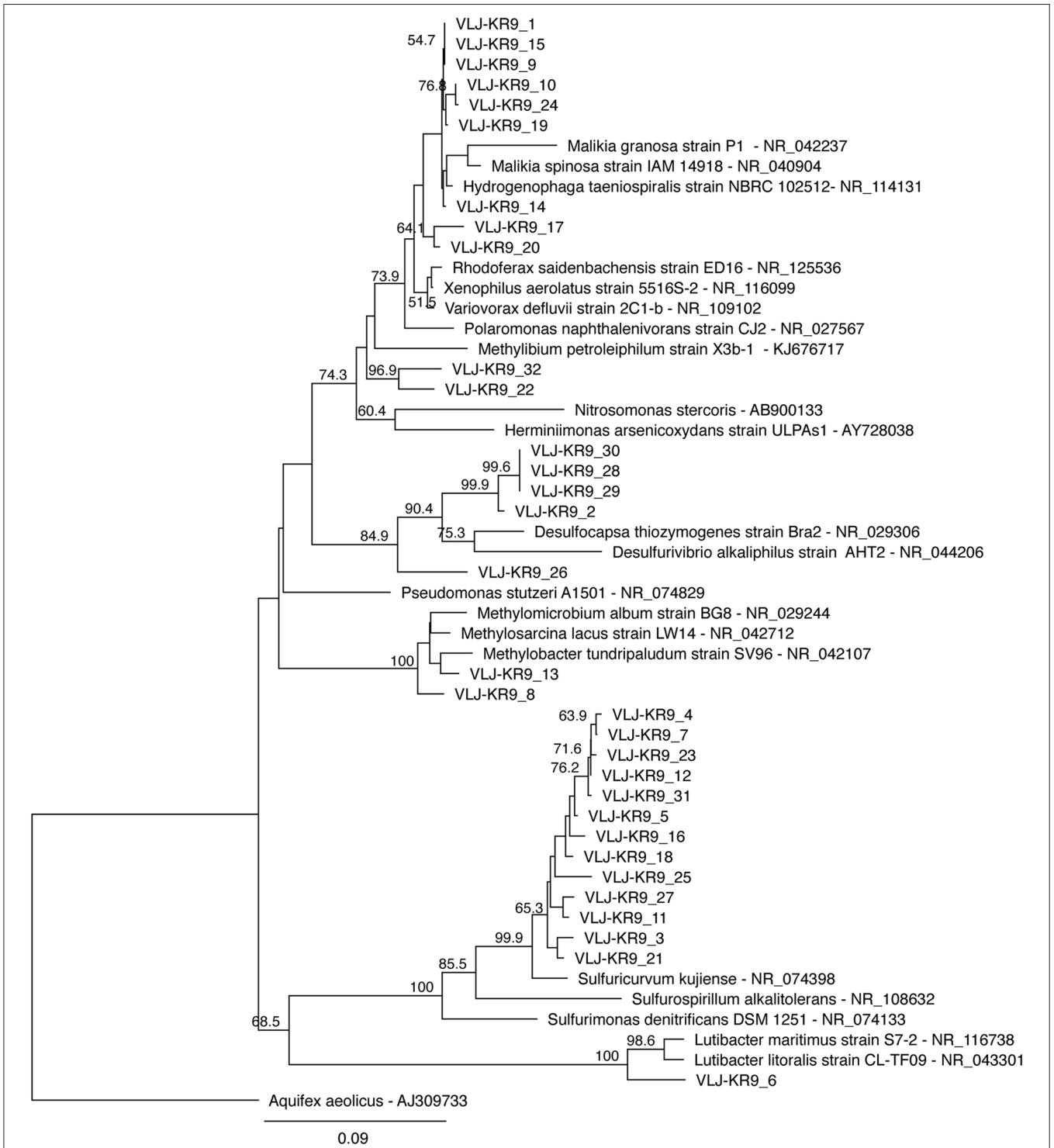

FIGURE 6 | A maximum likelihood tree displaying the sequences obtained from the 16S rRNA gene DGGE bands. The sequences of this study are designated with the identifier VLJ-KR9 and the number at the end of the identifier describes the isolated DGGE band, corresponding to the bands in **Figure 4**. Bootstrap support for nodes was calculated with 1000 random repeats; nodes with more than 50% support are indicated.

due to the lack of genes for nitrite ammonification (DNRA), *S. denitrificans* would have to incorporate ammonia from the environment. However, our results did not show any ε-proteobacterial enrichment in the ^{15}N DNA fraction in any of the treatments, indicating that they did not assimilate N from any N-substrates used here. Nevertheless, it should be noted

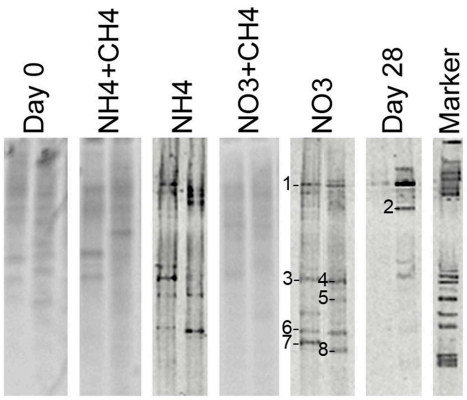

FIGURE 7 | Community profiles of PCR amplicons (*amo*A-targeted) from DNA of original groundwater (Day 0) and supplemented vs. control microcosms (Day 28). DGGE bands identified by sequencing are indicated by a number to the left of the band. The figure presents two replicate lanes out of 3 (Day 0 and Day 28) or 6 (NH_4+CH_4, NH_4, NO_3+CH_4, NO_3) replicate runs.

that we obtained very few sequences (24–180 reads per sample) from the ^{15}N-DNA fraction over all, and if ε-proteobacteria incorporated only low amounts of labeled N they may well have gone undetected in this assay. It is also possible that *Sulfuricurvum* sp. does not use nitrate of ammonium as N source, but only as energy source.

Bacterial taxa affiliating with the *Hydrogenophaga*/*Malikia* cluster (**Figure 6**) was another group that appeared to benefit from N-substrate supplementations, according to the DGGE analyses. In the 454 pyro sequencing *Hydrogenophaga*/*Malikia* bacteria were not detected from the original groundwater, but were the dominating bacteria found in all N-substrate amended microcosms (49.6–86.5% of the sequence reads) and their relative abundance in the 28d microcosms also increased (Table S1). *Hydrogenophaga* and *Malikia* species reduce nitrate to nitrite (Spring et al., 2005; Yoon et al., 2008). In addition, *Hydrogenophaga* are able to perform the DNRA process thus producing ammonia from nitrate (Yoon et al., 2008). However, as with *Sulfuricurvum* sp., *Hydrogenophaga/Malikia* sequences were undetectable in the

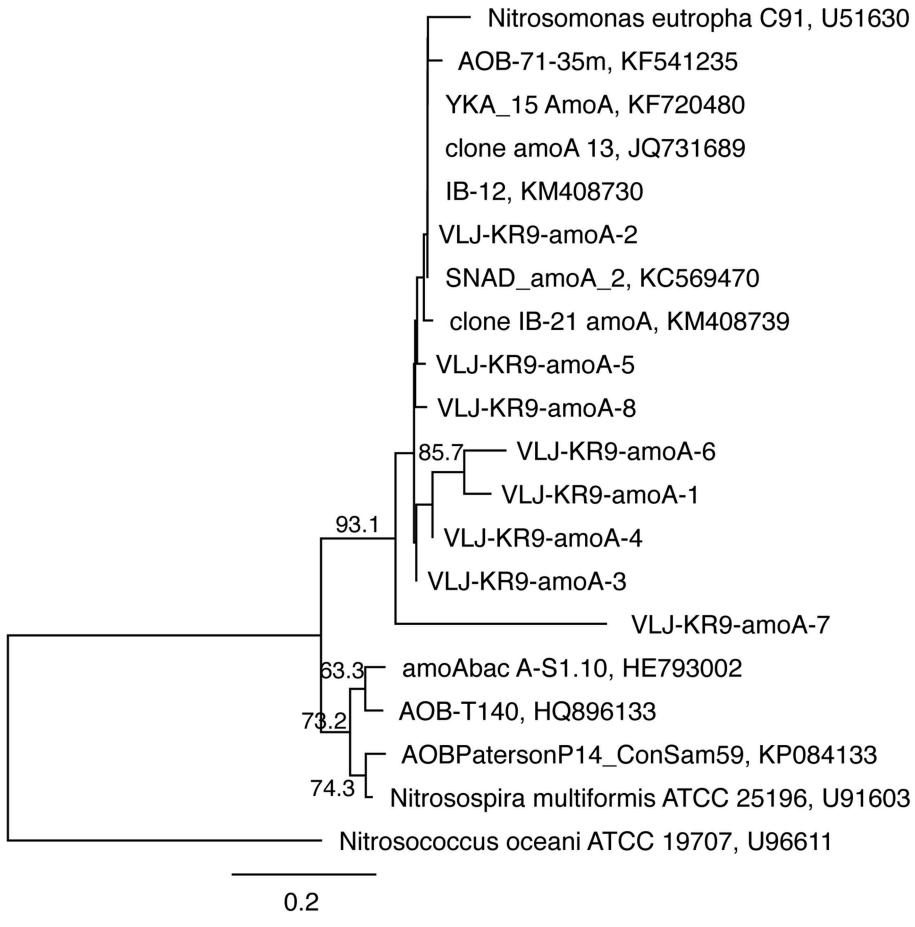

FIGURE 8 | The phylogenetic distribution of the *amo*A fragments detected in this study presented as a maximum likelihood tree. The gene sequences were translated into amino acid sequences prior to analysis. Bootstrap support for nodes was calculated with 1000 random repeats; nodes with more than 50% support are indicated. Sequences detected in this study are designated with the identifier VLJ-KR9-amoA; the number at the end of the identifier corresponds to the DGGE band indicated in **Figure 7**.

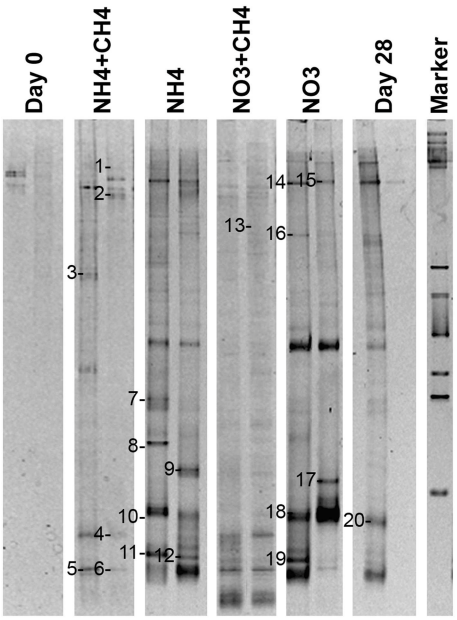

FIGURE 9 | Community profiles of PCR amplicons (*nar*G-targeted) from DNA of original groundwater (Day 0) and supplemented vs. control microcosms (Day 28). DGGE bands identified by sequencing are indicated by a number to the left of the band. The figure presents two replicate lanes out of 3 (Day 0 and Day 28) or 6 (NH_4+CH_4, NH_4, NO_3+CH_4, NO_3) replicate runs.

^{15}N-DNA fraction and may thus use other N sources that nitrate or ammonia.

Methylobacter sp. were found in all microcosms except the NO_3—amended ones according to the pyro sequencing profiles and in all microcosms that received NH_4+CH_4, NH_4, and NO_3+CH_4, i.e., in response to NH_4 and CH_4 according to DGGE (Table S1, **Figure 5**). Their relative abundance in the NH_4+CH_4– and NH_4–amended microcosms was 43.8 and 35.9% (**Figure 3**), respectively, and below 2.4% in the other treatments. In general, ammonia has been considered to inhibit methanotrophs. However, methanotrophic bacteria may oxidize ammonium to hydroxylamine using methane monooxygenase (Hanson and Hanson, 1996; Campbell et al., 2011) and in accordance with our results, Zhang et al. (2014) showed that the abundance of *Methylobacter* increased in landfill cover soil as a result of increased NH_4-N fertilization. Interestingly, Nyerges and Stein (2012) showed that ammonium had a distinct competitive effect on the oxidation of methane by methanotrophs.

The abundance of NRB increased in the microcosms during the incubations (**Figure 2B**). However, the ratio of *nar*G gene to bacterial 16S rRNA gene concentration was generally low. In addition to the membrane bound NAR enzyme many bacteria have a cytoplasmic NAP enzyme. Genes for this enzyme were not targeted in this study, i.e., we could detect only a part of the nitrate-reducing community. The detected *nar*G genes of NRB belonged to γ-proteobacterial *Pseudomonas* and β-proteobacterial *Methylibium*, *Alicycliphilus*, *Polaromonas, Herminiimonas,* and uncultured β-proteobacteria. *Methylibium* 16S rRNA gene sequences were not found in any treatment with either of the community profiling methods, although other Burkholderiales clades were detected. In contrast, *Pseudomonas* 16S rRNA genes or those of closely related groups were not found at all although *Pseudomonas* has been shown to be a major bacterial group at greater depth in Olkiluoto (Bomberg et al., 2015). *Polaromonas nar*G genes were detected in the NH_4+CH_4—amended and 28d control microcosms and similar DGGE bands were also faintly seen in most other samples. This is in accordance with the 454 pyro sequencing, which detected *Polaromonas* 16S rRNA gene sequences from all samples with the exception of the NH_4+CH_4—amended microcosms. It is possible that the *Polaromonas* escaped detection because the *Hydrogenophaga/Malikia* sequences were so dominating in this sample and the overall number of sequences obtained from this sample was low. *Herminiimonas nar*G were found only in the NH_4—amended microcosms, but their 16S rRNA gene sequences were detected in the NO_3+CH_4—amended microcosms. This is not surprising, because even in the sample where *Herminiimonas* was detected they were present at only 0.04% relative abundance (Table S1) indicating that they belong to the minority groups at this depth in Olkiluoto. The only N assimilating bacterial group for which a functional gene was also detected was the *Alicycliphilus*. *Alicycliphilus nar*G was detected in the NO_3—amended microcosms, but *Alicycliphilus* 16S rRNA genes were detected in the NH_4+CH_4 ^{15}N SIP fraction. It is possible that this group was present in the other treatments as well, but failed detection due to the overall low number of sequence reads obtained from the ^{15}N-DNA fractions.

The *nar*G gene specific primers we used here appear to have higher affinity to β- and γ-proteobacterial *nar*G genes than to those of the α- and ε-proteobacteria, which may lead to the α- and ε-proteobacteria being under-represented in this study (Nicolaisen and Ramsing, 2002). In addition, different primers were used for the *nar*G qPCR and *nar*G DGGE analyses, which may affect the detection efficiency to different *nar*G genes. In the *nar*G-qPCR assay the size of the produced amplicon was optimized for qPCR and was only 90 bp long. In order to increase sequence length a primer pair producing a 309 bp long amplicon was chosen for the *nar*G DGGE. However, the 90 bp long amplicon produced in the qPCR with primers *nar*G-1960m2f/*nar*G-2050m2F (López-Gutiérrez et al., 2004) have been shown to detect similar *nar*G sequences in Fennoscandian bedrock groundwater (Purkamo et al., 2015; Rajala et al., 2015a) as those detected with primers *nar*G-2179F/*nar*G2488R (Pastorelli et al., 2013) in this study.

*amo*A gene sequences were only obtained from the microcosms supplemented with NO_3 and from the unamended 28d controls and the rest of the sequences were unspecific. All *amo*A genes were similar to those of *Nitrosomonas* bacteria. Interestingly, *Nitrosomonas* 16S rRNA genes were not detected by DGGE or 454 pyro sequencing in any of the samples. However, other closely related Gallionellales groups were detected in all other treatments except the NH_4+CH_4—amended microcosms (Table S1), and the *amo*A genes between these groups may be similar to that of the *Nitrosomonas*. The number of AOB in

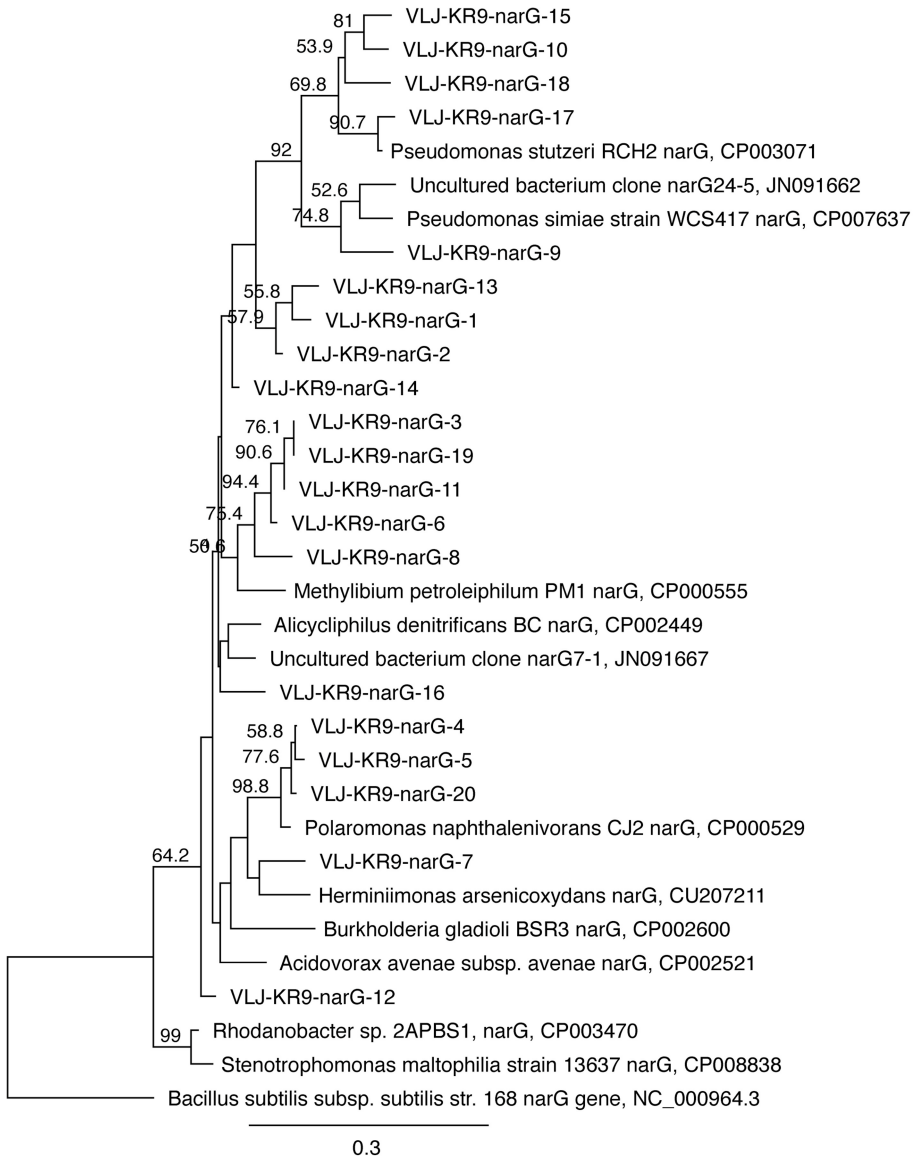

FIGURE 10 | The phylogenetic distribution of the *nar*G fragments detected in this study presented as a maximum likelihood tree. The gene sequences were translated into amino acid sequences prior to analysis. Bootstrap support for nodes was calculated with 1000 random repeats; nodes with more than 50% support are indicated. Sequences detected in this study are designated with the identifier VLJ-KR9-narG; the number at the end of the identifier corresponds to the DGGE band indicated in **Figure 9**.

deep crystalline bedrock groundwater overall is expected to be low, which was shown previously by Purkamo et al. (2015). The fact that *amo*A genes were only successfully detected in the NO_3-amended and 28d control microcosms is curious. It is, however, possible that the DGGE assay for *amo*A genes was not suitable for our sample matrix. We experienced some issues with the specificity of the primers used and in addition the DGGE bands obtained may have consisted of a mixture of amplicons. In the microcosms from which *amo*A gene fragments were successfully identified the number of interfering amplicons was probably lower and thus allowing us to detect clean sequences of the gene. Nevertheless, the AOB detected in this study in the NO_3-amended and 28d control microcosms may have benefited from the slowly released lower concentration ammonia in the NO_3—amended microcosms originating from the conversion of nitrate to ammonia through the DNRA process. In addition, it may also be possible that instead of typical ammonia oxidizers methanotrophic bacteria able to oxidize ammonium using their methane monooxygenase (Hanson and Hanson, 1996; Campbell et al., 2011) increased, and this group would not be detected by the *amo*A-gene targeted assays.

In the N-assimilating community, bacteria belonging to Rhizobiales genera were the most abundantly detected and were found in the ^{15}N DNA fraction in all of the treatments (**Figure 3**, Table S1). Rhizobiales represented 72 and 61% of the N-assimilating bacterial community in the in the NH_4- and NO_3-amended microcosms. In the microcosms that received CH_4 in addition to the N-substrates, their relative abundance in the N-assimilating community was lower, 4 and 35% in the NH_4+$CH_4$and NO_3+CH_4 treatments, respectively. In addition to Rhizobiales types, Burkholderiales were detected in the ^{15}N DNA fraction of all treatments, but was especially abundant in the NH_4+CH_4 incubations. Interestingly, in the original groundwater approximately 8% of the 16S rRNA gene sequence reads obtained by 454 sequencing belonged to Rhizobiales, while by the end of the incubation period Rhizobiales-related sequence reads decreased to <0.5%.

The pyro sequencing and DGGE assays used in this study generally produced similar profiles of the dominating bacterial taxa in the sample although the pyro sequencing provided much more detail as well as abundance information. While DGGE is a visual method for fast detection of microbial community profiles and is excellent for comparison of microbial community development between a low number of samples, it has some restrictions. It could be concluded from e.g., the present work and from other groundwater studies (e.g., Bomberg et al., 2014) that the method generally only presents the main groups of the community. In addition, many microbial groups dominating in a specific environment have been shown to go undetected by the DGGE method due to their incompatibility with the method of detection, low amounts of target template or high level of intra-species microdiversity, which makes optimization of the DGGE conditions very demanding (e.g., Costa et al., 2006; Alonso-Sáez et al., 2007; Sánchez et al., 2009). This was the case also here, where the DGGE failed to detect e.g., the *Parcubacteria* present at high relative abundance in both the original groundwater and the 28d incubation control (Table S1). However, the pyro sequencing approach failed to detect *Sulfuricurvum* in the original groundwater and the NH_4+CH_4-supplemented microcosms, although they were found in all samples according to the DGGE analysis.

The primers chosen for a study may also greatly affect the results. In this study we showed that microbial profile results depend on the detection method and primers used for characterizing microbial communities. For example the primers U968fGC/U1401r (Nübel et al., 1996) used for DGGE detected *Desulfocapsa* in the 28d incubation controls, but the primers 8F (Edwards et al., 1998) and P2 (Muyzer et al., 1993) used for 454-pyrosequencing did not.

Conclusions

The bacterial community of groundwater from 100 m depth in the VLJ-cave situated in the crystalline bedrock of the Fennoscandian Shield was affected by ammonia and nitrate supplementation. The bacterial population increased when N compounds were available, enriching specific bacterial groups. Known NRB belonging to ε-proteobacterial *Sulfuricurvum* and β-proteobacterial *Hydrogenophaga/Malikia* clades were greatly enriched when groundwater microcosms were supplemented with ammonium or nitrate with or without methane. *Methylobacter* was enriched in microcosms that had received ammonium with and without the addition of methane, indicating that the *Methylobacter* may also oxidize ammonia. In addition, it was demonstrated that bacterial clades belonging to Rhizobiales and Burkholderiales from nitrogen-poor deep crystalline bedrock groundwater were able to assimilate N from added nitrate and ammonium substrates. Here, the study of the N cycle in crystalline bedrock groundwater was restricted to specific enzymes of specific bacterial groups. In future investigations the N cycling genes of different taxonomic groups as well as different enzymes, such as the soluble nitrate reductase NAP, should be included. It would also be of value to investigate the N_2 fixation and anaerobic ammonia oxidation (ANAMMOX) and archaeal ammonia oxidation in order to obtain a complete picture of the N cycle in deep crystalline bedrock environments. Nevertheless, we show here that despite the low abundance of N cycling bacteria in the pristine groundwater of Olkiluoto, N assimilating, ammonia oxidizing and nitrate reducing bacteria increase when the concentration of ammonia and nitrate increase, which may influence the long-term safety of the underground repository for low and intermediate level radioactive waste.

Author Contributions

HK, PR, LC, and MB conceived, designed and performed the experiments, analyzed the data and wrote the paper.

Funding

The work was performed on funding provided by the Finnish Research Program on Nuclear Waste Management 2011–2014 (project MICCU), and the Academy of Finland (project 261220).

Acknowledgments

The assistance of the staff of TVO Olkiluoto Nuclear Power Plant during sampling is gratefully acknowledged.

Supplementary Material

The Supplementary Material for this article can be found online at: http://journal.frontiersin.org/article/10.3389/fmicb.2015.01079

References

Alonso-Sáez, L., Balagué, V., Sà, E. L., Sánchez, O., González, J. M., Pinhassi, J., et al. (2007). Seasonality in bacterial diversity in north-west Mediterranean coastal waters: assessment through clone libraries, fingerprinting and FISH. *FEMS Microbiol. Ecol.* 60, 98–112. doi: 10.1111/j.1574-6941.2006.00276.x

Beller, H. R., Madrid, V., Hudson, G. B., McNab, W. W., and Carlsen, T. (2004). Biogeochemistry and natural attenuation of nitrate in groundwater at an explosives test facility. *Appl. Geochem.* 19, 1483–1494. doi: 10.1016/j.apgeochem.2003.12.010

Bomberg, M., Nyyssönen, M., Nousiainen, A., Hultman, J., Paulin, L., Auvinen, P., et al. (2014). Evaluation of molecular techniques in characterization of deep terrestrial biosphere. *Open J. Ecol.* 4, 468–487. doi: 10.4236/oje.2014.48040

Bomberg, M., Nyyssönen, M., Pitkänen, P., Lehtinen, A., and Itävaara, M. (2015). Active microbial communities inhabit sulphate-methane interphase in deep bedrock fracture fluids in Olkiluoto, Finland. *BMRI* 2015:979530. doi: 10.1155/2015/979530

Bothe, H., Ferguson, S. J., and Newton, W. E. (2007). *Biology of Nitrogen Cycle*. Amsterdam: Elsevier Science.

Buckley, D. H., Huangyutitham, V., Hsu, S. F., and Nelson, T. A. (2007). Stable isotope probing with ^{15}N achieved by disentangling the effects of genome G+C content and isotope enrichment on DNA density. *Appl. Environ. Microbiol.* 73, 3189–3195. doi: 10.1128/AEM.02609-06

Campbell, B. J., Engel, A. S., Porter, M. L., and Takai, K. (2006). The versatile epsilon-proteobacteria: key players in sulphidic habitats. *Nat. Rev. Microbiol.* 4, 458–468. doi: 10.1038/nrmicro1414

Campbell, M. A., Nyerges, G., Kozlowski, J. A., Poret-Peterson, A. T., Stein, L. Y., and Klotz, G. M. (2011). Model of the molecular basis for hydroxylamine oxidation and nitrous oxide production in methanotrophic bacteria. *FEMS Microbiol. Lett.* 322, 82–89. doi: 10.1111/j.1574-6968.2011.02340.x

Costa, R., Götz, M., Mrotzek, N., Lottmann, J., Berg, G., and Smalla, K. (2006). Effects of site and plant species on rhizosphere structure revealed by molecular analysis of microbial guilds. *FEMS Microbiol. Ecol.* 56, 236–249. doi: 10.1111/j.1574-6941.2005.00026.x

D'Hondt, S., Rutherford, S., and Spivack, A. (2002). Metabolic activity of subsurface life in deep-sea sediments. *Science* 295, 2067–2070. doi: 10.1126/science.1064878

Edwards, U., Rogall, T., Blöcker, H., Emde, M., and Böttger, E. C. (1998). Isolation and direct complete nucleotide determination of entire genes. Characterization of a gene coding for 16S ribosomal RNA. *Nucleic Acids Res.* 17, 7843–53. doi: 10.1093/nar/17.19.7843

Guidon, S., and Gascuel, O. (2003). A simple, fast, and accurate algorithm to estimate large phylogenies by maximum likelihood. *Syst. Biol.* 52, 696–704. doi: 10.1080/10635150390235520

Handley, K. M., Bartels, D., O'Loughlin, E. J., Williams, K. H., Trimble, W. L., Skinner, K., et al. (2014). The complete genome sequence for putative H2-and S-oxidizer *Candidatus Sulfuricurvum* sp., assembled de novo from an aquifer-derived metagenome. *Environ. Microbiol.* 16, 3443–3462. doi: 10.1111/1462-2920.12453

Hanson, R., and Hanson, T. (1996). Methanotrophic bacteria. *Microbiol. Rev.* 60, 439–471.

Iker, B. C., Kambesis, P., Oehrle, S. A., Groves, C., and Barton, H. A. (2010). Microbial atrazine breakdown in a karst groundwater system and its effect on ecosystem energetics. *J. Environ. Qual.* 19, 509–518. doi: 10.2134/jeq 2009.0048

Jukes, T. H., and Cantor, C. R. (1969). "Evolution of protein molecules," in *Mammalian protein metabolism*, ed H. N. Munro (New York, NY: Academic Press), 21–123.

Kodama, Y., and Watanabe, K. (2004). *Sulfuricurvum kujiense* gen. nov., sp. nov., a facultatively anaerobic, chemolithoautotrophic, sulfur-oxidizing bacterium isolated from an underground crude-oil storage cavity. *ISME J.* 54, 2297–2300. doi: 10.1099/ijs.0.63243-0

López-Gutiérrez, J., Henry, S., Hallet, S., Martin-Laurent, F., Catroux, G., and Philippot, L. (2004). Quantification of a novel group of nitrate-reducing bacteria in the environment by real-time PCR. *J. Microbiol. Methods* 57, 399–407. doi: 10.1016/j.mimet.2004.02.009

Luque-Almagro, V. M., Gates, A. J., Moreno-Vivián, C., Ferguson, S. J., Richardson, D. J., and Roldan, M. D. (2011). Bacterial nitrate assimilation: gene distribution and regulation. *Biochem. Soc. Trans.* 39, 1838–1843. doi: 10.1042/BST20110688

Muyzer, G., de Waal, E. C., and Uitterlinden, A. G. (1993). Profiling of complex microbial populations by denaturing gradient gel electrophoresis analysis of polymerase chain reaction-amplified genes coding for 16S rRNA. *Appl. Environ. Microbiol.* 59, 695–700.

Nicolaisen, M., and Ramsing, N. (2002). Denaturing gradient gel electrophoresis (DGGE) approaches to study the diversity of ammonia-oxiding bacteria. *J. Microbiol. Methods* 50, 189–203. doi: 10.1016/S0167-7012(02)00026-X

Nübel, U., Engelen, B., Felske, A., Snaidr, J., Wieshuber, A., Amann, R. I., et al. (1996). Sequence heterogeneities of genes encoding 16S rRNAs in *Paenibacillus polymyxa* detected by temperature gradient gel electrophoresis. *J. Bacteriol.* 78, 5636–5643.

Nyerges, G., and Stein, L. Y. (2012). Ammonia cometabolism and product inhibition vary considerably among species of methanotrophic bacteria. *FEMS Microbiol. Ecol. Lett.* 297, 131–136. doi: 10.1111/j.1574-6968.2009.01674.x

Nyyssönen, M., Hultman, J., Ahonen, L., Kukkonen, I., Paulin, L., Laine, P., et al. (2014). Taxonomically and functionally diverse microbial communities in deep crystalline rocks of the Fennoscandian Shield. *ISME J.* 8, 126–138. doi: 10.1038/ismej.2013.125

Pastorelli, R., Piccolo, R., Simoncini, S., and Landi, S. (2013). New Primers for Denaturing gradient gel electrophoresis analysis of nitrate-reduction bacterial community in soil. *Pedoshere* 23, 340–349. doi: 10.1016/S1002-0160(13) 60025-9

Pedersen, K. (2008). Numbers, biomass and cultivable diversity of microbial populations relate to depth and borehole-specific conditions in groundwater from depths of 4–450 min Olkiluoto, Finland. *ISME J.* 2, 760–775. doi: 10.1038/ismej.2008.43

Posiva. (2009). *Olkiluoto Site Description 2008, Part 1*. Report POSIVA 2009–01, Posiva Oy.

Pruesse, E., Quast, C., Knittel, K., Fuchs, B. M., Ludwig, W., Peplies, J., et al. (2007). SILVA: a comprehensive online resource for quality checked and aligned ribosomal RNA sequence data compatible with ARB. *Nucleic Acids Res.* 35, 7188–7196. doi: 10.1093/nar/gkm864

Purkamo, L., Bomberg, M., Nyyssönen, M., Kukkonen, I., Ahonen, L., and Itävaara, M. (2015). Heterotrophic communities supplied by ancient organic carbon predominate in deep fennoscandian bedrock fluids. *Microb. Ecol.* 69, 319–332. doi: 10.1007/s00248-014-0490-6

Rajala, P., Bomberg, M., Kietäväinen, R., Kukkonen, I., Ahonen, L., Nyyssönen, M., et al. (2015a). Deep subsurface microbes rapidly reactivate in the presence of C-1 Compounds. *Microorganisms* 3, 17–33. doi: 10.3390/microorganisms3010017

Rajala, P., Carpén, L., Vepsäläinen, M., Raulio, M., Sohlberg, E., and Bomberg, M. (2015b). Microbially induced corrosion of carbon steel in deep groundwater environment. *Front. Microbiol.* 6:647. doi: 10.3389/fmicb.2015.00647

Ray, K., Painter, R., and Byl, T. (2010). *Ammonia Oxidation by Bacteria Collected from a Karst-Bedrock Well*. USGS Scientific Investigations Report 2008–5023, U.S. Geological Survey.

Rinke, C., Schwientek, P., Sczyrba, A., Ivanova, N. N., Anderson, I. J., Cheng, J.-F., et al. (2012). Insights into the phylogeny and coding potential of microbial dark matter. *Nature* 499, 431–437. doi: 10.1038/nature12352

Sánchez, O., Gasol, J. M., Balagué, V., Massana, R., Mas, J., and Pedrós-Alió, C. (2009). Influence of primer mismatch and microdiversity on DGGE results: a case study with SAR11. *Aquat. Microb. Ecol.* 54, 211–216. doi: 10.3354/ame01267

Schloss, P. D., Westcott, S. L., Ryabin, T., Hall, J. R., Hartmann, M., Hollister, E. B., et al. (2009). Introducing MOTHUR: open-source, platform-independent, community-supported software for describing and comparing microbial communities *Appl. Environ. Microbiol.* 75, 7537–7541. doi: 10.1128/AEM.01541-09

Sievert, S. M., Scott, K. M., Klotz, M. G., Chain, P. S., Hauser, L. J., Hemp, J., et al. (2008). Genome of the epsilonproteobacterial chemolithoautotroph *Sulfurimonas denitrificans*. *Appl. Environ. Microbiol.* 74, 1145–1156. doi: 10.1128/AEM.01844-07

Spring, S., Wagner, M., Schumann, P., and Kämpfer, P. (2005). *Malikia granosa* gen. nov., sp. nov., a novel polyhydroxylalkanoate- and polyphosphate-accumulating bacterium isolated from activated sludge, and reclassification of *Pseudomonas spinosa* as *Malikia spinosa* comb. nov. *Int. J. Syst. Evol. Microbiol.* 55, 621–629. doi: 10.1099/ijs.0.63356-0

Wang, F., Zhou, H., Meng, J., Peng, X., Jiang, L., Sun, P., et al. (2009). GeoChip-based analysis of metabolic diversity of microbial communities at the Juan de Fuca Ridge hydrothermal vent. *Proc. Natl. Ac. Sci. U.S.A.* 106, 4840–4845. doi: 10.1073/pnas.0810418106

Weisburg, W. G., Barns, S. M., Pelletier, D. A., and Lane, D. J. (1991). 16S ribosomal DNA amplification for phylogenetic study. *J. Bacteriol.* 173, 697–703.

Whelan, S., and Goldman, N. (2001). A general empirical model of protein evolution derived from multiple protein families using a maximum-likelihood approach. *Mol. Biol. Evol.* 18, 691–699. doi: 10.1093/oxfordjournals.molbev.a003851

Yoon, K.-S., Tsukada, N., Sakai, Y., Ishii, M., Igarashi, Y., and Nishihara, H. (2008). Isolation and characterization of a new facultatively autotrophic hydrogen-oxidizing Betaproteobacterium, *Hydrogenophaga* sp. AH-24. *FEMS Microbiol. Lett*. 278, 94–100. doi: 10.1111/j.1574-6968.2007.00983.x

Zhang, X., Kong, J.-Y., Xia, F.-F., Su, Y., and He, R. (2014). Effects of ammonium on the activity and community of methanotrophs in landfill biocover soils. *Syst. Appl. Microbiol*. 37, 296–304. doi: 10.1016/j.syapm.2014.03.003

Conflict of Interest Statement: The authors declare that the research was conducted in the absence of any commercial or financial relationships that could be construed as a potential conflict of interest.

frontiers in Microbiology

REVIEW
published: 17 July 2015
doi: 10.3389/fmicb.2015.00725

The origin, source, and cycling of methane in deep crystalline rock biosphere

Riikka Kietäväinen[1]* *and Lotta Purkamo*[2]*

[1] Geological Survey of Finland, Espoo, Finland, [2] VTT Technical Research Centre of Finland, Espoo, Finland

The emerging interest in using stable bedrock formations for industrial purposes, e.g., nuclear waste disposal, has increased the need for understanding microbiological and geochemical processes in deep crystalline rock environments, including the carbon cycle. Considering the origin and evolution of life on Earth, these environments may also serve as windows to the past. Various geological, chemical, and biological processes can influence the deep carbon cycle. Conditions of CH_4 formation, available substrates and time scales can be drastically different from surface environments. This paper reviews the origin, source, and cycling of methane in deep terrestrial crystalline bedrock with an emphasis on microbiology. In addition to potential formation pathways of CH_4, microbial consumption of CH_4 is also discussed. Recent studies on the origin of CH_4 in continental bedrock environments have shown that the traditional separation of biotic and abiotic CH_4 by the isotopic composition can be misleading in substrate-limited environments, such as the deep crystalline bedrock. Despite of similarities between Precambrian continental sites in Fennoscandia, South Africa and North America, where deep methane cycling has been studied, common physicochemical properties which could explain the variation in the amount of CH_4 and presence or absence of CH_4 cycling microbes were not found. However, based on their preferred carbon metabolism, methanogenic microbes appeared to have similar spatial distribution among the different sites.

Keywords: abiotic methane, deep subsurface, Precambrian bedrock, carbon cycle, methanogenesis, methanotrophy, isotopic fractionation

OPEN ACCESS

Edited by:
Paul Bodelier, Netherlands Institute of Ecology (NIOO-KNAW), Netherlands

Reviewed by:
Tillmann Lueders, Helmholtz Zentrum München, Germany
Sascha M. B. Krause, University of Washington, USA

***Correspondence:**
Riikka Kietäväinen, Geological Survey of Finland, PO Box 96, 02151 Espoo, Finland
riikka.kietavainen@gtk.fi;
Lotta Purkamo, VTT Technical Research Centre of Finland, Tietotie 2, 02044 VTT, Espoo, Finland
lotta.purkamo@vtt.fi

Specialty section:
This article was submitted to Terrestrial Microbiology, a section of the journal Frontiers in Microbiology

Received: *09 April 2015*
Accepted: *02 July 2015*
Published: *17 July 2015*

Citation:
Kietäväinen R and Purkamo L (2015) The origin, source, and cycling of methane in deep crystalline rock biosphere. Front. Microbiol. 6:725. doi: 10.3389/fmicb.2015.00725

Introduction and Historical Perspective

Methane is a key compound in the global carbon cycle. In the shallow subsurface CH_4 is mainy produced by anaerobic digestion of organic matter. Deeper in the geological strata CH_4 is found in large quantities within sedimentary formations and unconventional resources, such as shale gas, have also proven to be important reserves of CH_4 (Arthur and Cole, 2014). Other sources of CH_4 include methane hydrates and clathrates in deep lake sediments and seafloor (Walter et al., 2006; Ruppel, 2011; Kretschmer et al., 2015; Treat et al., 2015). In addition, CH_4 is a dominant gas in many Precambrian continental bedrock formations (Fritz et al., 1987; Karus et al., 1987; Nurmi et al., 1988; Sherwood Lollar et al., 1993a,b; Ward et al., 2004; Sherwood Lollar et al., 2006; Pitkänen and Partamies, 2007; Hallbeck and Pedersen, 2008a; Stotler et al., 2010; Kietäväinen et al., 2013, 2014).

Table 1 describes the carbon geochemistry of several continental study sites in Fennoscandia, South Africa, and North America within the depth range from few hundred meters down to 3.4 km. Microbes involved in methane cycling have been detected in many of these sites.

The emerging interest in using stable bedrock formations for industrial purposes (e.g., nuclear waste disposal sites or carbon dioxide or natural gas storages) has increased the need for understanding the complete carbon cycling scheme in deep crystalline rock environments. CH_4 can have effects on industrial utilization of the deep bedrock: It can promote growth of microorganisms in the subsurface by providing an ample source of energy and carbon. Increased microbial activity can lead to pH changes inducing corrosion and alteration of geochemistry resulting to mineral precipitation and scaling, or mobilization of hazardous compounds such as radiocarbon, thus damaging the infrastructure or imposing a risk to the environment. Therefore, research has been conducted for several years for example related to the long-term geological disposal of spent nuclear fuel to deep subsurface facilities in Canada, Sweden, USA, Finland, and Belgium (Stroes-Gascoyne and West, 1996; Pedersen, 1996; Fredrickson et al., 2004; Wang and Francis, 2005; Nyyssönen et al., 2012; Wouters et al., 2013). These studies have provided not only an understanding of the microbial risks, but also knowledge of the active microbial communities living in deep geological surroundings. However, many aspects of origin, source, and cycling of CH_4 in deep continental bedrock environments still remain poorly understood. These include sources of carbon and hydrogen in different rock formations, importance of microbial involvement, timescales and quantities of CH_4 production, and movements within and fluxes from bedrock.

Potential formation pathways of CH_4 in deep crystalline bedrock are presented in **Figure 1**. In principle, hydrocarbons can form via two major ways: from break-up of organic matter ("from big to small") or due to organic synthesis of small C and H bearing molecules and further polymerization of these molecules into higher hydrocarbons ("from small to big"). The first way includes the formation of thermogenic CH_4 and microbial aceticlastic methanogenesis. The latter includes abiotic organic synthesis, such as Fischer-Tropsch or Sabatier type reactions, and microbial hydrogenotrophic methanogenesis. Thus, both ways can be facilitated by microorganisms but may also occur inorganically. Not only is CH_4 produced but is also consumed within bedrock by anaerobic and aerobic processes with and without microorganisms.

The occurrence and major sources for abiotic CH_4 was discussed in a recent review by Etiope and Sherwood Lollar (2013) and microbial biodiversity in terrestrial subsurface environments by Fredrickson and Balkwill (2006). Yet it has been over a decade since the microbial CH_4 cycling in deep subsurface has been reviewed (Kotelnikova, 2002). Since then the scientific community has been pushing the understanding of deep carbon cycling to new frontiers. Recent advances in molecular biological methods, such as high-throughput sequencing and "omics" methods have expanded the knowledge of microbial community composition and functions in the deep biosphere (Teske and Biddle, 2008; Brazelton et al., 2012; Nyyssönen et al., 2014). The development of new computational methods for processing, mining and assessing metagenomic data has provided tools for handling the vast amount of data generated (e.g., Schloss et al., 2009; Caporaso et al., 2010; Langille et al., 2013). Some novel methods have been used to assess the microbial ecology of the deep terrestrial subsurface. For example, a single-species ecosystem fully independent from surface life and photosynthesis, gaining energy from sulfate reduction was discovered at 2.8 km depth from South African gold mine in 2008 by Chivian et al. with metagenomics approach (Chivian et al., 2008). Nyyssönen et al. (2014) used high-throughput amplicon sequencing and metagenomics for characterization of the 2.5 km Outokumpu Deep Drill Hole microbial communities in Finland.

In this review we aim to revise methane cycling within continental bedrock, as well as to provide an overview of methodological and conceptual advances in this field with an emphasis on microbiology. Diversity and variation of geochemical and microbiological characteristics in CH_4 containing deep bedrock environments are introduced through several case studies. Finally, we point out some key remaining unknowns and give suggestions for further research.

Geological Methane

Two main types of geological CH_4 are depicted in **Figure 1** which summarizes CH_4 cycling in the continental deep biosphere. Of these, thermogenic CH_4 is formed from the break-up of organic matter at elevated temperatures and pressures. This is thought to be the dominant CH_4 type in sedimentary basins and is the economically most important source of natural gas (e.g., Galimov, 1988; Milkov, 2011). However, even though some rocks found in continental shields, most notably black schists, also originate from organic rich material, the occurrence and preservation of "fossil" organic compounds in highly metamorphosed crystalline rocks is questionable (but see Karus et al., 1987 and Taran et al., 2011 for examples of organic compounds such as bitumen found in metamorphic and even igneous rocks of Archaean to Proterozoic age). Instead, carbon is mostly found in the form of graphite and carbonate minerals. Thus, and taking into account the low temperatures presently prevailing in continental shield sites (**Table 1**), any thermogenic CH_4 component would likely be relic. Where hydrocarbon-bearing sedimentary formations are nearby, thermogenic CH_4 may find its way into metamorphic and igneous rocks by diffusion or advective flow (Etiope and Martinelli, 2002 and references therein).

Probably the more important source of geological CH_4 in crystalline bedrock environments is abiotic. This refers to CH_4 that has formed from inorganic compounds without the involvement of biological activity. Abiotic CH_4 can be either magmatic or produced in water-rock reactions, the latter of which may take place even at low temperatures and pressures (Etiope and Sherwood Lollar, 2013). Within the habitable zone in the upper crust, high temperature abiotic CH_4 may be provided by a gas flux from deeper, hotter regions (**Figure 1**) or leak from fluid inclusions. However, abiotic CH_4 can also potentially form *in situ* in low temperature processes which include Sabatier and

TABLE 1 | Characteristics of deep Precambrian continental bedrock sites where microbes contributing to the methane cycle have been studied.

Site	Main rock types	Age (rock)	Depth[1]	T[1]	pH	Salinity[1]	CH_4^1	CH_4^1	$\delta^{13}C_{CH4}$	$\delta^2H^2_{CH4}$	$\delta^{13}C_{DIC}$	DIC	TOC	DOC	Methane-cycling microbes[6]	References[7]
		Ma	mbs	°C		TDS g L^{-1}	mM	Vol-%	‰ VPDB	‰ VSMOW	‰ VPDB	mM	mM	mM		
CANADA																
Lupin	Metagraywacke, slate, banded iron formation	2600	1130	11	7.9 …9.2	40	35	86.7	−56.1 …−42.4	−340/−324	−5.2 …10.5	0.088 …0.21	0.12 …0.33	0.15 …0.36	ND	26, 37, 38
FINLAND																
Hästholmen	Rapakivi granite	1630	985		6.8 …8.5	31.8	0.009	0.09	−63 …−28		−21.5 …−11.5	0.38 …2.22	0.30 …0.34	0.08 …0.82	ND	10, 20
Kivetty	Granite, granodiorite	1880	855		7.8 …9.0	0.23	0.006	0.09	−75.5 …−15		−24.2 …−18.3	0.99 …2.15	0.18	0.14 …1.27	ND	2, 10, 32
Olkiluoto	Migmatitic gneiss, mica gneiss, granite	1850	960	20	7.8 …8.3	84	41.4	80.5	−63.5 …−22.4	** [3]		0.04 …5.9	0.12 …0.14		MG, MT, ANME	3, 10, 24, 30
Outokumpu	Mica schist, black schist, granodiorite, serpentinite	1900	2480	40	8.4 …10.1	68.9	32.3	80	−31.2 …−24.4	−283/−279					MG, MT	11, 15, 25, 33, 34, 35
Palmottu	Garnet-cordierite gneiss, granite	1900	417		6.2 …9.4	1.6					−28.6 …−6.1	0.5 …3[4]			ND	1, 12, 29
Romuvaara	Tonalite gneiss	2700	566		8.4	0.17	0.003	0.2	−59.5 …−37			1.85	1.05		ND	10, 31
SOUTH AFRICA																
Beatrix	Conglomerate, quartzite	2900	1390	40	7.7 …7.9		35.2	89.6	−52.8 …−43.5	−195/−214	−32	0.34	0.14 …0.18	0.14	MG	4, 6, 18, 39
Driefontein	Andesite, quartzite	2700	3300	43	6.0 …7.4		17.5		−55.5 …−40.2	−218/−368	−17.8 …−8.0	0.41 …0.57	0.40 …1.83	0.67	MG, ANME	4, 6, 18, 22, 23, 36
Evander	Conglomerate, quartzite	2900	2230	45	7.2 …8.6		15.8	78.8	−61.2 …−40.7	−211/−281			0.22 …0.61		MG, ANME	6, 18, 39
Kloof	Andesite	2700	3400	59	7.6 …8.5		29.8	57.3	−40 …−28.7	−253/−300	−14.7	0.02[5]	0.46 …1.67		ND	14, 18, 36, 39
Mponeng	Metabasalt	2700	3300	52	9.3		20		−33.2 …−27.8	−390/−349			0.43		MG	6, 18, 19, 36
SWEDEN																
Äspö	Granite, granodiorite	1800	860	20	6.8 …7.8	16	1					0.16 …0.34[4]	0.11 …0.57	0.025 …1.5	MG, MT	5, 7, 13, 16, 17, 28
Forsmark	Meta-granite	1900	1002		7.3 …8.3	15	0.21					0.04 …1.5[4]		0.12 …0.13	MG, MT	5, 7, 9
Laxemar	Granite, quartz monzodiorite	1800	922	20	7.5 …8.4	18	0.039	1.4				0.13 …5.4[4]	0.12 …1.67	0.12 …1.75	MG	7, 8, 9, 28
USA																
Homestake, SURF	Metasediments	2000	1478	33	6.6 …8.5		0.00037								MG, MT	21, 27

[1] *Maximum values are given for depth, temperature (T), salinity and CH_4 concentration.*

[2] *For the same samples as min. and max. values of $\delta^{13}C_{CH4}$.*

[3] *Not determined for these particular samples. Overall range of δ^2H_{CH4} in Olkiluoto is from −309 to −175 ‰ VSMOW.*

[4] *HCO_3^- concentration.*

[5] *TIC.*

[6] *ND, not detected; MG, methanogens; MT, aerobic methanotrophs; ANME, anaerobic methanotrophs.*

[7] *[1] Ahonen et al., 2004, [2] Anttila et al., 1999, [3] Bomberg et al., 2015, [4] Borgonie et al., 2011, [5] Chi Fru, 2008, [6] Gihring et al., 2006, [7] Hallbeck and Pedersen, 2008a, [8] Hallbeck and Pedersen, 2008b, [9] Hallbeck and Pedersen, 2012, [10] Haveman et al., 1999, [11] Itävaara et al., 2011a, [12] Kaija et al., 1998, [13] Kalyuzhnaya et al., 1999, [14] Kieft et al., 2005, [15] Kietäväinen et al., 2013, [16] Kotelnikova and Pedersen, 1997, [17] Kotelnikova and Pedersen, 1998, [18] Lin et al., 2005a, [19] Lin et al., 2006b, [20] Luukkonen et al., 1999, [21] Morelli et al., 2010 and references therein, [22] Moser et al., 2003, [23] Moser et al., 2005, [24] Nyyssönen et al., 2012, [25] Nyyssönen et al., 2014, [26] Onstott et al., 2009, [27] Osburn et al., 2014, [28] Pedersen and Ekendahl, 1990, [29] Pedersen and Haveman, 1999, [30] Pitkänen and Partamies, 2007, [31] Pitkänen et al., 1996, [32] Pitkänen et al., 1998, [33] Purkamo et al., 2013, [34] Purkamo et al., 2015, [35] Rajala et al., 2015, [36] Sherwood Lollar et al., 2006, [37] Stotler et al., 2009, [38] Stotler et al., 2010, [39] Ward et al., 2004.*

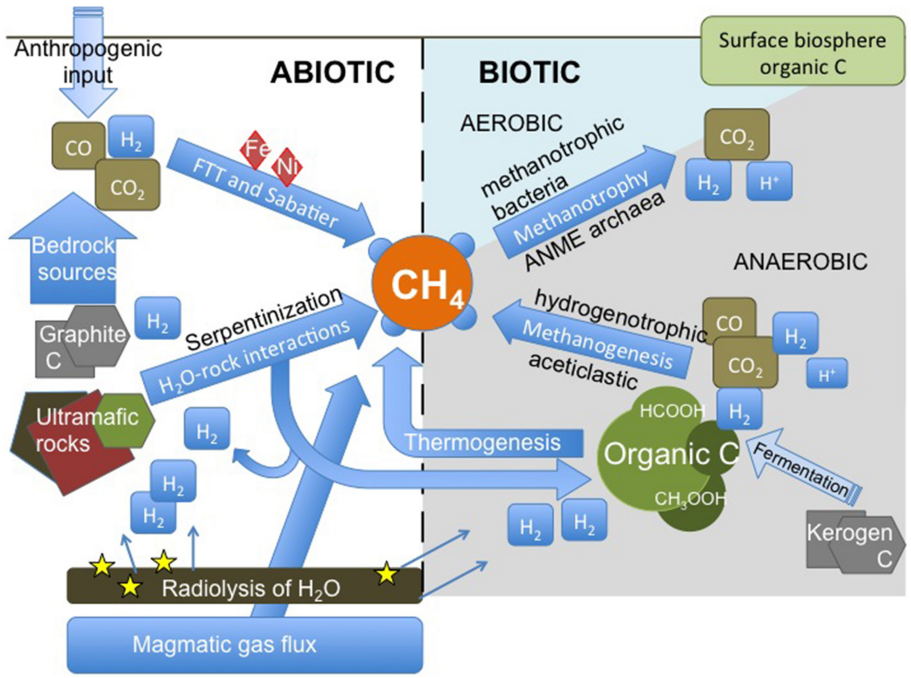

FIGURE 1 | Methane cycling scheme in the deep continental biosphere. Methane can originate either from low temperature abiotic reactions in the upper crust, as a gas flux deeper from the crust or mantle or as a result of microbial activity. CO_2 and organic matter are common carbon sources, while hydrogen can be derived from breakdown of water in radiolysis, from water-rock interactions or from microbial metabolism. Biological consumption of CH_4 can be divided to aerobic and anaerobic methane oxidation, the former being more abundant in shallower depths and the latter in greater depths. Hydrogenotrophic methanogens use inorganic carbon for the production of CH_4, as aceticlastic or methylotrophic methanogens use organic carbon molecules, such as formate or acetate. Bacterial fermentation of complex carbon-containing materials, such as kerogen, may produce hydrogen and small organic molecules for methanogens. FTT, Fischer-Tropsch type synthesis of hydrocarbons; ANME archaea, anaerobic methanotrophic archaea.

Fischer-Tropsch type (FTT) synthesis of CH_4 (Jacquemin et al., 2010; McCollom et al., 2010; Etiope and Sherwood Lollar, 2013; Zhang et al., 2013). These reactions are most likely catalyzed by metals, such as Fe and Ni or certain mineral phases, such as clay minerals (Jacquemin et al., 2010; McCollom et al., 2010; McCollom, 2013; Etiope and Ionescu, 2014). More detailed description of the possible mechanisms of abiotic CH_4 formation can be found in recent reviews by Etiope and Sherwood Lollar (2013) and McCollom (2013).

Microbial Contribution to CH_4 Budget in the Bedrock

Methanogenesis

Microbial methanogenesis is constrained to the domain Archaea. Methanogens can be divided to two groups depending on their CH_4 production pathways: chemolithoautotrophic methanogens utilizing solely CO_2 and H_2 for their cellular building blocks and energy production and organotrophic methanogens utilizing an array of different carbon molecules containing methyl group such as acetate, methanol, methylamines, and methylsulfides as substrates (**Figure 1**) (e.g. Garcia et al., 2000; Thauer et al., 2008; Ferry, 2010, 2011).

Methanogens thrive in many environments considered extreme from an anthropocentric point of view. These include deep, dark, isolated, and nutrient-depleted subsurface environments. Typically methanogenic archaea can be found in anaerobic environments where all other electron acceptors but CO_2 are limiting. Methanogenic archaea are an essential part of the microbial communities in deep continental crystalline biosphere as several studies from over the last 20 years have demonstrated (**Table 1** and e.g., Sherwood Lollar et al., 1993a; Kotelnikova and Pedersen, 1997, review by Kotelnikova, 2002).

Today, seven methanogenic archaeal orders are known: *Methanopyrales*, *Methanococcales*, *Methanobacteriales*, *Methanocellales*, and *Methanomicrobiales* (all of which depend on H_2 and CO_2 and some of them can utilize formate as carbon source) and *Methanosarcinales* (with more versatile carbon metabolism) (Thauer et al., 2008; Costa and Leigh, 2014). In addition to these, the representatives of the recently proposed seventh order "*Methanoplasmatales*" are methylotrophic methanogens utilizing methanol, methylamines, and H_2 (Paul et al., 2012; Borrel et al., 2013). Methanogenesis involves several enzymes and cofactors, resulting in a complex metabolic process.

In all methanogenic pathways, the final step in production of methane is performed by methyl-coenzyme M reductase. The gene *mcr*A, coding for the alpha subunit of this enzyme,

has been used widely as a marker gene for methanogenesis in various environmental studies (e.g., Luton et al., 2002; Chin et al., 2004; Dhillon et al., 2005; Juottonen et al., 2006). Heterodisulfide reductase, which is required in the final step of methanogenesis, can be either membrane-bound (*Methanosarcinales*) or cytoplasmic (other methanogens). It has been observed that *Methanosarcinales* with membrane bound cytochromes have higher growth yields but methanogens with cytoplasmic heterosulfide reductase enzyme have lower threshold level for H_2 partial pressure. Consequently, methanogenesis from carbon dioxide is dependent on hydrogen ion concentration, while electrons from the methanogenesis process are bound to hydrogen ions to drive ATP synthase and ultimately produce the energy for the methanogens (Thauer et al., 2008). Due to the lower threshold level for H_2, hydrogenotrophic methanogens can outcompete *Methanosarcinales* -methanogens in environments with low hydrogen concentration. There are more hydrogenotrophic methanogens than methanogens utilizing methylotrophic or aceticlastic pathways (Liu and Whitman, 2008). Whether this is because of the hydrogenotrophic CO_2-pathway is more favorable energetically, or hydrogenotrophic pathway being more ancient and thus has had more time to spread and diversify in the archaeal populations, or there has been more success in cultivating hydrogenotrophic methanogens, is still debatable.

Methane Oxidation

In addition to methane-producing archaea, the deep subsurface environments host microbes utilizing CH_4 for their sole source of carbon and energy, called methanotrophic microorganisms (**Figure 1**). Electron acceptors can vary from oxygen to sulfate, nitrate and nitrite, iron and manganese (Hanson and Hanson, 1996; Orphan et al., 2002; Raghoebarsing et al., 2006; Beal et al., 2009; Knittel and Boetius, 2009; Ettwig et al., 2010; Haroon et al., 2013). As most of the deep crystalline bedrock habitats are mainly anaerobic, other electron acceptors than oxygen could be more relevant in these environments. Nevertheless, the detection of both aerobic and anaerobic methanotrophs from deep crystalline bedrock prove that both of these microbial groups have a niche in the depths (**Table 1**) (Kalyuzhnaya et al., 1999; Chi Fru, 2008; Hirayama et al., 2011; Nyyssönen et al., 2012; Bomberg et al., 2015; Purkamo et al., 2015; Rajala et al., 2015). In addition, aerobic methylotrophs appear to frequently occupy geological lignite and coal formations that are usually considered anaerobic, at depths of over 1 km (Mills et al., 2010; Stępniewska et al., 2013, 2014). Anaerobic methanotrophic archaea (ANME archaea) are frequently found from deep subseafloor sediments (e.g., Mills et al., 2003; Knittel et al., 2005; Lazar et al., 2011a,b) and even in deeply buried Juan de Fuca Ridge flank basalts (Lever et al., 2013). They are more rarely encountered in continental deep biosphere. However, ANME archaea have been recently detected in groundwaters in Olkiluoto of the Fennoscandian Shield, Finland (Nyyssönen et al., 2012; Bomberg et al., 2015).

Aerobic Methane Oxidation

Representatives of aerobic methanotrophic bacteria can be found from alpha- and gamma-proteobacterial families and class *Verrucomicrobiae*. Aerobic methanotrophs use two types of biosynthesis pathways for incorporation of methane, either serine pathway or ribulose monophosphate pathway (RuMP) (Chistoserdova et al., 2009; Nazaries et al., 2013).

The aerobic methanotrophic bacteria have distinct intracellular membrane features. These intracellular membranes are arranged as stacks of disc-shaped features or as paired membranes following the brim of the cell interior. Methane monooxygenase, the key enzyme of aerobic CH_4 oxidation is located in these intracellular membrane structures. Methane monooxygenase mediates the first step of methanotrophy by oxidation of CH_4 to methanol. Two types of methane monooxygenases exist: membrane-bound particulate MMO, which is the common type and soluble cytoplasmic MMO that is found irregularly in a few methanotrophic strains. Soluble methane monooxygenase can oxidize a wide range of different types of substrates from simple alkanes to cyclic compounds, thus evoking industrial interest (Bowman, 2006).

Anaerobic Oxidation of Methane (AOM)

All but one currently recognized anaerobic methanotrophs are archaea. The single exception is a bacterium *Methylomirabilis oxyfera*, which will be discussed in the next paragraph. Anaerobic methanotrophic archaea often referred to as ANME archaea usually live in a symbiotic relationship with sulfate reducers and are therefore abundant in sulfate-methane transition zones (SMTZ). SMTZs can be found in all anaerobic aquatic ecosystems where sulfate is available, such as marine sediments and deep terrestrial crystalline bedrock formations (e.g., Knittel and Boetius, 2009; Bomberg et al., 2015). ANME-1 and ANME-2 groups are usually associated with deltaproteobacterial *Desulfosarcina* and *Desulfococcus*. There is limited evidence that some ANME-2 archaea can form symbiotic relationships with alpha-proteobacterial *Sphingomonas* sp. or with betaproteobacterial *Burkholderia* sp. (Orphan et al., 2001, 2002; Knittel and Boetius, 2009). In addition, ANME-2d archaea have been demonstrated to oxidize CH_4 and reduce nitrate in co-culture with an anaerobic ammonia oxidizer *Kuenenia* sp. (Haroon et al., 2013). Iron and manganese oxide minerals can be used as electron acceptors for anaerobic methane oxidation (Beal et al., 2009). ANME-3 archaea are typically associated with *Desulfobulbus* -type of sulfate reducers (Knittel and Boetius, 2009).

The only bacterial representative of an anaerobic methane oxidizer was found in anaerobic sediment from a Dutch canal and is candidatively named *Methanomirabilis oxyfera* (Ettwig et al., 2010). These peculiar bacteria grow anaerobically reducing nitrite to dinitrogen by nitric oxide dismutation simultaneously producing oxygen as an intermediate during this process within the cell. Oxygen is then used in the aerobic oxidation of CH_4 to methanol with methane monooxygenase inside the cell.

The biochemical mechanism of anaerobic methane oxidation remains elusive. One hypothesis is that ANME archaea are reversing the methanogenic pathway and taking into use the key enzymes of this pathway. Released hydrogen from this process is removed by reducing electron acceptors such as sulfate by the syntrophic partner of ANMEs (Hallam et al.,

2004; Knittel and Boetius, 2009). Results from metagenomic studies have fortified the reverse methanogenesis hypothesis (Krüger et al., 2003; Meyerdierks et al., 2005). Another suggested mechanism is acetogenic methanotrophy, in which acetate and hydrogen are produced from two molecules of CH_4, or from CO_2 and CH_4 and subsequently consumed by sulfate reducing bacteria (SRB). Yet another proposed hypothesis involves CO_2 reducing, methane-oxidizing archaea producing methyl sulfides following a pathway similar to methanogenesis. In this methylogenesis model, methyl groups are transferred to sulfide allowing the regeneration of coenzyme M. SRB capable of utilizing methyl sulfides are crucial partner in these type of AOM consortiums (review by Caldwell et al., 2008 and references within). While SRB have in general a significant role in AOM, a recent study by Milucka et al. (2012) showed that methanotrophic ANME-2 archaea can perform dissimilatory sulfate reduction without the syntrophic sulfate-reducing bacterial partner.

Origin of Substrates for Methanogenesis in Deep Crystalline Rock Biosphere

Biological production and consumption of CH_4 in deep crystalline bedrock is illustrated on the right in **Figure 1**. Abiotically produced carbon dioxide and hydrogen provide a useful source of carbon and energy for chemolithoautotrophic methanogens (Pedersen, 1997, 2000; Chapelle et al., 2002; Nealson et al., 2005; Schrenk et al., 2013). Within crystalline bedrock H_2 needed for autotrophic CH_4 synthesis can be produced during water-rock interactions such as serpentinization and other iron oxidation reactions (McCollom and Bach, 2009; Neubeck et al., 2011; Mayhew et al., 2013). It can also be produced through the dissociation of water molecules by energy released from radioactive decay, i.e., in radiolysis (Vovk, 1987; Lin et al., 2005a,b). The source of hydrogen may also be microbial (reviews by e.g., Nandi and Sengupta, 1998; Wang and Wan, 2009). Fermentative bacteria producing H_2, such as clostridia have been detected in several deep continental rock formations (e.g., Moser et al., 2003; Rastogi et al., 2010; Itävaara et al., 2011b; Purkamo et al., 2013; Schrenk et al., 2013). Overall, H_2 is common in these environments (Sherwood Lollar et al., 2014). Inorganic carbon can be found as carbonate minerals, graphite, and dissolved in groundwater (DIC). The speciation of DIC is controlled by pH. In alkaline conditions, typical of deep groundwaters within crystalline rocks, DIC is commonly found in the form of bicarbonate (HCO_3^-) and the concentrations may be quite low (**Table 1**).

In addition to inorganic carbon, methanogens can utilize organic compounds possibly produced in abiotic reactions, such as serpentinization of olivine-bearing ultramafic rocks (Lang et al., 2012). This principle can be turned inside out; in a recent review, Schrenk et al. (2013) suggested that heterotrophs might be the primary producers in serpentinizing environments. Thus, these heterotrophs utilizing organic materials (produced in abiotic reactions in deep Earth's crust or mantle) biologically produce inorganic end-products such as H_2 and CO_2. These can be used by organisms considered autotrophic, such as hydrogenotrophic methanogens.

Methanogenic archaea can also have the same function in the deep biosphere as in surface ecosystems, i.e., contributing to the degradation of organic matter in anaerobic conditions. Crystalline rock formations may contain refractory organic carbon materials such as kerogen or bitumoids for example in interlayers of black shales or black schist (Karus et al., 1987; Taran et al., 2011). During the formation of these rocks through diagenesis and maturation of sedimentary organic matter, carbon content, and aromaticity increase and volatile hydrocarbons usually migrate away (e.g., Strąpoć et al., 2011; Buseck and Beyssac, 2014). Further increase in temperature during metamorphosis will eventually turn the residual carbonaceous matter into graphite.

There are reports of microbes utilizing organic material trapped in sedimentary rocks such as shales and sandstones. Kerogen of black shales can be the sole carbon source for heterotrophs, such as *Clostridium* -type of bacteria, which in turn can support methanogenesis through the production of substrates for methanogens (Krumholz et al., 1997; Petsch et al., 2001, 2005). For example, clostridial fermenters can provide H_2 and carbon to methanogens in a syntrophic consortium (Kimura et al., 2010; Rosewarne et al., 2013a,b). Thus, methanogens living in a syntrophic relationship with specialized bacteria can mediate anaerobic biodegradation of refractory complex compounds comparable to those found within crystalline bedrock (Strąpoć et al., 2011 and references within).

Fungal contribution to degradation of refractory material, such as organic polymers and polyaromatic hydrocarbons is well known (e.g., Haritash and Kaushik, 2009; Harms et al., 2011). In addition, fungal degradation of refractory organic matter of black shale has been demonstrated (Wengel et al., 2006). As the presence of fungi in deep Fennoscandian bedrock has been verified (Ekendahl et al., 2003; Sohlberg et al., 2015), fungi with the capacity for degradation of refractory and ancient organic and inorganic materials and efficient elemental cycling in addition to bioweathering ability might play a role in providing carbon sources for microbial methanogenesis in deep continental crystalline bedrock environments.

Organic matter from dead microbial biomass is an additional source of carbon in deep biosphere. Bacteriophages are present in deep crystalline bedrock groundwater. If these viruses are active and lytic, they can control the numbers of living microorganisms and therefore increase the dead cell mass in the deep subsurface (Kyle et al., 2008). Recently, Pedersen (2013) concluded that bacteriophages control the cell numbers in flow cells operating in *in situ* conditions in deep crystalline bedrock. The cell number in the flow cells never exceeded the cell densities observed in pristine groundwater (Pedersen, 2013).

Carbon sources for biological CH_4 cycling can be anthropogenic and derived from the surface environments, such as in deep subsurface storage facilities for carbon dioxide or oil. Introduction of such carbon sources to microbial communities in the deep subsurface might induce a formidable activation of dormant microbes as Rajala et al. (2015) demonstrated. H_2 can be released through a chemical reaction between freshly crushed rock and water for example during drilling and blasting of rock (Kita et al., 1982), or oxidation of metals

such as iron casing which is often used to support drill hole walls.

To summarize, H_2 seems to be abundant and available in continental crust (Sherwood Lollar et al., 2014). Despite the several possible sources of organic carbon in the crystalline rock formations discussed above, organic carbon is either absent, scarce or available only as a refractory material (Fredrickson et al., 1997; Fredrickson and Balkwill, 2006). Likewise, concentrations of dissolved inorganic carbon in deep bedrock formations are commonly low (**Table 1**). Thus, it might be carbon which actually limits the formation of CH_4 and other hydrocarbons in continental bedrock.

Geochemical Methods to Study Origin, Source, and Cycling Of CH_4 - Principles and Limitations

Stable Isotope Composition of CH_4

The attempts to separate different CH_4 sources are mainly based on the isotopic composition of CH_4. Typically this includes the determination of stable isotope ratios of carbon ($^{13}C/^{12}C$) and hydrogen ($^2H/^1H$, also called D/H where D stands for deuterium) separately. The resulting isotopic compositions are commonly reported using δ-notation per mill (‰) relative to the isotopic composition of H and C in sea water (VSMOW, Vienna Standard Mean Ocean Water and VPDB, Vienna Pee Dee Belemnite):

$$\delta^2\mathrm{H} = \left(\frac{(^2H/^1H)_{sample}}{(^2H/^1H)_{VSMOW}} - 1\right) \times 1000$$

$$\delta^{13}C = \left(\frac{(^{13}C/^{12}C)_{sample}}{(^{13}C/^{12}C)_{VPDB}} - 1\right) \times 1000$$

Fundamentals of stable isotope methods in geochemistry can be found from books by Clark and Fritz (1997) and Hoefs (2004). In brief, the isotopic composition of CH_4 (or any chemical substance) is controlled by equilibrium and kinetic isotope effects, which arise from equilibrium isotope exchange and differences in reaction rates, respectively. Equilibrium isotope effects are mainly dependent on temperature. Kinetic fractionation is related to incomplete and unidirectional reactions such as those associated with microbial metabolism, and will lead to the depletion of lighter isotopes (^{12}C and ^1H) in the reaction product. These principles also form the basis for traditional classification of $CH_4$with $\delta^{13}C$ vs. δ^2H diagram (Schoell, 1980; Whiticar, 1999; Etiope and Sherwood Lollar, 2013; Etiope and Schoell, 2014).

The isotopic composition of CH_4 is ultimately dependent on the starting material(s) and is further affected by microbial activity, openness of the system, temperature and time, to name a few. Along with increasing amount of data from various settings, it has become clear that CH_4 from different origins may have similar isotopic composition. For example, unusual ^{13}C enriched microbial CH_4 has been found from saline substrate limited environments (Kelley et al., 2012; Tazaz et al., 2013). Carbon limited conditions were also thought to be responsible for ^{13}C enriched metabolic products found from the Lost City Hydrothermal Field by Bradley et al. (2009). Valentine et al. (2004a) found that the fractionation associated with methanogenesis was correlated with temperature and metabolic rate. Likewise, abiotic CH_4 may have a wide range of isotopic compositions. When compared to both microbial and thermogenic CH_4, abiotic CH_4 is typically enriched in ^{13}C (Etiope and Sherwood Lollar, 2013). However, abiotic CH_4 produced in laboratory experiments has been rather depleted in ^{13}C, down to around −50 ‰ VPDB (Horita and Berndt, 1999; Taran et al., 2007).

Difference in the source of hydrogen (methyl group vs. water) forms the basis for separating aceticlastic from autotrophic microbial CH_4 by means of hydrogen isotopic composition of CH_4 (Sugimoto and Wada, 1995; Whiticar, 1999). Hydrogenase enzymes are known to rapidly equilibrate the isotopic compositions of H_2 and H_2O (Sugimoto and Wada, 1995; Valentine et al., 2004b). Furthermore, hydrogen isotope fractionation in the system CH_4-H_2O-H_2 can be used as a thermometer in a system where isotopic equilibrium has been attained, or it may help to reveal the amount of kinetic fractionation caused by biological processes (Bradley and Summons, 2010; Suda et al., 2014).

After formation, the isotopic composition of CH_4 may change as the result of isotope exchange and equilibration, kinetic fractionation by abiotic or microbial oxidation (either aerobic or anaerobic) or migration (e.g., Coleman et al., 1981; Whiticar, 1999; Etiope et al., 2011). Compared to carbon, information on the CH_4 source carried by hydrogen may be more easily lost by isotope exchange, especially when geological time scales are considered (Ni et al., 2011; Reeves et al., 2012). A further complication is brought up by mixing of CH_4 originating from different sources.

Co-existing CO_2 and C_{2+} Hydrocarbons

CO_2 is usually a minor constituent in deep groundwaters within crystalline bedrock and, because of high pH typical for these environments, is mainly found in its dissolved form as HCO_3^- (e.g., Clark and Fritz, 1997; Frape et al., 2003). Nevertheless, considering CO_2 is a potential carbon source for both microbial and abiotic CH_4, it would be essential to know its isotopic composition (or the isotopic composition of DIC at least) in order to study the origin of CH_4. ^{13}C depleted DIC has also been used as an indication of microbial CH_4 oxidation as kinetic fractionation caused by this process will favor depletion of ^{13}C in the product CO_2 (Kotelnikova, 2002; Onstott et al., 2006). When recorded in minerals, such as calcite, this isotopic shift has been used for tracing carbon cycling in the past (e.g., Schidlowski, 2001; Drake and Tullborg, 2009; Sahlstedt et al., 2010).

Information on the origin and cycling of CH_4 may also be obtained by comparing the abundance of CH_4 to longer chained ("higher" or C_{2+}) hydrocarbons. Longer chained hydrocarbons most commonly found in deep groundwaters within crystalline rocks are ethane and propane (Fritz et al., 1987; Nurmi et al., 1988; Sherwood Lollar et al., 1993a,b; Haveman et al., 1999; Ward et al., 2004; Kietäväinen et al., 2013). As microbial processes

produce almost solely CH_4 and not higher hydrocarbons, the ratio between CH_4 and C_{2+} is very high ($>10^3$), while CH_4 produced by thermogenic break-up of organic matter tends to contain significant amounts of C_{2+} compounds (e.g., Whiticar, 1999). Hydrocarbon formation due to abiotic organic synthesis at geologically relevant conditions is more poorly constrained (McCollom, 2013). Formation of longer chained alkanes and alkenes is a typical feature of FTT synthesis (e.g., Taran et al., 2007; McCollom et al., 2010; Zhang et al., 2013). However, no longer chained hydrocarbons were formed in the low temperature (298 K) FTT experiment conducted by Jacquemin et al. (2010) using CO_2 and H_2 as starting materials. The study by Horita and Berndt (1999) also suggest that the CH_4 to C_{2+} ratio of abiotic gas might be closer to that of microbial than thermogenic gas. To summarize, variation in the CH_4 to C_{2+} ratio of abiotic gas should be expected. Moreover, mixing of gases originating from different sources as well as microbial and inorganic reactions are capable of modifying the CH_4 to C_{2+} ratio. For example, the ratio will be increased by both abiotic and microbial oxidation of CH_4. Decrease in the ratio will take place if longer hydrocarbons are consumed in microbial CH_4 production (Zengler et al., 1999).

A further approach is to compare the isotopic compositions of longer chained hydrocarbons and CH_4. In typical thermogenic gas, the isotopic composition of carbon proceeds toward more ^{13}C depleted compositions in the series propane-ethane-methane while isotopic depletion of ^{13}C along with increasing chain length (reversed pattern) has been suggested to characterize abiotic hydrocarbons (e.g., Sherwood Lollar et al., 2002; Zhang et al., 2013). Both trends can be explained by reaction kinetics, as lighter ^{12}C will both break and react faster. However, similarly to the concentration data, isotopic trends obtained from laboratory scale production of abiotic hydrocarbons vary (McCollom, 2013). Furthermore, it is not uncommon to see patterns in natural samples which are somewhere between these two. Zhang et al. (2013) proposed that different trends could be related to thermal history. According to their study, cracking of earlier formed longer chained hydrocarbons with increasing temperature would produce a typical thermogenic pattern while the reversed carbon isotope trend could be preserved in decreasing temperature. Kinnaman et al. (2007) found that large isotopic enrichment of both ^2H and ^{13}C in the substrate was associated with aerobic microbial CH_4 oxidation. Thus the isotopic pattern could likely be changed by microbial processes. They also found that the fractionation clearly decreased with increasing chain length and/or when the substrate became limiting. This has important implications for deep continental subsurface environments which are characteristically substrate-limited. There, isotope fractionation by microbial processes is expected to diminish and may even be absent if the substrate is completely consumed.

Other Co-existing Gases

In addition to carbon containing gases, other co-existing gases such as noble gases and N_2 can be used to trace the origin of CH_4. A major drawback related to using co-existing gases is the possible decoupling of these gases and CH_4.

As they are inert, noble gases are very useful in tracing gas migration. For example they may be used to distinguish between mantle and crustal sources of gases (Kipfer et al., 2002; Prinzhofer, 2013; Sano and Fischer, 2013). Noble gases have also been used to determine residence times of deep groundwaters within crystalline shields in Canada (Bottomley et al., 1990; Greene et al., 2008; Holland et al., 2013), Fennoscandia (Kietäväinen et al., 2014; Trinchero et al., 2014), and South Africa (Lippmann et al., 2003). These studies have revealed ancient fluids within these formations extending from several millions of years to over a billion years old. Even though the information on residence times obtained from noble gases is indirect, and often comes with high uncertainties, it can be potentially utilized in estimating timing and rates of CH_4 production as well as isolation of the subsurface ecosystems. Examples of this method are included in the studies by Lin et al. (2006b) and Schlegel et al. (2011).

Isotopic composition of N_2 in groundwaters of the Fennoscandian and Canadian shields was used by Sherwood Lollar et al. (1993a) to show that hydrocarbons were not related to shallow atmosphere derived fluids but originated from the crystalline basement. Attempts to separate between inorganic and organic sources of hydrocarbons may also benefit from determination of N_2 isotopes, as ^{15}N depleted values are suggested to be representative of organic origin (Sano et al., 1993; Zhu et al., 2000; Etiope et al., 2011). As N_2 is the main constituent of air, atmospheric contamination during sampling or analysis is a real risk to be aware of.

Radiocarbon

Attempts have also been made to estimate the age of CH_4 by using radiocarbon (^{14}C) dating. One such study was performed by Slater et al. (2006) among the deep continental bedrock sites in Witwatersrand Basin, South Africa. By comparing the ^{14}C isotopic composition of DIC and CH_4 they concluded that the majority of the CH_4 was produced in the distant past. Potential problems of this method include the contamination of typically CO_2-undersaturated groundwater samples by atmospheric CO_2, and recent formation of CH_4 from ancient (or "^{14}C dead") carbon source. In the former case, the apparent age of DIC may be underestimated, while in the latter case CH_4 from on-going processes could be interpreted as ancient. Nevertheless, ^{14}C determination could help with tracing the carbon source. For example, Stotler et al. (2010) found that the carbon source for CH_4 in the Lupin mine in Canada was older than could be dated with ^{14}C, i.e., more than 50 ka.

Clumped Isotopes

Recently, clumped isotope methods have also been developed which are capable of determining the isotopologues of CH_4 molecules (Stolper et al., 2014; Wang et al., 2015). Potential applications of the method include determination of CH_4 formation temperature (CH_4 thermometry), and detection of kinetic isotope fractionation, both of which might be used in separating biotic from abiotic CH_4 (Stolper et al., 2014; Wang et al., 2015). More applications are expected when this method comes more widely attainable.

Microbes Involved in Methane Cycling in the Fennoscandian Shield and Other Deep Precambrian Continental Subsurface Environments

Outokumpu Deep Drill Hole

Formation waters at the 2.5 km deep scientific drill hole in Outokumpu, eastern Finland are characterized by high salinity and abundant dissolved gas phase of which CH_4 covers up to 80 vol-% (**Table 1**). The bedrock in Outokumpu is composed of several geochemically different rock types. These include serpentinites which have gained a lot of attention recently in the studies of abiotic CH_4, along with black schists which contain abundant C. To date, Outokumpu Deep Drill Hole is the deepest site within the Fennoscandian Shield where CH_4 cycling microbes have been studied.

Marker genes for methanogenesis, *mcr*A were detected throughout the drill hole water column to 1500 m depth with a quantitative PCR assay (Itävaara et al., 2011a). Thus the existence of methanogens in Outokumpu could be verified, even though the copy numbers in a ml of drill hole water were essentially low (around 1×10^2 copies mL^{-1}). The overall ratio of methanogens vs. total number of bacteria was less than 1%. Cloning of the methanogenesis marker gene from the drill hole water suggested that at depths of 900 m or shallower, aceticlastic *Methanosarcina* were present in the methanogenic communities. Methylotrophic *Methanolobus* -type of OTUs were detected by cloning and high-throughput sequencing methods from 1.1, 1.3, and 1.5 km depths (Nyyssönen et al., 2014; Purkamo et al., 2015). Lithology of the latter depths is dominated by serpentinites and black schists and statistically corresponds with the detection of *mcr*A genes of *Methanolobus* (Västi, 2011; Purkamo et al., 2015). Majority of the *mcr*A clones and pyrosequenced archaeal 16S rRNA OTUs from the deepest part of the drill hole (1.9 km depth and below) were related to *Methanobacterium* -associated methanogens (Nyyssönen et al., 2014; Purkamo et al., 2015). Further proof for autotrophic methanogenesis in the deepest part of the drill hole was received from the metagenome of the sample from 2.3 km depth, in which genes involved in autotrophic methanogenesis were detected (Nyyssönen et al., 2014).

The bedrock fracture zones represent different microbial community as the drill hole at the same depth. When observing the intrinsic archaeal communities in bedrock fracture zones at different depths of Outokumpu bedrock, Purkamo et al. (2013) confirmed that hydrogenotrophic *Methanobacteriaceae* were dominating the archaeal community in the fracture zones at 500 and 2260 m levels. In addition, a small part of the archaeal community at these depths contained aceticlastic *Methanosarcina*. The results were based both on DNA and RNA, thus it can be presumed that these methanogens were active in these fractures. Despite of confirmed methanogenic activity in Outokumpu, CH_4 is ^{13}C rich (**Table 1**). Thus, it cannot be classified as microbial within traditional limits for isotopic composition of biological CH_4.

In addition to methanogens, the existence and activity of methanotrophic microbes in Outokumpu groundwater is established. By cloning of the marker gene for particulate methane monooxygenase enzyme (*pmo*A), Purkamo et al. (2015) demonstrated that aerobic methanogens are part of the microbial communities at 600, 900, and 1500 m depths of the drill hole water column. All clones in this study were affiliated with a γ-proteobacterial *Methylomonas methanica*. Rajala et al. (2015) verified that methanotrophs at 500 m fracture zone could be rapidly activated with CH_4, methanol and sulfate. No ANME-associated *mcr*A was found in these studies, suggesting either that an another type of anaerobic methane oxidation pathway than reverse methanogenesis could be more likely in Outokumpu, or aerobic oxidation of CH_4 by bacteria is more likely in Outokumpu, or the *mcr*A primers used in these studies do not detect ANME-type of *mcr*A.

Olkiluoto

Olkiluoto in southwestern Finland is the future repository site for nuclear waste. The bedrock in Olkiluoto is comprised of migmatitic mica gneisses. Similarly to Outokumpu, the deep groundwater in Olkiluoto is anaerobic and saline (Nyyssönen et al., 2012). Concentration of CH_4 is among the highest observed today from any Precambrian crystalline bedrock site (**Table 1**). The microbial communities in different parts and depths of Olkiluoto site have been under observation for several years. Traditional most probable number (MPN) cultivation methods have described methylotrophs in shallow depths and methanogens to the depth of at least 450 m. Methanogens were present in small numbers, 1×10^0 from 1×10^1 cells mL^{-1} (Pedersen et al., 2008). Using molecular biological methods, Nyyssönen et al. (2012) reported that the majority of *mcr*A clones acquired from shallow (< 400 m) depths of different drill holes in Olkiluoto fell within a metabolically diverse group of methanogens, namely *Methanosarcinales*. In addition, *Methanoregula boonei* of the *Methanomicrobiales mcr*A sequences were detected, while hydrogenotrophic *Methanobacteriales* -type of *mcr*A were found below 500 m depth. The *mcr*A copy numbers detected with qPCR varied from less than 200 copies to below detection limit mL^{-1} of groundwater. Apparently the archaeal communities are diverse in Olkiluoto but methanogenic archaea represent only a minority ranging from 10 to 0.4 % of the archaeal community (Bomberg et al., 2014).

Nyyssönen et al. (2012) detected *mcr*A of putative anaerobic methane oxidizers, i.e., ANME archaea in a single sample from 350 m depth. In addition, this sample had the highest number of *mcr*A gene copies, 660 copies mL^{-1}. This depth is considered to be within the sulfate-methane transition zone in the Olkiluoto bedrock. A flow cell cultivation study provided further evidence of existence of ANME archaea in Olkiluoto (Pedersen, 2013). In addition, it was shown that the active archaeal communities at depths of from 300 to 800 m in Olkiluoto consisted of, among others, ANME-2D archaea (Bomberg et al., 2015). These findings of ANME archaea are further proof for the hypothesis of Pedersen et al. (2008) that the anaerobic oxidation of methane is an active microbial process in the Olkiluoto bedrock.

Äspö, Laxemar, and Forsmark

Another important Fennoscandian shield sites where deep biosphere studies have been conducted are in Sweden. Probably the most famous is the Äspö Hard Rock Laboratory (HRL) that has been running since 1995, in addition to Laxemar-Simpevarp and Forsmark which have been suggested for the final repository sites for nuclear waste. Äspö HRL extends to 450 m depth in porphyritic granite/granodiorite bedrock, whereas Forsmark lithology comprises of granites and Laxemar-Simpevarp granites and quartz monzodiorite (**Table 1**). Both salinity and CH_4 concentrations are much lower in all Swedish sites compared to Olkiluoto and Outokumpu (**Table 1**). To our knowledge, no information on isotopic composition of CH_4 detected at the Swedish sites exists. Pedersen (1997) demonstrated that methylotrophic and aceticlastic methanogens dominated at shallower depths above 200 m, where more organic carbon was available. In the deeper depths where organic carbon content was lower, autotrophic methanogens were more frequent. Kotelnikova et al. (1998) isolated an autotrophic methanogen from Äspö groundwater, *Methanobacterium subterraneum*. Hallbeck and Pedersen (2008a, 2012) found low numbers of methanogens based on the most probable number method from samples of all these three sites.

In addition to methanogens, methanotrophs have also been detected from deep bedrock of Äspö and Forsmark. Clone libraries of methanotrophy marker gene *pmo*A were dominated by *Methylomonas* and *Methylocystis* (Chi Fru, 2008). *Methylomonas* and *Methylobacter* dominated enrichment cultures from Äspö groundwater from below 400 m depth (Kalyuzhnaya et al., 1999). To conclude, methanotrophs are detected approximately at the same depths in all Fennoscandian Shield sites, mainly above 1 km.

Witwatersrand and Other Deep Precambrian Continental Subsurface Study Sites

Another widely studied deep biosphere is located in the Witwatersrand Basin in South Africa. The geological formation is composed of quartzite and shale with overlying basaltic and andesitic rocks, on top of the schist basement (Ward et al., 2004). Several sites in the Witwatersrand Basin have been studied and methanogenic as well as ANME archaea have been detected with cloning of 16s rRNA gene (Takai et al., 2001; Ward et al., 2004; Moser et al., 2005; Lin et al., 2005a, 2006a,b; Gihring et al., 2006). CH_4 is a common constituent of the gas phase in all of these sites (**Table 1**). A wide range of isotopic compositions have been reported, including ^{13}C poor CH_4. In the Beatrix mine methanogens have been detected from 718 to 1390 m depths (Ward et al., 2004). At the depth of 866 mbls (BE16) *Methanobacterium*—type of clones were most abundant, while other detected methanogens affiliated with aceticlastic *Methanosarcina* and *Methanosaeta* (Lin et al., 2006a). The archaeal communities in the Evander mine at the depth of 1950 m (EV818) were composed of *Methanosarcina, Methanosaeta* in addition to *Methanolobus* (Ward et al., 2004; Gihring et al., 2006). *Methanobacterium*-type hydrogenotrophic methanogens were found typically in deeper samples in the Witwatersrand Basin, such as from the Mponeng and Driefontein mines from over 2.7 km depth (Moser et al., 2005; Gihring et al., 2006). In the Driefontein mine site D8A, at more than 3 km depth the archaeal community comprised about 10% of the total microbial community and was dominated by *Methanobacterium* (Moser et al., 2005). *Methanobacterium* - affiliating 16s rRNA sequences were detected also from the Mponeng mine at 2825 m depth (Lin et al., 2005a). Aceticlastic methanogens were typically found in depths shallower than 2 km at the Witwatersrand Basin whereas hydrogenotrophic methanogens such as *Methanobacterium* dominated at deeper depths. Gihring et al. (2006) suggested that high temperature and reducing conditions were the determining geochemical factors for the occurrence of *Methanobacteriales* in the fractures of the Witwatersrand Basin.

Anaerobic oxidation of methane in the deep subsurface in the Witwatersrand Basin is plausible, while archaeal 16s rRNA clones similar to methanotrophic ANME-1 archaea in Driefontein dolomitic aquifer and the Evander mine sites have been detected (Gihring et al., 2006).

Although life in the deep biosphere has been characterized in several sites as discussed above, there are some studies from deep continental bedrock sites where methanogens and methanotrophs could not be detected. These include the subsurface groundwaters from Palmottu, Kivetty, Romuvaara, and Hästholmen areas in the Fennoscandian Shield (Haveman et al., 1999; Haveman and Pedersen, 2002). Methanogenic archaea have not been detected from Kloof mine in the Witwatersrand Basin (Takai et al., 2001; Ward et al., 2004; Kieft et al., 2005). Neither did Onstott et al. (2009) detect any archaea from the Canadian Shield site in the Lupin mine. These results might indicate either real absence of methane cycling microbes at the sites or could be due to extremely low numbers of cells and/or inadequate sensitivity of analytical methods or because acquiring representative samples at field conditions is often challenging.

Conclusions and Future Prospects

The possibility of abiotic CH_4 synthesis at low temperatures, together with findings of methanogenic microbes indicates that the formation of CH_4 is an on-going process in deep Precambrian continental bedrock. In addition, the detection of aerobic, and recently also anaerobic methanotrophs deep within crystalline bedrock provide ecological evidence of microbial contribution to CH_4 consumption in these environments. So far, the identified carbon sources of microbes range from inorganic CO_2 to CH_4 and other small organic carbon molecules, but there are intriguing hypotheses on microbial utilization of refractory organic carbon of minerals. Thus, the participation of heterotrophic microbes in carbon cycling in deep crystalline bedrock should not be dismissed.

As deep continental crystalline bedrock environments are commonly carbon-deprived, the traditional isotopic separation between biologically produced and abiotically produced CH_4 can be difficult. When carbon sources are limited, the small amount of carbon available will be utilized without the preference for lighter isotope that is considered to happen in "normal" (surface) circumstances with abundant organic carbon. In addition,

microbial activities, such as syntrophy or competition, especially in substrate-limited environments, can result to similar isotopic composition of CH_4 produced in abiogenic reactions. Thus, further studies are needed especially considering the effect of syntrophy or competitiveness of microbial species, substrate availability and reaction rates on the isotopic composition of CH_4. Furthermore, more studies on different forms of inorganic carbon (including minerals) available for both abiotic and biological organic synthesis will be advantageous.

Metabolically diverse methanoges were found at shallower depths while hydrogenotrophic methanogenesis appeared to be more common at greater depths throughout the sites. However, transition between the zones is not sharp and the depth varies among the sites. Considering the evolution of methanogenesis, the hydrogenotrophic pathway may be as old as life itself on Earth, while the capability to use acetate is considered to have evolved more recently during the Cambrian period (Costa and Leigh, 2014 and references within). As the oldest bedrock fluids are dated to be Precambrian (over 1 billion years old; Holland et al., 2013) it will be interesting to see if there are any methanogenic communities in these isolated fracture fluids, and will the hydrogenotrophic pathway dominate in these communities, as the hypothesis of the methanogenesis evolution implies. Similarly, further studies on depth dependence and the extent of isolation of different methanogens can shed light on the evolution of deep bedrock biosphere as well as CH_4 cycling.

Growing industrial interest in utilizing deep rock formations as a natural resource such as mining of valuable metals or extracting shale gas, as storage for CO_2, hydrocarbons or other fuels, as a part of infrastructure such as traffic tunnels, and production of geothermal heat and/or energy has increased the need for understanding the origin, source and cycling of CH_4 in these environments. The natural state of the bedrock will be disturbed during these activities and release, production, and consumption of CH_4 can affect industrial operations. CH_4 may enhance biological activity by providing energy and carbon for microbial communities. In turn, this may increase the concentrations of reactive compounds such as hydrogen and sulfide, especially in the presence of SO_4, and change pH of the system thus increasing the corrosion risk. As a gaseous component, CH_4 can also be important in mobilization of radiocarbon.

In order to understand CH_4 cycling at depths, and the role of microorganisms within it, it is important to study the environmental conditions such as reduction-oxidation potential, isolation, and availability of substrates of the particular site together with microbiology. Geochemical methods may help to identify biotic from abiotic sources of CH_4. Yet, no common characteristics in terms of pH, T, depth, lithology, abundance, and isotopic composition of CH_4 could have been determined which would serve as diagnostic tools for estimating importance of microbial contribution in CH_4 cycle in these environments. However, potential of new findings exists in all continental regions as to date very few sites have been studied at great detail or even superficially. For example, such studies would be beneficial in some Canadian Shield sites where extensive geochemical data on CH_4 is available and world's oldest isolated bedrock fluids have been identified. In Sweden, on the other hand, more detailed geochemical characterization, including isotopic analyses could be helpful. In addition, development of new geochemical and microbiological methods, such as clumped isotopes and high-throughput sequencing can open new opportunities also in this field.

Acknowledgments

RK would like to thank Dr. Lasse Ahonen for commenting the manuscript and the Finnish Research Program on Nuclear Waste Management (grants SALAMI and RENGAS) for funding. LP would like to acknowledge M.Sc Elina Sohlberg for valuable discussions and criticism when compiling this review and Kone Foundation for financial support. Dr. Verity Flett is thanked for critical language revision. Reviewers are thanked for their constructive comments on the manuscript.

References

Ahonen, L., Kaija, J., Paananen, M., Hakkarainen, V., and Ruskeeniemi, T. (2004). *Palmottu Natural Analogue: A Summary of the Studies*. Geological Survey of Finland, Nuclear Waste Disposal Research, Report YST-121. Available online at: http://tupa.gtk.fi/julkaisu/ydinjate/yst_121.pdf

Anttila, P., Ahokas, H., Front, K., Heikkinen, E., Hinkkanen, H., Johansson, E., et al. (1999). *Final Disposal of Spent Nuclear Fuel in Finnish Bedrock - Kivetty Site Report*. Posiva report 99-09, Posiva Oy, Olkiluoto. Available online at: http://www.posiva.fi/files/2691/POSIVA-99-09_web.pdf

Arthur, M. A., and Cole, D. R. (2014). Unconventional hydrocarbon resources: prospects and problems. *Elements* 10, 257–264. doi: 10.2113/gselements.10.4.257

Beal, E. J., House, C. H., and Orphan, V. J. (2009). Manganese- and iron-dependent marine methane oxidation. *Science* 325, 184–187. doi: 10.1126/science.1169984

Bomberg, M., Nyyssönen, M., Nousiainen, A., Hultman, J., Paulin, L., Auvinen, P., et al. (2014). Evaluation of molecular techniques in characterization of deep terrestrial biosphere. *Open J. Ecol.* 4, 468–487. doi: 10.4236/oje.2014.48040

Bomberg, M., Nyyssönen, M., Pitkänen, P., Lehtinen, A., and Itävaara, M. (2015). Active microbial sulphate-methane interphase in deep bedrock fracture fluids in Olkiluoto, Finland. *BioMed Res. Int.* 979530. (in press).

Borgonie, G., García-Moyano, A., Litthauer, D., Bert, W., Bester, A., van Heerden, E., et al. (2011). Nematoda from the terrestrial deep subsurface of South Africa. *Nature* 474, 79–82. doi: 10.1038/nature09974

Borrel, G., O'Toole, P. W., Harris, H. M., Peyret, P., Brugere, J. F., and Gribaldo, S. (2013). Phylogenomic data support a seventh order of Methylotrophic methanogens and provide insights into the evolution of Methanogenesis. *Genome Biol. Evol.* 5, 1769–1780. doi: 10.1093/gbe/evt128

Bottomley, D. J., Gascoyne, M., and Kamineni, D. C. (1990). The geochemistry, age, and origin of groundwater in a mafic pluton, East Bull Lake, Ontario, Canada. *Geochim. Cosmochim. Acta* 54, 933–1008. doi: 10.1016/0016-7037(90)90433-L

Bowman, J. (2006). The methanotrophs—the families Methylococcaceae and Methylocystaceae. *Prokaryotes* 5, 266–289. doi: 10.1007/0-387-30745-1_15

Bradley, A. S., Hayes, J. M., and Summons, R. E. (2009). Extraordinary ^{13}C enrichment of diether lipids at the Lost City Hydrothermal Field indicates a carbon-limited ecosystem. *Geochim. Cosmochim. Acta* 73, 102–118. doi: 10.1016/j.gca.2008.10.005

Bradley, A. S., and Summons, R. E. (2010). Multiple origins of methane at the Lost City Hydrothermal Field. *Earth Planet. Sci. Lett.* 297, 34–41. doi: 10.1016/j.epsl.2010.05.034

Brazelton, W. J., Nelson, B., and Schrenk, M. O. (2012). Metagenomic evidence for H_2 oxidation and H_2production by serpentinite-hosted subsurface microbial communities. *Front. Microb.* 2:268. doi: 10.3389/fmicb.2011.00268

Buseck, P. R., and Beyssac, O. (2014). From organic matter to graphite: graphitization. *Elements* 10, 421–426. doi: 10.2113/gselements.10.6.421

Caldwell, S. L., Laidler, J. R., Brewer, E. A., Eberly, J. O., Sandborgh, S. C., and Colwell, F. S. (2008). Anaerobic oxidation of methane: mechanisms, bioenergetics, and the ecology of associated microorganisms. *Environ. Sci. Technol.* 42, 6791–6799. doi: 10.1021/es800120b

Caporaso, J. G., Kuczynski, J., Stombaugh, J., Bittinger, K., Bushman, F. D., Costello, E. K., et al. (2010). QIIME allows analysis of high-throughput community sequencing data. *Nat. Methods* 7, 335–336. doi: 10.1038/nmeth.f.303

Chapelle, F. M., O'Neill, K., Bradley, P. M., Methé, B. A., Ciufo, S., and A., Knobel, L. L., et al. (2002). A hydrogen-based subsurface microbial community dominated by methanogens. *Nature* 415, 312–315. doi: 10.1038/415312a

Chi Fru, E. (2008). Constraints in the colonization of natural and engineered subterranean igneous rock aquifers by aerobic methane-oxidizing bacteria inferred by culture analysis. *Geobiology* 6, 365–375. doi: 10.1111/j.1472-4669.2008.00164.x

Chin, K., Lueders, T., Friedrich, M., Klose, M., and Conrad, R. (2004). Archaeal community structure and pathway of methane formation on rice roots. *Microb. Ecol.* 47, 59–67. doi: 10.1007/s00248-003-2014-7

Chistoserdova, L., Kalyuzhnaya, M. G., and Lidstrom, M. E. (2009). The expanding world of methylotrophic metabolism. *Annu. Rev. Microbiol.* 63, 477–499. doi: 10.1146/annurev.micro.091208.073600

Chivian, D., Brodie, E. L., Alm, E. J., Culley, D. E., Dehal, P. S., DeSantis, T. Z., et al. (2008). Environmental genomics reveals a single-species ecosystem deep within Earth. *Science* 10, 275–278. doi: 10.1126/science.1155495

Clark, I., and Fritz, P. (1997). *Environmental Isotopes in Hydrogeology*. Boca Raton, FL: Lewis Publishers.

Coleman, D. D., Risatti, J. B., and Schoell, M. (1981). Fractionation of carbon and hydrogen isotopes by methane-oxidizing bacteria. *Geochim. Cosmochim. Acta* 45, 1033–1037. doi: 10.1016/0016-7037(81)90129-0

Costa, K. C., and Leigh, J. A. (2014). Metabolic versatility in methanogens. *Curr. Opin. Biotechnol.* 29, 70–75. doi: 10.1016/j.copbio.2014.02.012

Dhillon, A., Lever, M., Lloyd, K. G., Albert, D. B., Sogin, M. L., and Teske, A. (2005). Methanogen diversity evidenced by molecular characterization of methyl coenzyme M reductase A (mcrA) genes in hydrothermal sediments of the Guaymas Basin. *Appl. Environ. Microbiol.* 71, 4592–4601. doi: 10.1128/AEM.71.8.4592-4601.2005

Drake, H., and Tullborg, E.-L. (2009). Paleohydrogeological events recorded by stable isotopes, fluid inclusions and trace elements in fracture minerals in crystalline rock, Simpevarp area, SE Sweden. *Appl. Geochem.* 24, 715–732. doi: 10.1016/j.apgeochem.2008.12.026

Ekendahl, S., O'Neill, A. H., Thomsson, E., and Pedersen, K. (2003). Characterization of yeasts isolated from deep igneous rock aquifers of the Fennoscandian shield. *Microb. Ecol.* 46, 416–428. doi: 10.1007/s00248-003-2008-5

Etiope, G., Baciu, C. L., and Schoell, M. (2011). Extreme methane deuterium, nitrogen and helium enrichment in natural gas from the Homorod seep (Romania). *Chem. Geol.* 280, 89–96. doi: 10.1016/j.chemgeo.2010.10.019

Etiope, G., and Ionescu, A. (2014). Low-temperature catalytic CO2 hydrogenation with geologic quantities of ruthenium: a possible abiotic CH4 source in chromitite-rich serpentinized rocks. *Geofluids*. doi: 10.1111/gfl.12106. [Epub ahead of print].

Etiope, G., and Martinelli, G. (2002). Migration of carrier and trace gases in the geosphere: an overview. *Phys. Earth Planet. Inter.* 129, 185–204. doi: 10.1016/S0031-9201(01)00292-8

Etiope, G., and Schoell, M. (2014). Abiotic gas: atypical, but not rare. *Elements* 10, 291–296. doi: 10.2113/gselements.10.4.291

Etiope, G., and Sherwood Lollar, B. (2013). Abiotic methane on Earth. *Rev. Geophys.* 51, 276–299. doi: 10.1002/rog.20011

Ettwig, K. F., Butler, M. K., Le Paslier, D., Pelletier, E., Mangenot, S., Kuypers, M. M., et al. (2010). Nitrite-driven anaerobic methane oxidation by oxygenic bacteria. *Nature* 464, 543–548. doi: 10.1038/nature08883

Ferry, J. G. (2010). The chemical biology of methanogenesis. *Planet. Space Sci.* 58, 1775–1783. doi: 10.1016/j.pss.2010.08.014

Ferry, J. G. (2011). Fundamentals of methanogenic pathways that are key to the biomethanation of complex biomass. *Curr. Opin. Biotechnol.* 22, 351–357. doi: 10.1016/j.copbio.2011.04.011

Frape, S. K., Blyth, A., Blomqvist, R., McNutt, R. H., and Gascoyne, M. (2003). Deep fluids in the continents: II. Crystalline rocks. *Treatise Geochem.* 5, 541–580. doi: 10.1016/B0-08-043751-6/05086-6

Fredrickson, J. K., and Balkwill, D. L. (2006). Geomicrobial processes and biodiversity in the deep terrestrial subsurface. *Geomicrobiol. J.* 23, 345–356. doi: 10.1080/01490450600875571

Fredrickson, J. K., McKinley, J. P., Bjornstad, B. N., Ringelberg, D. B., White, D. C., Krumholz, L. R., et al. (1997). Pore-size constraints on the activity and survival of subsurface bacteria in a late Cretaceous shale-sandstone sequence, northwestern New Mexico. *Geomicrobiol. J.* 14,183–202. doi: 10.1080/01490459709378043

Fredrickson, J. K., Zachara, J. M., Balkwill, D. L., Kennedy, D., Li, S. M., Kostandarithes, H. M., et al. (2004). Geomicrobiology of high-level nuclear waste-contaminated vadose sediments at the hanford site, washington state. *Appl. Environ. Microbiol.* 70, 4230–4241. doi: 10.1128/AEM.70.7.4230-4241.2004

Fritz, P., Frape, S. K., and Miles, M. (1987). Methane in the crystalline rocks of the Canadian Shield. *Geol. Assoc. Canada* 33, 211–223. doi: 10.1016/0009-2541(88)90117-9

Galimov, E. M. (1988). Sources and mechanisms of formation of gaseous hydrocarbons in sedimentary rocks. *Chem. Geol.* 71, 77–95. doi: 10.1016/0009-2541(88)90107-6

Garcia, J., Patel, B. K., and Ollivier, B. (2000). Taxonomic, phylogenetic, and ecological diversity of methanogenic archaea. *Anaerobe* 6, 205–226. doi: 10.1006/anae.2000.0345

Gihring, T., Moser, D., Lin, L., Davidson, M., Onstott, T., Morgan, L., et al. (2006). The distribution of microbial taxa in the subsurface water of the Kalahari Shield, South Africa. *Geomicrobiol. J.* 23, 415–430. doi: 10.1080/01490450600875696

Greene, S., Battye, N., Clark, I., Kotzer, T., and Bottomley, D. (2008). Canadian Shield brine from the Con Mine, Yellowknife, NT, Canada: Noble gas evidence for an evaporated Palaeozoic seawater origin mixed with glacial meltwater and Holocene recharge. *Geochim. Cosmochim. Acta* 72, 4008–4019. doi: 10.1016/j.gca.2008.05.058

Hallam, S. J., Putnam, N., Preston, C. M., Detter, J. C., Rokhsar, D., Richardson, P. M., et al. (2004). Reverse methanogenesis: testing the hypothesis with environmental genomics. *Science* 305, 1457–1462. doi: 10.1126/science.1100025

Hallbeck, L., and Pedersen, K. (2008a). Characterization of microbial processes in deep aquifers of the Fennoscandian Shield. *Appl. Geochem.* 23, 1796–1819. doi: 10.1016/j.apgeochem.2008.02.012

Hallbeck, L., and Pedersen, K. (2008b). *Explorative Analyses of Microbes, Colloids, and Gases Together with Microbial Modeling: Site Description Model SDM-Site Laxemar*. SKB Report R-08-109, Swedish Nuclear Fuel and Waste Management Co., Stockholm. Available online at: http://www.iaea.org/inis/collection/NCLCollectionStore/_Public/40/021/40021023.pdf

Hallbeck, L., and Pedersen, K. (2012). Culture-dependent comparison of microbial diversity in deep granitic groundwater from two sites considered for a Swedish final repository of spent nuclear fuel. *FEMS Microbiol. Ecol.* 81, 66–77. doi: 10.1111/j.1574-6941.2011.01281.x

Hanson, R. S., and Hanson, T. E. (1996). Methanotrophic bacteria. *Microbiol. Rev.* 60, 439–471.

Haritash, A. K., and Kaushik, C. P. (2009). Biodegradation aspects of polycyclic aromatic hydrocarbons (PAHs): a review. *J. Hazard. Mater.* 169, 1–15. doi: 10.1016/j.jhazmat.2009.03.137

Harms, H., Schlosser, D., and Wick, L. Y. (2011). Untapped potential: expoiting fungi in bioremediation of hazardous chemicals. *Nat. Rev. Microbiol.* 9, 177–192. doi: 10.1038/nrmicro2519

Haroon, M. F., Hu, S., Shi, Y., Imelfort, M., Keller, J., Hugenholtz, P., et al. (2013). Anaerobic oxidation of methane coupled to nitrate reduction in a novel archaeal lineage. *Nature* 500, 567–570. doi: 10.1038/nature12375

Haveman, S. A., and Pedersen, K. (2002). Distribution of culturable microorganisms in Fennoscandian Shield groundwater. *FEMS Microbiol. Ecol.* 39, 129–137. doi: 10.1111/j.1574-6941.2002.tb00914.x

Haveman, S. A., Pedersen, K., and Ruotsalainen, P. (1999). Distribution and metabolic diversity of microorganisms in deep igneous rock aquifers of Finland. *Geomicrobiol. J.* 16, 277–294. doi: 10.1080/014904599270541

Hirayama, H., Suzuki, Y., Abe, M., Miyazaki, M., Makita, H., Inagaki, F., et al. (2011). Methylothermus subterraneus sp. nov., a moderately thermophilic methanotroph isolated from a terrestrial subsurface hot aquifer. *Int. J. Syst. Evol. Microbiol.* 61, 2646–2653. doi: 10.1099/ijs.0.028092-0

Hoefs, J. (2004). *Stable Isotope Geochemistry*. Berlin; Heidelberg: Springer-Verlag. doi: 10.1007/978-3-662-05406-2

Holland, G., Sherwood Lollar, B., Li, L., Lacrampe-Couloume, G., Slater, G. F., and Ballentine, C. J. (2013). Deep fracture fluids isolated in the crust since the Precambrian era. *Nature* 497, 357–360. doi: 10.1038/nature12127

Horita, J., and Berndt, M. E. (1999). Abiogenic methane formation and isotopic fractionation under hydrothermal conditions. *Science* 285, 1055–1057. doi: 10.1126/science.285.5430.1055

Itävaara, M., Nyyssönen, M., Bomberg, M., Kapanen, A., Nousiainen, A., Ahonen, L., et al. (2011a). Microbiological sampling and analysis of the Outokumpu Deep Drill Hole biosphere in 2007–2009. *Geol. Surv. Finland* 51, 199–206.

Itävaara, M., Nyyssönen, M., Kapanen, A., Nousiainen, A., Ahonen, L., and Kukkonen, I. (2011b). Characterization of bacterial diversity to a depth of 1500 m in the Outokumpu deep borehole, Fennoscandian Shield. *FEMS Microbiol. Ecol.* 77, 295–309. doi: 10.1111/j.1574-6941.2011.01111.x

Jacquemin, M., Beuls, A., and Ruiz, P. (2010). Catalytic production of methane from CO_2 and H_2 at low temperature: insight on the reaction mechanism. *Catal. Today* 157, 462–366. doi: 10.1016/j.cattod.2010.06.016

Juottonen, H., Galand, P. E., and Yrjälä, K. (2006). Detection of methanogenic Archaea in peat: comparison of PCR primers targeting the *mcr*A gene. *Res. Microbiol.* 157, 914–921. doi: 10.1016/j.resmic.2006.08.006

Kaija, J., Blomqvist, R., Ahonen, L., and Hakkarainen, V. (1998). *The Hydrogeochemical Database of Palmottu*. The Palmottu Natural Analogue Project, Technical Report 98-08. Available online at: http://tupa.gtk.fi/raportti/arkisto/y50_98_08.pdf

Kalyuzhnaya, M. G., Khmelenina, V. N., Kotelnikova, S., Holmquist, L., Pedersen, K., and Trotsenko, Y. A. (1999). Methylomonas scandinavica sp. nov., a new methanotrophic psychrotrophic bacterium isolated from deep igneous rock ground water of Sweden. *Syst. Appl. Microbiol.* 22, 565–572. doi: 10.1016/S0723-2020(99)80010-1

Karus, E. W., Nartikoyev, V. D., Bartashevich, O. V., Gigashvili, G. M., Ikorsky, S. V., Pavlolva, M. A., et al. (1987). "Gases and organic matter," in *The Superdeep Well of the Kola Peninsula*, ed Y. A. Kozlovsky (Berlin; Heidelberg: Springer-Verlag), 243–270.

Kelley, C. A., Poole, J. A., Tazaz, A. M., Chanton, J. P., and Bebout, B. M. (2012). Substrate limitation for methanogenesis in hypersaline environments. *Astrobiology* 12, 89–97. doi: 10.1089/ast.2011.0703

Kieft, T. L., McCuddy, S. M., Onstott, T. C., Davidson, M., Lin, L., Mislowack, B., et al. (2005). Geochemically generated, energy-rich substrates and indigenous microorganisms in deep, ancient groundwater. *Geomicrobiol. J.* 22, 325–335. doi: 10.1080/01490450500184876

Kietäväinen, R., Ahonen, L., Kukkonen, I. T., Hendriksson, N., Nyyssönen, M., and Itävaara, M. (2013). Characterisation and isotopic evolution of saline waters of the Outokumpu Deep Drill Hole, Finland–Implications for water origin and deep terrestrial biosphere. *Appl. Geochem.* 32, 37–51. doi: 10.1016/j.apgeochem.2012.10.013

Kietäväinen, R., Ahonen, L., Kukkonen, I. T., Niedermann, S., and Wiersberg, T. (2014). Noble gas residence times of saline waters within crystalline bedrock, Outokumpu Deep Drill Hole, Finland. *Geochim. Cosmochim. Acta* 145, 159–174. doi: 10.1016/j.gca.2014.09.012

Kimura, H., Nashimoto, H., Shimizu, M., Hattori, S., Yamada, K., Koba, K., et al. (2010). Microbial methane production in deep aquifer associated with the accretionary prism in Southwest Japan. *ISME J.* 4, 531–541. doi: 10.1038/ismej.2009.132

Kinnaman, F. S., Valentine, D. L., and Tyler, S. C. (2007). Carbon and hydrogen isotope fractionation associated with the aerobic microbial oxidation of methane, ethane, propane and butane. *Geochim. Cosmochim. Acta* 71, 271–283. doi: 10.1016/j.gca.2006.09.007

Kipfer, R., Aeschbach-Hertig, W., Peeters, F., and Stute, M. (2002). Noble gases in lakes and ground waters. *Rev. Mineral. Geochem.* 47, 615–700. doi: 10.2138/rmg.2002.47.14

Kita, I., Matsuo, S., and Wakita, H. (1982). H_2 generation by reaction between H_2O and crushed rock: an experimental study on H_2 degassing from the active fault zone. *J. Geophys. Res.* 87, 10,789–10,795.

Knittel, K., and Boetius, A. (2009). Anaerobic oxidation of methane: progress with an unknown process. *Annu. Rev. Microbiol.* 63, 311–334. doi: 10.1146/annurev.micro.61.080706.093130

Knittel, K., Losekann, T., Boetius, A., Kort, R., and Amann, R. (2005). Diversity and distribution of methanotrophic archaea at cold seeps. *Appl. Environ. Microbiol.* 71, 467–479. doi: 10.1128/AEM.71.1.467-479.2005

Kotelnikova, S. (2002). Microbial production and oxidation of methane in deep subsurface. *Earth-Sci. Rev.* 58, 367–395. doi: 10.1016/S0012-8252(01)00082-4

Kotelnikova, S., Macario, A. J., and Pedersen, K. (1998). Methanobacterium subterraneum sp. nov., a new alkaliphilic, eurythermic and halotolerant methanogen isolated from deep granitic groundwater. *Int. J. Syst. Bacteriol.* 48, 357–367. doi: 10.1099/00207713-48-2-357

Kotelnikova, S., and Pedersen, K. (1997). Evidence for methanogenic archaea and homoacetogenic bacteria in deep granitic rock aquifers. *FEMS Microbiol. Rev.* 20, 339–349. doi: 10.1111/j.1574-6976.1997.tb00319.x

Kotelnikova, S., and Pedersen, K. (1998). Distribution and activity of methanogens and homoacetogens in deep granitic aquifers at Äspö Hard Rock Laboratory, Sweden. *FEMS Microbiol. Ecol.* 26, 121–134. doi: 10.1016/S0168-6496(98)00028-2

Kretschmer, K., Biastoch, A., Rupke, L., and Burwicz, E. (2015). Modeling the fate of methane hydrates under global warming. *Global Biogeochem. Cycles* 29, 610–625. doi: 10.1002/2014GB005011

Krüger, M., Meyerdierks, A., Glockner, F. O., Amann, R., Widdel, F., and Kube, M., et al. (2003). A conspicuous nickel protein in microbial mats that oxidize methane anaerobically. *Nature* 426, 878–881. doi: 10.1038/nature02207

Krumholz, L. R., McKinley, J. P., Ulrich, G. A., and Suflita, J. M. (1997). Confined subsurface microbial communities in Cretaceous rock. *Nature* 386, 64–66 doi: 10.1038/386064a0

Kyle, J. E., Eydal, H. S., Ferris, F. G., and Pedersen, K. (2008). Viruses in granitic groundwater from 69 to 450 m depth of the Äspö hard rock laboratory, Sweden. *ISME J.* 2, 571–574. doi: 10.1038/ismej.2008.18

Lang, S. Q., Früh-Green, G. L., Bernasconi, S. M., Lilley, M. D., Proskurowski, G., Méhay, S., et al. (2012). Microbial utilization of abiogenic carbon and hydrogen in a serpentinite-hosted system. *Geochim. Cosmochim. Acta* 92, 82–99. doi: 10.1016/j.gca.2012.06.006

Langille, M. G., Zaneveld, J., Caporaso, J. G., McDonald, D., Knights, D., Reyes, J. A., et al. (2013). Predictive functional profiling of microbial communities using 16S rRNA marker gene sequences. *Nat. Biotechnol.* 31, 814–821. doi: 10.1038/nbt.2676

Lazar, C. S., Dinasquet, J., L'Haridon, S., Pignet, P., and Toffin, L. (2011a). Distribution of anaerobic methane-oxidizing and sulfate-reducing communities in the G11 Nyegga pockmark, Norwegian Sea. *A. Van Leeuw.* 100, 639–653. doi: 10.1007/s10482-011-9620-z

Lazar, C. S., L'Haridon, S., Pignet, P., and Toffin, L. (2011b). Archaeal populations in hypersaline sediments underlying orange microbial mats in the Napoli mud volcano. *Appl. Environ. Microbiol.* 77, 3120–3131. doi: 10.1128/AEM.01296-10

Lever, M. A., Rouxel, O., Alt, J. C., Shimizu, N., Ono, S., Coggon, R. M., et al. (2013). Evidence for microbial carbon and sulfur cycling in deeply buried ridge flank basalt. *Science* 339, 1305–1308. doi: 10.1126/science.1229240

Lin, L., Hall, J., Lippmann-Pipke, J., Ward, J. A., Sherwood Lollar, B., DeFlaun, M., et al. (2005a). Radiolytic H_2in continental crust: nuclear power for deep subsurface microbial communities. *Geochem. Geophys. Geosyst.* 6, Q07003. doi: 10.1029/2004GC000907

Lin, L., Hall, J., Onstott, T., Gihring, T., Lollar, B. S., Boice, E., et al. (2006a). Planktonic microbial communities associated with fracture-derived groundwater in a deep gold mine of South Africa. *Geomicrobiol. J.* 23, 475–497. doi: 10.1080/01490450600875829

Lin, L.-H., Slater, G. F., Sherwood Lollar, B., Lacrampe-Couloume, G., and Onstott, T. C. (2005b). The yield and isotopic composition of radiolytic H_2, a potential energy source for the deep subsurface biosphere. *Geochim. Cosmochim. Acta* 69, 893–903. doi: 10.1016/j.gca.2004.07.032

Lin, L.-H., Wang, P.-L., Rumble, D., Lippmann-Pipke, J., Boice, E., Pratt, L. M., et al. (2006b). Long-term sustainability of a high-energy, low-diversity crustal biome. *Science* 314, 479–482. doi: 10.1126/science.1127376

Lippmann, J., Stute, M., Torgersen, T., Moser, D. P., and Hall, J. A., Lin, et al. (2003). Dating ultra-deep mine waters with noble gases and ^{36}Cl, Witwatersrand Basin, South Africa. *Geochim. Cosmochim. Acta* 67, 4597–4619. doi: 10.1016/S0016-7037(03)00414-9

Liu, Y., and Whitman, W. B. (2008). Metabolic, phylogenetic, and ecological diversity of the methanogenic Archaea. *Ann. N. Y. Acad. Sci.* 1125, 171–189. doi: 10.1196/annals.1419.019

Luton, P. E., Wayne, J. M., Sharp, R. J., and Riley, P. W. (2002). The *mcr*A gene as an alternative to 16S rRNA in the phylogenetic analysis of methanogen populations in landfill. *Microbiology* 148, 3521–3530.

Luukkonen, A., Pitkänen, P., Ruotsalainen, P., Leino-Forsman, H., and Snellman, M. (1999). *Hydrogeochemical Conditions at the Hästholmen site*. Posiva report 99-26, Posiva Oy, Helsinki. Available online at: http://www.posiva.fi/files/2708/POSIVA-99-26_web.pdf

Mayhew, L. E., Ellison, E. T., McCollom, T. M., Trainor, T. P., and Templeton, A. S. (2013). Hydrogen generation from low-temperature water-rock reactions. *Nat. Geosci.* 6, 478–484. doi: 10.1038/ngeo1825

McCollom, T. M. (2013). Laboratory simulations of abiotic hydrocarbon formation in Earth's deep subsurface. *Rev. Mineral. Geochem.* 75, 467–494. doi: 10.2138/rmg.2013.75.15

McCollom, T. M., and Bach, W. (2009). Thermodynamic constraints on hydrogen generation during serpentinization of ultramafic rocks. *Geochim. Cosmochim. Acta* 73, 856–875. doi: 10.1016/j.gca.2008.10.032

McCollom, T. M., Sherwood Lollar, B., Lacrampe-Couloume, G., and Seewald, J. S. (2010). The influence of carbon source on abiotic organic synthesis and carbon isotope fractionation under hydrothermal conditions. *Geochim. Cosmochim. Acta* 74, 2717–2740. doi: 10.1016/j.gca.2010.02.008

Meyerdierks, A., Kube, M., Lombardot, T., Knittel, K., Bauer, M., Glöckner, F. O., et al. (2005). Insight into the genomes of archaea mediating the anaerobic oxidation of methane. *Environ. Microbiol.* 7, 1937–1951. doi: 10.1111/j.1462-2920.2005.00844.x

Milkov, A. V. (2011). Worldwide distribution and significance of secondary microbial methane formed during petroleum biodegradation in conventional reservoirs. *Org. Geochem.* 42, 184–207. doi: 10.1016/j.orggeochem.2010.12.003

Mills, C. T., Amano, Y., Slater, G. F., Dias, R. F., Iwatsuki, T., and Mandernack, K. W. (2010). Microbial carbon cycling in oligotrophic regional aquifers near the Tono Uranium Mine, Japan as inferred from δ 13 C and Δ 14 C values of *in situ* phospholipid fatty acids and carbon sources. *Geochim. Cosmochim. Acta* 74, 3785–3805. doi: 10.1016/j.gca.2010.03.016

Mills, H. J., Hodges, C., Wilson, K., MacDonald, I. R., and Sobecky, P. A. (2003). Microbial diversity in sediments associated with surface-breaching gas hydrate mounds in the Gulf of Mexico. *FEMS Microbiol. Ecol.* 46, 39–52. doi: 10.1016/S0168-6496(03)00191-0

Milucka, J., Ferdelman, T. G., Polerecky, L., Franzke, D., Wegener, G., Schmid, M., et al. (2012). Zero-valent sulphur is a key intermediate in marine methane oxidation. *Nature* 491, 541–546. doi: 10.1038/nature11656

Morelli, R. M., Bell, C. C., Creaser, R. A., and Simonetti, A. (2010). Constraints on the genesis of gold mineralization at the Homestake Gold Deposit, Black Hills, South Dakota from rhenium–osmium sulfide geochronology. *Miner. Deposita.* 45, 461–480. doi: 10.1007/s00126-010-0284-9

Moser, D. P., Gihring, T. M., Brockman, F. J., Fredrickson, J. K., Balkwill, D. L., Dollhopf, M. E., et al. (2005). *Desulfotomaculum* and *Methanobacterium* spp. dominate a 4- to 5-kilometer-deep fault. *Appl. Environ. Microbiol.* 71, 8773–8783. doi: 10.1128/AEM.71.12.8773-8783.2005

Moser, D. P., Onstott, T. C., Fredrickson, J. K., Brockman, F. J., Balkwill, D. L., Drake, G. R., et al. (2003). Temporal shifts in the geochemistry and microbial community structure of an ultradeep mine borehole following isolation. *Geomicrobiol. J.* 20, 517–548. doi: 10.1080/713851170

Nandi, R., and Sengupta, S. (1998). Microbial production of hydrogen: an overview. *Crit. Rev. Microbiol.* 24, 61–84. doi: 10.1080/10408419891294181

Nazaries, L., Murrell, J. C., Millard, P., Baggs, L., and Singh, B. K. (2013). Methane, microbes and models: fundamental understanding of the soil methane cycle for future predictions. *Environ. Microbiol.* 15, 2395–2417. doi: 10.1111/1462-2920.12149

Nealson, K. H., Inagaki, F., and Takai, K. (2005). Hydrogen-driven subsurface lithoautotrophic microbial ecosystems (SLiMEs): do they exist and why should we care? *Trends Microbiol.* 13, 405–410. doi: 10.1016/j.tim.2005.07.010

Neubeck, A., Than Duc, N., Bastviken, D., Crill, P., and Holm, N. G. (2011). Formation of H_2 and CH_4 by weathering of olivine at temperatures between 30 and 70°C. *Geochem. Trans.* 12, 6. doi: 10.1186/1467-4866-12-6

Ni, Y., Ma, Q., Ellis, G. S., Dai, J., Katz, B., Zhang, S., et al. (2011). Fundamental studies on kinetic isotope effect (KIE) of hydrogen isotope fractionation in natural gas systems. *Geochim. Cosmochim. Acta* 75, 2696–2707. doi: 10.1016/j.gca.2011.02.016

Nurmi, P. A., Kukkonen, I. T., and and, Lahermo, P. W. (1988). Geochemistry and origin of saline groundwaters in the Fennoscandian Shield. *Appl. Geochem.* 3, 185–203. doi: 10.1016/0883-2927(88)90007-8

Nyyssönen, M., Bomberg, M., Kapanen, A., Nousiainen, A., Pitkänen, P., and Itävaara, M. (2012). Methanogenic and sulphate-reducing microbial communities in deep groundwater of crystalline rock fractures in Olkiluoto, Finland. *Geomicrobiol. J.* 29, 863–878. doi: 10.1080/01490451.2011.635759

Nyyssönen, M., Hultman, J., Ahonen, L., Kukkonen, I., Paulin, L., Laine, P., et al. (2014). Taxonomically and functionally diverse microbial communities in deep crystalline rocks of the Fennoscandian shield. *ISME J.* 8, 126–138. doi: 10.1038/ismej.2013.125

Onstott, T. C., Lin, L.-H., Davidson, M., Mislowack, B., Borcsik, M., Hall, J., et al. (2006). The origin and age of biogeochemical trends in deep fracture water of the Witwatersrand Basin, South Africa. *Geomicrobiol. J.* 23, 369–414. doi: 10.1080/01490450600875688

Onstott, T. C., McGown, D. J., Bakermans, C., Ruskeeniemi, T., Ahonen, L., Telling, J., et al. (2009). Microbial communities in subpermafrost saline fracture water at the Lupin Au Mine, Nunavut, Canada. *Microb. Ecol.* 58, 786–807. doi: 10.1007/s00248-009-9553-5

Orphan, V. J., House, C. H., Hinrichs, K. U., McKeegan, K. D., and DeLong, E. F. (2001). Methane-consuming archaea revealed by directly coupled isotopic and phylogenetic analysis. *Science* 293, 484–487. doi: 10.1126/science.1061338

Orphan, V. J., House, C. H., Hinrichs, K. U., McKeegan, K. D., and DeLong, E. F. (2002). Multiple archaeal groups mediate methane oxidation in anoxic cold seep sediments. *Proc. Natl. Acad. Sci. U.S.A.* 99, 7663–7668. doi: 10.1073/pnas.072210299

Osburn, M. R., LaRowe, D. E., Momper, L. M., and Amend, J. P. (2014). Chemolithotrophy in the continental deep subsurface: Sanford Underground Research Facility (SURF), USA. *Front. Microbiol.* 5:610. doi: 10.3389/fmicb.2014.00610

Paul, K., Nonoh, J. O., Mikulski, L., and Brune, A. (2012). '*Methanoplasmatales*," Thermoplasmatales-related archaea in termite guts and other environments, are the seventh order of methanogens. *Appl. Environ. Microbiol.* 78, 8245–8253. doi: 10.1128/AEM.02193-12

Pedersen, K. (1996). Investigations of subterranean bacteria in deep crystalline bedrock and their importance for the disposal of nuclear waste. *Can. J. Microbiol.* 42, 382–391. doi: 10.1139/m96-054

Pedersen, K. (1997). Microbial life in deep granitic rock. *FEMS Microbiol. Rev.* 20, 399–414. doi: 10.1111/j.1574-6976.1997.tb00325.x

Pedersen, K. (2000). Exploration of deep intraterrestrial microbial life: current perspectives. *FEMS Microbiol. Lett.* 185, 9–16. doi: 10.1111/j.1574-6968.2000.tb09033.x

Pedersen, K. (2013). Metabolic activity of subterranean microbial communities in deep granitic groundwater supplemented with methane and H_2. *ISME J.* 7, 839–849. doi: 10.1038/ismej.2012.144

Pedersen, K., Arlinger, J., Eriksson, S., Hallbeck, A., Hallbeck, L., and Johansson, J. (2008). Numbers, biomass and cultivable diversity of microbial populations relate to depth and borehole-specific conditions in groundwater from depths of 4–450 m in Olkiluoto, Finland. *ISME J.* 2, 760–775. doi: 10.1038/ismej.2008.43

Pedersen, K., and Ekendahl, S. (1990). Distribution and activity of bacteria in deep granitic groundwaters of Southeastern Sweden. *Microb. Ecol.* 20, 37–52. doi: 10.1007/BF02543865

Pedersen, K., and Haveman, S. (1999). *Analysis of Diversity and Distribution of Microorganisms in Palmottu Groundwater and Evaluation of their Influence on Redox Potential and Uranium (VI) Reduction*. The Palmottu Natural Analogue Project, Technical Report 99-14. Available online at: http://tupa.gtk.fi/raportti/arkisto/y50_99_14.pdf

Petsch, S. T., Edwards, K., and Eglinton, T. I. (2005). Microbial transformations of organic matter in black shales and implications for global biogeochemical cycles. *Palaeogeogr. Palaeoclimatol. Palaeoecol.* 219, 157–170. doi: 10.1016/j.palaeo.2004.10.019

Petsch, S. T., Eglinton, T. I., and Edwards, K. J. (2001). 14C-dead living biomass: evidence for microbial assimilation of ancient organic carbon during shale weathering. *Science* 292, 1127–1131. doi: 10.1126/science.1058332

Pitkänen, P., Luukkonen, A., Ruotsalainen, P., Leino-Forsman, H., and Vuorinen, U. (1998). *Geochemical Modelling of Groundwater Evolution and Residence Time at the Kivetty Site*. Posiva report 98-07, Posiva Oy, Helsinki. Available online at: http://www.posiva.fi/files/2672/POSIVA-98-07_web.pdf

Pitkänen, P., and Partamies, S. (2007). *Origin and Implications of Dissolved Gases in Groundwater at Olkiluoto*. Posiva report 2007-04, Posiva Oy, Olkiluoto. Available online at: http://www.posiva.fi/files/341/Posiva2007-04web.pdf

Pitkänen, P., Snellman, M., Vuorinen, U., and Leino-Forsman, H. (1996). *Geochemical Modelling Study on the Age and Evolution of the Groundwater at the Romuvaara Site*. Posiva report 96-06, Posiva Oy, Helsinki. Available online at: http://www.posiva.fi/files/3458/Posiva-96-06.pdf

Prinzhofer, A. (2013). "Noble gas in oil and gas accumulations," in *The Noble Gases as Geochemical Tracers*, ed P. Burnard (Berlin; Heidelberg: Springer-Verlag), 225–247. doi: 10.1007/978-3-642-28836-4_9

Purkamo, L., Bomberg, M., Nyyssönen, M., Kukkonen, I., Ahonen, L., and Itävaara, M. (2015). Heterotrophic communities supplied by ancient organic carbon predominate in deep Fennoscandian bedrock fluids. *Microb. Ecol.* 69, 319–332. doi: 10.1007/s00248-014-0490-6

Purkamo, L., Bomberg, M., Nyyssönen, M., Kukkonen, I., Ahonen, L., Kietäväinen, R., et al. (2013). Dissecting the deep biosphere: retrieving authentic microbial communities from packer-isolated deep crystalline bedrock fracture zones. *FEMS Microbiol. Ecol.* 85, 324–337. doi: 10.1111/1574-6941.12126

Raghoebarsing, A. A., Pol, A., Van de Pas-Schoonen, K. T., Smolders, A. J., Ettwig, K. F., Rijpstra, W. I. C., et al. (2006). A microbial consortium couples anaerobic methane oxidation to denitrification. *Nature* 440, 918–921. doi: 10.1038/nature04617

Rajala, P., Bomberg, M., Kietäväinen, R., Kukkonen, I., Ahonen, L., Nyyssönen, M., et al. (2015). Rapid reactivation of deep subsurface microbes in the presence of C-1 compounds. *Microorganisms* 3, 17–33. doi: 10.3390/microorganisms3010017

Rastogi, G., Osman, S., Kukkadapu, R., Engelhard, M., Vaishampayan, P. A., Andersen, G. L., et al. (2010). Microbial and mineralogical characterizations of soils collected from the deep biosphere of the Former Homestake Gold Mine, South Dakota. *Microb. Ecol.* 60, 539–550. doi: 10.1007/s00248-010-9657-y

Reeves, E. P., Seewald, J. S., and Sylva, S. P. (2012). Hydrogen isotope exchange between *n*-alkanes and water under hydrothermal conditions. *Geochim. Cosmochim. Acta* 77, 582–599. doi: 10.1016/j.gca.2011.10.008

Rosewarne, C. P., Greenfield, P., Li, D., Tran-Dinh, N., Bradbury, M. I., Midgley, D. J., et al. (2013a). Draft genome sequence of *Clostridium* sp. Maddingley, Isolated from coal-seam gas formation water. *Genome Announc.* 1:e00081-12. doi: 10.1128/genomeA.00081-12

Rosewarne, C. P., Greenfield, P., Li, D., Tran-Dinh, N., Midgley, D. J., and Hendry, P. (2013b). Draft genome sequence of *Methanobacterium* sp. Maddingley, reconstructed from metagenomic sequencing of a methanogenic microbial consortium enriched from coal-seam gas formation water. *Genome Announc.* 1:e00082-12. doi:10.1128/genomeA.00082-12

Ruppel, C. (2011). Methane hydrates and contemporary climate change. *Nat. Educ. Knowl.* 3, 29. Available online at: http://www.nature.com/scitable/knowledge/library/methane-hydrates-and-contemporary-climate-change-24314790

Sahlstedt, E., Karhu, J. A., and Pitkänen, P. (2010). Indications for the past redox environments in deep groundwaters from the isotopic composition of carbon and oxygen in fracture calcite, Olkiluoto, SW Finland. *Isot. Environ. Health Stud.* 46, 370–391. doi: 10.1080/10256016.2010.505981

Sano, Y., and Fischer, T. (2013). "The analysis and interpretation of noble gases in modern hydrothermal systems," in *The Noble Gases as Geochemical Tracers*, ed P. Burnard (Berlin; Heidelberg: Springer-Verlag), 249–317. doi: 10.1007/978-3-642-28836-4_10

Sano, Y., Urabe, A., and Wakita, H. (1993). Origin of hydrogen-nitrogen gas seeps, Oman. *Appl. Geochem.* 8, 1–8. doi: 10.1016/0883-2927(93)90053-J

Schidlowski, M. (2001). Carbon isotopes as biogeochemical recorders of life over 3.8 Ga of Earth history: evolution of a concept. *Precambrian Res.* 106, 117–134. doi: 10.1016/S0301-9268(00)00128-5

Schlegel, M. E., Zhou, Z., McIntosh, J. C., Ballentine, C. J., and Person, M. A. (2011). Constraining the timing of microbial methane generation in an organic-rich shale using noble gases, Illinois Basin, USA. *Chem. Geol.* 287, 27–40. doi: 10.1016/j.chemgeo.2011.04.019

Schloss, P. D., Westcott, S. L., Ryabin, T., Hall, J. R., Hartmann, M., Hollister, E. B., et al. (2009). Introducing mothur: open-source, platform-independent, community-supported software for describing and comparing microbial communities. *Appl. Environ. Microbiol.* 75, 7537–7541. doi: 10.1128/AEM.01541-09

Schoell, M. (1980). The hydrogen and carbon isotopic composition of methane from natural gases of various origins. *Geochim. Cosmochim. Acta* 44, 649–661. doi: 10.1016/0016-7037(80)90155-6

Schrenk, M. O., Brazelton, W. J., and Lang, S. Q. (2013). Serpentinization, carbon, and deep life. *Rev. Mineral. Geochem.* 75, 575–606. doi: 10.2138/rmg.2013.75.18

Sherwood Lollar, B., Frape, S. K., Fritz, P., Macko, S. A., Welhan, J. A., Blomqvist, R., et al. (1993a). Evidence for bacterially generated hydrocarbon gas in Canadian Shield and Fennoscandian Shield rocks. *Geochim. Cosmochim. Acta* 57, 5073–5085. doi: 10.1016/0016-7037(93)90609-Z

Sherwood Lollar, B., Frape, S. K., Weise, S. M., Fritz, P., Macko, S. A., and Welhan, J. A. (1993b). Abiogenic methanogenesis in crystalline rocks. *Geochim. Cosmochim. Acta* 57, 5087–5097. doi: 10.1016/0016-7037(93)90610-9

Sherwood Lollar, B., Lacrampe-Couloume, G., Slater, G. F., Ward, J., Moser, D. P., Gihring, T. M., et al. (2006). Unravelling abiogenic and biogenic sources of methane in the Earth's deep subsurface. *Chem. Geol.* 226, 328–339. doi: 10.1016/j.chemgeo.2005.09.027

Sherwood Lollar, B., Onstott, T. C., Lacrampe-Couloume, G., and Ballentine, C. J. (2014). The contribution of the Precambrian continental lithosphere to global H_2 production. *Nature* 516, 379–382. doi: 10.1038/nature14017

Sherwood Lollar, B., Westgate, T. D., Ward, J. A., Slater, G. F., and Lacrampe-Couloume, G. (2002). Abiogenic formation of alkanes in the Earth's crust as a minor source for global hydrocarbon reservoirs. *Nature* 416, 522–524. doi: 10.1038/416522a

Slater, G. F., Lippmann-Pipke, J., Moser, D. P., Reddy, C. M., Onstott, T. C., Lacrampe-Couloume, G., et al. (2006). ^{14}C in methane and DIC in the deep terrestrial subsurface: Implications for microbial methanogenesis. *Geomicrobiol. J.* 23, 453–462. doi: 10.1080/01490450600875787

Sohlberg, E., Bomberg, M., Miettinen, H., Nyyssönen, M., Salavirta, H., Vikman, M., et al. (2015). Revealing the unexplored fungal communities in deep groundwater of crystalline bedrock fracture zones in Olkiluoto, Finland. *Front. Microbiol.* 6:573. doi: 10.3389/fmicb.2015.00573

Stępniewska, Z., Pytlak, A., and Kuźniar, A. (2013). Methanotrophic activity in carboniferous coalbed rocks. *Int. J. Coal Geol.*106, 1–10. doi: 10.1016/j.coal.2013.01.003

Stępniewska, Z., Pytlak, A., and Kuźniar, A. (2014). Distribution of the methanotrophic bacteria in the Western part of the Upper Silesian Coal Basin (Borynia-Zofiówka and Budryk coal mines). *Int. J. Coal Geol.* 130, 70–78. doi: 10.1016/j.coal.2014.05.003

Stolper, D. A., Lawson, M., Davis, C. L., Ferreira, A. A., Santos Neto, E. V., Ellis, G. S., et al. (2014). Formation temperatures of thermogenic and biogenic methane. *Science* 344, 1500–1503. doi: 10.1126/science.1254509

Stotler, R. L., Frape, S. K., Ahonen, L., Clark, I., Greene, S., Hobbs, M., et al. (2010). Origin and stability of a permafrost methane hydrate occurrence in the Canadian Shield. *Earth Planet. Sci. Lett.* 296, 384–394. doi: 10.1016/j.epsl.2010.05.024

Stotler, R. L., Frape, S. K., Ruskeeniemi, T., Ahonen, L., Onstott, T. C., and Hobbs, M. Y. (2009). Hydrogeochemistry of groundwaters in and below the base of thick permafrost at Lupin, Nunavut, Canada. *J. Hydrol.* 373, 80–95. doi: 10.1016/j.jhydrol.2009.04.013

Strąpoć, D., Mastalerz, M., Dawson, K., Macalady, J., Callaghan, A. V., Wawrik, B., et al. (2011). Biogeochemistry of microbial coal-bed methane. *Annu. Rev. Earth Planet. Sci.* 39, 617–656. doi: 10.1146/annurev-earth-040610-133343

Stroes-Gascoyne, S., and West, J. M. (1996). An overview of microbial research related to high-level nuclear waste disposal with emphasis on the Canadian concept for the disposal of nuclear fuel waste. *Can. J. Microbiol.* 42, 349–366. doi: 10.1139/m96-051

Suda, K., Ueno, Y., Yoshizaki, M., Nakamura, H., Kurokawa, K., Nishiyama, E., et al. (2014). Origin of methane in serpentinite-hosted hydrothermal systems: the CH_4-H_2-H_2O hydrogen isotope systematics of the Hakuba Happo hot spring. *Earth Planet. Sci. Lett.* 386, 112–125. doi: 10.1016/j.epsl.2013.11.001

Sugimoto, A., and Wada, E. (1995). Hydrogen isotopic composition of bacterial methane: CO_2/H_2 reduction and acetate fermentation. *Geochim. Cosmochim. Acta* 59, 1329–1337. doi: 10.1016/0016-7037(95)00047-4

Takai, K., Moser, D. P., DeFlaun, M., Onstott, T. C., and Fredrickson, J. K. (2001). Archaeal diversity in waters from deep South African gold mines. *Appl. Environ. Microbiol.* 67, 5750–5760. doi: 10.1128/AEM.67.21.5750-5760.2001

Taran, L. N., Onoshko, M. P., and Mikhailov, N. D. (2011). Structure and composition of organic matter and isotope geochemistry of the Palaeproterozoic graphite and sulphide-rich metasedimentary rocks from the Outokumpu Deep Drill Hole, Eastern Finland. *Geol. Surv. Finland* 51, 219–228.

Taran, Y. A., Klinger, G. A., and Sevastianov, V. S. (2007). Carbon isotope effects in the open-system Fischer-Tropsch synthesis. *Geochim. Cosmochim. Acta* 71, 4474–4487. doi: 10.1016/j.gca.2007.06.057

Tazaz, A. M., Bebout, B. M., Kelley, C. A., Poole, J., and Chanton, J. P. (2013). Redefining the isotopic boundaries of biogenic methane: Methane from endoevaporites. *Icarus* 224, 268–275. doi: 10.1016/j.icarus.2012.06.008

Teske, A., and Biddle, J. (2008). "Analysis of deep subsurface microbial communities by functional genes and genomics," in *Links Between Geological Processes, Microbial Activities and Evolution of Life,* eds Y. Dilek, H. Furnes and K. Muehlenbachs (New York, NY: Springer Science+Business Media, B.V.), 159–176.

Thauer, R. K., Kaster, A., Seedorf, H., Buckel, W., and Hedderich, R. (2008). Methanogenic archaea: ecologically relevant differences in energy conservation. *Nat. Rev. Microbiol.* 6, 579–591. doi: 10.1038/nrmicro1931

Treat, C., Natali, S. M., Ernakovich, J., Iversen, C. M., Lupascu, M., McGuire, A. D., et al. (2015). A pan-Arctic synthesis of CH4 and CO2 production from anoxic soil incubations. *Glob. Change Biol.* 21, 2787–2803. doi: 10.1111/gcb.12875

Trinchero, P., Delos, A., Molinero, J., Dentz, M., and Pitkänen, P. (2014). Understanding and modelling dissolved gas transport in the bedrock of three Fennoscandian sites. *J. Hydrol.* 512, 506–517. doi: 10.1016/j.jhydrol.2014.03.011

Valentine, D. L., Chidthaisong, A., Rice, A., Reeburgh, W. S., and Tyler, S. C. (2004a). Carbon and hydrogen isotope fractionation by moderately thermophilic methanogens. *Geochim. Cosmochim. Acta* 68, 1571–1590. doi: 10.1016/j.gca.2003.10.012

Valentine, D. L., Sessions, A. L., Tyler, S. C., and Chithaisong, A. (2004b). Hydrogen isotope fractionation during H_2/CO_2 acetogenesis: hydrogen utilization efficiency and the origin of lipid-bound hydrogen. *Geobiology* 2, 179–188. doi: 10.1111/j.1472-4677.2004.00030.x

Västi, K. (2011). Petrology of the Drill hole R2500 at Outokumpu, Eastern Finland - the deepest drill hole ever drilled in Finland. *Geol. Surv. Finland* 51, 17–46.

Vovk, I. F. (1987). Radiolytic salt enrichment and brines in the crystalline basement of the East European Platform. *Geol. Assoc. Canada* 33, 197–210.

Walter, K. M., Zimov, S., Chanton, J. P., Verbyla, D., and Chapin, F. S. (2006). Methane bubbling from Siberian thaw lakes as a positive feedback to climate warming. *Nature* 443, 71–75. doi: 10.1038/nature05040

Wang, D. T., Gruen, D. S., Sherwood Lollar, B., Hinrichs, K.-U., Stewart, L. C., Holden, J. F., et al. (2015). Nonequilibrium clumped isotope signals in microbial methane. *Science* 348, 428–431. doi: 10.1126/science.aaa4326

Wang, J., and Wan, W. (2009). Factors influencing fermentative hydrogen production: a review. *Int. J. Hydrogen Energ.* 34, 799–811. doi: 10.1016/j.ijhydene.2008.11.015

Wang, Y., and Francis, A. J. (2005). Evaluation of microbial activity for long-term performance assessments of deep geologic nuclear waste repositories. *J. Nucl. Radiochem. Sci.* 6, 43–50. doi: 10.14494/jnrs2000.6.43

Ward, J., Slater, G., Moser, D., Lin, L., Lacrampe-Couloume, G., Bonin, A., et al. (2004). Microbial hydrocarbon gases in the Witwatersrand Basin, South Africa: implications for the deep biosphere. *Geochim. Cosmochim. Acta* 68, 3239–3250. doi: 10.1016/j.gca.2004.02.020

Wengel, M., Kothe, E., Schmidt, C. M., Heide, K., and Gleixner, G. (2006). Degradation of organic matter from black shales and charcoal by the wood-rotting fungus Schizophyllum commune and release of DOC and heavy metals in the aqueous phase. *Sci. Total Environ.* 367, 383–393. doi: 10.1016/j.scitotenv.2005.12.012

Whiticar, M. J. (1999). Carbon and hydrogen isotope systematics of bacterial formation and oxidation of methane. *Chem. Geol.* 161, 291–314. doi: 10.1016/S0009-2541(99)00092-3

Wouters, K., Moors, H., Boven, P., and Leys, N. (2013). Evidence and characteristics of a diverse and metabolically active microbial community in deep subsurface clay borehole water. *FEMS Microbiol. Ecol.* 86, 458–473. doi: 10.1111/1574-6941.12171

Zengler, K., Richnow, H. H., Rosselló-Mora, R., Michaelis, W., and Widdel, F. (1999). Methane formation from long-chain alkanes by anaerobic microorganisms. *Nature* 401, 266–269. doi: 10.1038/45777

Zhang, S., Mi, J., and He, K. (2013). Synthesis of hydrocarbon gases from four different carbon sources and hydrogen gas using a gold-tube system by Fischer-Tropsch method. *Chem. Geol.* 349–350, 27–35. doi: 10.1016/j.chemgeo.2013.03.016

Zhu, Y., Shi, B., and Fang, C. (2000). The isotopic composition of molecular nitrogen: implications on their origins in natural s accumulations. *Chem. Geol.* 164, 321–330. doi: 10.1016/S0009-2541(99)00151-5

Conflict of Interest Statement: The authors declare that the research was conducted in the absence of any commercial or financial relationships that could be construed as a potential conflict of interest.

frontiers in Microbiology

ORIGINAL RESEARCH
published: 16 July 2015
doi: 10.3389/fmicb.2015.00719

Marinobacter subterrani, a genetically tractable neutrophilic Fe(II)-oxidizing strain isolated from the Soudan Iron Mine

*Benjamin M. Bonis and Jeffrey A. Gralnick**

BioTechnology Institute and Department of Microbiology, University of Minnesota – Twin Cities, Saint Paul, MN, USA

We report the isolation, characterization, and development of a robust genetic system for a halophilic, Fe(II)-oxidizing bacterium isolated from a vertical borehole originating 714 m below the surface located in the Soudan Iron Mine in northern Minnesota, USA. Sequence analysis of the 16S rRNA gene places the isolate in the genus *Marinobacter* of the Gamma*proteobacteria*. The genome of the isolate was sequenced using a combination of short- and long-read technologies resulting in two contigs representing a 4.4 Mbp genome. Using genomic information, we used a suicide vector for targeted deletion of specific flagellin genes, resulting in a motility-deficient mutant. The motility mutant was successfully complemented by expression of the deleted genes *in trans*. Random mutagenesis using a transposon was also achieved. Capable of heterotrophic growth, this isolate represents a microaerophilic Fe(II)-oxidizing species for which a system for both directed and random mutagenesis has been established. Analysis of 16S rDNA suggests *Marinobacter* represents a major taxon in the mine, and genetic interrogation of this genus may offer insight into the structure of deep subsurface communities as well as an additional tool for analyzing nutrient and element cycling in the subsurface ecosystem.

Keywords: Fe(II)-oxidizing bacteria, genetic system, dark biosphere, deep subsurface, cultivation, characterization

OPEN ACCESS

Edited by:
Malin Bomberg, VTT Technical Research Centre of Finland, Finland

Reviewed by:
Hongchen Jiang, Miami University, USA
Daan R. Speth, Radboud University Nijmegen, Netherlands

***Correspondence:**
Jeffrey A. Gralnick, BioTechnology Institute and Department of Microbiology, University of Minnesota – Twin Cities, 1479 Gortner Avenue, Saint Paul, MN 55108, USA
gralnick@umn.edu

Specialty section:
This article was submitted to Terrestrial Microbiology, a section of the journal Frontiers in Microbiology

Received: *10 April 2015*
Accepted: *30 June 2015*
Published: *16 July 2015*

Citation:
Bonis BM and Gralnick JA (2015) Marinobacter subterrani, a genetically tractable neutrophilic Fe(II)-oxidizing strain isolated from the Soudan Iron Mine. Front. Microbiol. 6:719. doi: 10.3389/fmicb.2015.00719

Introduction

Ubiquitous and abundant in marine environments, the genus *Marinobacter* contains a metabolic diversity and environmental versatility that has gained recent attention as a prospective biocatalyst for wax ester synthesis (Holtzapple and Schmidt-Dannert, 2007; Lenneman et al., 2013) and remediation of hydrocarbon contaminated environments (Strong et al., 2013; Fathepure, 2014). *Marinobacter* species become initially enriched in hydraulic fracturing effluent, suggesting an ability to thrive in harsh environments and in the deep subsurface (Cluff et al., 2014). Coupled with the prominent contribution of *Marinobacter* to geochemical cycling (Handley et al., 2009; Wang et al., 2012; Handley and Lloyd, 2013) and various ecosystem roles such as hydrocarbon degradation (Handley and Lloyd, 2013) and marine snow precipitation (Kaeppel et al., 2012), a greater understanding and control of these bacteria is necessary to fully harness and explore the processes they influence and are able to perform. Though traditionally thought to be a genus comprised exclusively of marine organisms (Handley and Lloyd, 2013), *Marinobacter* species isolated from salinous non-marine sources are challenging this definition of the genus, which includes members from wastewater (Liebgott et al., 2006), salinous soil (Martin et al., 2003), and now the deep subsurface.

The Soudan Underground Mine State Park, home of the Soudan Iron Mine, is located in the Archean Soudan Iron Formation of northern Minnesota, USA. The mine reaches a depth of 714 m below the surface, and produced high-grade hematite ore until it closed operations in 1962. In an effort to expand the depth of the mine prior to closing, core samples were drilled to locate ore-rich veins. Water from the surrounding rock, a calcium- and sodium-rich brine that reaches salinities as high as 4.2% (w/v), emerges from these boreholes. Anaerobic and containing up to 150 mM dissolved iron, the water carries with it microbes from still deeper in the earth (Edwards et al., 2006). Opposing concentration gradients of Fe(II) and oxygen form as the effluent contacts the air in the mineshaft, creating an environment conducive for aerobic microbial Fe(II) oxidation. A bacterium belonging to the genus *Marinobacter*, designated isolate JG233, was isolated from a downwardly oriented borehole located on the lowest level of the mine, approximately 714 m below the surface. A previous study conducted by Edwards et al. (2006) focusing on microbial ecology of the Soudan Iron Mine, found abundant Gamma*proteobacteria* in this level of the mine (Edwards et al., 2006). Heterotrophic cultivation estimates concentration of *Marinobacter* to be approximately 10^5 CFU/mL from the site where JG233 was isolated (data not shown). These findings are further supported by cultivation-independent analysis where *Marinobacter* species constituted a significant fraction of 16S rDNA sequences from several sites within the mine (unpublished work). The presence of *Marinobacter* suggests the genus is well suited to survival in the high salinity and Fe(II) found in the mine, and as such is likely to influence nutrient and geochemical cycling.

The quantity of iron in the earth's crust and its availability for electron transfer reactions enable it to significantly impact the cycling of other elements, and has been implicated in the change of state of carbon, sulfur, oxygen, nitrogen, and manganese (Ghiorse, 1984; Konhauser et al., 2011; Johnson et al., 2012). These elements play critical roles in the environment; further extending the already considerable influence of iron alone. The oxidation state of iron also influences soil structure, dissolved carbon stability (Chan et al., 2009), and enzyme activity (Baldock and Skjemstad, 2000; Bronick and Lal, 2005), affecting microbial communities and soil fertility. Additionally, microaerophilic Fe(II)-oxidizing bacteria have been implicated in the accelerated corrosion and occlusion of water-associated iron-bearing constructs, biofouling, and corroding pipes, as well as other iron-containing structures (Emerson et al., 2010; McBeth et al., 2010; Lee et al., 2013). In the environment, Fe(II)-oxidizing organisms facilitate weathering and cycling, affecting the oxidation state, bioavailability, and solubility of a variety of important elements including carbon, oxygen, nitrogen, and sulfur. Despite the importance and prevalence of these organisms, little is known regarding the biochemistry of microaerophilic Fe(II) oxidation. To our knowledge there exists no genetically tractable representative of the Fe(II)-oxidizing bacteria, and only recently has genomic work become possible. This lack of knowledge arises from two complicating factors inherent to Fe(II)-oxidizing metabolisms: the quantities of Fe(III) precipitates that result as a product of Fe(II) oxidation are inhibitory to biochemical and genetic analysis, and it is difficult to obtain sufficient biomass for analysis. These problems are coupled in current model organisms for microaerophilic Fe(II) oxidation, as growth on Fe(II) is obligatory for these organisms. For this study we set out to isolate, characterize, and describe a model organism for the study of Fe(II) oxidation capable of heterotrophic growth, and to develop a robust genetic system for this model organism. Here we describe an environmental isolate that represents a microaerophilic Fe(II)-oxidizing strain capable of heterotrophic growth, uncoupling an increase in cell density from a proportional increase in Fe(III) byproducts. Heterotrophic growth allows for the use of established molecular techniques without the complications of growth on Fe(II) normally observed in Fe(II)-oxidizing model organisms.

Materials and Methods

Isolation

Samples were obtained from the effluent of a descending exploratory borehole, Soudan Mine Diamond Drill Hole 942, located in the bottom (level 27) of the Soudan Underground Mine State Park in Soudan, Minnesota, USA. The effluent is an iron-rich, primarily calcium chloride brine with a circumneutral pH (6.31 $\pm$ 0.48). Strain JG233 was isolated aerobically on agar-solidified Difco Marine Broth (MB) medium (Becton Dickinson and Company, NJ, USA).

Media and Growth Conditions

Escherichia coli cultures were grown at 37° C in Difco LB (Luria-Bertani) medium. When cultivated in rich medium, isolate strain JG233 was grown at 30° C in MB medium. In defined-media experiments, isolate strain JG233 was cultured at 30° C in *Marinobacter* Iron Medium (MIM) containing per liter: 50.0 g NaCl, 5.3 g $MgCl_2{\cdot}6H_2O$, 0.75g KCl, 0.1 g $MgSO_4{\cdot}6H_2O$, 50 mg K_2HPO_4, 1.0 g NH_4Cl, 0.740 g $CaCl_2{\cdot}2H_2O$, 0.42 g $NaHCO_3$, 2.38 g HEPES (4-(hydroxyethyl)-1-piperazineethanesulfonic acid) and pH adjusted to 7.0 with 1 M HCl. LBMB (Luria-Bertani Marine Broth) medium used during conjugation contained 750 mL prepared Difco LB and 250 mL prepared Difco MB per liter. MB25RB medium used in preparation of competent cells contained per liter: 3.75 g tryptone, 1.875 g yeast extract, 1.875 g NaCl, 1mL 1N NaOH, 4.39 g $MgSO_4{\cdot}6H_2O$, and 4.675 g Difco MB powder. For growth under kanamycin selection, media contained 50 μg/mL kanamycin sulfate (Fisher Scientific, MA, USA). Diaminopimelic acid was used at a concentration of 360 μM when growing *E. coli* strain WM3064. Media were supplemented with 1.5% (w/v) agar for growth on solid media.

Growth conditions were assayed aerobically in MIM at 30° C unless varied for the conditions of the assay as noted. Heterotrophic growth of isolate strain JG233 in liquid media was monitored using optical density at 600 nm, unless the opacity of the media proved prohibitive, in which case growth was determined by counting colony forming units (CFU) on MB solid medium. Electron donors were assayed at 20 mM or 0.03% unless noted. Media for anaerobic growth were prepared by

sparging MIM with N_2 gas for 15 min in Balch tubes prior to autoclaving sterilization. Media were amended with 10 mM sodium lactate as the electron donor and 40 mM electron acceptor. Following growth in tubes containing nitrate, nitrogen speciation was determined using 0.8% N,N-dimethyl-α-naphthylamine solubilized in 5 M acetic acid and 0.6% sulfanilic acid solubilized in 5 M acetic acid, followed by the addition of powdered zinc. Salinity assays utilized 40 mM sodium lactate as the electron donor and varied concentrations of NaCl and $CaCl_2$ in MIM media from 0 to 2.22 M, and 0 to 300 mM, respectively. Hydrochloric acid and sodium hydroxide were used to adjust MIM for pH assays, and contained 40 mM sodium lactate as the electron donor. Media for assaying pH tolerance contained 10 mM 3-(N-morpholino)propanesulfonic acid (MOPS) and N-cyclohexyl-2-aminoethanesulfonic acid (CHES) to extend buffering capacity. Antibiotic susceptibility was assayed using antibiotic disks AM10, N30, E15, TE30, P10, S10, and B10 (Cypress Diagnostics, Belgium) on solid LB medium.

Fe(II) Oxidation Assay

The gel-stabilized gradient tube system from Emerson and Floyd (2005) was adapted for Fe(II) oxidation assays (Emerson and Floyd, 2005). In brief, FeS or $FeCO_3$ stabilized in 1.0% agarose was deposited in the bottom of sterile Balch tubes and allowed to solidify. A low-melt agarose (SeaKem LE Agarose, Lonza, ME, USA) stabilized MIM at pH 7.0 and lacking HEPES, was gently overlaid on the Fe(II)-plugs and gassed for 1 min using 20% CO_2 gas with a balance of N_2. Tubes were then stoppered with butyl rubber bungs and allowed to set overnight at ambient temperature. Heterotrophically grown strain JG233 cultures were washed in defined medium lacking organic carbon before inoculation into the gradient tubes. Inoculation was performed by removing the bung from the tube, allowing atmospheric gas into the headspace, and injecting cells throughout the length of the tube. Gradient tubes were incubated statically in the dark at 30° C. During respiratory inhibition, gradient tubes of varied maturity were amended to a final concentration of 2 mM sodium azide or 20 μM N,N-dicyclohexylcarbodiimide (DCCD) solubilized in 200 proof ethanol.

Genomic DNA Isolation and Genome Assembly

For Illumina sequencing, genomic DNA was isolated using the Wizard Genomic DNA Purification Kit (Promega, WI, USA) from an overnight culture of isolate strain JG233 grown in MB medium. Purified DNA was sequenced at the University of Minnesota Genomics Center using an Illumina platform sequencing 100 bp paired-end reads. For PacBio sequencing, pooled samples from 5 mL overnight outgrowths of isolate strain JG233 were isolated using phenol/chloroform extraction. Purified DNA was sent to the Mayo Clinic Bioinformatics Core for sequencing on a PacBio platform using size selected reads on 4 SMRT cells. Assembly was done using the Hierarchical Genome Assembly Process with 100X coverage. The genome was assembled to two contigs and polished to accuracy greater than 99.99%. Auto-annotation was performed using the RAST Annotation Server through the SEED <http://www.theseed.org/> (Aziz et al., 2008; Overbeek et al., 2014).

Bacterial Strains and Mutant Construction

The bacterial strains, plasmids, and primers used in this study are listed in **Table 1**. Primers were purchased from Integrated DNA Technologies. DNA modification enzymes were purchased from New England BioLabs. DNA purification for plasmid construction was achieved using the Invitrogen Quick PCR Cleanup Kit and Quick Plasmid Miniprep Kit.

For *flaBG* mutant construction, 1 kb regions flanking the *flaBG* genes from isolate strain JG233 were amplified by polymerase chain reaction (PCR) in two reactions, one using primers Flagellin UF/Flagellin UR, and the other with Flagellin DF/Flagellin DR (**Table 1**) in GoTaq Green Master Mix (Promega, WI, USA). Purified upstream and downstream amplicons were digested using either BamHI/AflII or AflII/SpeI, respectively. The vector, pSMV3 (Saltikov and Newman, 2003), was digested using BamHI/SpeI and gel purified. Fragments and vector were ligated using T4 ligase prior to transformation into *E. coli* strain UQ950.

Preparation of Competent Cells

Chemically competent isolate strain JG233 stocks were prepared using an adapted protocol for rubidium chloride treatment. Briefly, cultures were grown to an optical density at 600 nm of 0.75 in MB25RM medium then kept on ice for the remainder of the preparation. Cultures were centrifuged and pellets resuspended in TFB1 containing per 500 mL: 1.45 g potassium acetate, 6 g rubidium chloride, 0.75g $CaCl_2 \cdot 2H_2O$, 4.95 g $MnCl_2 \cdot 4H_2O$, 94.5 g glycerol, and pH adjusted to 5.8 with acetic acid. Again, cells were centrifuged and pellets resuspended in TFB2 containing per 100 mL: 0.2 g MOPS, 1.1 g $CaCl_2 \cdot 2H_2O$, 0.12 g rubidium chloride, and 18.9 g glycerol, and pH adjusted to 6.5 with KOH. Stocks were stored at -80° C until use. For transformation of competent isolate strain JG233, aliquots were incubated with 120 ng pBBR1MCS-2::*gfp*mut3 for 30 min on ice. Following heat shock at 45° C for 5 min, cells were incubated for an additional 2 min on ice before dilution in MB25RB. After a 60 min recovery at 30° C, cells were plated to MB plates and MB plates supplemented with kanamycin.

Conjugation

Escherichia coli donor strain WM3064 was used to conjugate plasmids into isolate strain JG233. Cultures of donor and recipient were grown in LB amended with kanamycin and MB, respectively, and then diluted to an optical density at 600 nm of 1.0 with LBMB. Donor cultures were washed once with LBMB to remove kanamycin, pelleted, and decanted. After recipient cells were heat shocked at 45° C for 5 min, 1 mL was removed and used to resuspend the donor pellets. Cultures were pelleted, resuspended in 100 μL LBMB, and spotted onto LBMB plates. Following an 18 h incubation at 30° C, spots were resuspended in LBMB and spread to MB plates devoid of diaminopimelic acid and amended with kanamycin for selection against the donor strain and for the selection of merodiploid mutants, respectively. Kanamycin resistant colonies were verified by PCR using insertion-specific primers. Selection on MB plates amended with 100 mM sucrose yielded kanamycin-sensitive colonies. Mutants were confirmed via Sanger sequencing of the 16S rRNA gene using 27F and genomic DNA using Flagellin UF and Flagellin DR primers to assure no contamination had occurred.

TABLE 1 | Bacterial strains, vectors, and primers.

Strain or vector	Relevant trait(s)	Source
Strains		
Marinobacter subterrani		
JG233	Wild Type	This study
JG2729	Δ*flaBG*	This study
JG3126	Wild Type with pBBR1MCS-2	This study
JG2756	Δ*flaBG* with pBBR1MCS-2 containing *flaBG*	This study
JG2791	JG233 with pBBR1MCS-2 containing *gfp*mut3	This study
Escherichia coli		
UQ950	DH5α vector construction host	Saltikov and Newman (2003)
WM3064	DAP auxotroph donor strain for conjugation	Saltikov and Newman (2003)
Vectors		
pSMV3	Deletion vector, Km^r, *sacB*	Saltikov and Newman (2003)
pSMV3Δ*fla*BG	Deletion construct for *flaBG*	This study
pBBR1MCS-2	Broad range cloning vector, Km^r	Kovach et al. (1995)
pBBR1MCS-2::*fla*BG	Δ*flaBG* complementation vector	This study
pBBR1MCS-2::*gfp*mut3	*gfp* containing vector	Laboratory stock
pMiniHimar RB1	Transposon-carrying plasmid	Bouhenni et al. (2005)
Primers		
Flagellin UF	catg**GGATCC**TTCTTCCTGTTTGGGACCGAC	This study
Flagellin UR	catg**CTTAAG**GGCTAATGCCCCTCCAGTATC	This study
Flagellin DF	cagt**CTTAAG**CAGTAAACTCAGAACGCCC	This study
Flagellin DR	cagt**ACTAGT**GTGCCGGTTTCCTCGGAG	This study
Flagellin CompF	cagt**AAGCTT**GATACTGGAGGGGCATTAGCC	This study
Flagellin CompR	cagt**ACTAGT**GGGCGTTCTGAGTTTACTG	This study
27F	AGA GTT TGA TCM TGG CTC AG	Wilson et al. (1990)
M13F	GTA AAA CGA CGG CCA GT	Universal Primer List (n.d.)
M13R	CAG GAA ACA GCT ATG AC	Universal Primer List (n.d.)

Restriction site indicated in bold.

Phylogeny

Phylogenetic analysis was done using the two identical complete 16S rRNA genes of isolate strain JG233 obtained from the genome assembly. All sequences were size-adjusted, aligned, and a tree was constructed using the MEGA6.06 software package (Tamura et al., 2013) with the Neighbor-Joining statistical method with a Jukes-Cantor substitution model and 1000 bootstrap replications (Jukes and Cantor, 1969). Analysis of *gyrB* was conducted similarly to the 16S rRNA genes using the MEGA6.06 software package (Tamura et al., 2013) utilizing the Maximum Likelihood method and the Tamura-Nei model with 1000 bootstrap replications (Tamura and Nei, 1993). Genome comparison was conducted using the Average Nucleotide Identity calculator developed by the Konstantinidis Lab, Georgia Institute of Technology, GA, USA (Goris et al., 2007).

Results

Growth Conditions

Growth in MIM was supported by acetate, citrate, fumarate, fructose, glucose, glutamine, glycerol, lactate, n-hexane, n-tetradecane, succinate, and sucrose. No growth was observed in defined media containing arabinose, galactose, glucosamine, lactose, malate, or *N*-acetylglucosamine as the sole electron donor. Anaerobic oxidation of lactate was coupled to the reduction of nitrate to nitrite. Anaerobic growth was not supported by nitrite, sulfate, fumarate, DMSO, or TMAO, and no growth was observed in controls lacking a terminal electron acceptor. Isolate strain JG233 grew at temperatures between 2 and 37° C, and between pH 5 and 9, with optimum growth rates at 37° C and pH 6. Strain JG233 is capable of growth in NaCl concentrations of 0.5–13% with an optimum at 7%. Isolate strain JG233 displayed zones of clearing around diffusion disks containing ampicillin, neomycin, erythromycin, tetracycline, penicillin, and streptomycin and no apparent growth defect from bacitracin.

Genome Properties

The draft genome of strain JG233 consists of two contigs of a single amplicon, encompassing 4,453,613 bp, 4,155 possible coding regions, and a G+C content of 58.9%. The assembly finished had an N_{50} of 3,410,286 bp and a length cutoff of 15,849 bp. Despite read lengths up to 40 kb, the assembly was unable to resolve two repetitive regions containing phage sequences of high similarity. Analysis of the SEED metabolic reconstruction using the KEGG database supports strain JG233 prototrophic for amino acid biosynthesis, which is empirically supported by growth in defined media. Analysis of the genome also suggests complete glycolysis, Entner-Doudoroff, pentose phosphate, and tricarboxylic acid cycle pathways. Carbon source utilization is supported by the genomic annotation. Based on genomic analysis, strain JG233 should be capable of fermentation and be able to utilize nitrite as a terminal electron acceptor, though cultivation-based efforts have failed to demonstrate either.

In an effort to identify gene products that may be involved in Fe(II) oxidation, sequences of proteins thought to be involved with Fe(II) oxidation in other organisms were queried against the strain JG233 translated genome. Though a putative protein

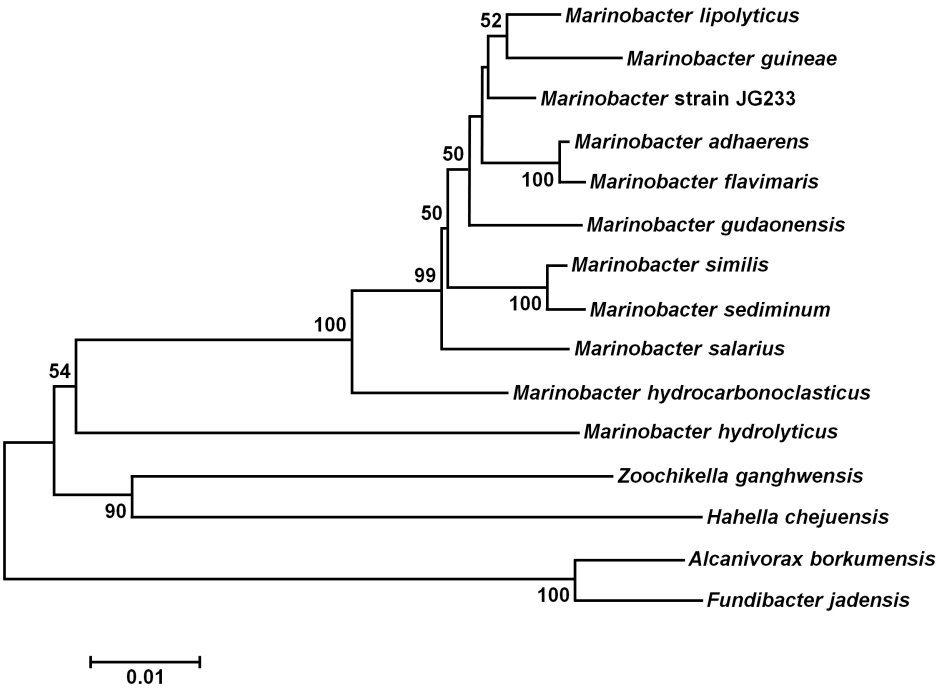

FIGURE 1 | Maximum Likelihood phylogenetic tree of the 16S rRNA gene placing *Marinobacter subterrani* JG233 in the genus *Marinobacter*. Evolutionary relatedness was inferred using the Neighbor-Joining method (Saitou and Nei, 1987) based on the Jukes-Cantor method (Jukes and Cantor, 1969). Branch lengths are measured in the number of substitutions per site. Sequences were obtained from the National Center for Biotechnology Information, and were trimmed to as to attain a total of 1417 positions in the final dataset representing similar regions of the 16S rRNA gene. Evolutionary analyses were conducted in MEGA6 (Tamura et al., 2013). Accession numbers for included species are as follows: *Marinobacter adhaerens* (NR_074765), *Marinobacter similis* (KJ547704), *Marinobacter gudaonensis* (NR_043796), *Marinobacter salarius* (KJ547705), *Marinobacter lypolyticus* (NR_025671), *Marinobacter flavimaris* (NR_025799), *Marinobacter sediminum* (NR_029028), *Marinobacter guineae* (NR_042618), *Marinobacter hydrocarbonoclasticus* (NR_074619), *Zooshikella ganghwensis* (AY130994), *Microbulbifer hydrolyticus* (AJ608704), *Alcanivorax borkumensis* (Y12579), *Fundibacter jadensis* (AJ001150), and *Hahella chejuensis* (AF195410).

with 32% identity to the CycA1 of the acidophilic Fe(II)-oxidizer *Acidothiobacillus ferrooxidans* was identified, the lack of genes encoding Cyc2 or Rusticyanin fails to suggest that a similar Fe(II) oxidation system is employed by strain JG233. Strain JG233 lacks homologs to proposed photosynthetic Fe(II) oxidation systems PioABC (Jiao and Newman, 2007) and FoxEYZ (Croal et al., 2007) from *Rhodopseudomonas palustris* TIE-1 and *Rhodobacter ferrooxidans* SW-2, respectively, as well as the proposed MtoAB and $CymA_{ES-1}$ (Liu et al., 2012) of the neutrophilic Fe(II)-oxidizer *Sideroxydans lithotrophicus* ES-1. PioAB and MtoAB share high sequence identity with MtrAB of the Fe(III)-reducing system of *Shewanella oneidensis* MR-1. Homology between these systems suggests other genes involved with Fe(III) reduction may share orthologs in Fe(II)-oxidizing organisms, and the genome of JG233 was queried and found to be lacking homologs to MtrABCDEF, DmsEF, OmcA, and the translated products of SO_4359 and SO_4360 of *Shewanella oneidensis* MR-1. The relevance of *c*-type cytochromes in electron transfer systems was also exploited to identify candidate genes for Fe(II) oxidation. The translated genome of strain JG233 was searched for proteins containing the characteristic *c*-type cytochrome binding CXXCH motif (Kranz et al., 2009), yielding 33 possible *c*-type cytochromes. Of these, four contained two heme *c*-binding motifs, and none more than two.

Phylogeny

Analysis of the 16S rRNA gene of isolate JG233 places it in the genus *Marinobacter*, however, members of the genus *Marinobacter* often share a greater than an 97% identity of the 16S rRNA gene (**Figure 1**). Few of the *Marinobacter* have additional publicly available sequences, making further sequence-based analysis difficult. Taxonomic classification of isolate JG233 was refined though comparison of gene *gyrB*, average nucleotide identity, and phenotypic properties. The *gyrB* gene is commonly used as an indicator of phylogenetic relatedness, as it contains sufficient length to tolerate subtle mutations that accumulate during speciation, but remains a highly conserved supplement or alternative to classification based on the 16S rRNA genes (Rajendhran and Gunasekaran, 2011). Establishment of strain JG233 as a distinct species from *M. adhaerens*, *M. salarius*, *M. similis*, and *M. flavimaris* is supported by comparison of *gyrB*, which clusters isolate JG233 solely, but distinctly, with *M. guineae* (**Figure 2**). Genomes publicly available for species with an identity higher than 97% to the 16S rRNA gene of isolate JG233 include *M. adhaerens*, *M. salarius*, *M. similis*, and *M. lypoliticus*. Two-way average nucleotide identity comparison to the strain JG233 genome yield values of 84.73, 79.51, 80.15, and 77.23% respectively. These values fall conservatively outside the 95% threshold put forth by Goris et al. (2007) for speciation.

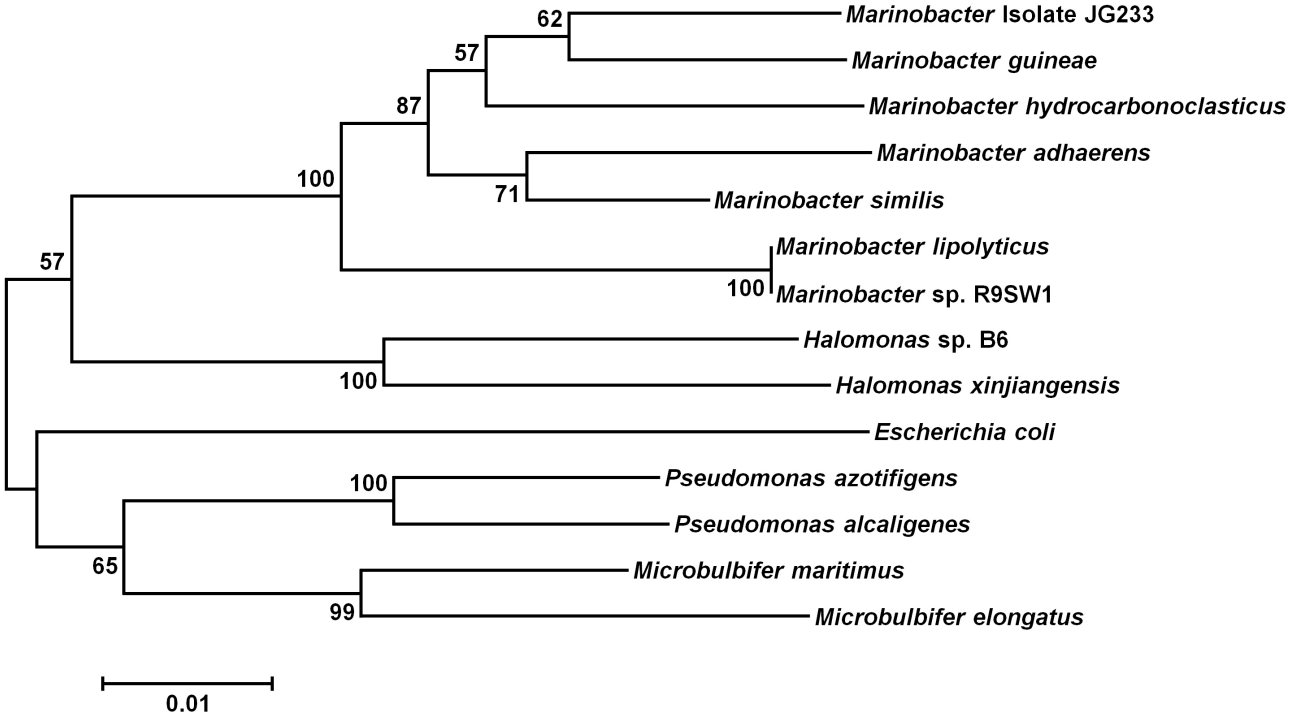

FIGURE 2 | Maximum Likelihood phylogenetic tree of the *gyrB gene*. Evolutionary relatedness was inferred using the Maximum Likelihood method based on the Tamura-Nei model (Tamura and Nei, 1993). Branch lengths are measured in the number of substitutions per site. Sequences were obtained from the National Center for Biotechnology Information, and were trimmed so as to attain a total of 851 positions in the final dataset representing similar regions of the *gyrB* as constrained by sequence available from the National Center for Biotechnology Information. Evolutionary analyses were conducted in MEGA6 (Tamura et al., 2013). Accession numbers for included species are as follows: *Marinobacter adhaerens* (KF811467), *Marinobacter salarius* (KJ547705), *Marinobacter similis* (CP007151), *Marinobacter guinea* (KJ467768), *Marinobacter* sp. R9SW1 (KF811464), *Marinobacter hydrocarbonoclasticus* (KF811470), *Halomonas sp. B6* (KC935335), *Halomonas xinjiangensis* (KC967623), *Pseudomonas azotifigens* (KM103930), *Pseudomonas alcaligenes* (AB039388), *Microbulbifer maritimus* (AB243198), *Microbulbifer elongatus* (AB243199), *Escherichia coli* (AB083821).

Genetic System

Conjugation of the pMiniHimar RB1 transposon vector into wild-type isolate strain JG233 resulted in kanamycin-resistant colonies. Presence of the transposon was confirmed by sequencing purified genomic DNA using transposon specific primers (data not shown). Direct transformation of isolate strain JG233 with plasmid pBBR1MCS-2::*gfp*mut3 was achieved by chemically induced competency with an efficiency of 1.36×10^4 CFU/μg plasmid DNA. Directed deletion of the chromosomal region containing flagellin encoding genes *flaG* and three copies of *flaB* was conducted via conjugation of the suicide vector pSMV3Δ*flaBG* into wild type isolate strain JG233, followed by sucrose counter selection. Flagellin deletion mutants were confirmed by Sanger sequencing and a lack of motility in 0.3% agar MB plates (**Figure 3**). Motility was recovered upon conjugation of the pBBR1MCS-2::*flaBG* complementation construct into motility-deficient mutants (**Figure 3C**), and motility was not observed by the pBBR1MCS-2 empty-vector controls (data not shown).

Fe(II) Oxidation

Isolate strain JG233 was tested for Fe(II) oxidation in gradient tubes and positively demonstrated Fe(II) oxidation with either FeS (**Figure 4**) or $FeCO_3$ (results not shown) as the Fe(II) source as compared to abiotic and *E. coli* UQ950 controls. Growth was not observed in gradient tubes when compared to controls lacking Fe(II). Use of respiratory inhibitors sodium azide and N,N-dicyclohexylcarbodiimide abolished the distinct band of Fe(II)-oxides associated with microbially facilitated Fe(II) oxidation, resulting in banding consistent with abiotic Fe(II) oxidation (**Figure 5**). Ethanol was found to have no effect on the system in the volumes used to solubilize N,N-dicyclohexylcarbodiimide (results not shown). Scanning electron microscopy suggests cells do not form biogenically templated Fe(III) structures such as stalks or sheaths (results not shown).

Discussion

Prior to the cessation of mining operations in 1962, expansion of the Soudan Iron Mine was actively underway and involved the drilling of cores to survey the surrounding rock. Shortly after, anaerobic and Fe(II)-rich water started welling from the deeper of these boreholes. The effluent of these boreholes is ideal for microaerophilic Fe(II)-oxidizing bacteria as oxygen diffusion forms opposing Fe(II) and oxygen gradients. Isolated from one such vertical borehole originating 714 m below the surface and

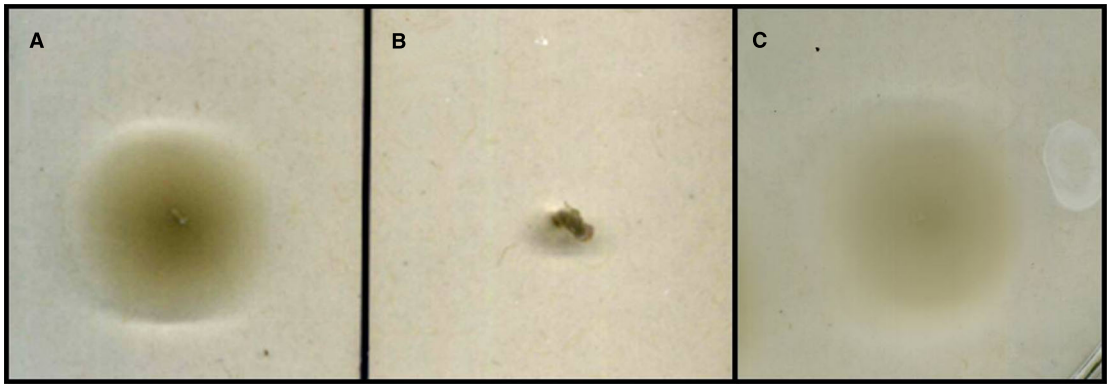

FIGURE 3 | Swimming motility assay. Comparison of wild type *Marinobacter* strain JG233 **(A)** with Δ*flaBG* **(B)** and the Δ*flaBG* mutant complemented with pBBR1-MCS2:: *flaBG* **(C)** on 0.3% agar Marine Broth plates.

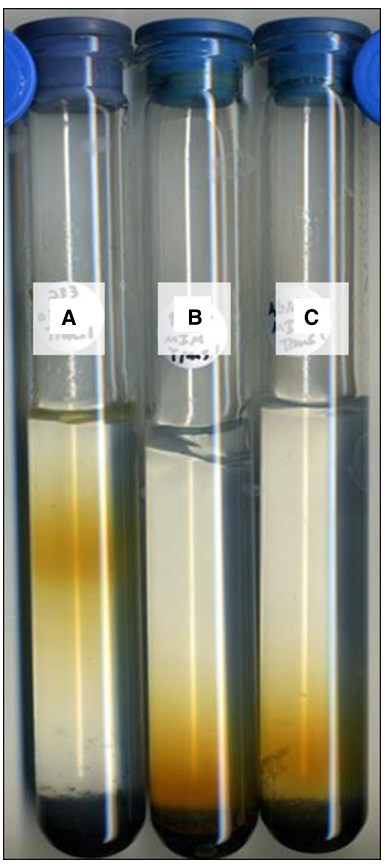

FIGURE 4 | Fe(II) oxidation by *Marinobacter strain JG233 in gradient tubes*. Representative set of tubes ($n = 3$) demonstrating Fe(II) oxidation by *Marinobacter* strain JG233 **(A)** compared to *Escherichia coli* strain UQ950 **(B)** and an abiotic control **(C)** in tubes containing FeS as the Fe(II) source and MIM +0.15% low melt agarose as the medium overlay.

almost 1,600 km from an ocean, isolate JG233 attests to the ubiquity of the genus *Marinobacter*, a genus thought to primarily consist of marine organisms. *Marinobacter* constitutes a dominant genus in the mine, with representation in some mine samples greater than 70% based on 16S rDNA sequencing (unpublished data).

Description of *Marinobacter subterrani* sp. nov

Marinobacter subterrani (suhb.tuh.reyn.ahy. Genitive noun *subterrani* meaning "of the subterrane," referring to the ecosystem from which the strain was isolated). Cells are motile rods approximately 1.8–2.0 μm in length and 0.4 μm wide under Fe(II)-oxidizing conditions and 1.5 μm in length and 0.7 μm wide when grown under heterotrophic conditions. Colonies on MB agar are smooth, convex, circular, and have a diameter of approximately 1–2 mm after 48 h of growth at 30° C. Growth occurs from pH 5–9 with an optimum around 6. Strain is moderately halophilic and capable of growth between NaCl concentrations of 0.5–13% (w/v) with an optimum at 7% (w/v). Interestingly, calcium is required for growth, with an optimum concentration of 0.54% (w/v) and a maximum tolerated concentration of 3.5% (w/v), though strontium can substitute for calcium to support growth. Divalent calcium is a major cation in the mine, reaching concentrations of 1.8% (w/v) at the sampling site.

The similarity to mine conditions of *Marinobacter subterrani* JG233 optima for salinity and pH, tolerance to calcium, and growth at 11° C, coupled with the prevalence of *Marinobacter* in the mine, suggest *M. subterrani* is not only able to propagate but is well acclimated to the conditions from which it was isolated and has not recently been introduced to this environment. Despite significant 16S rDNA similarity to other members of the *Marinobacter*; average nucleotide identity, comparison of *gyr*B, distinct environmental niche, and physiological differences support the establishment of *M. subterrani* as a distinct species (**Table 2**).

The genome of *M. subterrani* does not contain components of any known carbon fixation pathways, and lithoautotrophic growth is neither expected nor observed (data not shown). The lack of autotrophic growth with Fe(II) as an electron donor presents a challenge to determine the role of Fe(II) oxidation by this organism, as growth in the absence of alternative electron donors normally implicates the electrons from Fe(II) oxidation are used electrogenically. The inhibition of facilitated Fe(II)

FIGURE 5 | Fe(II) oxidation under respiratory inhibition. Representative set of *Marinobacter* strain JG233 in tubes containing FeS as the Fe(II) source and MIM +0.15% low melt agarose as the medium overlay. Results were consistent regardless of incubation time prior to respiratory inhibition, as long as inhibitor was added prior to rust-colored band formation. Tubes **(A)** and **(B)** contain sodium azide to 2 mM both abiotic and with *Marinobacter* strain JG233, respectively. N,N-dicyclohexylcarbodiimide solubilized in 200 proof ethanol was added to a final concentration of 20 μM to an abiotic control **(C)** and a tube with *Marinobacter* strain JG233 **(D)**. The tubes containing respiratory inhibitors exhibited rust-colored bands dissimilarly to uninhibited *Marinobacter* strain JG233 **(E)** and are located in similar positions as the abiotic control **(F)**, indicating Fe(II) oxidation by *Marinobacter* strain JG233 required actively metabolizing cells.

oxidation by respiratory inhibitors supports Fe(III)-precipitation by *M. subterrani* requires actively metabolizing cells, and thus is not thought to occur due to an unmediated process, such as production of acidic exopolysaccharides (Chan et al., 2009), which would persist regardless of viability. Regardless of mechanism or function of Fe(II) oxidation by *M. subterrani*, the prevalence of this organism, and the abundance of *Marinobacter* species isolated from cathodic enrichments from other oxic-anoxic interface environments (Rowe et al., 2015; Wang et al., 2015), imply this genus plays a major role in the communities that dominate Fe(II)-oxidizing environments.

Current models for the study of microaerophilic Fe(II) oxidation lack the necessary genetic tools to properly interrogate the possible mechanisms responsible for Fe(II) oxidation. This lack of a robust genetic system stems from the obligate nature of these model organisms for ferrotrophy, inherently coupling the growth of the organism to be studied to the production of Fe(III) oxides. The ability to grow *M. subterrani* under heterotrophic conditions enables the use of well established methods for genetic manipulation separately from phenotypic observations when incubated with Fe(II). The establishment of a robust genetic system in *M. subterrani* has application beyond the study of Fe(II)

TABLE 2 | *Marinobacter subterrani* JG233 and defining species attributes of related species.

Characteristics	1	2	3	4	5	6	7
DNA G+C Content (mol%)	52.7%	57.1%	58.9%	56.9	58%	57.6	57.1
Salinity range (%[a] of Na^+)	0.5–20.5	1–15	1–13	0.5–20	20	0.5–20	0.5–20
Temperature range (C^o)	10–45	4–42	2–37	4–45	4–45	4–40	4–40
pH Range	6–9.5	5–9.5	5–9	5.5–10	5.5–8.0	6–9	6–9
Plasmids	2 (0.2 Mb)		0	2		0	0
Utilization of:							
Acetate	+		+			−	+
Citrate	+	−	+	−		−	−
Fumarate	+		+				
Lactate			+	+		+	+
Malate			−	+			
Succinate	+		+			−	+
Arabinose	−		−	−	−	−	−
Fructose	−	+	+		+	−	+
Glucose	−	+	+	−	−	−	−
Glycerol	−	+	+	−	−	−	+
Lactose	−		−		−	−	−
Mannitol		−		−	−	−	−
NAG	−	+	−	−		−	−
Starch		+					
Sucrose	−		+	−	−	−	−
Hydrocarbons	+		+				
Reduction of nitrate	+	+	+	−	+	+	−
Reduction of nitrite	+	+	−		−	−	−
Fermentative		+	−				

[a]*in weight per volume.*

NAG, N-acetyl-glucosamine.

Spaces left blank were not assayed in the original characterization paper of the species.1, M. hydrocarbonoclasticus *(Gauthier et al., 1992); 2,* M. guinea *(Montes et al., 2008); 3,* Marinobacter subterrani *JG233; 4,* M. adhaerens *(Kaeppel et al., 2012); 5,* M. flavimaris *(Yoon et al., 2004); 6,* M. similis *(Hooi et al., 2014); 7,* M. salarius *(Hooi et al., 2014).*

oxidation. Phylogenetic analysis using 16S rRNA gene would suggest inclusion of *M. subterrani* in the genus *Marinobacter* of the Gamma*proteobacteria*. *Marinobacter* are well regarded as a metabolically diverse clade, containing representatives capable of many biotechnologically and industrially relevant biochemical processes. The development of a genetic system for *M. subterrani* JG233 expands upon the genetic system for *M. adhaerens* reported by Sonnenschein et al. (2011) for the analysis and development of the genus *Marinobacter* and establishes a crucial genetic system for the study of microaerophilic Fe(II)-oxidizing species (Sonnenschein et al., 2011). The genetic tools outlined in this study allow methods previously unavailable in a microaerophilic Fe(II)-oxidizing strain to be utilized. Transposon mutagenesis, markerless deletion, and complementation via expression from a plasmid enable the interrogation of the function of specific gene products, as well as the use of hypothesis generating experiments.

The isolation, description, and development of a genetic system in *M. subterrani* JG233 establishes a foundation for the genetic study of dominant organisms contributing to Fe(II) oxidation in the subsurface. As *Marinobacter* species are increasingly found in diverse environments, including hydraulic fracturing effluent, deep marine sediments, and beneath the iron ranges of Minnesota, a greater understanding of these microbes will shed light on survival and metabolism in the dark biosphere. Future studies should focus on the mechanism of the demonstrated Fe(II) oxidation and the contribution and mode of *M. subterrani* metabolism to the microbial community structure and its functioning in the native environment.

Acknowledgments

We would like to thank Daniel Bond and Jon Badalamenti for their diligence in the refinement and completion of the *M. subterrani* genome. We also thank Michael Donald and Ryan Lesniewski who helped initially characterize this strain while undergraduates in the Gralnick Lab. Funding for this research comes from the Minnesota Environment and Natural Resources Trust Fund.

References

Aziz, R. K., Bartels, D., Best, A. A., DeJongh, M., Disz, T., Edwards, R. A., et al. (2008). The RAST server: rapid annotations using subsystems technology. *BMC Genomics* 9:75. doi: 10.1186/1471-2164-9-75

Baldock, J. A., and Skjemstad, J. O. (2000). Role of soil matrix and minerals in protecting natural organic materials against biological attacks. *Org. Geochem.* 31, 697–710. doi: 10.1016/S0146-6380(00)00049-8

Bouhenni, R., Gehrke, A., and Saffarini, D. (2005). Identification of genes involved in cytochrome c biogenesis in *Shewanella oneidensis*, using a modified mariner transposon. *Appl. Environ. Microbiol.* 71, 4935–4937. doi: 10.1128/AEM.71.8.4935-4937.2005

Bronick, J. C., and Lal, R. (2005). Soil structure and management: a review. *Geoderma* 124, 3–22. doi: 10.1016/j.geoderma.2004.03.005

Chan, C. S., Fakra, S., Edwards, D. C., Emerson, D., and Banfield, J. F. (2009). Iron oxyhydroxide mineralization on microbial polysaccharides.

Geochim. Cosmochim. Acta 73, 3807–3818. doi: 10.1016/j.gca.2009.02.036

Cluff, M. A., Hartsock, A., MacRae, J. D., Carter, K., and Mouser, P. J. (2014). Temporal changes in microbial ecology and geochemistry in produced water from hydraulically fractured Marcellus shale gas wells. *Environ. Sci. Technol.* 46, 6508–6517. doi: 10.1021/es501173p

Croal, L. R., Jiao, Y., and Newman, D. K. (2007). The fox operon from *Rhodobacter strain* SW2 promotes phototrophic Fe(II) oxidation in *Rhodobacter capsulatus* SB1003. *J. Bacteriol.* 189, 1774–1782. doi: 10.1128/JB.01395-06

Edwards, E. A., Rodriguez-Brito, B., Wegley, L., Haynes, M., Breitbart, M., Peterson, D. M., et al. (2006). Using pyrosequencing to shed light on deep mine microbial ecology. *BMC Genomics* 7:57. doi: 10.1186/1471-2164-7-57

Emerson, D., Fleming, E. J., and McBeth, J. M. (2010). Iron-oxidizing bacteria: an environmental and genomic perspective. *Ann. Rev. Microbiol.* 64, 561–583. doi: 10.1146/annurev.micro.112408.134208

Emerson, D., and Floyd, M. M. (2005). Enrichment and isolation of iron-oxidizing bacteria at neutral pH. *Methods Enzymol.* 397, 112–123. doi: 10.1016/S0076-6879(05)97006-7

Fathepure, B. Z. (2014). Recent studies in microbial degradation of petroleum hydrocarbons in hypersaline environments. *Front. Microbiol.* 5:173. doi: 10.3389/fmicb.2014.00173

Gauthier, M. J., Lafay, B., Christen, R., Fernandez, L., Acquaviva, M., Bonin, P., et al. (1992). *Marinobacter hydrocarbonoclasticus* gen. nov., sp. nov., a new, extremely halotolerant, hydrocarbon-degrading marine bacterium. *Int. J. Syst. Bacteriol.* 42, 568–576. doi: 10.1099/00207713-42-4-568

Ghiorse, W. C. (1984). Biology of iron- and manganese-depositing bacteria. *Ann. Rev. Microbiol.* 38, 515–550. doi: 10.1146/annurev.mi.38.100184.002503

Goris, J., Konstantinidis, K. T., Klappenbach, J. A., Coenye, T., Vandamme, P., and Tiedje, J. M. (2007). DNA-DNA hybridization values and their relationship to whole-genome sequence similarities. *Int. J. Syst. Evol. Microbiol.* 57, 81–91. doi: 10.1099/ijs.0.64483-0

Handley, K. M., Héry, M., and Lloyd, J. R. (2009). *Marinobacter santoriniensis* sp. nov., an arsenate-respiring and arsenite-oxidizing bacterium isolated from hydrothermal sediment. *Int. J. Syst. Evol. Microbiol.* 59, 886–892. doi: 10.1099/ijs.0.003145-0

Handley, K. M., and Lloyd, J. R. (2013). Biogeochemical implications of the ubiquitous colonization of marine habitats and redox gradients by *Marinobacter species*. *Front. Microbiol.* 4:136. doi: 10.3389/fmicb.2013.00136

Holtzapple, E., and Schmidt-Dannert, C. (2007). Biosynthesis of isoprenoid wax ester in *Marinobacter hydrocarbonoclasticus* DSM 8798: identification and characterization of isoprenoid coenzyme a synthetase and wax ester synthases. *J. Bacteriol.* 189, 3804–3812. doi: 10.1128/JB.01932-06

Hooi, J. N., López-Pérez, M., Webb, H. K., Gomez, D., Sawabe, T., Ryan, J., et al. (2014). *Marinobacter salaries* sp. nov. and *Marinobacter similis* sp. nov., isolated from sea water. *PLOS ONE* 9:e106514. doi: 10.1371/journal.pone.0106514

Jiao, Y., and Newman, D. K. (2007). The pio operon is essential for phototrophic Fe(II) oxidation in *Rhodopseudomonas palustris* TIE-1. *J. Bacteriol.* 189, 1764–1773. doi: 10.1128/jb.00776-06

Johnson, D. B., Kanao, T., and Hedrich, S. (2012). Redox transformations of iron at extremely low pH: fundamental and applied aspects. *Front. Microbiol.* 3:96. doi: 10.3389/fmicb.2012.00096

Jukes T. H., and Cantor, C. R. (1969). "Evolution of protein molecules," in *Mammalian Protein Metabolism*, ed. H. N. Munro (New York, NY: Academic Press), 21–132. doi: 10.1016/b978-1-4832-3211-9.50009-7

Kaeppel, E. C., Gärdes, A., Seebah, S., Grossart, H. P., and Ullrich, M. S. (2012). *Marinobacter adhaerens* sp. nov. isolated from marine aggregates formed with the diatom *Thalassiosira weissflogii*. *Int. J. Syst. Evol. Microbiol.* 62, 124–128. doi: 10.1099/ijs.0.030189-0

Konhauser, K. O., Kappler, A., and Roden, E. E. (2011). Iron in microbial metabolisms. *Elements* 7, 89–93. doi: 10.2113/gselements.7.2.89

Kovach, M. E., Elzer, P. H., Hill, D. S., Robertson, G. T., Farris, M. A., and Roop, R. M. II, et al. (1995). Four new derivatives of the broad-host-range cloning vector pBBR1MCS, carrying different antibiotic-resistance cassettes. *Gene* 166, 175–176. doi: 10.1016/0378-1119(95)00584-1

Kranz, R. G., Richard-Fogal, C., Taylor, J., and Frawley, E. R. (2009). Cytochrome c biogenesis: mechanisms for covalent modifications and trafficking of heme and for heme-iron redox control. *Microbiol. Mol. Biol. Rev.* 73, 510–528. doi: 10.1128/MMBR.00001-09

Lee, J. S., McBeth, J. M., Ray, R. I., Little, B. J., and Emerson, D. (2013). Iron cycling at corroding carbon steel surfaces. *Biofouling* 29, 1243–1252. doi: 10.1080/08927014.2013.836184

Lenneman, E. M., Ohlert, J. M., Palani, N. P., and Barney, B. M. (2013). Fatty alcohols for wax esters in *Marinobacter aquaeolei* VT8: two optional routes in the wax biosynthesis pathway. *Appl. Environ. Microbiol.* 79, 7055–7062. doi: 10.1128/AEM.02420-13

Liebgott, P., Casalot, L., Paillard, S., Lorquin, J., and Labat, M. (2006). *Marinobacter vinifirmus* sp. nov., a moderately halophilic bacterium isolated from a wine-barrel-decalcification wastewater. *Int. J. Syst. Evol. Microbiol.* 56, 2511–2516. doi: 10.1099/ijs.0.64368-0

Liu, J., Wang, Z., Belchik, S. M., Edwards, M. J., Liu, C., Kennedy, D. W., et al. (2012). Identification and characterization of MtoA: a decaheme c-type cytochrome of the neutrophilic Fe(II)-oxidizing bacterium *Sideroxydans lithotrophicus* ES-1. *Front. Microbiol.* 3:37. doi: 10.3389/fmicb.2012.00037

Martin, S., Márqus, M. C., Sánchez-Porro, C., Mellado, E., Arahal, D. R., and Ventosa, A. (2003). *Marinobacter lipolyticus* sp. nov., a novel moderate halophile with lipolytic activity. *Int. J. Syst. Evol. Microbiol.* 53, 1383–1387. doi: 10.1099/ijs.0.02528-0

McBeth, M. J., Little, B. J., Ray, R. I., Farrar, K. M., and Emerson, D. (2010). Neutrophilic iron-oxidizing "*Zetaproteobacteria*" and mild steel corrosion in nearshore marine environments. *App. Environ. Microbiol.* 77, 1405–1412. doi: 10.1128/AEM.02095-10

Montes, M. J., Bozal, N., and Mercadé, E. (2008). *Marinobacter guinea* sp. nov., a novel moderately halophilic bacterium from an Antarctic environment. *Int. J. Syst. Evol. Microbiol.* 58, 1346–1349. doi: 10.1099/ijs.0.65298-0

Overbeek, R., Olson, R., Pusch, G. D., Olsen, G. J., Davis, J. J., Disz, T., et al. (2014). The SEED and the rapid annotation of microbial genomes using subsystems technology (RAST). *Nucleic Acids Res.* 42, D206–D214. doi: 10.1093/nar/gkt1226

Rajendhran, J., and Gunasekaran, P. (2011). Microbial phylogeny and diversity: small subunit ribosomal RNA sequence analysis and beyond. *Microbial Res.* 166, 99–110. doi: 10.1016/j.micres.2010.02.003

Rowe, A. R., Chellamuthu, P., Lam, B., Okamoto, A., and Nealson, K. H. (2015). Marine sediments microbes capable of electrode oxidation as a surrogate for lithotrophic insoluble substrate metabolism. *Front. Microbiol.* 5:784. doi: 10.3389/fmicb.2014.00784

Saltikov, C. W., and Newman, D. K. (2003). Genetic identification of a respiratory arsenate reductase. *Proc. Natl. Acad. Sci. U.S.A.* 100, 10983–10988. doi: 10.1073/pnas.1834303100

Saitou, N., and Nei, M. (1987). The neighbor-joining method: a new method for reconstructing phylogenetic trees. *Mol. Biol. Evol.* 4, 406–425

Sonnenschein, E. C., Gärdes, A., Seebah, S., Torres-Monroy, I., Grossart, H. P., and Ullrich, M. S. (2011). Development of a genetic system for *Marinobacter adhaerens* HP15 involved in marine aggregate formation by interaction with diatom cells. *J. Microbiol. Methods* 87, 176–183. doi: 10.1016/j.mimet.2011.08.008

Strong, L. C., Gould, T., Kasinkas, L., Sadowsky, M. J., Aksan, A., and Wackett, L. P. (2013). Biodegradation in waters from hydraulic fracturing: chemistry, microbiology, and engineering. *J. Environ. Eng.* 140:B4013001. doi: 10.1061/(ASCE)EE.1943-7870.0000792

Tamura, K., and Nei, M. (1993). Estimation of the number of nucleotide substitutions in the control region of mitochondrial DNA in humans and chimpanzees. *Mol. Biol. Evol.* 10, 512–526.

Tamura, K., Stecher, G., Peterson, D., Filipski, A., and Kumar, S. (2013). MEGA6: molecular evolutionary genetics analysis version 6.0. *Mol. Biol. Evol.* 30, 2725–2729. doi: 10.1093/molbev/mst197

Universal Primer List. (n.d.). *ACGT, Inc. Universal Primer List*. Available at: https://www.acgtinc.com/primerlist.htm [accessed April 08, 2015]

Wang, H., Li, H., Shao, Z., Liao, S., Johnstone, L., Rensing, C., et al. (2012). Genome sequence of deep-sea manganese-oxidizing bacterium *Marinobacter manganoxydans* Mnl7-9. *J. Bacteriol.* 194, 899–900. doi: 10.1128/JB.06551-11

Wang, Z., Leary, D. H., Malanoski, A. P., Li, R. W., Hervey, W. J. IV., Eddie, B. J., et al. (2015). A previously uncharacterized, nonphotosynthetic member of

the *Chromatiaceae* is the primary CO2-fixing constituent in a self-regenerating biocathode. *Appl. Environ. Microbiol.* 81, 699–712. doi: 10.1128/AEM.02947-14

Wilson, K. H., Blitchington, R. B., and Greene, R. C. (1990). Amplification of bacterial 16S ribosomal DNA with polymerase chain reaction. *J. Clin. Microbiol.* 28, 1942–1946.

Yoon, J. H., Yeo, S. H., Kim, I. G., and Oh, T. K. (2004). *Marinobacter flavimaris* sp. nov. and *Marinobacter daepoensis* sp. nov., slightly halophilic organisms isolated from sea water of the Yellow Sea in Korea. *Int. J. Syst. Evol. Microbiol.* 54, 1799–1803. doi: 10.1099/ijs.0.63151-0

Conflict of Interest Statement: The authors declare that the research was conducted in the absence of any commercial or financial relationships that could be construed as a potential conflict of interest.

frontiers in
MICROBIOLOGY

ORIGINAL RESEARCH ARTICLE
published: 03 March 2015
doi: 10.3389/fmicb.2015.00152

Diversity and role of plasmids in adaptation of bacteria inhabiting the Lubin copper mine in Poland, an environment rich in heavy metals

Lukasz Dziewit[1]*, Adam Pyzik[1], Magdalena Szuplewska[1], Renata Matlakowska[2], Sebastian Mielnicki[2], Daniel Wibberg[3], Andreas Schlüter[3], Alfred Pühler[3] and Dariusz Bartosik[1]

[1] Department of Bacterial Genetics, Institute of Microbiology, Faculty of Biology, University of Warsaw, Warsaw, Poland
[2] Laboratory of Environmental Pollution Analysis, Faculty of Biology, University of Warsaw, Warsaw, Poland
[3] Institute for Genome Research and Systems Biology, Center for Biotechnology (CeBiTec), Bielefeld University, Bielefeld, Germany

Edited by:
Malin Bomberg, VTT Technical Research Centre of Finland, Finland

Reviewed by:
Angel Valverde, University of Pretoria, South Africa
Miguel Angel Cevallos, Centro de Ciencias Genomicas-Universidad Nacional Autónoma de México, Mexico

***Correspondence:**
Lukasz Dziewit, Department of Bacterial Genetics, Institute of Microbiology, Faculty of Biology, University of Warsaw, Miecznikowa 1, Warsaw, 02-096, Poland
e-mail: ldziewit@biol.uw.edu.pl

The Lubin underground mine, is one of three mining divisions in the Lubin-Glogow Copper District in Lower Silesia province (Poland). It is the source of polymetallic ore that is rich in copper, silver and several heavy metals. Black shale is also significantly enriched in fossil organic matter in the form of long-chain hydrocarbons, polycyclic aromatic hydrocarbons, organic acids, esters, thiophenes and metalloporphyrins. Biological analyses have revealed that this environment is inhabited by extremophilic bacteria and fungi. Kupfershiefer black shale and samples of water, bottom and mineral sediments from the underground (below 600 m) Lubin mine were taken and 20 bacterial strains were isolated and characterized. All exhibited multi-resistant and hypertolerant phenotypes to heavy metals. We analyzed the plasmidome of these strains in order to evaluate the diversity and role of mobile DNA in adaptation to the harsh conditions of the mine environment. Experimental and bioinformatic analyses of 11 extrachromosomal replicons were performed. Three plasmids, including a broad-host-range replicon containing a Tn*3* family transposon, carried genes conferring resistance to arsenic, cadmium, cobalt, mercury and zinc. Functional analysis revealed that the resistance modules exhibit host specificity, i.e., they may increase or decrease tolerance to toxic ions depending on the host strain. The other identified replicons showed diverse features. Among them we identified a catabolic plasmid encoding enzymes involved in the utilization of histidine and vanillate, a putative plasmid-like prophage carrying genes responsible for NAD biosynthesis, and two *repABC*-type plasmids containing virulence-associated genes. These findings provide an unique molecular insight into the pool of extrachromosomal replicons and highlight their role in the biology and adaptation of extremophilic bacteria inhabiting terrestrial deep subsurface.

Keywords: plasmid, Tn*3* transposon, underground copper mine, terrestrial deep subsurface, extremophilic bacteria, heavy metal

INTRODUCTION

Bacterial plasmids, as extrachromosomal mobile genetic elements, are components of many microbial genomes. They have modular structures, since it is possible to dissect them into several functional genetic modules. The plasmid backbone is composed of a set of conserved modules, coding for replication, stability and conjugal transfer functions, which are crucial for plasmid maintenance and spread. Many plasmids also carry accessory genes determining various phenotypes, e.g., antibiotics resistance and utilization of toxic compounds. Such genetic information is not crucial for host viability, but it may play an important role in the adaptation of bacteria to various environments, including terrestrial deep subsurface habitats (Sobecky and Coombs, 2009; Heuer and Smalla, 2012; Nojiri, 2013).

It was shown that one of the most frequently found phenotypic modules carried by bacterial plasmids are heavy metal resistance genes (Silver, 1996). Moreover, metal resistance genes are often co-localized on plasmids together with antibiotic resistance genes, and they are frequently present within transposable and integrative mobile elements (Rahube et al., 2014). Such plasmid-encoded heavy metal resistance systems are usually related to chromosomally-encoded determinants found in other bacteria, which exemplifies the naturally occurring gene flow (Silver, 1996).

Horizontal gene transfer is a major mechanism contributing to bacterial diversification and adaptation, and plasmids are the main players in this process (Heuer and Smalla, 2012). Many plasmids are self-transmissible or mobilizable replicons, which can be transferred from one host to another, together with various

"passenger" genes (often embedded within transposons), which can be useful under particular selection pressures (Tamminen et al., 2012). This phenomenon is extremely profitable for bacteria and, in effect, speeds up the process of evolution. To explain the link between environmental conditions and the diversity of bacterial plasmids a complex molecular analyses or, so called, meta-analyses of plasmidomes of bacteria inhabiting various (especially unique) extremophilic environments are needed (Dziewit and Bartosik, 2014).

The Lubin underground mine, is one of the three mining divisions in the Lubin-Glogow Copper District located in the Lower Silesia province (Poland). This mine is the source of polymetallic ore that is highly rich in copper (10 wt.%) and silver (100 mg kg^{-1}) (Oszczepalski, 1999). Besides these two elements As, Co, V, Ni, Pb, and Zn at high concentrations were also detected (Speczik, 1994, 1995; Oszczepalski, 1999). All mentioned elements occur in the form of sulfides and sulphosalts [e.g., bornite (Cu_5FeS_4), chalcopyrite ($CuFeS_2$)], gersdorffite (NiAsS), nickeline (NiAs), cobaltite (CoAsS), minerals belonging to the tennantite-tetrahedrite series [$(Cu, Fe)_{12}As_4S_{13}$—$(Cu, Fe)_{12}Sb_4S_{13}$, sphalerite (ZnS) and galena (PbS)]. A characteristic feature of these deposits is a neutral or slightly alkaline pH reaching 8.5. Black shale is also significantly enriched in fossil organic matter (up to 30%) in the form of long-chain saturated and unsaturated hydrocarbons, polycyclic aromatic hydrocarbons, organic acids and esters, as well as thiophenes and metalloporphyrins (Sklodowska et al., 2005; Matlakowska and Sklodowska, 2011). Biological analyses have revealed that this hostile environment is inhabited by endemic and extremophilic microorganisms, including bacteria and fungi (Matlakowska and Sklodowska, 2009; Rajpert et al., 2013).

In our previous work we analyzed several strains of the genus *Pseudomonas* originating from the Lubin copper mine (Szuplewska et al., 2014). Using a trap plasmid strategy to capture functional transposable elements, we identified several insertion sequences and transposons (autonomous and non-autonomous), some of which carry predicted genetic modules of adaptive value (Szuplewska et al., 2014). In this study we extended our investigation of the mobilome of bacteria inhabiting this deep underground environment. We isolated and analyzed the plasmids of strains representing various taxonomic groups, focusing on replicons conferring heavy metal resistance. Such plasmids (and their bacterial hosts) may be exploited in industrial processes, e.g. bioleaching of metals or biormediation. Moreover, the naturally occurring plasmids are good candidates for the construction of vectors for the genetic manipulations of biotechnologically important bacteria. However, this requires an in-depth understanding of the plasmid biology.

MATERIALS AND METHODS

BACTERIAL STRAINS, PLASMIDS AND CULTURE CONDITIONS

The bacterial strains and plasmids used in this study are listed in Table S1. The strains were grown in LB (Luria-Bertani) medium (Sambrook and Russell, 2001) at 37°C (*E. coli*) or 22 and 30°C (other strains). Where necessary, the medium was supplemented with sucrose (10%) and the antibiotics, kanamycin (50–1000 μg/ml) and rifampicin (50 μg/ml).

SAMPLE COLLECTION AND BACTERIAL ISOLATION

Samples of black shale, mineral sediment, bottom sediment and water, collected from various sites within the Lubin underground copper mine (below 600 m), were placed in sterile plastic tubes and held at 4°C until they were processed in the laboratory.

To isolate bacterial strains, samples of solid matter (10 g) were resuspended in 20 ml of 0.85% NaCl (pH 7.0) and shaken at 22°C for 2 h. Then a series of dilutions were prepared in saline solution and plated onto solid LB medium. Diluted water samples were plated directly onto LB medium. The plates were incubated at 22°C for 2 weeks. All operations were carried out aseptically.

AMPLIFICATION AND SEQUENCING OF 16S rRNA GENES

A colony PCR method was used for the amplification of 16S rRNA gene fragments (Gathogo et al., 2003). PCR was performed with the primers 27f and 1492r (Lane, 1991). The amplified 16S rDNA fragments were used as templates for DNA sequencing with an ABI Prism 377 automatic sequencer (Applied Biosystems).

PHYSIOLOGICAL ANALYSES OF THE BACTERIAL STRAINS

The temperature, pH and salinity tolerance of bacteria were analyzed by monitoring changes in the optical density of cultures (in comparison with non-inoculated controls) according to the procedures described previously (Dziewit et al., 2013). For the motility assay LB soft agar plates containing 0.3, 0.35, or 0.4% (w/v) agar were inoculated with the bacteria using a sterile toothpick and incubated at 30°C for 48 h.

The minimum inhibitory concentrations (MICs) of selected heavy metal ions were established. For this purpose, analytical grade salts ($3CdSO_4 \times 8H_20$; $CoSO_4 \times 7H_20$; $CuSO_4$; $HgCl_2$; $K_2Cr_2O_7$; $NaAsO_2$; $Na_2HAsO_4 \times 7H_2O$; $NiCl_2 \times 6H_20$; NaO_3V; $ZnSO_4 \times 7H_20$) were used in an assay procedure described previously (Dziewit et al., 2013). Isolates that grew in the presence of at least the following metal ion concentrations were considered resistant: (i) 20 mM V^{5+}, (ii) 10 mM As^{5+}, (iii) 1 mM As^{3+}, Cd^{2+}, Co^{2+}, Cu^{2+}, Ni^{2+}, Zn^{2+}, or Cr^{6+}, and (iv) 0.1 mM Hg^{2+} (Nieto et al., 1987; Abou-Shanab et al., 2007).

The ability to produce siderophores was examined by application of the modified chrome azurol S (CAS) agar plate method (Schwyn and Neilands, 1987). The plates were incubated at 30°C for 72 h in the dark and the formation of halos around colonies was recorded.

DNA MANIPULATIONS, PLASMID ISOLATION AND INTRODUCTION OF PLASMID DNA INTO BACTERIAL CELLS

Bacterial plasmids were isolated according to the method of Birnboim and Doly (Birnboim and Doly, 1979), and when required, the DNA was further purified by CsCl-ethidium bromide gradient centrifugation (Sambrook and Russell, 2001). Plasmid DNA was also isolated using a Plasmid Mini Kit (A&A Biotechnology), Plasmid Miniprep Kit Gene Matrix (EUR_x) and GeneJET Plasmid Miniprep Kit (Thermo SCIENTIFIC). The visualization of mega-sized replicons was achieved by in-gel lysis and DNA electrophoresis according to a method described previously (Wheatcroft et al., 1990). The common DNA manipulations were performed as described earlier (Sambrook and Russell, 2001). PCR was performed in a Mastercycler (Eppendorf) using

Taq DNA polymerase (Qiagen; with supplied buffer), dNTP mixture and appropriate primer pairs (Table S1). Triparental mating was performed as described previously (Bartosik et al., 2001).

PLASMID DNA SEQUENCING AND ASSEMBLY

The complete nucleotide sequences of plasmids pLM16A1, pLM20P1-5, pLM8P1, and pLM12P1 were determined in the Laboratory of DNA Sequencing and Oligonucleotide Synthesis (oligo.pl) at the Institute of Biochemistry and Biophysics, Polish Academy of Sciences, Warsaw, Poland. Plasmids pLM19O1, pLM19O2, and pLM21S1 were sequenced at the Center for Biotechnology (CeBiTec), Bielefeld University, Germany. High-throughput sequencing of the MID-tagged shotgun plasmid-libraries was performed using a Genome Sequencer FLX system (Roche/454 Life Sciences). The GS *de novo* assembler software (Roche) was applied for the sequence assemblies. Primer walking and polymerase chain reaction (PCR) were used to close physical gaps between assembled contigs. The amplified DNA fragments were sequenced using an ABI3730xl DNA Analyzer (Applied Biosystems).

IDENTIFICATION OF ACTIVE TRANSPOSABLE ELEMENTS (TEs)

The identification of functional TEs using trap plasmid pMAT1 was performed as described previously (Szuplewska and Bartosik, 2009; Dziewit et al., 2012).

PHAGE INDUCTION

Phage of *Sinorhizobium* sp. LM21 was induced using mitomycin C as described previously (Dziewit et al., 2014b).

FUNCTIONAL ANALYSIS OF THE HEAVY METAL RESISTANCE MODULES

A restriction fragment or PCR-amplified DNA regions containing the resistance genes of plasmids pLM20P1 (ARS module), pLM20P2 (CZC) and pLM16A1 (MER) were cloned into the broad-host-range mobilizable vector pBBR1MCS-2, to produce plasmids pBBR-CZCLM20, pBBR-ARSLM20 and pBBR-MERLM16 (Table S1). For comparison, two resistance cassettes of functional transposable elements identified within *Pseudomonas* spp. strains LM7 and LM14 (Szuplewska et al., 2014) were also included. Those were (i) the CZC module of insertion sequence IS*Ppu12*a (3372 bp, IS*L3* family), encoding a predicted CzcD protein, possibly involved in resistance to Co^{2+}, Zn^{2+}, and Cd^{2+}, and (ii) MER, a mercury resistance operon of the Tn*3* family transposon Tn*5563*a (6253 bp), containing three genes—*merP, merT* (encoding mercury transporters) and *merR* (encoding a transcription regulator). To analyze these modules we used two previously obtained derivatives of the pBBR1MCS-2-based broad host range mobilizable trap plasmid pMAT1, namely pMAT-ISPPU12A and pMAT-TN5563A, carrying inserted IS*Ppu12*a and Tn*5563*a, respectively (Table S1) (Szuplewska et al., 2014).

All five plasmids containing predicted resistance modules were introduced into 13 bacterial strains (LM5, LM6, LM7, LM8, LM10, LM12, LM14, LM15, LM16, LM19, LM21, LM24, and LM25), representing *Alpha-*, *Beta-* and *Gammaproteobacteria*. As controls, two laboratory strains, *Agrobacterium tumefaciens* LBA288 (type strain of *Alphaproteobacteria*) and *E. coli* TG1 (*Gammaproteobacteria*), were also selected as the hosts for the plasmids. The resistance phenotypes of the obtained transconjugants (or transformants) were then tested by determining the minimum inhibitory concentrations (MICs) for As^{3+}, As^{5+}, Cd^{2+}, Co^{2+}, Zn^{2+}, and Hg^{2+} salts in liquid culture and the obtained values were compared with those of the wild-type strains.

PLASMID HOST RANGE TESTING

To analyze the host range of plasmids pLM16A1, pLM20P1, and pLM20P2, three mobilizable shuttle plasmids (pABW-LM20P1, pABW-LM20P2, and pABW-LM16A1) were constructed (Table S1), containing the replication modules of the resistance plasmids and an *E. coli*-specific pMB1 (ColE1-type) replication system [vector pABW1 (Bartosik et al., 1997)]. The obtained plasmids were introduced *via* conjugation into 14 strains (LM5, LM6, LM7, LM8, LM10, LM12, LM14, LM15, LM16, LM19, LM21, LM24, LM25, and LBA288). The plasmids were also introduced via transformation into *E. coli* BR825 (*Gammaproteobacteria*). Since the ColE1-type replication system is not functional in any of the recipient strains (*E. coli* BR825 carries a mutation within the DNA polymerase I gene that blocks ColE1-type replication), all functions required for replication of the shuttle plasmids in the tested hosts were provided by the REP modules of pLM20P1, pLM20P2 or pLM16A1.

BIOINFORMATIC ANALYSES

Plasmid nucleotide sequences were analyzed using Clone Manager Professional, version 9.0 (Sci-Ed software), Artemis (Carver et al., 2008) and GenDB 2.0 (Meyer et al., 2003). Similarity searches were performed using the BLAST programs (Altschul et al., 1997) and the PRIAM tool (Claudel-Renard et al., 2003). Putative tRNA genes were identified with the tRNAscan-SE program (Lowe and Eddy, 1997). Comparative genomic analyses were performed with the application of the ACT: the Artemis comparison tool (Carver et al., 2008). The reference data set for the computational prediction of metabolic pathways was obtained from the MetaCyc database (Caspi et al., 2014). Phylogenetic analysis was performed using MEGA6 (Tamura et al., 2013), applying the neighbor-joining algorithm with 1000 bootstrap replicates. The initial alignment obtained with ClustalW (Chenna et al., 2003) was manually refined. For the analysis 100 homologs (best BLAST hits) of proteins ArsB, ArsC, CzcD, and MerA retrived from the UniProt database (Apweiler et al., 2004) were used.

NUCLEOTIDE SEQUENCE ACCESSION NUMBERS

The sequences of 16S rRNA genes determined in this study have been deposited in GenBank (NCBI), with the following accession numbers: KF769960 (strain LM16), KF769961 (LM17), KF769962 (LM18), KF769963 (LM19), KF769964 (LM20), KF769965 (LM21), KF769966 (LM22), KF769967 (LM23), KF769968 (LM24), KF769970 (LM26).

The plasmid sequences determined in this study have been deposited in GenBank (NCBI), with the following accession numbers: KM659090 (plasmid pLM16A1), KM659091 (pLM19O1), KM659092 (pLM19O2), KM659093 (pLM20P1), KM659094 (pLM20P2), KM659095 (pLM20P3), KM659096 (pLM20P4), KM659097 (pLM20P5), KM659098 (pLM21S1), KM659088 (pLM8P1) and KM659089 (pLM12P1).

RESULTS

IDENTIFICATION AND CHARACTERIZATION OF BACTERIA ISOLATED FROM THE LUBIN COPPER MINE

In this study we analyzed 20 bacterial strains isolated from various samples collected from the terrestrial deep subsurface environment, namely Lubin copper mine: (i) black shale (strains LM5, LM6, LM7, LM8, LM17, LM18, LM20, LM23, LM25, LM26); (ii) water (LM10, LM12, LM24); (iii) mineral sediment (LM11, LM14, LM21) and (iv) bottom sediment (LM15, LM16, LM19, LM22). Ten of the strains (belonging to the genus *Pseudomonas* - LM5, LM6, LM7, LM8, LM10, LM11, LM12, LM14, LM15, and LM25) were identified and subjected to preliminary characterization in previous studies (Matlakowska and Sklodowska, 2009; Szuplewska et al., 2014). However, detailed physiological or genomic analyses have not been done for these *Pseudomonas* strains so far. The remaining 10 strains were classified on the basis of comparative analyses of the obtained 16S rDNA sequences applying the RDP (Ribosomal Database Project) (Cole et al., 2009) and GenBank (NCBI) databases. This analysis revealed that the majority of the uncharacterized bacterial isolates represented different classes of *Proteobacteria*: (i) 5 strains of *Alphaproteobacteria—Brevundimonas* sp. LM17 and LM18, *Ochrobactrum* sp. LM19, *Paracoccus yeei* LM20 and *Sinorhizobium* sp. LM21; (ii) 1 of *Betaproteobacteria—Achromobacter* sp. LM16; and (iii) 2 of *Gammaproteobacteria—Psychrobacter* sp. LM26 and *Stenotrophomonas* sp. LM24. The two remaining strains (LM22 and LM23) were identified as members of the genus *Sphingobacterium*, belonging to the *Bacteroidetes* phylum. Based on their 16S rDNA sequences three of the analyzed strains (LM7, LM10, and LM20) could be identified as *Pseudomonas mendocina* LM7, *Pseudomonas aeruginosa* LM10 and *Paracoccus yeei* LM20.

Preliminary physiological characterization of all identified bacterial strains revealed that 13 could grow at temperatures ranging from 15 to 37°C, or even 42°C (this growth pattern is typical for mesophilic bacteria), while 7 strains were psychrotrophs, able to grow at temperatures between 4 and 37°C (the optimum temperature for all strains was either 21 or 30°C) (Table S2). All strains grew in LB medium at pH values close to 7, which is characteristic for neutrophilic bacteria. Three strains (LM7, LM16, and LM19) displayed properties of facultative alkaliphiles, since they could tolerate pH values of up to 11 (Table S2) (Slonczewski et al., 2009). Salinity tolerance testing revealed that the majority (18) of the strains were non-halophilic bacteria, while LM14 and LM26 could tolerate a higher NaCl concentration (6%); thus they were classified as halotolerant (Table S2) (Larson, 1986). The motility assay revealed that 15 of the tested strains were motile (Table S2). Moreover, application of the universal chrome azurol S (CAS) agar plate assay indicated that 16 of the analyzed strains produced iron-chelating siderophores (Table S2).

GENERAL CHARACTERIZATION OF THE PLASMIDOME OF THE IDENTIFIED BACTERIA

Plasmid screening of all bacterial isolates revealed the presence of 12 circular replicons ranging in size from approx. 1.7 to 120 kb. Six strains contained plasmids: *Achromobacter* sp. LM16, *Ochrobactrum* sp. LM19, *P. yeei* LM20, *Pseudomonas* sp. LM8, *Pseudomonas* sp. LM12 and *Sinorhizobium* sp. LM21. The nucleotide sequences of all but one of these replicons [pLM8P2 of *Pseudomonas* sp. LM8 was described in our previous study (Szuplewska et al., 2014)], were obtained and analyzed. This revealed that the plasmids contained from 2 to 150 predicted genes and their average GC content varied between 53.5 and 67.3%. The plasmids carried as many as 22 types of predicted genetic modules, involved in various functions. The results of the overall characterization of the plasmids are shown in **Table 1**. A summary of genes identified in each plasmid, including their position, the size of the putative encoded proteins and their closest homologs, is presented in Tables S3–S7.

For each plasmid, a conserved backbone, composed of the maintenance and conjugal transfer modules (including modules responsible for mobilization for conjugal transfer) was distinguished. *In silico* analysis of the plasmid-encoded accessory modules showed plasmids containing genes of direct adaptive value: (i) heavy metal resistance plasmids (pLM16A1, pLM20P1 and pLM20P2), (ii) a catabolic plasmid (pLM20P5), and other replicons, including a (iii) plasmid-like prophage (pLM21S1), (iv) putative virulence plasmids (pLM19O1 and pLM19O2) and (v) cryptic plasmids (pLM20P3, pLM20P4, pLM8P1 and pLM12P1). In our analyses we mainly focused on heavy metal resistance plasmids.

GENOMICS OF HEAVY METAL RESISTANCE PLASMIDS

Three plasmids were found to carry predicted genetic modules involved in heavy metal resistance: pLM20P1 and pLM20P2 of *P. yeei* LM20, and pLM16A1 of *Achromobacter* sp. LM16 (**Figure 1**, Tables S3, S4). The average GC content of the nucleotide sequences of the plasmids is 62.7, 63.4, and 64.2% (**Table 1**), respectively, which is lower than the mean values determined for the total DNA of the bacteria belonging to *Achromobacter* and *Paracoccus* genus—66.4% (mean result for 11 genomes) and 67.3% (mean result for 27 genomes), respectively.

Two plasmids of *P. yeei* LM20 are small replicons (6 and 6.2 kb, respectively) encoding replication initiation proteins with homology to related proteins of plasmids occurring in several carotenoid-producing strains of *Paracoccus* spp. (Maj et al., 2013). Plasmid pLM20P1 carries three arsenic-tolerance genes (ARS module; pLM20P1_p3-pLM20P1_p5) encoding arsenate reductase (ArsC), an efflux pump (ArsB) and an ArsR family transcriptional repressor. The small cytoplasmatic arsenate reductase ArsC is responsible for the conversion of arsenate (As^{5+}) into arsenite (As^{3+}), while the membrane protein ArsB is an effective chemiosmotic efflux system mediating the removal of As^{3+} from the cell (Silver and Phung Le, 2005a,b). Interestingly, the ARS module of pLM20P1 shares 80% nucleotide sequence identity with the appropriate gene cluster of chromid pAMI5 of *Paracoccus aminophilus* JCM 7686 (Dziewit et al., 2014a). The second plasmid, pLM20P2 carries a CZC module, encoding a MerR family transcriptional regulator (pLM20P2_p3) and a predicted CzcD cation transport membrane protein (pLM20P2_p4) [member of the cation diffusion facilitator (CDF) protein family], which mediates cobalt (Co^{2+}), zinc (Zn^{2+}) and cadmium (Cd^{2+}) resistance (Anton et al., 2004). This DNA region shares

Table 1 | General features of plasmids of bacteria from the Lubin mine.

Plasmid name	Bacterial strain	Plasmid size (bp)	GC content (%)	Number of genes	Average gene length (bp)	Percentage of coding regions	Genetic modules*
pLM16A1	*Achromobacter* sp. LM16	25,026	64.2	28	817	91.7	REP, PAR, RM, MOB, TE, MER
pLM19O1	*Ochrobactrum* sp. LM19	78,679	53.5	75	806	76.9	REP, PAR, TA, TE, RT, VIR
pLM19O2	*Ochrobactrum* sp. LM19	107,804	54.7	100	870	80.7	REP, PAR, TA, TE, TRA, VIR
pLM20P1	*Paracoccus yeei* LM20	5982	62.7	9	582	87.6	REP, TA, ARS
pLM20P2	*Paracoccus yeei* LM20	6235	63.4	9	619	89.4	REP, MOB, CZC
pLM20P3	*Paracoccus yeei* LM20	7244	62.0	9	610	75.8	REP, TA, MOB, TE
pLM20P4	*Paracoccus yeei* LM20	20,746	57.8	21	784	79.4	REP, PAR, TA, MOB
pLM20P5	*Paracoccus yeei* LM20	28,489	66.2	28	940	92.3	REP, MRS, PAR, TA, ABC, ALN, HIS, HUT, LCT, MLR, VAN
pLM8P1	*Pseudomonas* sp. LM8	1679	58.1	2	651	77.5	REP
pLM12P1	*Pseudomonas* sp. LM12	5089	67.3	4	963	56.2	REP, MOB
pLM21S1	*Sinorhizobium* sp. LM21	117,539	59.5	150	685	87.4	REP, PAR, COB, NAD

**ABC, ABC-type transporter system; ALN, allantoate amidohydrolase; ARS, arsenic resistance module; COB, cobalamine biosynthesis module; CZC, cobalt, zinc, and cadmium resistance module; HIS, histidinol-phosphate aminotransferase; HUT, histidine catabolism module; LCT, D-lactate dehydrogenase; MER, mercury resistance module; MLR, microcystin LR degradation protein; MOB, mobilization to conjugal transfer module; MRS, multimer resolution module; NAD, NAD biosynthesis module; PAR, partitioning module; REP, replication module; RM, restriction-modification system; RT, group II intron; TA, toxin-antitoxin module; TE, transposable element; TRA, conjugal transfer module; VAN, vanillate utilization module; VIR, virulence factors.*

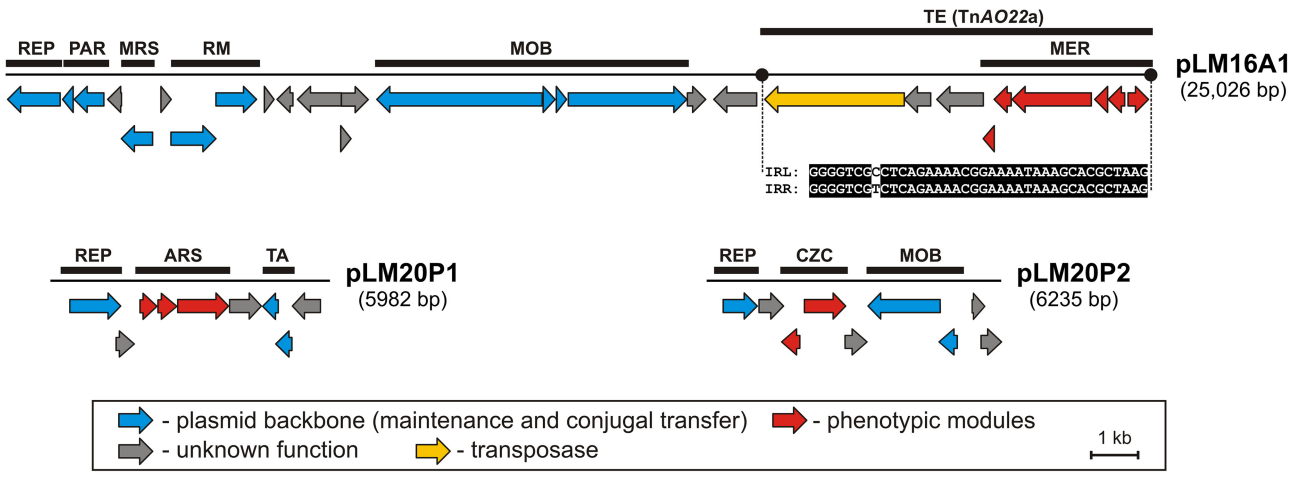

FIGURE 1 | Linear maps showing the genetic structure of the circular plasmids pLM20P1 and pLM20P2 of *P. yeei* LM20 and pLM16A1 of *Achromobacter* sp. LM16. The predicted genetic modules are indicated by black rectangles: ARS, arsenic resistance system; CZC, cobalt, zinc and cadmium resistance system; MER, mercury resistance system; MRS, multimer resolution system; PAR, partitioning system; REP, replication system; RM, restriction-modification system; TA, toxin-antitoxin system; TE, transposon Tn*AO22*a within pLM16A1. The nucleotide sequences of the left and right terminal inverted repeats (IRL and IRR) of Tn*AO22*a are presented. Arrows indicate genes and their transcriptional orientation.

high level (69%) of nucleotide sequence identity with appropriate CZC module of a large, extrachromosomal, alphaproteobacterial replicon—NT26_p1 of *Rhizobium* sp. NT-26 (Andres et al., 2013).

The third plasmid, pLM16A1 of *Achromobacter* sp. LM16 (25 kb), has a mosaic structure. More than half of the plasmid genome shares at least 84% nucleotide sequence identity with transposon TNCP23 of plasmid pKLC102, coexisting as an autonomous replicon and a genomic island in *Pseudomonas aeruginosa* (Klockgether et al., 2004; Bonnin et al., 2013). Plasmid pLM16A1 contains the following modules: (i) a replication system, encoding a RepA protein (pLM16A1_p1); (ii) a partitioning system (pLM16A1_p2- pLM16A1_p3); (iii) a putative multimer resolution system (pLM16A1_p5); (iv) a type II restriction-modification system (pLM16A1_p7-pLM16A1_p8), whose restriction endonuclease (predicted recognition sequence GCCGGC) shares 68% amino acid sequence identity with R.NgoMIV from *Neisseria gonorrhoeae* MS11 (Stein et al., 1992); (v) a MOB module; and (vi) a mercury resistance module (MER; pLM16A1_p23-pLM16A1_p28) (**Figure 1**).

The MER module consists of 6 genes encoding proteins responsible for the enzymatic conversion of Hg^{2+} ions to the less toxic form Hg^0 (metallic mercury). The key enzyme is the mercuric reductase (MerA), which reduces Hg^{2+} to Hg^0. The other five MER-encoded proteins include two mercury ion transporters (MerT and MerP), two transcriptional regulators (MerR and MerD) and an accessory membrane protein (MerE) of unknown function. The pLM16A1 MER module is embedded within a transposon (Tn*AO22*a; 8240 bp), which is an isoform (99% nucleotide sequence identity) of Tn*AO22*, previously identified in *Achromobacter* sp. AO22 (Ng et al., 2009). Using a positive-selection trap vector (pMAT1) to identify functional transposable elements, we demonstrated that Tn*AO22*a is capable of transposition and therefore may contribute to the dissemination of mercury resistance.

We also performed a phylogenetic analysis of the heavy metal resistance modules of plasmids pLM20P1, pLM20P2, and pLM16A1. For the analysis ArsB, ArsC, CzcD, and MerA proteins were used. We found that the close homologs of ArsB and ArcC proteins are encoded mostly within the genomes of *Alphaproteobacteria*, including several strains of *Paracoccus* spp. (**Figures S1**, **S2**). Interestingly, proteins related to CzcD are encoded not only by *Alphaproteobacteria*, but also by members of the phylum *Thaumarchaeota* (*Archaea*), which may suggest the inter-domain gene transfer (**Figure S3**). The fourth analyzed protein, MerA, has close relatives encoded within the genomes of various gram-negative (*Beta-* and *Gammaproteobacteria*), as well as gram-positive bacteria (*Mycobacterium* spp. and *Bacilli*) (**Figure S4**).

HOST RANGE AND FUNCTIONAL ANALYSES OF HEAVY METAL RESISTANCE PLASMIDS

Heavy metal tolerance of wild-type strains was determined. Ten heavy metal ions were examined: As^{3+}, As^{5+}, Cd^{2+}, Co^{2+}, Cr^{6+}, Cu^{2+}, Hg^{2+}, Ni^{2+}, V^{5+}, and Zn^{2+}. All tested strains showed resistance to at least 4 of the 10 tested ions. In total we found 146 (out of 200 tested) resistance phenotypes. One strain, *P. aeruginosa* LM10, exhibited resistance to all of the tested ions, while *Pseudomonas* sp. LM15 and LM25, *Achromobacter* sp. LM16, *Ochrobactrum* sp. LM19, *Sinorhizobium* sp. LM21, *Sphingobacterium* sp. LM22 and *Stenotrophomonas* sp. LM24 showed resistance to 9 of them (**Table 2**). All strains tolerated high levels of arsenate (60–1200 mM), nickel (1–6 mM) and copper (2–10 mM), while 19 isolates were resistant to arsenite (1–25 mM). In contrast, only 8 isolates showed (low level) resistance to chromium (VI) (**Table 2**).

Then, the functionality of the resistance modules (from plasmids pLM20P1, pLM20P2, and pLM16A1, and transposable elements IS*Ppu12*a and Tn*5563*a) was tested in various hosts and the obtained values were compared with those of the wild-type strains (**Figure 2**). This analysis revealed that the introduction of the plasmids to the recipient strains resulted in a significant increase (at least 2-fold) in the MICs in 30 (20%) of the transconjugants, while decreases in the MICs of at least 2-fold were observed in 22 (14.7%) (**Figure 2**, Table S8).

The putative CZC module of plasmid pLM20P2 (CZC-LM20) was active, but produced a resistance phenotype in only a limited number of strains: *Pseudomonas* spp. LM5, LM6 and LM8 (increased resistance to Cd^{2+}, Co^{2+}, Zn^{2+}; MIC increases of at

Table 2 | Heavy metals resistance of bacteria isolated from the Lubin mine.

	Heavy metals resistance (MICs) (mM)*									
	As^{3+}	As^{5+}	Cd^{2+}	Co^{2+}	Cr^{6+}	Cu^{2+}	Hg^{2+}	Ni^{2+}	V^{5+}	Zn^{2+}
Achromobacter sp. LM16	**25**	**1200**	**7**	**1.5**	0.8	**10**	**0.3**	**6**	**200**	**10**
Brevundimonas sp. LM17	**2**	**250**	0.1	0.6	0.2	**5**	0.01	**3**	1	**2**
Brevundimonas sp. LM18	**2**	**250**	0.1	0.7	0.4	**4**	0.02	**2**	**20**	**2**
Ochrobactrum sp. LM19	**9**	**1000**	**2**	**1**	**2**	**8**	0.02	**4**	**200**	**10**
Paracoccus yeei LM20	**6**	**400**	**1**	**1.5**	0.1	**3**	0.08	**2**	5	**1**
Pseudomonas sp. LM5	**1**	**400**	0.1	0.5	0.6	**3**	0.06	**2**	**75**	0.6
Pseudomonas sp. LM6	0.6	**75**	0.1	0.5	0.2	**3**	**0.2**	**3**	15	0.6
Pseudomonas mendocina LM7	**15**	**500**	0.6	0.4	**2**	**5**	**0.2**	**3**	**150**	0.9
Pseudomonas sp. LM8	**7**	**250**	0.1	0.5	0.3	**3**	**0.2**	**3**	15	0.4
Pseudomonas aeruginosa LM10	**4**	**250**	**6**	**2**	**2**	**9**	**0.2**	**3**	**30**	**15**
Pseudomonas sp. LM11	**3**	**500**	0.1	0.4	0.6	**2**	**0.2**	**3**	**75**	0.3
Pseudomonas sp. LM12	**2**	**400**	0.2	0.6	0.3	**4**	**0.2**	**3**	**75**	0.8
Pseudomonas sp. LM14	**15**	**250**	0.1	**1.5**	0.4	**9**	**0.1**	**4**	**250**	**6**
Pseudomonas sp. LM15	**7**	**500**	**1**	**4**	**3**	**8**	0.01	**6**	**40**	**6**
Pseudomonas sp. LM25	**6**	**500**	**4**	**3**	**2**	**8**	0.01	**6**	**30**	**5**
Psychrobacter sp. LM26	**4**	**200**	0.1	0.8	**2**	**5**	0.02	**1**	**100**	**2**
Sinorhizobium sp. LM21	**5**	**200**	**2**	**1.5**	**1**	**5**	0.02	**4**	**50**	**3**
Sphingobacterium sp. LM22	**3**	**250**	**2**	**2**	0.3	**7**	**0.2**	**5**	**100**	**9**
Sphingobacterium sp. LM23	**2**	**60**	**1**	0.3	0.2	**4**	0.02	**2**	**30**	**2**
Stenotrophomonas sp. LM24	**4**	**350**	**2**	0.9	**2**	**8**	**0.1**	**5**	**60**	**10**

**MICs considered to represent the heavy metal resistance phenotype were shown in bold.*

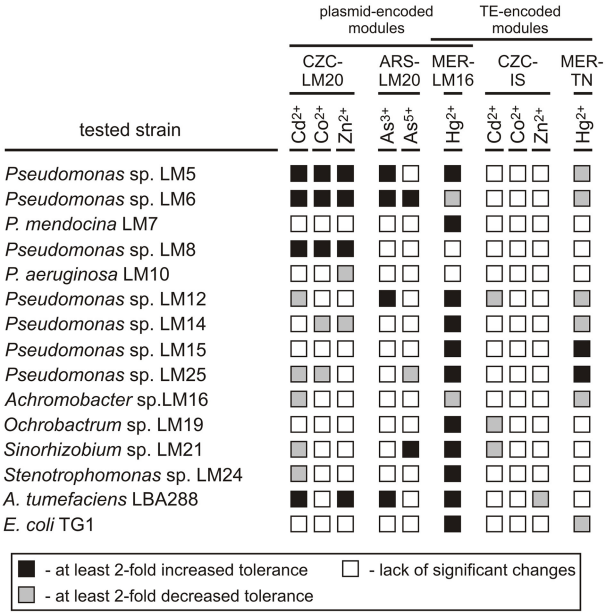

FIGURE 2 | Influence of the CZC, ARS, and MER modules on the heavy metal tolerance of bacterial strains inhabiting the Lubin copper mine, plus the controls *A. tumefaciens* and *E. coli*. CZC-LM20, cobalt, zinc and cadmium resistance module of plasmid pLM20P2; ARS-LM20, arsenic resistance module of pLM20P1; MER-LM16, mercury resistance module of plasmid pLM16A1; CZC-IS, cobalt, zinc and cadmium resistance module of IS*Ppu12*a; MER-TN, mercury resistance module of plasmid Tn*5563*a.

least 3-fold) and *A. tumefaciens* LBA288 (elevated resistance to Cd^{2+} and Zn^{2+}; MIC increases of 2- and 2.5-fold, respectively). In contrast, the CZC-IS module of IS*Ppu12*a did not confer resistance to Cd^{2+}, Co^{2+}, or Zn^{2+} in any of the tested transconjugant strains and hence probably was inactive. In a few cases, presence of the CZC-LM20 and CZC-IS modules resulted in a decrease in the MIC values (**Figure 2**, Table S8).

The arsenic resistance module of pLM20P1 (ARS-LM20) was tested for its ability to increase the tolerance of bacteria to arsenite and arsenate ions. Only 5 strains carrying pBBR-ARSLM20 (*Pseudomonas* spp. LM5, LM6, LM12, *Sinorhizobium* sp. LM21 and *A. tumefaciens* LBA288) exhibited at least 2-fold higher resistance to arsenite or arsenate compared to their parental wild-type strains (**Figure 2**, Table S8).

The MER modules analyzed in this study originated from plasmid pLM16A1 (MER-LM16 module) and transposon Tn*5563*a (MER-TN module) and were predicted to confer resistance to mercury ions. As mentioned above, the MER-LM16 module carries a complete set of genes commonly found in other well defined mercury resistance operons (Silver and Phung Le, 2005b), while MER-TN is a partial module, carrying only three genes (*merRTP*). Introduction of the MER-TN module resulted in a significant increase in the MIC for Hg^{2+} in only two strains, while the MICs of six other strains were at least 2-fold decreased. In contrast, presence of the MER-LM16 module increased tolerance to Hg^{2+} in 11 (73.3%) strains. Interestingly, introduction of plasmid pBBR-MERLM16 into two strains (LM6 and LM16) originally exhibiting high levels of resistance to mercury, resulted in an unexpected decrease in tolerance (**Figure 2**, Table S8).

We also tested the host range of plasmids pLM20P1, pLM20P2, and pLM16A1. The replication system of pLM16A1 was functional in all tested strains, which indicates its broad host range. In contrast, plasmids replication modules of pLM20P1 and pLM20P2 were found to have a relatively narrow host range, limited to a few strains of *Alphaproteobacteria*. Both plasmids were able to replicate in *A. tumefaciens* LBA288, and the latter one could also replicate in *Sinorhizobium* sp. LM21.

DIVERSITY AND GENOMICS OF OTHER PLASMIDS OF BACTERIA ISOLATED FROM THE LUBIN MINE

Amongst identified replicons we found one catabolic plasmid, pLM20P5 of *P. yeei* LM20. The plasmid carries 28 predicted genes (**Figure 3A**). Of these, 12 encode enzymes directly linked with: (i) purine metabolism, (ii) pyruvate metabolism, (iii) vanillate utilization and (iv) amino acid and peptide transport and metabolism (**Figure 3A**, Table S3). Two of the pLM20P5-encoded phenotypic modules are of particular interest. One, responsible for the utilization of vanillate (an important intermediate in the lignin degradation process), is composed of three genes encoding vanillate *O*-demethylase [VanA and VanB subunits; (EC 1.14.13.82)] and a predicted LysR family transcriptional regulator (VanR). The formaldehyde-producing monooxygenase-type vanillate *O*-demethylase VanAB is crucial for the utilization of vanillate by its demethylation to protocatechuate (**Figure 3A**), which can then be degraded to central metabolism intermediates using the *meta* or *ortho* cleavage pathways (Masai et al., 2007; Chen et al., 2012). The second distinguished module (HUT) is involved in histidine utilization. It is composed of 7 genes encoding histidine ammonia lyase (HutH, EC 4.3.1.3), urocanase (HutU, EC 4.2.1.49), imidazolone propionate amidohydrolase (HutI, EC 3.5.2.7), formiminoglutamate deiminase (HutF, EC 3.5.3.13), formylglutamate amidohydrolase (HutG, EC 3.5.1.68), plus a histidine utilization repressor (HutR) and a HutD-family protein. The final products of this utilization pathway are L-glutamate and formate (**Figure 3A**) (Bender, 2012).

Another plasmid, pLM21S1 of *Sinorhizobium* sp. LM21, was found to carry numerous phage-related genes, encoding proteins required for DNA packaging, capsid and tail assembly, and cell lysis. This predicted plasmid-like prophage lacks an integrase gene, which suggests that it is not able to integrate into chromosomal DNA. Interestingly, pLM21S1 carries a RepC-like replication system, commonly found within large alphaproteobacterial plasmids (Cevallos et al., 2008). To check whether pLM21S1 is an active phage, we treated cells of *Sinorhizobium* sp. LM21 with mitomycin C, a classical inducer of lambdoid prophages. This approach did not cause phage induction, although it resulted in the induction of another indigenous prophage residing in the bacterial genome (Dziewit et al., 2014b). We speculate that pLM21S1 may be an inactive prophage, or alternatively it may require specific, as yet unidentified, environmental factors for induction.

Plasmid/phage pLM21S1 carries 147 putative genes and 3 tRNA-encoding sequences (Table S5). In total 83 of its genes are conserved in the genome of a related phage, RHEph10 of *Rhizobium etli* CFN42 (Santamaria et al., 2014) (**Figure 3B**).

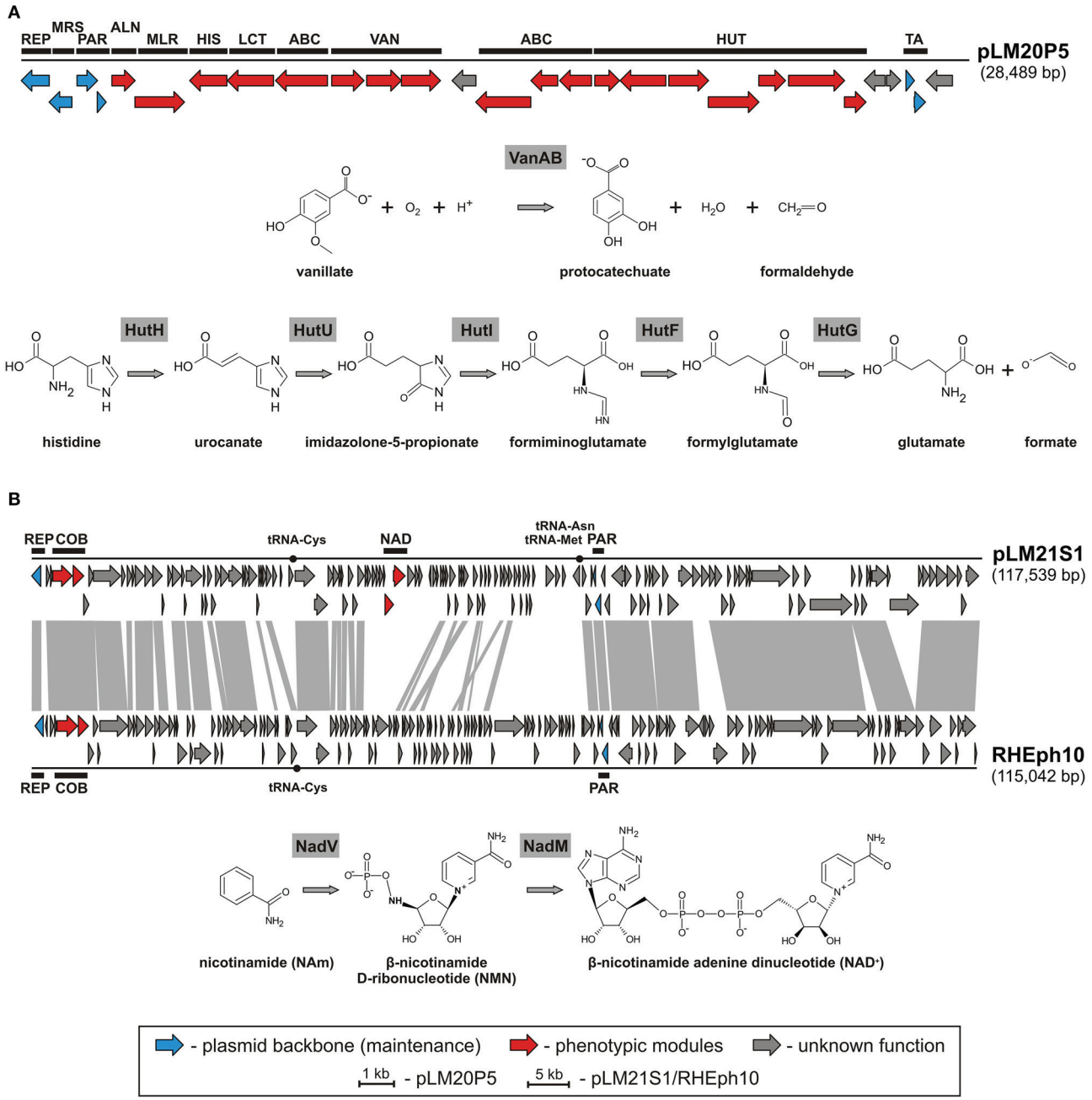

FIGURE 3 | Linear map showing the genetic structure of the circular plasmid pLM20P5 of *P. yeei* LM20 and schematic pathways for vanillate and histidine utilization (A), and linear map showing the genetic structures of the circular plasmid-like prophage pLM21S1 of *Sinorhizobium* sp. LM21 and *Rhizobium* phage RHEph10, and a schematic pathway for NAD biosynthesis (B). The predicted genetic modules are indicated by black rectangles: ABC, ABC-type transporter system; ALN, allantoate amidohydrolase; COB, part of a cobalamine biosynthesis module; HIS, histidinol-phosphate aminotransferase; HUT, histidine utilization system; LCT, *D*-lactate dehydrogenase; MLR, microcystin LR degradation protein; MRS, multimer resolution system; NAD, NAD^+ biosynthesis module; PAR, partitioning system; REP, replication system; TA, toxin-antitoxin system; VAN, vanillate utilization system. Arrows indicate genes and their transcriptional orientation. The tRNA-encoding sequences are marked by black dots. The gray-shaded area connects genes of plasmid pLM21S1 and phage RHEph10 that encode homologous proteins.

These two replicons carry homologous replication and partitioning systems, as well as putative genetic modules for cobalamine biosynthesis (*cobTS*) (**Figure 3B**). The CobT and CobS proteins form a complex, which together with an additional subunit, CobN (not encoded by the prophages) catalyzes cobalt incorporation into the corrin ring during the biosynthesis of coenzyme B12 (Debussche et al., 1992). Interestingly, pLM21S1 carries also genes involved in nicotinamide adenine

dinucleotide (NAD) biosynthesis, which are not present in RHEph10. Of these, pLM21S1_p57 encodes a bifunctional nicotinamide mononucleotide adenylyltransferase/ADP-ribose pyrophosphatase (NadM, EC 2.7.7.1), while pLM21S1_p58 encodes nicotinamide phosphoribosyltransferase (NadV, EC 2.4.2.12). NadV catalyzes the transformation of nicotinamide (NAm) to β-nicotinamide ribonucleotide (NMN), which is then converted to NAD by the NadM enzyme (**Figure 3B**) (Martin et al., 2001). It has been suggested that the *nadV-nadM* module is not only responsible for NAD biosynthesis, but also for overall recycling of endogenous nicotinamide, which may be generated by the hydrolysis of NAD (Gerdes et al., 2006).

Next two replicons identified in the course of this study originated from *Ochrobactrum* sp. LM19. The plasmids pLM19O1 and pLM19O2 contain *repABC* modules (replication and partitioning functions) and carry 75 and 100 genes, respectively (**Figure S5**, Table S6). The bioinformatic analyses revealed that both replicons encode several virulence-associated proteins, including: (i) outer membrane autotransporter barrel domain-containing proteins of the type V secretion system, (ii) three invasion-associated locus B (IalB-like) proteins, whose homologs determine the erythrocyte-invasive phenotype of *Bartonella bacilliformis* (Coleman and Minnick, 2001), (iii) a YadA-like autotransporter adhesin of the non-fimbrial adhesins family, whose representatives are responsible for adhesion in infected tissues and protection against lysis (Hoiczyk et al., 2000), and (iv) an ATP-binding ABC-type transporter (HlyB) and hemolysin D (HlyD) of the hemolysin A type I secretion system (Fath and Kolter, 1993) (**Figure S5**, Table S6).

The remaining four plasmids (pLM20P3 and pLM20P4 of *P. yeei* LM20, pLM8P1 of *Pseudomonas* sp. LM8 and pLM12P1 of *Pseudomonas* sp. LM12) identified in bacteria from the Lubin mine were designated as cryptic replicons, since they lack accessory modules (Tables S3, S7).

DISCUSSION

In this study we analyzed the plasmid content of 20 bacterial strains (representing eight genera of three classes of *Proteobacteria* and one genus of the *Bacteroidetes* phylum) isolated from the Lubin underground copper mine. The plasmidome of these strains comprised 12 replicons, whose genetic structure was revealed. We demonstrated the diversity of the plasmids and defined their adaptive value, focusing on heavy metal resistance, since these toxic elements are major contaminants of the Lubin copper mine environment influencing indigenous microoganisms.

The black shale horizon is exposed to the activity of oxygen, water, and microorganisms. These factors cause the chemical and biological weathering of the rock and strongly influences the geochemical cycles of heavy metals, as well as organic carbon, which results in further redistribution of the elements within the environment (Matlakowska et al., 2010, 2012; Matlakowska and Sklodowska, 2011). The geochemical examination of environmental samples of water and bottom sediment used in presented study confirmed the presence of heavy metals. For example, the concentrations of Cu, Pb, Zn, As and Ni in sample of bottom sediment originated from underground pond were 6839 mg kg^{-1}, 1128 mg kg^{-1}, 115 mg kg^{-1}, 110 mg kg^{-1} and 14 mg kg^{-1}, respectively. Similarly, the mineral sediment taken from the surface of black shale contained copper at concentration 721 mg kg^{-1}.

High concentrations of heavy metals act as a specific selection pressure permitting the survival of only well adapted indigenous strains expressing multi-resistant and hypertolerant phenotypes. Our analysis confirmed that all the strains analyzed in this work exhibited such characteristics. The majority of them were resistant to high levels of copper, arsenic and nickel, which correlates with the composition of Kupferschiefer black shale [35000 mg kg^{-1} for Cu, 398 mg kg^{-1} for As, 479 mg kg^{-1} for Ni (Matlakowska et al., 2012)]. We showed that some of the resistance phenotypes were confirmed by the mobile genetic elements.

Among the mobile genetic elements identified in the analyzed bacteria we found three plasmids (pLM16A1, pLM20P1, pLM20P2) and three transposable elements [Tn*AO22*a, Tn*5563*a, IS*Ppu12*a] that mediate resistance to arsenate, arsenite, cadmium, zinc, cobalt, and mercury. In-depth analyses demonstrated that the resistance phenotypes conferred by the particular elements are highly dependent on the host strain. Surprisingly, these results revealed that acquisition of a predicted resistance module is not always beneficial for the host, and may paradoxically lead to increased sensitivity. We speculate that this phenomenon may be the result of an unfavorable influence of the introduced genetic module on the overall homeostasis of the cell, e.g., by altering intracellular ion concentrations. All of the analyzed resistance modules encode influx/efflux pumps that are likely to have a relaxed substrate specificity [e.g., ArsB recognizes and functions with antimony, as well as arsenite (Silver and Phung Le, 2005a,b)], which may significantly influence ion fluxes.

An interesting example of a resistance module leading to increased sensitivity is the MER module of Tn*3* family transposon Tn*5563*a [deletion derivative of Tn*5044* of *Xanthomonas campestris*; (Kholodii et al., 2000)]. Transposon Tn*5563*a lacks *merA* (which is present in Tn*5044*), but it carries *merP* and *merT* genes encoding transporters responsible for the uptake of toxic mercuric ions. In six of the tested strains, the acquisition of this genetic module resulted in significant decreases in their MICs, which is probably the result of an increased intracellular concentration of toxic ions plus the inability of the strains to inactivate Hg^{2+} caused by the lack of MerA mercuric reductase. In contrast, increased tolerance was observed in two *Pseudomonas* spp. strains, possibly due to the presence of a chromosomal copy of the *merA* gene. Therefore it seems that the phenotypes determined by this module depend on the genetic background of the host strain.

The analyzed resistance modules are present on mobile genetic elements, so they may be readily transferred to other bacteria. We found that the replication system of the mobilizable plasmid pLM16A1 (containing MER) is functional in a broad range of hosts, which makes this replicon ideal for the horizontal dissemination of the mercury resistance phenotype. Moreover, the MER module of pLM16A1 (determining resistance in the great majority of tested strains) is located within an active Tn*3* family transposon (Tn*AO22*a), which enables its spread among different replicons co-residing in a single cell.

The host range of the tested plasmids correlates with the results of phylogenetic analyses, which showed that the close homologs of ArsB, ArcC, and CzcD proteins (whose genes are located within narrow host range plasmids, pLM20P1 and pLM20P2) are encoded mostly within the genomes of *Alphaproteobacteria*, while MerA protein (encoded by the broad host range plasmid pLM16A1) is conserved among various gram-negative and gram-positive bacteria. Interestingly, it was also found that the homologs of the MER module are frequently co-localized with antibiotic resistance genes in various plasmids of *Gammaproteobacteria* [e.g., pACM1 (Preston et al., 2014), pHCM1 (Parkhill et al., 2001), pKOX_R1 (Huang et al., 2013)]. Those findings reflect the pivotal role of broad host range replicons in the dissemination of various resistance genes.

In the course of this study other replicons which may contribute to adaptation of their bacterial hosts to harsh environmental conditions of the Lubin mine were also identified. Amongst them, there was a catabolic replicon pLM20P5 of *P. yeei* LM20. It carries genetic modules, enabling the utilization of histidine and vanillate. These substrates can be used as alternative sources of carbon, nitrogen and energy. Since there is a limited amount of easily degradable carbon sources in the Lubin mine, it is likely that acquisition of catabolic plasmids such as pLM20P5 may be beneficial to the host.

An intriguing finding was also the identification of an unusual plasmid-like prophage element in *Sinorhizobium* sp. LM21. The replicon pLM21S1 has features typical of both, plasmids (replication and stable maintenance modules) and phages (complete set of proteins necessary for the phage "life cycle"). Plasmid pLM21S1 is related to the phage RHEph10, which is able to infect various *Rhizbium etli* strains (Santamaria et al., 2014). Accordingly, both replicons may be considered as the archetypes of a novel group of plasmid-like prophages. Interestingly, pLM21S1 carries the *nadV-nadM* genes responsible for NAD biosynthesis. The introduction of such genes into bacteria that neither possess the NAD *de novo* biosynthesis pathway, nor the NAD salvage pathway (e.g., *Haemophilus influenzae*), may transform them into "NAD-independent" strains, able to synthesize NAD from nicotinamide (Martin et al., 2001). We postulate that the presence of pLM21S1 may be beneficial to the host because NAD production is likely to improve the overall fitness of the bacterium, since NAD (and its derivative, NADP) is the most important coenzyme in cellular redox reactions (Martin et al., 2001).

Current knowledge concerning the direction, frequency and range of DNA transfer among microorganisms living in extreme environments, and especially deep terrestrial habitats, is sparse. We believe that the approach followed in the present study, linking geochemical data with physiological characterization of bacteria and detailed analyses of their plasmidome, may considerably increase our understanding of the influence of mobile DNA and horizontal gene transfer on the biology of extremophilic bacteria.

ACKNOWLEDGMENT

This work was supported by the National Science Centre, Poland [grant number N N303 579238].

SUPPLEMENTARY MATERIALS

The Supplementary Material for this article can be found online at: http://www.frontiersin.org/journal/10.3389/fmicb.2015.00152/abstract

Figure S1 | Phylogenetic tree of the ArsB proteins homologous to ArsB efflux pomp encoded within pLM20P1. The analysis was based on 100 sequences retrieved from the UniProt database. The unrooted tree was constructed using the neighbor-joining algorithm and statistical support for the internal nodes was determined by 1000 bootstrap replicates. Values of ≥50% are shown. UniProt accession numbers of the protein sequences used for the phylogenetic analysis are given in parentheses. The underlined accession numbers indicate *Paracoccus* proteins.

Figure S2 | Phylogenetic tree of the ArsC proteins homologous to ArsC arsenate reductase encoded within pLM20P1. The analysis was based on 100 sequences retrieved from the UniProt database. The unrooted tree was constructed using the neighbor-joining algorithm and statistical support for the internal nodes was determined by 1000 bootstrap replicates. Values of ≥50% are shown. UniProt accession numbers of the protein sequences used for the phylogenetic analysis are given in parentheses. The underlined accession numbers indicate *Paracoccus* proteins.

Figure S3 | Phylogenetic tree of the CzcD proteins homologous to CzcD cation transport membrane protein encoded within pLM20P2. The analysis was based on 100 sequences retrieved from the UniProt database. The unrooted tree was constructed using the neighbor-joining algorithm and statistical support for the internal nodes was determined by 1000 bootstrap replicates. Values of ≥50% are shown. UniProt accession numbers of the protein sequences used for the phylogenetic analysis are given in parentheses. The underlined accession numbers indicate *Paracoccus* proteins.

Figure S4 | Phylogenetic tree of the MerA proteins homologous to MerA mercuric reductase encoded within pLM16A1. The analysis was based on 100 sequences retrieved from the UniProt database. The unrooted tree was constructed using the neighbor-joining algorithm and statistical support for the internal nodes was determined by 1000 bootstrap replicates. Values of ≥50% are shown. UniProt accession numbers of the protein sequences used for the phylogenetic analysis are given in parentheses. The underlined accession numbers indicate *Achromobacter* proteins.

Figure S5 | Linear map showing the genetic structure of the circular plasmids pLM19O1 and pLM19O2 of *Ochrobactrum* sp. LM19. The predicted genetic modules are indicated by black rectangles: PAR, partitioning system; REP, replication system; RT, group II intron; TA, toxin-antitoxin system; TE, transposable element; TRA, conjugal transfer system; VIR, virulence module. Arrows indicate genes and their transcriptional orientation. The gray-shaded area indicates the inversion region within pLM19O1.

REFERENCES

Abou-Shanab, R. A., Van Berkum, P., and Angle, J. S. (2007). Heavy metal resistance and genotypic analysis of metal resistance genes in gram-positive and gram-negative bacteria present in Ni-rich serpentine soil and in the rhizosphere of *Alyssum murale*. *Chemosphere* 68, 360–367. doi: 10.1016/j.chemosphere.2006.12.051

Altschul, S. F., Madden, T. L., Schaffer, A. A., Zhang, J., Zhang, Z., Miller, W., et al. (1997). Gapped BLAST and PSI-BLAST: a new generation of protein database search programs. *Nucleic Acids Res.* 25, 3389–3402. doi: 10.1093/nar/25.17.3389

Andres, J., Arsene-Ploetze, F., Barbe, V., Brochier-Armanet, C., Cleiss-Arnold, J., Coppee, J. Y., et al. (2013). Life in an arsenic-containing gold mine: genome and physiology of the autotrophic arsenite-oxidizing bacterium *Rhizobium* sp. NT-26. *Genome Biol. Evol.* 5, 934–953. doi: 10.1093/gbe/evt061

Anton, A., Weltrowski, A., Haney, C. J., Franke, S., Grass, G., Rensing, C., et al. (2004). Characteristics of zinc transport by two bacterial cation diffusion facilitators from *Ralstonia metallidurans* CH34 and *Escherichia coli*. *J. Bacteriol.* 186, 7499–7507. doi: 10.1128/JB.186.22.7499-7507.2004

Apweiler, R., Bairoch, A., Wu, C. H., Barker, W. C., Boeckmann, B., Ferro, S., et al. (2004). UniProt: the Universal Protein knowledgebase. *Nucleic Acids Res.* 32, D115–D119. doi: 10.1093/nar/gkh131

Bartosik, D., Białkowska, A., Baj, J., and Wlodarczyk, M. (1997). Construction of mobilizable cloning vectors derived from pBGS18 and their application for analysis of replicator region of a pTAV202 mini-derivative of *Paracoccus versutus* pTAV1 plasmid. *Acta Microbiol. Pol.* 46, 387–392.

Bartosik, D., Szymanik, M., and Wysocka, E. (2001). Identification of the partitioning site within the repABC-type replicon of the composite *Paracoccus versutus* plasmid pTAV1. *J. Bacteriol.* 183, 6234–6243. doi: 10.1128/JB.183.21.6234-6243.2001

Bender, R. A. (2012). Regulation of the histidine utilization (hut) system in bacteria. *Microbiol. Mol. Biol. Rev.* 76, 565–584. doi: 10.1128/MMBR.00014-12

Birnboim, H. C., and Doly, J. (1979). A rapid alkaline extraction procedure for screening recombinant plasmid DNA. *Nucleic Acids Res.* 7, 1513–1523. doi: 10.1093/nar/7.6.1513

Bonnin, R. A., Poirel, L., Nordmann, P., Eikmeyer, F. G., Wibberg, D., Puhler, A., et al. (2013). Complete sequence of broad-host-range plasmid pNOR-2000 harbouring the metallo-beta-lactamase gene blaVIM-2 from *Pseudomonas aeruginosa*. *J. Antimicrob. Chemother.* 68, 1060–1065. doi: 10.1093/jac/dks526

Carver, T., Berriman, M., Tivey, A., Patel, C., Bohme, U., Barrell, B. G., et al. (2008). Artemis and ACT: viewing, annotating and comparing sequences stored in a relational database. *Bioinformatics* 24, 2672–2676. doi: 10.1093/bioinformatics/btn529

Caspi, R., Altman, T., Billington, R., Dreher, K., Foerster, H., Fulcher, C. A., et al. (2014). The MetaCyc database of metabolic pathways and enzymes and the BioCyc collection of Pathway/Genome Databases. *Nucleic Acids Res.* 42, D459–D471. doi: 10.1093/nar/gkt1103

Cevallos, M. A., Cervantes-Rivera, R., and Gutierrez-Rios, R. M. (2008). The *repABC* plasmid family. *Plasmid.* 60, 19–37. doi: 10.1016/j.plasmid.2008.03.001

Chen, H. P., Chow, M., Liu, C. C., Lau, A., Liu, J., and Eltis, L. D. (2012). Vanillin catabolism in *Rhodococcus jostii* RHA1. *Appl. Environ. Microbiol.* 78, 586–588. doi: 10.1128/AEM.06876-11

Chenna, R., Sugawara, H., Koike, T., Lopez, R., Gibson, T. J., Higgins, D. G., et al. (2003). Multiple sequence alignment with the clustal series of programs. *Nucleic Acids Res.* 31, 3497–3500. doi: 10.1093/nar/gkg500

Claudel-Renard, C., Chevalet, C., Faraut, T., and Kahn, D. (2003). Enzyme-specific profiles for genome annotation: PRIAM. *Nucleic Acids Res.* 31, 6633–6639. doi: 10.1093/nar/gkg847

Cole, J. R., Wang, Q., Cardenas, E., Fish, J., Chai, B., Farris, R. J., et al. (2009). The Ribosomal Database Project: improved alignments and new tools for rRNA analysis. *Nucleic Acids Res.* 37, D141–D145. doi: 10.1093/nar/gkn879

Coleman, S. A., and Minnick, M. F. (2001). Establishing a direct role for the *Bartonella bacilliformis* invasion-associated locus B (IalB) protein in human erythrocyte parasitism. *Infect. Immun.* 69, 4373–4381. doi: 10.1128/IAI.69.7.4373-4381.2001

Debussche, L., Couder, M., Thibaut, D., Cameron, B., Crouzet, J., and Blanche, F. (1992). Assay, purification, and characterization of cobaltochelatase, a unique complex enzyme catalyzing cobalt insertion in hydrogenobyrinic acid a,c-diamide during coenzyme B12 biosynthesis in *Pseudomonas denitrificans*. *J. Bacteriol.* 174, 7445–7451.

Dziewit, L., Baj, J., Szuplewska, M., Maj, A., Tabin, M., Czyzkowska, A., et al. (2012). Insights into the transposable mobilome of *Paracoccus* spp. (*Alphaproteobacteria*). *PLoS ONE* 7:e32277. doi: 10.1371/journal.pone.0032277

Dziewit, L., and Bartosik, D. (2014). Plasmids of psychrophilic and psychrotolerant bacteria and their role in adaptation to cold environments. *Front. Microbiol.* 5:596. doi: 10.3389/fmicb.2014.00596

Dziewit, L., Czarnecki, J., Wibberg, D., Radlinska, M., Mrozek, P., Szymczak, M., et al. (2014a). Architecture and functions of a multipartite genome of the methylotrophic bacterium *Paracoccus aminophilus* JCM 7686, containing primary and secondary chromids. *BMC Genomics* 15:124. doi: 10.1186/1471-2164-15-124

Dziewit, L., Oscik, K., Bartosik, D., and Radlinska, M. (2014b). Molecular characterization of a novel temperate *Sinorhizobium* bacteriophage, ΦLM21, encoding DNA methyltransferase with CcrM-like specificity. *J. Virol.* 88, 13111–13124. doi: 10.1128/JVI.01875-14

Dziewit, L., Pyzik, A., Matlakowska, R., Baj, J., Szuplewska, M., and Bartosik, D. (2013). Characterization of *Halomonas* sp. ZM3 isolated from the Zelazny most post-flotation waste reservoir, with a special focus on its mobile DNA. *BMC Microbiol.* 13:59. doi: 10.1186/1471-2180-13-59

Fath, M. J., and Kolter, R. (1993). ABC transporters: bacterial exporters. *Microbiol. Rev.* 57, 995–1017.

Gathogo, E. W., Waugh, A. C., Peric, N., Redpath, M. B., and Long, P. F. (2003). Colony PCR amplification of actinomycete DNA. *J. Antibiot.* 56, 423–424. doi: 10.7164/antibiotics.56.423

Gerdes, S. Y., Kurnasov, O. V., Shatalin, K., Polanuyer, B., Sloutsky, R., Vonstein, V., et al. (2006). Comparative genomics of NAD biosynthesis in cyanobacteria. *J. Bacteriol.* 188, 3012–3023. doi: 10.1128/JB.188.8.3012-3023.2006

Heuer, H., and Smalla, K. (2012). Plasmids foster diversification and adaptation of bacterial populations in soil. *FEMS Microbiol. Rev.* 36, 1083–1104. doi: 10.1111/j.1574-6976.2012.00337.x

Hoiczyk, E., Roggenkamp, A., Reichenbecher, M., Lupas, A., and Heesemann, J. (2000). Structure and sequence analysis of *Yersinia* YadA and *Moraxella* UspAs reveal a novel class of adhesins. *EMBO J.* 19, 5989–5999. doi: 10.1093/emboj/19.22.5989

Huang, T. W., Wang, J. T., Lauderdale, T. L., Liao, T. L., Lai, J. F., Tan, M. C., et al. (2013). Complete sequences of two plasmids in a blaNDM-1-positive *Klebsiella oxytoca* isolate from Taiwan. *Antimicrob. Agents Chemother.* 57, 4072–4076. doi: 10.1128/AAC.02266-12

Kholodii, G., Yurieva, O., Mindlin, S., Gorlenko, Z., Rybochkin, V., and Nikiforov, V. (2000). Tn*5044*, a novel Tn*3* family transposon coding for temperature-sensitive mercury resistance. *Res. Microbiol.* 151, 291–302. doi: 10.1016/S0923-2508(00)00149-2

Klockgether, J., Reva, O., Larbig, K., and Tummler, B. (2004). Sequence analysis of the mobile genome island pKLC102 of *Pseudomonas aeruginosa* C. *J. Bacteriol.* 186, 518–534. doi: 10.1128/JB.186.2.518-534.2004

Lane, D. J. (1991). "16S/23S rRNA sequencing," in *Nucleic Acid Techniques in Bacterial Systematics,* eds E. Stackebrandt and M. Goodfellow. (New York, NY: Wiley), 115–175.

Larson, H. (1986). Halophilic and halotolerant microorganisms-an overview and historical perspective. *FEMS Microbiol. Rev.* 39, 3–7. doi: 10.1111/j.1574-6968.1986.tb01835.x

Lowe, T. M., and Eddy, S. R. (1997). tRNAscan-SE: a program for improved detection of transfer RNA genes in genomic sequence. *Nucleic Acids Res.* 25, 955–964. doi: 10.1093/nar/25.5.0955

Maj, A., Dziewit, L., Czarnecki, J., Wlodarczyk, M., Baj, J., Skrzypczyk, G., et al. (2013). Plasmids of carotenoid-producing *Paracoccus* spp. (*Alphaproteobacteria*) - structure, diversity and evolution. *PLoS ONE* 8:e80258. doi: 10.1371/journal.pone.0080258

Martin, P. R., Shea, R. J., and Mulks, M. H. (2001). Identification of a plasmid-encoded gene from *Haemophilus ducreyi* which confers NAD independence. *J. Bacteriol.* 183, 1168–1174. doi: 10.1128/JB.183.4.1168-1174.2001

Masai, E., Yamamoto, Y., Inoue, T., Takamura, K., Hara, H., Kasai, D., et al. (2007). Characterization of ligV essential for catabolism of vanillin by *Sphingomonas paucimobilis* SYK-6. *Biosci. Biotechnol. Biochem.* 71, 2487–2492. doi: 10.1271/bbb.70267

Matlakowska, R., Narkiewicz, W., and Sklodowska, A. (2010). Biotransformation of organic-rich copper-bearing black shale by indigenous microorganisms isolated from lubin copper mine (Poland). *Environ. Sci. Technol.* 44, 2433–2440. doi: 10.1021/es903298t

Matlakowska, R., and Sklodowska, A. (2009). The culturable bacteria isolated from organic-rich black shale potentially useful in biometallurgical procedures. *J. Appl. Microbiol.* 107, 858–866. doi: 10.1111/j.1365-2672.2009.04261.x

Matlakowska, R., and Sklodowska, A. (2011). Biodegradation of Kupferschiefer black shale organic matter (Fore-Sudetic Monocline, Poland) by indigenous microorganisms. *Chemosphere* 83, 1255–1261. doi: 10.1016/j.chemosphere.2011.03.003

Matlakowska, R., Sklodowska, A., and Nejbert, K. (2012). Bioweathering of kupferschiefer black shale (Fore-Sudetic Monocline, SW Poland) by indigenous

bacteria: implication for dissolution and precipitation of minerals in deep underground mine. *FEMS Microbiol. Ecol.* 81, 99–110. doi: 10.1111/j.1574-6941.2012.01326.x

Meyer, F., Goesmann, A., Mchardy, A. C., Bartels, D., Bekel, T., Clausen, J., et al. (2003). GenDB - an open source genome annotation system for prokaryote genomes. *Nucleic Acids Res.* 31, 2187–2195. doi: 10.1093/nar/gkg312

Ng, S. P., Davis, B., Palombo, E. A., and Bhave, M. (2009). A Tn*5051*-like mercontaining transposon identified in a heavy metal tolerant strain *Achromobacter* sp. AO22. *BMC Res. Notes* 2:38. doi: 10.1186/1756-0500-2-38

Nieto, J. J., Ventosa, A., and Ruiz-Berraquero, F. (1987). Susceptibility of halobacteria to heavy metals. *Appl. Environ. Microbiol.* 53, 1199–1202.

Nojiri, H. (2013). Impact of catabolic plasmids on host cell physiology. *Curr. Opin. Biotechnol.* 24, 423–430. doi: 10.1016/j.copbio.2012.09.014

Oszczepalski, S. (1999). Origin of the Kupferschiefer polymetallic mineralization in Poland. *Mineral. Deposita* 34, 599–613. doi: 10.1007/s001260050222

Parkhill, J., Dougan, G., James, K. D., Thomson, N. R., Pickard, D., Wain, J., et al. (2001). Complete genome sequence of a multiple drug resistant *Salmonella enterica* serovar Typhi CT18. *Nature* 413, 848–852. doi: 10.1038/35101607

Preston, K. E., Hitchcock, S. A., Aziz, A. Y., and Tine, J. A. (2014). The complete nucleotide sequence of the multi-drug resistance-encoding IncL/M plasmid pACM1. *Plasmid* 76, 54–65. doi: 10.1016/j.plasmid.2014.08.005

Rahube, T. O., Viana, L. S., Koraimann, G., and Yost, C. K. (2014). Characterization and comparative analysis of antibiotic resistance plasmids isolated from a wastewater treatment plant. *Front. Microbiol.* 5:558. doi: 10.3389/fmicb.2014.00558

Rajpert, L., Sklodowska, A., and Matlakowska, R. (2013). Biotransformation of copper from Kupferschiefer black shale (Fore-Sudetic Monocline, Poland) by yeast *Rhodotorula mucilaginosa* LM9. *Chemosphere* 91, 1257–1265. doi: 10.1016/j.chemosphere.2013.02.022

Sambrook, J., and Russell, D. W. (2001). *Molecular Cloning: A Laboratory Manual.* New York, NY: Cold Spring Harbor Laboratory Press.

Santamaria, R. I., Bustos, P., Sepulveda-Robles, O., Lozano, L., Rodriguez, C., Fernandez, J. L., et al. (2014). Narrow-host-range bacteriophages that infect *Rhizobium etli* associate with distinct genomic types. *Appl. Environ. Microbiol.* 80, 446–454. doi: 10.1128/AEM.02256-13

Schwyn, B., and Neilands, J. B. (1987). Universal chemical assay for the detection and determination of siderophores. *Anal. Biochem.* 160, 47–56. doi: 10.1016/0003-2697(87)90612-9

Silver, S. (1996). Bacterial resistances to toxic metal ions - a review. *Gene* 179, 9–19. doi: 10.1016/S0378-1119(96)00323-X

Silver, S., and Phung Le, T. (2005a). A bacterial view of the periodic table: genes and proteins for toxic inorganic ions. *J. Ind. Microbiol. Biotechnol.* 32, 587–605. doi: 10.1007/s10295-005-0019-6

Silver, S., and Phung Le, T. (2005b). Genes and enzymes involved in bacterial oxidation and reduction of inorganic arsenic. *Appl. Environ. Microbiol.* 71, 599–608. doi: 10.1128/AEM.71.2.599-608.2005

Sklodowska, A., Matlakowska, R., and Bal, K. (2005). Extracellular polymer produced in the presence of copper minerals during bioleaching. *Geomicrobiol. J.* 22, 1–9. doi: 10.1080/01490450590922596

Slonczewski, J. L., Fujisawa, M., Dopson, M., and Krulwich, T. A. (2009). Cytoplasmic pH measurement and homeostasis in bacteria and archaea. *Adv. Microb. Physiol.* 55, 317. doi: 10.1016/S0065-2911(09)05501-5

Sobecky, P. A., and Coombs, J. M. (2009). Horizontal gene transfer in metal and radionuclide contaminated soils. *Methods Mol. Biol.* 532, 455–472. doi: 10.1007/978-1-60327-853-9_26

Speczik, S. (1994). Kupferschiefer mineralization in the light of organic geochemistry and coal petrology studies. *Geol. Q.* 38, 639–650.

Speczik, S. (1995). The Kupferschiefer mineralization of Central Europe: new aspects and major areas of future research. *Ore. Geol. Rev.* 9, 411–426. doi: 10.1016/0169-1368(94)00022-G

Stein, D. C., Chien, R., and Seifert, H. S. (1992). Construction of a *Neisseria gonorrhoeae* MS11 derivative deficient in NgoMI restriction and modification. *J. Bacteriol.* 174, 4899–4906.

Szuplewska, M., and Bartosik, D. (2009). Identification of a mosaic transposable element of *Paracoccus marcusii* composed of insertion sequence ISP*mar4* (ISA*s1* family) and an IS*1247a*-driven transposable module (TMo). *FEMS Microbiol. Lett.* 292, 216–221. doi: 10.1111/j.1574-6968.2009.01495.x

Szuplewska, M., Ludwiczak, M., Lyzwa, K., Czarnecki, J., and Bartosik, D. (2014). Mobility and generation of mosaic non-autonomous transposons by Tn*3*-derived inverted-repeat miniature elements (TIMEs). *PLoS ONE* 9:e105010. doi: 10.1371/journal.pone.0105010

Tamminen, M., Virta, M., Fani, R., and Fondi, M. (2012). Large-scale analysis of plasmid relationships through gene-sharing networks. *Mol. Biol. Evol.* 29, 1225–1240. doi: 10.1093/molbev/msr292

Tamura, K., Stecher, G., Peterson, D., Filipski, A., and Kumar, S. (2013). MEGA6: molecular evolutionary genetics analysis version 6.0. *Mol. Biol. Evol.* 30, 2725–2729. doi: 10.1093/molbev/mst197

Wheatcroft, R., Mcrae, G. D., and Miller, R. W. (1990). Changes in the *Rhizobium meliloti* genome and the ability to detect supercoiled plasmids during bacteroid development. *Mol. Plant Microbe. Inter.* 3, 9–17. doi: 10.1094/MPMI-3-009

Conflict of Interest Statement: The authors declare that the research was conducted in the absence of any commercial or financial relationships that could be construed as a potential conflict of interest.

Received: 07 January 2015; accepted: 09 February 2015; published online: 03 March 2015.

Citation: Dziewit L, Pyzik A, Szuplewska M, Matlakowska R, Mielnicki S, Wibberg D, Schlüter A, Pühler A and Bartosik D (2015) Diversity and role of plasmids in adaptation of bacteria inhabiting the Lubin copper mine in Poland, an environment rich in heavy metals. Front. Microbiol. ***6****:152. doi: 10.3389/fmicb.2015.00152*

This article was submitted to Terrestrial Microbiology, a section of the journal Frontiers in Microbiology.

frontiers in Microbiology

ORIGINAL RESEARCH
published: 30 October 2015
doi: 10.3389/fmicb.2015.01203

Microbiome composition and geochemical characteristics of deep subsurface high-pressure environment, Pyhäsalmi mine Finland

Hanna Miettinen[1], Riikka Kietäväinen[2], Elina Sohlberg[1], Mikko Numminen[3], Lasse Ahonen[2] and Merja Itävaara[1]*

[1] Valtion Teknillinen Tutkimuskeskus Technical Research Centre of Finland Ltd., Espoo, Finland, [2] Geological Survey of Finland, Espoo, Finland, [3] Pyhäsalmi Mine Oy, First Quantum Minerals Ltd., Pyhäsalmi, Finland

Pyhäsalmi mine in central Finland provides an excellent opportunity to study microbial and geochemical processes in a deep subsurface crystalline rock environment through near-vertical drill holes that reach to a depth of more than two kilometers below the surface. However, microbial sampling was challenging in this high-pressure environment. Nucleic acid yields obtained were extremely low when compared to the cell counts detected (1.4×10^4 cells mL^{-1}) in water. The water for nucleic acid analysis went through high decompression (60–130 bar) during sampling, whereas water samples for detection of cell counts by microscopy could be collected with slow decompression. No clear cells could be identified in water that went through high decompression. The high-pressure decompression may have damaged part of the cells and the nucleic acids escaped through the filter. The microbial diversity was analyzed from two drill holes by pyrosequencing amplicons of the bacterial and archaeal 16S rRNA genes and from the fungal ITS regions from both DNA and RNA fractions. The identified prokaryotic diversity was low, dominated by Firmicute, Beta- and Gammaproteobacteria species that are common in deep subsurface environments. The archaeal diversity consisted mainly of Methanobacteriales. Ascomycota dominated the fungal diversity and fungi were discovered to be active and to produce ribosomes in the deep oligotrophic biosphere. The deep fluids from the Pyhäsalmi mine shared several features with other deep Precambrian continental subsurface environments including saline, Ca-dominated water and stable isotope compositions positioning left from the meteoric water line. The dissolved gas phase was dominated by nitrogen but the gas composition clearly differed from that of atmospheric air. Despite carbon-poor conditions indicated by the lack of carbon-rich fracture fillings and only minor amounts of dissolved carbon detected in formation waters, some methane was found in the drill holes. No dramatic differences in gas compositions were observed between different gas sampling methods tested. For simple characterization of gas composition the most convenient way to collect samples is from free flowing fluid. However, compared to a pressurized method a relative decrease in the least soluble gases may appear.

Keywords: microbiome, geochemical characterization, crystalline bedrock, gas, deep subsurface, high-pressure sampling

OPEN ACCESS

Edited by:
Gary M. King,
Louisiana State University, USA

Reviewed by:
Steffen Kolb,
Friedrich Schiller University Jena, Germany
Hongchen Jiang,
Miami University, USA
Kuk-Jeong (Kuki) Chin,
Georgia State University, USA

****Correspondence:***
Hanna Miettinen
hanna.miettinen@vtt.fi

Specialty section:
This article was submitted to Terrestrial Microbiology, a section of the journal Frontiers in Microbiology

Received: *24 April 2015*
Accepted: *15 October 2015*
Published: *30 October 2015*

Citation:
Miettinen H, Kietäväinen R, Sohlberg E, Numminen M, Ahonen L and Itävaara M (2015) Microbiome composition and geochemical characteristics of deep subsurface high-pressure environment, Pyhäsalmi mine Finland. Front. Microbiol. 6:1203. doi: 10.3389/fmicb.2015.01203

INTRODUCTION

Microbial life has been observed in deep subsurface continental bedrock fractures and aquifers despite the harsh conditions in terms of energy, nutrients, pressure, and space. Nutrient and energy sources in the form of dissolved gases, solutes, or colloids are available via fracture fluids as most crystalline rocks lack extensive and continuous water-filled porosity. In a fractured rock environment, rock itself may provide a nutritional and energetic substrate to sustain minimal metabolic activity (Fredrickson and Balkwill, 2006). Microbial cells in these settings catabolize 10^4–10^6 fold more slowly than model organisms in nutrient-rich cultures and subsist with energy fluxes that are 1000-fold lower than the typical culture-based estimates of maintenance requirements (Hoehler and Jørgensen, 2013). The total number of bacteria found in groundwater ecosystems may vary by several orders of magnitude between 10^2 and 10^6 cells per mL of groundwater (Griebler and Lueders, 2009; Itävaara et al., 2011; Nyyssönen et al., 2012). The dominant bacterial and archaeal groups in different deep subsurface bedrock environments vary based on prevailing lithology and hydrogeochemistry (Nyyssönen et al., 2014; Bomberg et al., 2015). The diverse microbial communities detected in deep subsurface exploit various metabolic pathways, including nitrate, sulfate, manganase, and iron reduction, sulfur oxidation, methanogenesis, acetogenesis, and anaerobic methane oxidation (AOM) (Kotelnikova and Pedersen, 1998; Haveman et al., 1999; Hallbeck and Pedersen, 2012; Bomberg et al., 2015). In addition fungi (Pedersen, 1987) and viruses (Eydal et al., 2009) have been detected in bedrock aquifers by cultivation and DNA-based methods. Furthermore, fungal communities are suggested to be active in continental and deep subseafloor sediments (Edgcomb et al., 2010; Orsi et al., 2013), and recently, evidence of rich and active fungal communities were found in continental crystalline bedrock facture zones (Sohlberg et al., 2015).

Physical parameters influencing microbial physiology and competitiveness are temperature and pressure to which microbes need to be adapted. The increase of temperature with depth in the Fennoscandian crystalline bedrock is about 15°C per kilometer (Kukkonen, 1989). Due to the low geothermal gradient, life can potentially thrive down to several kilometers in depth in these settings. Hydrostatic pressure created by the interconnected porosity of the fracture network increases by about 100 bar per kilometer. High-pressure is not only a distinctive feature of deep subsurface environment where microbial life needs to integrate, but also makes sampling of these environments particularly challenging. While water sampling is rather straightforward, representative sampling of dissolved gases can face problems such as uncontrolled degassing and air contamination. In addition, microbial sampling has its demands depending on the method of analysis. Intact cells are needed for microscopy, RNA analysis and culturing, whereas damaged cells are applicable for DNA analysis. Contamination, the effect of pressure and sampling time also need to be controlled for.

In order to gain samples for deep biosphere studies, sampling groundwater by pumping has the advantage of yielding large volumes of water from a defined depth range, which can also be isolated by packers to abstract water from a particular fracture zone (Purkamo et al., 2013). Pressure decrease in the water line can be controlled by pumping rate, but uncontrolled gas release due to the pressure decrease can take place in the ascending water line. Deep subsurface samples at *in situ* pressure can be obtained with pressure core samplers in oceanic sediments (Reed et al., 2002; Kubo et al., 2014) and from bedrock drill holes by samplers equipped with the ability to compensate for decreasing hydrostatic pressure during sample retrieval with e.g., Positive Displacement Sampler (PDS; Regenspurg et al., 2010; Kietäväinen et al., 2013) and PAVE-samplers, pressurized water sampling system (Hatanpää et al., 2005).

In general, mines, as drained bedrock systems, have the investigational advantage that spontaneous fluid flow from drill holes made for ore exploration and evaluation is common. Thus, mines have provided an access to deep subsurface microbial ecosystems e.g., in Arctic Canada (Stotler et al., 2009; Onstott et al., 2009) and South Africa (Moser et al., 2003, 2005; Davidson et al., 2011). On the other hand, the hydrostatic pressure field around operative mines is typically disturbed, because natural and excavation related active fractures drain the surrounding bedrock.

In recent years, information on microbial communities in deep subsurface has become increasingly important as deeper parts of the bedrock are utilized in construction, for example in the case of deep storages of nuclear waste and CO_2 as well as deep mining and production of geothermal energy. However, to date, only few sites within crystalline shields have been studied for their microbial communities below 2 km depth. Pyhäsalmi mine in central Finland provides an excellent opportunity to study microbial processes in deep subsurface crystalline rock environment. In addition to being one of the deepest mines in Europe (1400 m), near-vertical drill holes starting from the deepest levels of the mine reach the depth of more than two kilometers below the surface. Furthermore, due to the surrounding high hydrostatic pressure, the risk that some portion of the high-pressure flush water will remain in fractures and contaminate the samples is clearly smaller than in drilling from the surface. In this study microbial and geochemical samples from deep extreme subsurface mine environment from prospectively uncontaminated drill holes that produce high amounts of water were taken. The objective was to explore bacterial, archaeal, and fungal communities. The geochemical aim was to compare different geochemical sampling methods in order to find the most suitable ways of collecting fluid samples from high-pressure drill holes, as well as to reveal environmental and nutritional restrictions faced by the deep biosphere. By studying the results obtained from microbial and geochemical samples, we aimed to identify potential relationships between biological and geological factors.

MATERIALS AND METHODS

Description of the Site

Pyhäsalmi Mine is situated in a volcanogenic massive sulfide (VMS) deposit, which was formed during the Paleoproterozoic

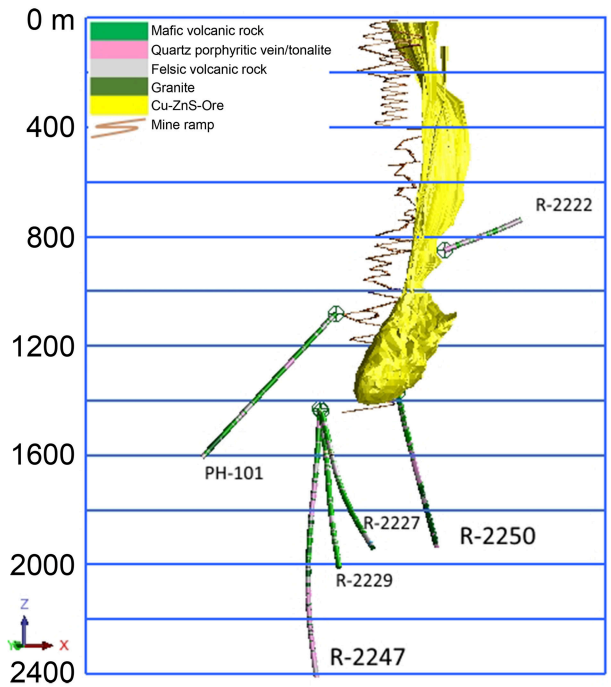

FIGURE 1 | Locations and under ground surface level depths (m) of the studied drill holes and the Pyhäsalmi ore in yellow.

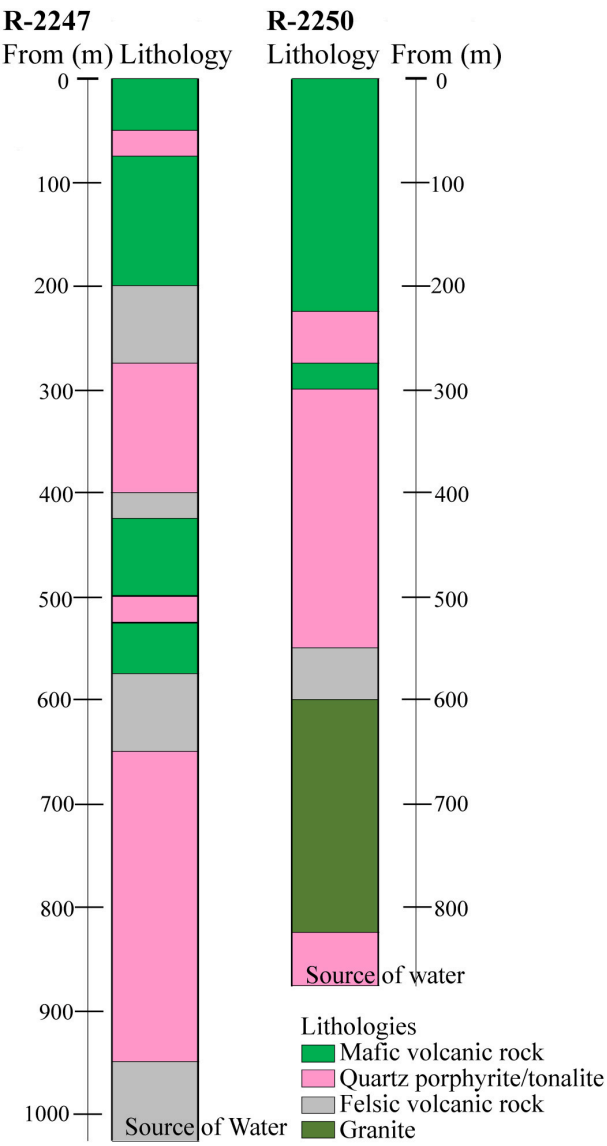

FIGURE 2 | Generalized lithologies in drill holes R-2247 and R-2250 starting from the mine levels of 1430 m and 1350 m below ground surface.

era (1.93–1.92 Ga). It is located within the Fennoscandian Shield in central Finland. The stratigraphy from the lower parts of the area is composed of felsic volcanites with tuffaceous and pyroclastic rocks. The upper part of the stratigraphy is composed of mafic massive lavas, pillow lavas, pillow breccias, and pyroclastic rocks. Related tonalitic subvolcanic intrusions are also present in the area. After formation, the Pyhäsalmi deposit was subjected to multiphase deformational history where all the formations were refolded in to an upright position (Laine et al., 2015).

The massive sulfide deposit (average grade: Cu 1%, Zn 2.5%, S 41%) is exploited for the production of copper, zinc and pyrite concentrates. The chalcopyrite, sphalerite, and pyrite containing ore is hosted by quartz-rich felsic volcanic rock. The main targets of the present study are the deep drill holes R-2250 and R-2247 drilled from 1350 and 1430 m levels below the surface (bsl), respectively (**Figure 1**). They are situated within the new deep ore body (1050–1425 m bsl) that was taken in production in 2001 and reaches a total depth of about 2000 and 2400 m bsl, respectively. The drilling method used was the common diamond drilling technique preserving a core sample of the rock, from which the rock types were determined (**Figure 2**). Flush water used in drilling was taken from a near-by Lake Pyhäjärvi. Diameters of the drill holes are 75.7 mm (R-2250) and 60.3 mm (R-2247). Additional drill holes situated at the level of 1430 m bsl (R-2227, R-2229), 1080 m bsl (PH-101) and 850 m bsl (R-2222) were also studied for geochemistry (**Figure 1**).

The drilling of both R-2250 and R-2247 was terminated because of a voluminous discharge of water from the drill hole, which exceeded the water injection pressure of the drilling machine (70 bar) and indicated that a water-conducting fracture zone was hit. The fresh drilling water was flushed out and replaced by the formation water before the drilling rods were removed and a plug was installed. The most prominent brittle tectonic feature in the area is the Oulujärvi shear zone (OSZ) (Kärki et al., 1993). It is unclear how the fracture systems that met during drilling are related to OSZ but the location (**Figure 1**) and lithologies (**Figure 2**) of the drill hole R-2250 fracture zone indicates close resemblance to it. The fracture zone perforated by the drill hole R-2247 could be evidence of an overthrust structure identified from previous seismic surveys (Laine et al., 2015). No graphite or carbonate fillings have been found in either of the fracture zones, demonstrative of a carbon-poor environment.

Geochemical Sample Collection and Analysis

Groundwater samples for detailed geochemical and microbiological analysis were collected from the drill holes R-2250 and R-2247 (**Figure 1**). Maximum pressures measured on the collars of the drill holes were 60 and 140 bar, respectively. R-2247 was sampled three times (in May and August 2013, and in June 2014) while samples from R-2250 were taken only once, in August 2013. In order to get a wider view on groundwater systematics in the mine four additional drill holes (R-2222, PH-101, R-2227, and R-2229) were studied for geochemistry. R-2222 was unplugged and was not sampled for gas composition. Samples for water stable isotopes of the drilling fluid (Pyhäjärvi lake water) were taken in February 2015.

Groundwater samples were taken directly from the free flowing fluid. Temperature, pH and electrical conductivity (EC) were measured at the site using handheld meters (WTW). Untreated groundwater samples of 500 mL each were taken for the determination of anions and alkalinity. Alkalinity was measured within the same day by titration to pH 4.5 using a digital titrator (Hach). Samples for the determination of water stable isotopes (60 mL) and cations (100 mL) were filtered (<0.45μm, Whatman FP). In addition, cation samples were acidified with ultra pure 65% HNO_3 (0.5 mL per 100 mL of water). Anions and cations were analyzed at Labtium Oy (Espoo, Finland) using ion chromatographic and spectrometric methods, respectively (Kietäväinen et al., 2013). Water stable isotopes were determined at the Geological Survey of Finland (Espoo, Finland) using a cavity ring-down spectrometer (Picarro) and reported as ‰ relative to Vienna Standard Mean Ocean Water (VSMOW). Total and dissolved organic carbon were determined from unfiltered and filtered (<0.45 μm, Whatman XP) samples (50 mL each), respectively, using a TOC analyzer at Labtium Oy. Sulfide samples were taken into 100 mL glass bottles (Winkler) and immediately fixed by adding 0.5 mL of 1 M NaOH and 0.5 mL of 1 M zinc acetate and were analyzed within 48 h at Ramboll Analytics (Vantaa, Finland) with a spectrophotometer.

Gas samples were collected in a bucket from the free flowing fluid into inverted glass bottles (Schott), which were kept under sample water, sealed with 2 cm thick black butyl rubber septa (Glasgerätebau Ochs) and closed with cut screw caps. The gas/water ratio was monitored during sampling. From the drill holes R-2247 and R-2227 gas samples were also taken by collecting the gas first into an inverted modified 1 L plastic syringe (Hamilton) and injecting it with a double-ended needle (Venoject) into evacuated glass bottles (Laborexin) sealed with blue butyl rubber septa (Bellco Glass) and aluminum open top crimp caps (Bellco Glass). A few grains of solid $HgCl_2$ were added into one of the Laborexin bottles prior to evacuation in order to provide a killed control to test if biological activity affects the gas composition during storage of untreated samples. In addition, one fluid sample from R-2247, R-2229, and R-2227 each was collected into pressure tight 500 mL stainless steel cylinders (Swagelok) that were attached directly to the collar. From the cylinders, the gas was later separated into smaller 25 or 50 mL Teflon coated stainless steel cylinders (Swagelok) in a vacuum line. Gas compositions were analyzed by gas chromatography at Ramboll Analytics or Isotech Laboratories Inc. (Illinois, USA).

Based on the determinations of groundwater and gas composition, reduction oxidation pairs [C(−4)/C(4), H(0)/H(1) and S(−2)/S(6)] were modeled at *in situ* T and pH using PHREEQC software wateq4f database (USGS, 2014).

Microbial Sample Collection

In August 2013 the groundwater from the drill holes R-2247 and R-2250 was sampled as triplicate samples for DNA and RNA study. The sample line was equipped with a pressure reduction valve (Swagelok) in order to reduce the pressure to less than 2 bar. In 2014 two microbial samples were taken from the drill hole R-2247 with a different pressure reduction system. Three pressure reduction valves (Swagelok) were used and 500 mL stainless steel pressure cylinders were installed between the first and the second, and between the second and the third reduction valves to allow some time for the sample water and microbes to recover from each pressure reduction step. The recovery times were around 15–20 s. The measured pressures during the sampling in each pressure reduction step before the actual sample collection are presented in **Table 1**. In 2013 cells in the groundwater were collected by filtration with Sterivex filter units (Millipore Corporation, USA) and in 2014 with Steripak (Millipore) 0.22 pore size filter units connected directly to the stainless steel sampling system with a sterile ¼inch NPT to a Luer connector (Adhesive Dispensing Ltd, UK) or silicon tube, respectively. Filters were immediately frozen on dry ice after sampling and stored at −80°C until use. The sample sizes are shown in **Table 1**. In 2013 samples for microbial cell counts were collected in acid-washed sterile, anaerobic 100 mL glass infusion flasks through butyl rubber septa with a sterile needle. In 2014 water was collected in sterile pressure cylinders. The pressure in the cylinders was initially 90 bar but when the inlet valve was closed the pressure dropped to 50 bar in the cylinders and as the valve between the two cylinders was closed the pressure dropped to 40 bar. The residual pressure was reduced before the cell count

TABLE 1 | Collected microbial groundwater samples from two drill holes: Sampling methods, measured pressures during sampling, and sample volumes.

Drill hole	Year	Sampling method	Pressures (bar)	Sample volume (L)
R-2250	2013	Filtration	60–2	0.5 (RNA), 1.0 (DNA)
		Head space bottle	60–1	0.1 (TNC)
R-2247	2013	Filtration	130–2	0.5 (RNA), 1.0 (DNA)
		Head space bottle	130–1	0.1 (TNC)
R-2247	2014	Filtration	130–90–60[a]-60-35-1	100 (DNA)
		Filtration	130–90[a]–60–35–1	155 (DNA)
		Pressure cylinder	130–90[a]–50–40	0.5 (TNC)

[a] *Represents a pressure drop due to gas leakage in the collar of the drill hole connection that changed during the collection. The pressure after leakage was measured every now and then and was found to be between 90 and 60 bar.*
TNC, Total number of microorganism.

analysis in the laboratory during a half hour in each of the six pressure reducing steps.

Microbiome Composition Analysis

Total Number of Cells

The total number of microbial cells (TNC) was estimated by epifluorescence microscopy based on DAPI staining. The number of microbial cells was determined by fluorescent staining with 4′,6-diamidino-2-phenylindole (DAPI) (Keppner and Pratt, 1994; Itävaara et al., 2008) from the headspace bottle and pressure cylinder waters. Two 50 mL subsamples of each groundwater sample were stained with 1 μg mL^{-1} of DAPI for 20 min at room temperature in the dark under aerobic conditions and filtered on black 0.2 μm pore-size polycarbonate membrane filters (Isopore™ Membrane filters, 0.2 μm GTBP, Millipore) with a Millipore 1225 Sampling Manifold (Millipore) using low vacuum suction. The number of cells in the sample was then calculated from 30 random microscopy fields according to the magnification factor (Olympus BX60, Olympus Optical Ltd., Tokyo, Japan and 100 × magnification). The groundwater samples from 2014 (50 mL) were also stained with Live/Dead stain (Life Technologies) according to manufacturer's instructions and the portions of live and dead cells were counted.

DNA Extraction

DNA was extracted and purified from the frozen Sterivex samples (1 L) separately from each of the triplicate samples per drill hole by aseptically breaking filter units and by cutting the filter and moving it to PowerWater DNA Isolation kit tube (MoBio Laboratiories, USA). The isolation was performed according to the manufacturer's instructions. Extracted DNA amounts were measured with a Qubit-fluorometer (Life Technologies) according to the manufacturer's instructions from 20 μL of undiluted sample.

DNA from the two Steripak filters (100 and 155 L) was separately extracted as follows. The outlet of the filter was closed with ethanol treated parafilm. 15 mL of SET-buffer (50 mM Tris-HCl, 40 mM EDTA, 0.75 M sucrose, pH 7.8) and 500 μL acid washed sterile glass beads (Sigma 150–212 μm) was added to the filter and shaken (900 r min^{-1}) for 10 min at room temperature. Lysozyme (final concentration in buffer 0.8 mg mL^{-1}) was added and the filter units were incubated for 30 min at 37°C. Proteinase K (final concentration in buffer 0.2 mg mL^{-1}) and 1 mL of 20% sodium dodecyl sulfate was added and the incubation was continued for 90 min at 65°C. The buffer liquid was drained out from the inlet and the treatment was repeated. DNA was precipitated from the combined buffer liquids by adding 95% ethanol (78 mL) and freezing at −80°C over night. The sample was thawed and DNA was centrifuged (30 min, 11.000 g). Liquid was removed and the precipitate was washed with 70% ethanol. DNA was further purified with the PowerWater DNA Isolation kit (MoBio Laboratiories). The isolated and purified DNA was stored frozen at −80°C until use.

RNA Extraction and Reverse Transcription

Total RNA from triplicate 0.5 L groundwater samples collected on the Sterivex filter units (0.22 μm pore-size) was isolated with the PowerWater RNA isolation kit (MoBio Laboratories). The filters were thawed on ice and care was taken to minimize the time of thawing. The filter units were aseptically broken and the filter membranes were removed using sterile scalpels. The intact filters were inserted into the bead tubes with flame-sterilized forceps and the RNA extraction was performed according to the manufacturer's instructions. Negative isolation controls were also included in all nucleic acid extractions. DNA contamination of the RNA extracts was checked by PCR with bacteria 16S rRNA gene specific primers U968 and U1401 (Nübel et al., 1996). If no PCR product was obtained, no DNA contamination was assumed. If a PCR product was obtained, the RNA extract was first treated with DNase (Promega) according to the manufacturer's instructions. The RNA was subsequently subjected to cDNA synthesis. Aliquots of 11.5 μL of RNA were incubated together with 250 ng random hexamers (Promega) and 0.83 mM final concentration dNTP (Finnzymes, Finland) at 65°C for 5 min and cooled on ice for 1 min. The cDNA was synthesized with the Superscript III kit (Invitrogen), by adding 4 μL 5× First strand buffer, 40 u DTT and 200 u Superscript III to the cooled reactions. To protect the RNA template from degradation, 40 u recombinant RNase inhibitor, RNaseOut (Promega), was used. The reactions were incubated at 25°C for 5 min, 50°C for 1 h and 70°C for 15 min. Duplicate reactions per sample as well as no template controls were performed. The duplicate reactions were subsequently pooled. RT-PCR was also performed on the negative RNA extraction controls as well as negative reagent RT-PCR controls to ensure that these steps had remained uncontaminated during the process.

Quantitative PCR

The abundances of bacterial 16S rRNA genes were estimated by real-time quantitative PCR (qPCR). 1 μL of DNA extract was used as template from each samples as triplicate. The qPCR was performed with KAPA™ SYBR® Fast 2× Master mix for Roche LightCycler 480 (Kapa Biosystems, USA) and triple reactions were performed for each sample. The amplifications were performed with primers P1 and P2 (Muyzer et al., 1993), which specifically target the V3 region of the bacterial 16S rRNA gene. Each reaction contained 3 pmol of each primer. The amplification was performed for 45 cycles, with denaturation (10 s at 95°C), annealing (35 s at 57°C), and extension (30 s at 72°C). The number of bacterial 16S rRNA genes was determined by comparing the amplification result (Cp) to that of a dilution series (10^1–10^7 copies μl^{-1}) of *Esherichia coli* (ATCC 31608) 16S rRNA genes in plasmid. Inhibition of PCR was tested with comparing the amplification of standard to standard with sample liquid addition (1 μL).

Amplicon Library Preparation

The amplicon libraries for high throughput pyrosequencing were prepared by PCR from the DNA and cDNA samples from 2013. Amplicons were made as duplicates from each triplicate sample. All amplicons were produced by nested PCR as follows: the bacterial 16S rRNA genes were first amplified with primers fD1 (Weisburg et al., 1991) and U1401 (Nübel et al., 1996) and then for the V1-V3 variable regions with tagged primers 8F

(Edwards et al., 1989) and P2 (Muyzer et al., 1993). Archaeal 16S rRNA gene fragments were amplified first with primers A109f (Großkopf et al., 1998) and Arch915R (Stahl and Amann, 1991) for an 806 bp long fragment of the 16S rRNA gene. Then, a second PCR with tagged ARC344f (Bano et al., 2004) and Ar774r primers (modified from Barns et al., 1994) was used to produce the tagged product for sequencing (covering the V3-V4 variable areas). For the fungal ITS fragments a 420-825 bp long fragment was first amplified with primers ITS1F and ITS4 (White et al., 1990; Gardes and Bruns, 1993). The product of this PCR was used as a template in a secondary PCR with tagged primers ITS1F and ITS2 (Buée et al., 2009) generating a ca. 400 bp product. Amplifications were also made of PCR reagent controls. The first step of PCR amplification was performed in 10 μL and second step in 50 μL reactions containing 1× KAPA Fidelity buffer (Kapa Biosystems), 0.3 mM final concentration of dNTP, 6 pmol of each primer in 10μL reaction and 25 pmol in 50 μL reaction, 1 unit of KAPA Hifi polymeraze enzyme (Kapa Biosystems) and 1μL in 10 μL reaction, and 2 μL in 50 μL reaction of template. The PCR program for both PCR steps consisted of an initial denaturation step at 98°C for 5min, 39 cycles of 20 s at 98°C, 15 s at 53°C (for archaea and fungi at 50°C), and 30 s at 72°C. A final elongation step of 5 min was performed at 72°C. The products were cleaned with NucleoSpin PCR Clean-up kit (Macherey-Nagel) according to manufacturer's instructions. The amplicon products from the six replicates of each sample were pooled and the pyrotag libraries were sent to Beckman Coulter Genomics (USA) for pyrosequencing with a Genome Sequencer FLX 454 titanium platform according to manufacturer's protocol (454 Life Sciences/Roche Applied Biosystems).

Sequence Processing and Analysis

The bacterial and archaeal sequence reads obtained from the sequencing center were batch processed with an in-house developed pipeline (Miettinen et al., 2015). Briefly, the sequence reads were first subjected to quality control using the Mothur software version 1.31.2 (Schloss et al., 2009). Adapters, barcodes and primers were removed from the reads, and the quality of base-calls was assessed in order to remove erroneous reads from the data set. Chimeric sequence reads were identified in the data set with the USEARCH algorithm (Edgar, 2010) by *de novo* detection and through similarity searches against the 97% representative OTU set of the Greengenes reference database of 13_8 version (DeSantis et al., 2006) and were removed from the analyses. Operational Taxonomic Units (OTUs) were detected from the chimera-filtered sequence data set following the open-reference OTU-picking protocol of QIIME version 1.7.0 (Caporaso et al., 2010) against the 97% identity Greengenes 13_8 OTU sets. OTU clustering was performed with UCLUST v. 1.2.22q (Edgar, 2010), and the cluster seed sequences were selected as the representative OTU sequences. OTUs with less than two members were discarded. Taxonomy was assigned with RDP classifier v. 2.2 (Wang et al., 2007).

The raw fungal ITS sequence data were analyzed as above, except that the reference database was UNITE (Kõljalg et al., 2013), and the taxonomic assignments were made by the BLAST algorithm with a maximum *E*-value of 0.001 (Altschul et al., 1990). OTUs found in bacterial and fungal negative controls were filtered from the sample data. Alpha diversity chao1 was calculated for all microorganism types (Chao, 1984).

Accession Number

The bacterial and archaeal 16S rDNA and 16S rRNA and fungal ITS gene region sequences have been submitted to the European Nucleotide Archive (ENA) under accession number PRJEB9160 (http://www.ebi.ac.uk/ena/data/view/PRJEB9160).

RESULTS

Geochemistry

A summary of the results of geochemical characterization of groundwater in the drill holes R-2247 and R-2250 at the time of microbiological sampling is given in **Table 2**. A full geochemical dataset, including the other time points and drill holes, is provided in Supplementary Tables 1 and 2.

In situ temperature at the sampling sites and of the groundwater was approximately 23°C at 1430 and 1350 m bsl. Groundwater from R-2247 was saline [total dissolved solids (TDS) up to 76 g L^{-1}] and of Ca-Na-Cl type. Water from the drill hole R-2250 was approximately 4 times more dilute, less Ca-dominated and more sulfide rich compared to R-2247. Water from the both drill holes contained 1–2 mM of sulfate. Nitrate was below detection, i.e., <0.16 and <3.2 mM in R-2247 and R-2250, respectively. Based on alkalinity and TOC measurements carbon contents were found to be low. The amount of DOC was 70–80% of the total organic carbon. Dissolved gas phase in both R-2250 and R-2247 was comprised mostly of nitrogen and helium (**Figure 3**). R-2250 also contained a significant amount of methane. CO_2 was detected only in two samples, which were either fixed with $HgCl_2$ (PYS-1B, R-2247) or collected using a pressure cylinder (PYH-2A, R-2229; Supplementary Table 2). Small amounts of oxygen were present in all other samples but the one sample pressurized from R-2247. However, based on C(–4)/C(4), H(0)/H(1), and S(–2)/S(6) redox pairs, *Eh*-values are between –0.3 and –0.4 V in both R-2247 and R-2250 indicating clearly reductive conditions. CO was not detected but small amounts of C_{2+} hydrocarbons up to pentane (C_5) were found. The amount of gas in the drill hole R-2247 in 2014 was approximately doubled compared to the same sample in August 2013. The most notable change was the increase in H_2, while relative amounts of other gases stayed relatively constant. Furthermore, He and H_2 were more enriched in the pressurized samples compared to other samples taken at the same time.

Within groundwater samples δ^2H and $\delta^{18}O$ vary from −96.8 to −69.8‰ VSMOW and −13.70 to −11.96‰ VSMOW, respectively (Supplementary Table 1). Isotopic composition of the most saline water (R-2247) plots clearly left from the Finnish Meteoric Water Line (FMWL, Kortelainen 2007) while groundwaters sampled from the shallower levels of –1080 m (PH-101) and –850 m (R-2222) feature compositions typical for meteoric, fresh groundwater (**Figure 4**). Both compositions are clearly distinct from the lake water used for drilling with δ^2H of −73.3‰ VSMOW and of $\delta^{18}O$ of −9.33‰ VSMOW.

TABLE 2 | Geochemistry of groundwater in the drill holes R-2247 and R-2250 in the Pyhäsalmi mine.

Drill hole		R-2247	R-2247	R-2250
Sampling date		13.8.2013	11.6.2014	14.8.2013
pH		8.6	8.7	8.8
EC	mS cm^{-1}	103.3	102.0	34.0
Alk.	mM	0.09	0.08	0.09
TOC	mM	0.092		0.117
DOC	mM	0.066		0.085
Ca	mM	565	488	119
Fe	mM	0.0024	<0.0009	0.0006
K	mM	0.83	0.97	0.14
Mg	mM	0.14	0.13	0.04
Na	mM	324	320	112
P	mM	0.005	0.004	0.003
S	mM	1.23	1.30	1.16
Si	mM	0.14	0.10	0.18
Sr	mM	3.06	3.02	0.61
Br	mM	7.48	6.65	2.17
Cl	mM	1272	1097	285
SO_4	mM	1.78	1.58	1.23
Sulfide	mM	0.0023	0.0020	0.057
TDS	g L^{-1}	76.2	66.9	17.7
Gas_{tot}	mL L^{-1}	56	119	60
Ar	mL L^{-1}	0.58	1.06	0.40
O_2	mL L^{-1}	0.31	0.40	0.19
N_2	mL L^{-1}	39	73	26
H_2	mL L^{-1}	0.10	9.0	0.74
He	mL L^{-1}	14	30	19
CH_4	mL L^{-1}	1.6	3.9	14
C_2H_6	mL L^{-1}	0.24	0.46	0.08
C_3H_8	mL L^{-1}	0.007	0.014	0.002
Iso-butane	mL L^{-1}		0.0002	
N-butane	mL L^{-1}		0.0012	
N-pentane	mL L^{-1}		0.00012	

EC, electrical conductivity; Alk, alkalinity; TOC, total organic carbon; DOC, dissolved organic carbon; TDS, total dissolved solids.

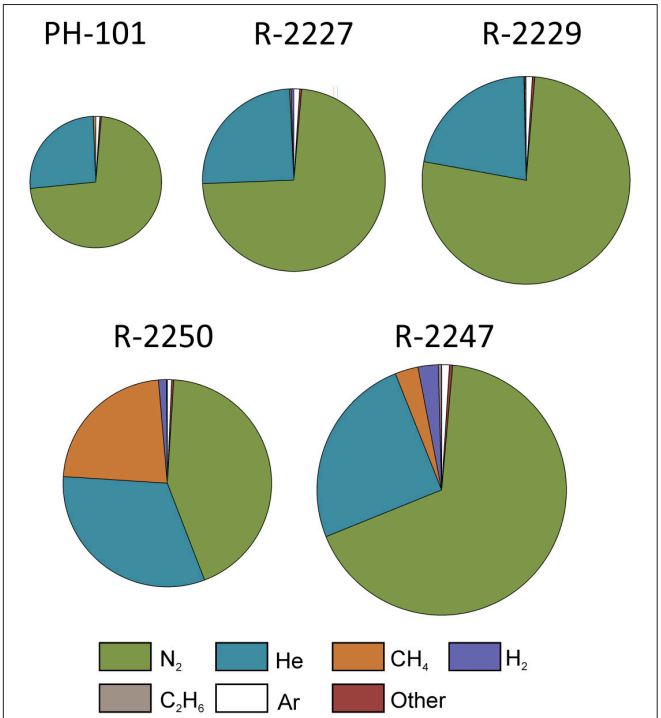

FIGURE 3 | Relative compositions of dissolved gases in the drill holes sampled in the Pyhäsalmi mine. Areas of the charts are proportional to the average gas volumes measured in each of the drill holes, with the largest chart (R-2247) corresponding to a gas volume of 90 mL per 1 L of groundwater. Other gases include O_2, CO_2, propane, butane, and pentane (Supplementary Table 2).

Microbiology

Microbial cells could not be detected in the water samples from 2013 by microscopy. Only some blurred stains were visible that could not be identified as cells. In 2014 the number of microbial cells detected in the groundwater by microscopy was 1.4×10^4 cells mL^{-1} at R-2247 (drill hole bottom at ~2400 m bsl) from the pressure cylinder groundwater stained with DAPI. The amount of live cells determined with Live/Dead staining was 1.2×10^4 cells mL^{-1} and the injured cell count was 1.5×10^2 cells mL^{-1}.

The amount of isolated DNA from both of the drill holes (2013; 1 L samples) was less than 0.05 ng. In 2014 the total isolated DNA amount from 100 and 155 L groundwater was 1.1 and 1.3 ng, respectively. Even though more DNA was obtained from the samples from 2014 compared to those from 2013, no PCR product was obtained from the 16S rRNA gene qPCR in either year. However, no PCR inhibition was seen. As 16S rRNA qPCR was not successful no other qPCRs were performed for marker genes. Amplicon sequencing analysis targeting the bacterial and archaeal 16S ribosomal genes and fungal internal transcribed spacer (ITS) gene region were done with the nested PCR products of the year 2013 samples. As no products were obtained from the year 2014 samples with 16S rRNA gene qPCR, the samples were considered not to represent the original drill hole diversity any better than the year 2013 samples and no high-throughput amplicon sequencing analysis was performed on these samples.

Bacterial and archaeal 16S rRNA gene sequences were obtained from all samples. Most of the sequences were obtained from the shallower drill hole R-2250, consisting of around 3000 archaeal sequences from both DNA and RNA fractions but less than a thousand sequences were obtained from each bacterial amplicon library (Supplementary Table 3). From the deeper drill hole R-2247 the sequence amounts from each sample (<138 sequences) serve only as an exemplary of the drill hole prokaryotic diversity. Fungal sequences dominated in both drill hole samples (over 11,700 sequences from each sample type). Rarefaction curves from all samples with more than 300 sequences are presented in Supplementary Image 1. Different operational taxonomic unit (OTU) counts were lowest in the case of archaea (<7 OTUs) and the highest number of OTUs was found in deeper R-2247 fungal DNA fraction (77 OTUs).

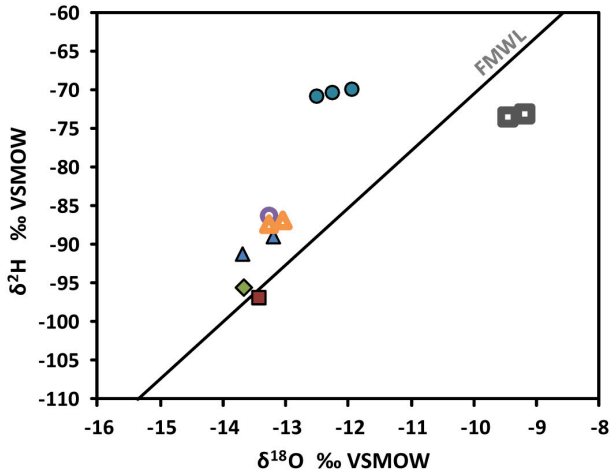

FIGURE 4 | Stable isotope compositions of groundwaters in the Pyhäsalmi mine. Values are given in ‰ relative to Vienna Standard Mean Ocean Water (VSMOW). FMWL, Finnish Meteoric Water Line (Kortelainen, 2007) depicts the average composition of precipitation in Finland. Most of the samples plot left from the FMWL. This is typical for deep saline groundwaters within crystalline rocks, which have been modified by water-rock interaction (e.g., Frape et al., 2003). Circles = R-2247, open circle = R-2250, triangles = R-2227, open triangles = R-2229, diamond = PH-101, square = R-2222, open squares = drilling water from Lake Pyhäjärvi.

The bacterial, archaeal, and fungal community compositions are shown in **Figure 5**.

Bacterial diversity was low and the highest number of detected OTUs was only 45 OTUs found from R-2250 with 946 sequences. The sequences found in all samples grouped into three phyla: Proteobacteria, Firmicutes, and Cyanobacteria (**Figure 5**). All samples included also unidentified bacterial sequences especially in the RNA fraction describing a potentially active community (20–38% of the sequences). In both drill holes the DNA fraction describing the total community was dominated by sequences affiliating with the phyla Firmicutes and Proteobacteria. The majority of the bacterial 16S rRNA sequences (63 and 42%) were classified to genus *Alicyclobacillus* of the phylum Firmicutes in both R-2250 and R-2247, respectively. The bacterial diversity detected from the RNA fraction was higher than that of the DNA fraction in R-2250. The sequence reads belonged especially to Gammaproteobacteria (44%) and Firmicutes (13%) lineages. The Solimonadaceae (39%) was the most abundant separate family.

The archaeal diversity was very low. The number of sequences (5) found from R-2247 does not describe any real diversity in this sample. In R-2250 sample the sequencing depth seemed to be sufficient (over 3000 sequences in each sample) as the rarefaction curve stabilized and the chao1 estimate was the same as the actual number of identified OTUs (Supplementary Image 1 and Supplementary Table 3). However, the archaeal diversity was very low as only 4 and 6 OTUs were found in DNA and RNA fractions, respectively. These OTUs belonged to three euryarchaeotal orders: Methanobacteriales, Methanosarcinales, and Thermoplasmata and one OTU to crenarchaeotal MCG class. The majority of the archaeal sequences belonged to the order Methanobacteriales.

Fungal diversity detected from the DNA fraction was highest in R-2247 with 77 OTUs identified. In R-2250 28 OTUs were detected in the DNA fraction and 13 OTUs in the RNA fraction. The sequencing efficiency was appropriate for the fungal communities as the number of detected OTUs was close to the chao1 estimated OTU numbers (Supplementary Table 3). Ascomycota was the dominating fungal phylum detected in both of the drill holes (**Figure 5**). The dominating ascomycotal class was Eurotiomycetes (67 and 98%) in DNA fraction in both of the drill holes. These OTUs related most closely to genera *Penicillium* and *Aspergillus*. Sequences similar to the fungal class Dothideomycetes (7%) were detected in R-2247 in the total fungal community. Basidiomycota constituted the minor fungal phylum detected in the R-2247 DNA fraction (5%). Basidiomycota sequences belonged to Microbotryomycetes and more specifically *Rhodosporidium*-like yeasts. 17% of the sequences in the DNA fraction of the R-2250 were identified to represent other fungal phylotypes. However, their exact phylogenetic affiliation remains elusive. In the active fungal community of both of the drill holes most of the fungal sequences were similar to ascomycotal class Sordariomycetes and more closely to genus *Nectria*. In R-2250 in the RNA fraction also fungal sequences belonging to ascomycotal class Eurotiomycetes and to genus *Paecilomyces* were found.

DISCUSSION

Geochemical Aspects on Representativeness and Limits of the Deep Biosphere

Deep fluids from the Pyhäsalmi mine have several features in common with other deep Precambrian continental subsurface environments (e.g., Nurmi et al., 1988; Frape et al., 2003): they are saline, Ca-dominated and have water stable isotope compositions left from the meteoric water line. Even though the dissolved gas phase is dominated by nitrogen, the gas composition clearly differs from the atmosphere. These features may indicate long-term water-rock interactions. Estimated residence times of saline fluids within the Fennoscandian Shield vary between 4 and 60 Ma (Kietäväinen et al., 2014; Trinchero et al., 2014). High concentrations of helium likely indicate similar residence times of the saline groundwaters also analyzed in our study. Even though we cannot exclude other sources due to a lack of information on the isotopic composition of helium, it is likely that this helium originates from long-term accumulation due to radioactive decay of U and Th in the crust (e.g., Ballentine et al., 2002). No mantle helium was detected from the 2.5 km deep Outokumpu Deep Drill Hole located within the Precambrian bedrock some 160 km SE from the Pyhäsalmi mine in a similar tectonic setting (Kietäväinen et al., 2014).

Small amounts of oxygen detected in the gas samples likely originate from atmospheric contamination during sampling or analysis. This is because no O_2 could be found in the pressure cylinder sample collected from R-2247. This sampling technique does not include any injection of sample into sample container or

Taxon Bacteria	R-2250 DNA	R-2250 RNA	R-2247 DNA	R-2247 RNA
Bacteria;Other	1.1	37.6	3.0	20.0
Cyanobacteria; Nostocophycideae; Nostocales	5.6	0	0	0
Firmicutes; Bacilli; Bacillales; Alicyclobacillaceae; Other	2.6	0	0	0
Firmicutes; Bacilli; Bacillales; Alicyclobacillaceae; Alicyclobacillus	62.8	0	42.4	0
Firmicutes; Bacilli; Lactobacillales; Lactobacillaceae; Lactobacillus	0	13.2	0	0
Proteobacteria; Other	0	2.0	0	0
Proteobacteria; Alphaproteobacteria; Other	0	0.2	0	13.3
Proteobacteria; Alphaproteobacteria; Rhizobiales; Other	0	0.8	1.5	0
Proteobacteria; Alphaproteobacteria; Rhizobiales; Bradyrhizobiaceae	5.6	1.3	0.8	0
Proteobacteria; Alphaproteobacteria; Rhizobiales; Brucellaceae; Pseudochrobactrum	0	0	2.3	0
Proteobacteria; Alphaproteobacteria; Rhizobiales;Methylobacteriaceae; Methylobacterium	1.1	0	0	0
Proteobacteria; Alphaproteobacteria; Rhizobiales; Rhizobiaceae; Agrobacterium	7.9	0.3	0	6.7
Proteobacteria; Alphaproteobacteria; Sphingomonadales; Sphingomonadaceae	0.8	0.2	0.8	0
Proteobacteria; Betaproteobacteria; Burkholderiales; Other	0.8	0.2	0	0
Proteobacteria; Betaproteobacteria; Burkholderiales; Comamonadaceae; Other	0	0	2.3	0
Proteobacteria; Betaproteobacteria; Burkholderiales; Comamonadaceae; Comamonas	0	0	3.8	0
Proteobacteria; Betaproteobacteria; Burkholderiales; Comamonadaceae; Delftia	0.4	0	0.8	46.7
Proteobacteria; Betaproteobacteria; Burkholderiales; Oxalobacteraceae	6.4	0.4	0.8	13.3
Proteobacteria; Gammaproteobacteria; Other	0	0.6	2.3	0
Proteobacteria; Gammaproteobacteria; Pseudomonadales; Moraxellaceae; Other	0	0	3.8	0
Proteobacteria; Gammaproteobacteria; Pseudomonadales; Moraxellaceae; Acinetobacter	4.9	0	2.3	0
Proteobacteria; Gammaproteobacteria; Pseudomonadales; Moraxellaceae; Enhydrobacter	0	0	32.6	0
Proteobacteria; Gammaproteobacteria; Pseudomonadales; Pseudomonadaceae	0	2.4	0	0
Proteobacteria; Gammaproteobacteria; Xanthomonadales: Other	0	1.5	0	0
Proteobacteria; Gammaproteobacteria; Xanthomonadales; Solimonadaceae; Other	0	38.8	0.8	0
Proteobacteria; Gammaproteobacteria; Xanthomonadales; Solimonadaceae; Nevskia	0	0.2	0	0
Proteobacteria; Gammaproteobacteria; Xanthomonadales; Xanthomonadaceae	0	0.2	0	0

Taxon Archaea	R-2250 DNA	R-2250 RNA	R-2247 DNA	R-2247 RNA
Crenarchaeota; MCG	0.0	0.1	0.0	0.0
Euryarchaeota; Methanobacteria; Methanobacteriales; MSBL1; SAGMEG-1	100.0	99.6	75.0	0.0
Euryarchaeota; Methanomicrobia; Methanosarcinales; ANME-2D	0.0	0.2	0.0	0.0
Euryarchaeota; Thermoplasmata; E2; TMEG	0.0	0.1	25.0	100.0

Taxon Fungi	R-2250 DNA	R-2250 RNA	R-2247 DNA	R-2247 RNA
Ascomycota; Dothideomycetes; Capnodiales; Mycosphaerellaceae; Cercospora	0.0	0.0	6.9	0.0
Ascomycota; Dothideomycetes; Capnodiales; Mycosphaerellaceae; unidentified	1.6	0.0	0.0	0.0
Ascomycota; Eurotiomycetes; Eurotiales; Trichocomaceae; Aspergillus	2.0	0.0	8.4	< 0.1
Ascomycota; Eurotiomycetes; Eurotiales; Trichocomaceae; Byssochlamys	0.0	0.0	0.5	0.0
Ascomycota; Eurotiomycetes; Eurotiales; Trichocomaceae; Paecilomyces	0.0	19.2	0.0	0.0
Ascomycota; Eurotiomycetes; Eurotiales; Trichocomaceae; Penicillium	95.7	0.0	59.9	0.1
Ascomycota; Sordariomycetes; Hypocreales; Nectriaceae; Nectria	0.1	80.7	0.0	99.8
Ascomycota; Sordariomycetes; Xylariales; Xylariaceae; Xylaria	0.6	0.0	2.1	0.0
Basidiomycota; Microbotryomycetes; Sporidiobolales; Incertae_sedis; Rhodosporidium	0.0	0.0	3.8	0.0
Basidiomycota; Microbotryomycetes; Sporidiobolales; Incertae_sedis; Rhodotorula	0.0	< 0.1	0.0	0.0
Basidiomycota; Ustilaginomycetes; Ustilaginales; Ustilaginaceae; Pseudozyma	0.0	0.0	1.6	0.0
Chytridiomycota; Chytridiomycetes; Rhizophydiales; unidentified	< 0.1	0.1	0.0	0.0
Unidentified	< 0.1	0.1	16.8	0.1

Relative abundance (%)
0
50
100

FIGURE 5 | Bacterial, archaeal, and fungal taxonomy in deep groundwaters of the Pyhäsalmi mine in drill holes R-2247 and R-2250. Taxonomic classification of the bacterial, archaeal, and fungal sequence reads obtained by high throughput sequencing of the total (DNA) and potentially active (RNA) communities presented at the genus level.

analysis line, which clearly decreases the risk of contamination. However, not all pressure cylinder samples were O_2 free. Further evidence of strictly anaerobic conditions is brought by reduction oxidation pairs of carbon, hydrogen and sulfur, which give negative values down to −0.4 V, indicative of clearly reductive conditions. The hydrogen pair gives the most negative values, which could be related to the mobility of H_2 in the system and thus redox disequilibrium within the samples.

It was observed that gases with the lowest solubility, i.e., H_2 and He, were preferably found in the pressurized samples. This is likely an indication of escape of these gases during sampling from free flowing fluid. However, it may also be due to partial degassing and preferential enrichment of less soluble gases during gas separation from the pressure cylinders. Variability in the concentration of H_2 between different samplings can also be explained in terms of solubility as H_2 is easily enriched if there is a gas pulse. Such a gas pulse might be caused by a pressure drop within the formation. In a mine environment this may include opening of fractures due to blasting and drilling operations. These operations might also trigger chemical reactions between freshly crushed rock and water, releasing H_2 (Kita et al., 1982; Hirose et al., 2011). Episodic release of H_2 from fracture networks has been proposed to provide energy for deep microbial communities within crystalline shields (Sherwood Lollar et al., 2007). H_2 can accumulate into sealed pockets within crystalline bedrock as a result of radiolysis of water (Lin et al., 2005a,b) or through reactions including oxidation of Fe(III)hydroxides (e.g., Mayhew et al., 2013). Due to the co-existence of H_2 with high

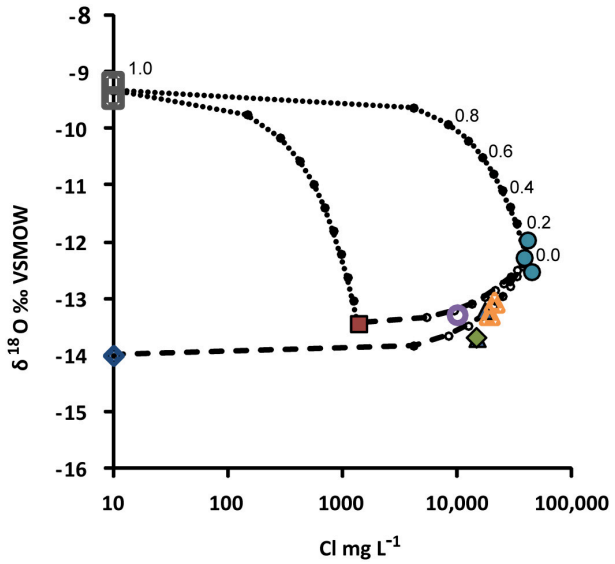

FIGURE 6 | Mixing model for groundwaters collected from the Pyhäsalmi mine. The model is based on oxygen isotopic composition of water ($\delta^{18}O$ ‰ Vienna Standard Mean Ocean Water, VSMOW) and salinity (represented by the concentration of Cl). End-members used are (1) drilling water (open squares), (2) deep saline formation water (R-2247, circles), (3) shallow groundwater (R-2222, square), and (4) approximated composition of local precipitation/fresh groundwater (open diamond). Due to the semi-logarithmic scale, simple two-component mixing appears as a curve in this plot. Mixing of drilling water with the end-members (2) and (3) is illustrated by the dotted lines, and mixing with the end-member (2) with (3) and (4) is shown by the dashed lines. Proportions of the end-members are indicated by small circles, as exemplified for the mixing between (1) and (2). Composition of groundwater from the drill hole R-2250 (open circle) can be explained by mixing of the end-member (2) with either (3) or (4), with the proportion of saline formation water around 0.2 or 0.3 i.e., 20 or 30%, respectively, without significant mixing with drilling water. Symbols are as in **Figure 4**.

amounts of most likely radiogenic helium, the radiolytic origin seems more probable for H_2 in the Pyhäsalmi mine.

Despite the carbon poor conditions indicated by the lack of carbon-rich fracture fillings and only minor amounts of dissolved carbon detected in the formation waters, some methane was found especially in the drill hole R-2250 (**Table 2**). There a surface driven, more carbon-rich groundwater may mix with deep sourced H_2-rich formation water (**Figure 6**) producing methane either through microbial metabolism or abiotically. Microbial involvement may be substantiated by the presence of CO_2 in the $HgCl_2$ treated sample, but not in the comparative samples. However, more data would be needed to confirm this relationship.

Compared to natural variability, no dramatic differences were observed between the different gas sampling methods. Thus, for a simple characterization of gas composition the most convenient way to collect samples is from a free flowing fluid. However, changes may appear in the amounts of the least soluble gases as discussed above. Drawbacks of the pressurized method include the laborious separation of gas from the sample cylinder and the relatively small sample volume obtained. In addition, quantitative gas separation still needs to be confirmed. Nevertheless, dissolved gas phase forms the most interesting part of the fluid geochemistry in terms of availability of energetic compounds in deep subsurface environments.

Microbial Diversity

The bacterial 16S rRNA gene diversity was low and only describes the most abundant species or the cells most resistant to the decompression. Despite the low sequence counts the diversities in the total community of the drill holes R-2247 and R-2250 were quite similar. The dominating OTU was a sequence similar to the Firmicutes genus *Alicyclobacillus*. Representatives of this genus inhabit mostly acidic geothermal environments (Imperio et al., 2008) and a few strains of *Alicyclobacillus* are known to reduce nitrate to nitrite and some strains also reduce Fe^{3+} (Da Costa and Rainey, 2009). *Alicyclobacillus* are spore-forming, which may explain its abundant presence due to better decompression tolerance. In addition, alphaproteobacterial orders Rhizobiales and Sphingomonadales, betaproteobacterial order Burkholderiales, and gammaproteobacterial order Pseudomonadales sequences were frequently found in the DNA fractions of both samples. These lineages are often found in deep subsurface terrestrial aquifers (Moser et al., 2003; Itävaara et al., 2011; Nyyssönen et al., 2014). A small portion of the sequences (6%) in R-2250 was similar to Cyanobacteria and was further grouped to order Nostocales. Low numbers of sequences belonging to the Cyanobacteria have previously been reported from deep extreme environments (Kormas et al., 2003; Bomberg and Itävaara, 2013), however their presence as photosynthetic bacteria in the deep dark subsurface seems unclear and their role is not known.

The diversity of the potentially active community was higher than that of the community detected from the DNA fraction in the shallower drill hole R-2250 (**Figure 5**). There were especially sequences similar to Gammaproteobacteria (44%) and Firmicutes (13%), the gammaproteobacterial Solimonadaceae (39%) being the most abundant separate lineage. Members of the Solimonadaceae are usually associated with soil and freshwater and described for their ability to decompose chemical pollutants (Zhou et al., 2014). The RNA fraction of the sample from R-2247 yielded only few sequences of which most grouped with betaproteobacterial *Delftia* genus. Similar sequences have been found from river estuary sediment in southern China (GenBank accession EU880508.1) and saline hydrothermal water in a Mexican mine (Ragon et al., 2013).

Archaeal sequences obtained in the deeper drill hole R-2247 identify only a few species likely present in this environment and give a hint that there might be more archaea to be found. In R-2250 the sequencing was more successful but again only a portion of the diversity was detected as the initial DNA and RNA amounts were small. The majority of the archaeal sequences belonged to the Euryarchaeota while a low number of crenarchaeotal sequences were detected only in R-2250 (**Figure 5**). Almost all sequences from R-2250 DNA and RNA fractions and also in R-2247 DNA fraction belonged to the Methanobacteriales order, which are generally hydrogenotrophic and use H_2 to reduce CO_2 to CH_4 (Bonin and Boone, 2006). These sequences were

further affiliated within the SAGMEG1 (South African Cold Mine Euryarchaeal Group 1) group that was first detected in deep South African gold mines (Takai et al., 2001). The first of the two additional rare euryarchaeal groups found from R-2250 RNA fraction was similar to the Methanomicrobia class and was further grouped with the anaerobic methane oxidizing ANME-2D family. The second rare sequence type was similar to the Thermoplasmata and belonged to the E2 order, which is known to associate with anoxic environments and includes methanogens (Yashiro et al., 2011).

More fungal than bacterial and archaeal OTUs were detected in the deeper R-2247 drill hole (82 and 21 OTUs in DNA and RNA fractions, respectively). Moreover, the fungal diversity was higher in R-2247 than in R-2250 contrary to the bacterial and archaeal diversities. Similar or higher fungal diversity (7–163 OTUs) have been detected in the Fennoscandian deep subsurface groundwater in several drill holes using the same 454 pyrosequencing method for fungal ITS regions as used here (Sohlberg et al., 2015), and up to 43 fungal OTUs in deep-sea environments have been detected by sequencing clone libraries constructed with three different primer sets of the fungal ITS gene region (Nagano et al., 2010). The dominating fungal class in the total community of both of the drill holes was Eurotiomycetes and these sequences were most closely related to *Penicillium* and *Aspergillus*. These fungi are known to be ubiquitous and cosmopolitan and function in virtually all ecosystems. They have been detected in deep-sea environments where they were found to be adapted to the aquatic environment (Damare and Raghukumar, 2008) and to tolerate high salt concentrations and anaerobic conditions (Raghukumar, 2012) that also prevail in the Pyhäsalmi mine bedrock. Another abundant sequence type found from the total community of the drill hole R-2247 was affiliated with the class Dothideomycetes and was closely related to the genus *Cercospora*. Species within the *Cercospora* act as parasites of plants and are globally distributed and spores of *Cercospora* are easily aerosolized (Kellogg and Griffin, 2006). Their role in deep terrestrial groundwater is unknown. The total community in R-2247 also included fungal sequences similar to the Basidiomycota phylum, which is closely related to the genera *Rhodosporidium* and *Pseudozyma*. *Rhodosporidium* is the sexual state of several species of *Rhodotorula*. The genus *Rhodotorula* is thought to be of polyphyletic origin and is phylogenetically a mixed grouping with the genus *Rhodosporidium* (Nagahama et al., 2001). These yeasts have been previously detected with cultivation-based methods from groundwaters within Fennoscandian crystalline rocks (Ekendahl et al., 2003) and from deep-sea environments (Nagahama et al., 2006). Both *Rhodosporium*- and *Pseudozyma*-species have been detected in deep-sea environments (Nagahama et al., 2001) and brackish and sea water environments (Fell et al., 1988). Interestingly, *Rhodosporium*—species have been able to grow at as high as 400 bar pressure (Lorenz and Molitoris, 1997).

In the active community the dominant fungi belonged to the class Sordariomycetes (81–99%) and more closely to the genus *Nectria* in both of the drill holes. The Nectricea includes facultative anaerobic microscopic fungal genera able to use nitrate or nitrite as a final electron acceptor as an alternative to oxygen (Kurakov et al., 2008). In terrestrial environments they act as parasites of plants and are saprophytes. Their origin and role in the deep terrestrial environment is unknown although *Nectria* -species have been isolated from deep-sea sediments (Singh et al., 2012). The active community in the shallower drill hole also has a smaller amount (19%) of sequences grouping with the class Eurotiomycetes and further classified to genus *Paecilomyces*. *Paecilomycetes*—species have been isolated from marine sediments. They have been found to be capable of growing in anoxic conditions and to perform denitrification (Cathrine and Raghukumar, 2009). Overall, the dominant fungal taxa found both in the DNA and RNA fractions were also detected abundantly in a study from Fennoscandian Shield crystalline bedrock in Olkiluoto, Finland (Sohlberg et al., 2015). This indicates that these fungal classes could be characteristic to the deep terrestrial biosphere.

This study performed in the Fennoscandian Shield crystalline bedrock, with groundwater samples from 2.4 km below the ground surface level with high salinity (TDS up to 76 g L^{-1}) and especially high calcium and magnesium concentrations (22 and 0.4 g L^{-1}, respectively), found the bacterial taxa *Alicyclobacillus* genus and Solimonadaceae that are not found as dominant bacterial groups in the Fennoscandian Shield bedrock studies earlier. The fungal taxa identified here provide further evidence for the fungal core microbiome detected recently from the Fennoscandian Shield bedrock (Sohlberg et al., 2015). In addition, the fungal genus *Cercospora* was detected. To the best of our knowledge, this genus has not been found in either deep subsurface bedrock or sediment environments before.

Microbial Sampling in High-pressure Environment

The microbiological results of the first sampling session were surprising as no recognizable microorganisms were microscopically detected. In addition, very low DNA and RNA amounts were obtained from the groundwater filtration samples and microbial communities could only be detected with a nested PCR approach. It is possible that the abrupt pressure drop of 58 or 128 bar during sampling may have ruptured at least a part of the microbial cells and therefore the nucleic acids could escape through the filters. Hemmingsen and Hemmingsen (1980) have shown that fast (1–2 s) decompression from gas saturation pressures (25–50 bar) ruptured cell envelopes and decreased the counts of viable cells of three different species of Gram negative gas vesicle containing bacteria. Pressure drops between 50 and 100 bar ruptured the majority of these cells, however cells that did not have gas vesicles were not affected by decompression from gas saturation pressures of up to 300 bar (Hemmingsen and Hemmingsen, 1980). However, the cell envelope can be ruptured regardless of whether a membrane-enclosed vacuole is present as was seen in the case of a deep-sea methanogen *Methanococcus jannaschii* that ruptured upon rapid decompression (1 s) from 260 bar of hyperbaric pressure to atmospheric pressure (Park and Clark, 2002). To avoid this possible reason for the low nucleic acid yield we added two pressure-decreasing steps for the second sampling session. In practice altogether four pressure-reduction steps occurred as the drill hole's first joint started to leak during the microbiological sampling and gases were partly escaping

which caused a pressure drop estimated to be as high as 40–70 bar. We also included some time difference between the pressure reductions by placing cylinders between the pressure reduction points.

In addition to having a better control of the pressure, we wanted to maximize the amount of harvested microorganisms from groundwater with extremely low microbial counts by collecting larger sample volumes. Thus, we used Steripak filter units that are designed for pressure driven tissue media filtration but are substantially faster and have bigger filtration capacity than that of the small Sterivex filters. However, the filters cannot be cut out from the Steripak filter unit and moved to commercial extraction kits. Instead, the microbial cells need to be released and lysed to the liquid phase inside the intact filter unit. To ensure that we would get at least a confirmation that there really were microorganisms present in the Pyhäsalmi mine groundwater, we took a small water sample without the harsh pressure decrease procedure into a pressure cylinder and lowered the residual pressure with small steps in the laboratory. The microbial cell count from this pressure cylinder was 1.4×10^4 cells mL^{-1} (DAPI) with 1.2×10^4 live cells mL^{-1} (Live/Dead) from the R-2247 drill hole. The injured cells were a minority (1.5×10^2 cells mL^{-1}). This cell count is consistent with the average cell counts from this depth of groundwater (McMahon and Parnell, 2013) and is 10-fold higher than that detected from 2.3 km depth from the Outokumpu Deep Drill Hole (Purkamo et al., 2013; Nyyssönen et al., 2014). This also confirms that microorganisms are present in the deepest groundwater of the Pyhäsalmi mine.

Another reason for the low DNA and RNA amounts isolated might be the filter breakage during sampling. However, this seems unlikely as the maximum inlet pressure for both used filter types is over 3 bar, according to the manufacturer, and during sampling the pressures were mainly 1 bar and at most 2 bar. A more probable cause for the low DNA and RNA extraction amount could be inhibitory substances within the filtered groundwater, as the water was very saline with a calcium concentration over 20 g L^{-1}. Both microbial cells and nucleic acids tend to have high adsorption on soil components (Frostegård et al., 1999). This may be especially relevant if part of the cells were damaged during collection and nucleic acids became susceptible to environmental conditions. The adsorption of nucleic acids to surface-reactive soil fractions such as mineral matrixes can result in low extraction yields (Direito et al., 2011). The filters collecting samples overnight were turned from white to gray and almost black throughout indicating particle accumulation and/or chemical reactions occurring on the filter surface. Especially in clay silicates (Direito et al., 2011) and iron rich clays, DNA and RNA yields can be minimal or absent, primarily due to nucleic acid adsorption (Hurt et al., 2014). The polyanionic property of the phosphate groups of the nucleic acids support a large number of binding sites for divalent or multivalent cations that further bind to negatively charged mineral particles (Hurt et al., 2014). The effect of mono- or divalent cations has also been shown to be dependent on the species of cation species, with a greater adsorption of DNA in the order of Ca^{2+}, Mg^{2+} and Na^{+} (Paget et al., 1992; Nguyen and Elimelech, 2007). The Pyhäsalmi mine groundwater contained a high concentration of Na^{+} and especially Ca^{2+}. It is probable that at least part of the DNA was bound to mineral particles due to presence of high Ca^{2+} concentration. To prevent DNA adsorption supported by cations, chelating agents removing metal ions from aqueous solutions, are often incorporated into the lysis buffer. The extraction method used for Steripak filters included some chelating EDTA in the lysis buffer but more attention could have been paid to desorption of DNA from the solid particles. The commercial isolation kit used was functioning in terms of purification as no PCR inhibition was found. However, efficient purification is again a source of decreased DNA yield.

There were probably several reasons for the very low nucleic acid gain as described above. However, the most probable reason for this was the strong pressure drop causing rupture of at least part of the cells and nucleic acid drift through the sampling filters. This is supported by the fact that no whole cells were seen by microscopy in decompressed water sample compared to clear cells seen in water collected into pressure cylinder without harsh decompression. In addition higher sequence counts were obtained from the drill hole R-2250 than from R-2247 as the pressure drop during sampling in R-2250 was half of that compared to the deeper R-2247.

Microbial Contamination of Drill Holes

In the Pyhäsalmi mine the possible microbial contamination of the drill hole waters has to be considered as the drill holes were plugged and not continuously flowing after drilling. Contamination due to drilling water is relevant especially in R-2250 as it was newly drilled. However, the high hydrostatic pressure in the drill hole caused by the depth, and the voluminous discharge of groundwater encountered during drilling, decrease the risk of microbial contamination. R-2247 was drilled more than a year prior to our sampling and it had been allowed to flow freely for about a month before it was plugged and the water flow amount was estimated to be around 500 m^3, equivalent to approximately 175 borehole volumes. The isotopic composition of water from the drill hole R-2250 can be explained by mixing of a saline formation water end-member such as that represented by R-2247 with shallower fresh groundwater, such as the one collected from R-2222 (**Figure 6**). No evident contribution of drilling water was observed. As the geochemical parameters of both of the R-2250 and R-2247 were also very different from the lake water that was used as a drilling water, this confirms that the sample water originated from the bedrock fractures. In addition, the conditions in the deep bedrock are extreme and very different from those in the water used for drilling. For this reason any possible contaminating agent could survive only as fungal or bacterial spores that may better endure extreme environments. The dominant bacterial sequences found were related to a spore-forming genus in the total community analysis. However, whether this is due to contamination or strong decompression during sampling destroying most live cells is difficult to determine. Nevertheless, the detection of potentially active bacterial, archaeal and fungal taxa suggests that the identified microorganisms were adapted to deep terrestrial subsurface conditions and are able to live in this environment.

Yet, evidence indicates that rRNA has some limitations when used as an indicator of current activity as dormant cells could also contain high number of ribosomes (Blazewicz et al., 2013). However, the ITS1 gene region used in this study is present between the 5.8D and 18S units of the mRNA transcript only when the genomic copy of the genes is being actively transcribed. After transcription, the ITS area is quickly spliced out in order for the rRNA units to fold properly and thus is conclusive evidence that the fungi are active and produce ribosomes in the deep biosphere of the Pyhäsalmi mine.

CONCLUSIONS

The presence of deep saline fluids was confirmed in the Pyhäsalmi mine, which supports the previous findings from crystalline shield areas elsewhere in Finland and around the world that these fluids are common below a relatively thin layer of fresh groundwater. The successful geochemical sampling campaign also revealed dissolved gases with compositions clearly distinct from atmospheric air and indicative of long term water-rock interaction. As a mobile phase, dissolved gases such as H_2 form a potential source of energy for microbial communities in deep terrestrial environments. The microbial high-pressure sampling succeeded only partially as the amount of prokaryotic DNA/RNA collected was especially low. This was probably due to the high-pressure decompression that may have damaged part of the cells and the nucleic acids likely have passed through the filter. The fungal community was discovered to be live and active in the deep subsurface oligotrophic environment, since fungal ITS-sequences were found in the samples. The fungal taxa discovered assist in confirming the fungal core microbiome recently detected from the Fennoscandian Shield bedrock (Sohlberg et al., 2015). The identified prokaryotic diversity was low, however it consisted of species often found from other subsurface environments, but also included taxa such as *Alicyclobacillus* genus and Solimonadaceae that have not been found as dominant bacterial groups in the Fennoscandian Shield bedrock environments before. The majority of the archaeal community was closely-related species to methanogens that use H_2 and carbon dioxide to produce methane. The geochemical results identified H_2 and methane as being present, but carbon dioxide was detected at very low levels in two samples. Carbon dioxide may be a limiting factor for these archaea and it may be used rapidly in this highly oligotrophic environment. Conversely, in an alkaline environment (pH over 8), carbon dioxide is present in water as HCO_3^- and in the Pyhäsalmi drill holes low concentrations of HCO_3^- was detected. Carbonate minerals, indicative of the precipitation of dissolved carbon, have not been found on fracture surfaces in the studied drill holes. As a result of these experiments we note that a better way to perform microbial sampling in an environment with high water pressure is to maintain high-pressure throughout the filtering and allow for a slow decompression afterwards.

ACKNOWLEDGMENTS

Arto Pullinen (Geologial Survey of Finland) and Toni Leskinen (Pyhäsalmi Mine Oy) are acknowledged for assistance in sampling and logistics, respectively. Arja Henttinen and Nina Hendriksson from the Research Laboratory of the Geological Survey of Finland performed the water stable isotope analyses. Mirva Pyrhönen is acknowledged for skillful assistance in sampling and the microbial analysis at VTT. Andrew Rushby is thanked for English language editing. The Finnish Research Programme for Nuclear Waste Management KYT2014 and KYT2018 (projects SALAMI, RENGAS, GEOMICRO, and GEOBIOKIERTO) is thanked for the funding of this research.

SUPPLEMENTARY MATERIAL

The Supplementary Material for this article can be found online at: http://journal.frontiersin.org/article/10.3389/fmicb.2015.01203

REFERENCES

Altschul, S. F., Gish, W., Miller, W., Myers, E. W., and Lipman, D. J. (1990). Basic local alignment search tool. *J. Mol. Biol.* 215, 403–410. doi: 10.1016/S0022-2836(05)80360-2

Ballentine, C. J., Burgess, R., and Marty, B. (2002). Tracing fluid origin, transport and interaction in the crust. *Rev. Mineral. Geochem.* 47, 539–614. doi: 10.2138/rmg.2002.47.13

Bano, N., Ruffin, S., Ransom, B., and Hollibaugh, J. T. (2004). Phylogenetic composition of Arctic Ocean archaeal assemblages and comparison with Antarctic assemblages. *Appl. Environ. Microbiol.* 70, 781–789. doi: 10.1128/AEM.70.2.781-789.2004

Barns, S. M., Fundyga, R. E., Jeffries, M. W., and Pace, N. R. (1994). Remarkale archaeal diversity detected in Yellowstone National Park hot spring environment. *Proc. Natl. Acad. Sci. U.S.A.* 91, 1609–1613. doi: 10.1073/pnas.91.5.1609

Blazewicz, S. J., Barnard, R. L., Daly, R. A., and Firestone, M. K. (2013). Evaluating rRNA as an indicator of microbial activity in environmental communities: limitations and uses. *ISME J.* 7, 2061–2068. doi: 10.1038/ismej.2013.102

Bomberg, M., and Itävaara, M. (2013). *The Diversity of Mirobial Communities in Olkiluoto Groundwater Fracture Zones Charaxterized by DNA and RNA Based 16S rRNA-Targeted 454 Pyro Sequencing and qPCR*. Posiva Working Report, 2012-27.

Bomberg, M., Nyyssönen, M., Pitkänen, P., Lehtinen, A., and Itävaara, M. (2015). Active microbial communities inhabit sulphate-methane interphase in deep bedrock fracture fluids in Olkiluoto, Finland. *BioMed. Res. Int.* 2015:979530. doi: 10.1155/2015/979530

Bonin, A. S., and Boone, D. R. (2006). "The order methanobacteriales," in *The Prokaryotes,* Vol. 3, eds. M. Dworkin, S. Falkow, E. Rosenberg, K.-H. Schleifer, and E. Stackebrandt (New York, NY: Springer), 231–243.

Buée, M., Reich, M., Murat, C., Morin, E., Nilsson, R. H., Uroz, S., et al. (2009). 454 Pyrosequencing analyses of forest soils reveal an unexpectedly high fungal diversity. *New Phytol.* 184, 449–456. doi: 10.1111/j.1469-8137.2009.03003.x

Caporaso, J. G., Kuczynski, J., Stombaugh, J., Bittinger, K., Bushman, F. D., Costello, E. K., et al. (2010). QIIME allows analysis of high-throughput community sequencing data. *Nat. Methods* 7, 335–336. doi: 10.1038/nmeth.f.303

Cathrine, S. J., and Raghukumar, C. (2009). Anaerobic denitrification in fungi from the coastal marine sediments off Goa, India. *Mycol. Res.* 113, 100–109. doi: 10.1016/j.mycres.2008.08.009

Chao, A. (1984). Non-parametric estimation of the number of classes in a population. *Scand. J. Stat.* 11, 265–270.

Da Costa, M. S., and Rainey, F. A. (2009). "Family II. Alicyclobacillaceae fam. Nov," in *Bergeys Manual® of Systematic Bacteriology*, Vol. 3, eds P. De Vos, G. M. Garrity, D. Jones, N. R. Krieg, W. Ludwig, F. A. Rainey, K.-H. Schleifer, and W. B. Whitman (New York, NY: Springer), 229.

Damare, S., and Raghukumar, C. (2008). Fungi and macroaggregation in deep-sea sediments. *Microb. Ecol.* 56, 168–177. doi: 10.1007/s00248-007-9334-y

Davidson, M. M., Silver, B. J., Onstott, T. C., Moser, D. P., Gihring, T. M., Pratt, L. M., et al. (2011). Capture of planktonic microbial diversity in fractures by long-term monitoring of flowing boreholes, Evander Basin, South Africa. *Geomicrobiol. J.* 28, 275–300. doi: 10.1080/01490451.2010.499928

DeSantis, T. Z., Hugenholtz, P., Larsen, N., Rojas, M., Brodie, E. L., Keller, K., et al. (2006). Greengenes, a chimera-checked 16S rRNA gene database and workbench compatible with ARB. *Appl. Environ. Microbiol.* 72, 5069–5072. doi: 10.1128/AEM.03006-05

Direito, S. O. L., Ehrenfreund, P., Marees, A., Staats, M., Foing, B., and Röling, W. F. M. (2011). A wide variety of putative extremophiles and large beta-diversity at the Mars Desert Research Station (Utah). *Int. J. Astrobiol.* 10, 191–207. doi: 10.1017/S1473550411000012

Edgar, R. C. (2010). Search and clustering orders of magnitude faster than BLAST. *Bioinformatics* 26, 2460–2461. doi: 10.1093/bioinformatics/btq461

Edgcomb, V. P., Beaudoin, D., Gast, R., Biddle, J. F., and Teske, A. (2010). Marine subsurface eukaryotes: the fungal majority. *Environ. Microbiol.* 13, 172–183. doi: 10.1111/j.1462-2920.2010.02318.x

Edwards, U., Rogall, T., Böcker, H., Emde, M., and Böttger, E. C. (1989). Isolation and direct complete nucleotide determination of entire genes. characterization of a gene coding for 16S ribosomal RNA. *Nucleic Acids Res.* 17, 7843–7853. doi: 10.1093/nar/17.19.7843

Ekendahl, S., O'Neill, A. H., Thomsson, E., and Pedersen, K. (2003). Characterisation of yeasts isolated from deep igneous rock aquifers of the Fennoscandian shield. *Microb. Ecol.* 46, 416–428. doi: 10.1007/s00248-003-2008-5

Eydal, H. S. C., Jägevall, S., Hermansson, M., and Pedersen, K. (2009). Bacteriophage lytic to *Desulfovibrio aespoeensis* isolated from deep groundwater. *ISME J.* 3, 1139–1147. doi: 10.1038/ismej.2009.66

Fell, J. W., Kurtzman, C. P., Tallman, A. S., and Buck, J. D. (1988). Rhodosporidium fluviale sp. nov., a homokaryotic red yeast from a subtropical brackish environment. *Mycologia* 80, 560–564. doi: 10.2307/3807858

Frape, S. K., Blyth, A., Blomqvist, R., McNutt, R. H., and Gascoyne, M. (2003). Deep fluids in the continents: II. Crystalline rocks. *Treatise Geochem.* 5, 541–580. doi: 10.1016/B0-08-043751-6/05086-6

Fredrickson, J. K., and Balkwill, D. L. (2006). Geomicrobial processes and biodiversity in the deep terrestrial subsurface. *Geomicrobiol. J.* 23, 345–356. doi: 10.1080/01490450600875571

Frostegård, Å., Courtois, S., Ramisse, V., Clerc, S., Bernillon, D., Le Gall, F., et al. (1999). Quantification of bias related to the extraction of DNA directly from soils. *Appl. Environ. Microbiol.* 65, 5409–5420.

Gardes, M., and Bruns, T. D. (1993). ITS primers with enhanced specificity for basidiomycetes—application to the identification of mycorrhizae and rusts. *Mol. Ecol.* 2, 113–118. doi: 10.1111/j.1365-294X.1993.tb00005.x

Griebler, C., and Lueders, T. (2009). Microbial biodiversity in groundwater ecosystems. *Freshw. Biol.* 54, 649–677. doi: 10.1111/j.1365-2427.2008.02013.x

Großkopf, R., Stubner, S., and Liesack, W. (1998). Novel euryarchaeotal lineages detected on rice roots and in the anoxic bulk soil of flooded rice microcosms. *Appl. Environ. Microbiol.* 64, 4983–4989.

Hallbeck, L., and Pedersen, K. (2012). Culture-dependent comparison of microbial diversity in deep granitic groundwater from two sites considered for a swedish final repository of spent nuclear fuel. *FEMS Microbiol. Ecol.* 81, 66–77. doi: 10.1111/j.1574-6941.2011.01281.x

Hatanpää, E., Manninen, P., and Apilo, S. (2005). *Representativity of Gas Samples Taken with the Pressurized Water Sampling System (PAVE) 1995–2004*. Posiva Working Report, 5005-55.

Haveman, S. A., Pedersen, K., and Ruotsalainen, P. (1999). Distribution and metabolic diversity of microorganisms in deep igneous rock aquifers of Finland. *Geomicrobiol. J.* 16, 277–294. doi: 10.1080/014904599270541

Hemmingsen, B. B., and Hemmingsen, E. A. (1980). Rupture of the cell envelope by induced intracellular gas phase expansion in gas vacuolate bacteria. *J. Baceriol.* 143, 841–846.

Hirose, T., Kawagucci, S., and Suzuki, K. (2011). Mechanoradical H_2 generation during simulated faulting: Implications for an earthquake-driven subsurface biosphere. *Geophys. Res. Lett.* 38, L17303. doi: 10.1029/2011GL048850

Hoehler, T. M., and Jørgensen, B. B. (2013). Microbial life under extreme energy limitation. *Nat. Rev.* 11, 83–94. doi: 10.1038/nrmicro2939

Hurt, R. A. Jr., Robeson, M. S. II., Shakya, M., Moberly, J. G., Vishnivetskaya, T. A., Gu, B., et al. (2014). Improved yield of high molecular weight DNA coincides with increased microbial diversity access from iron oxide cemented subsurface clay environments. *PLoS ONE* 9:e102826. doi: 10.1371/journal.pone.0102826

Imperio, T., Viti, C., and Marri, L. (2008). *Alicyclobacillus pohliae* sp. nov., a thermophilic, endospore-forming bacterium isolated from geothermal soil of the north-west slope of Mount Melbourne (Antarctica). *Int. J. Syst. Ecol. Microbiol.* 58, 221–225. doi: 10.1099/ijs.0.65092-0

Itävaara, M., Nyyssönen, M., Kapanen, A., Nousiainen, A., Ahonen, L., and Kukkonen, I. (2011). Characterization of bacterial diversity down to a depth of 1500 m in the Outokumpu deep borehole, Fennoscandian shield. *FEMS Microbiol. Ecol.* 77, 295–309. doi: 10.1111/j.1574-6941.2011.01111.x

Itävaara, M., Vehkomäki, M. L., and Nousiainen, A. (2008). *Sulphate-Reducing Bacteria in Ground Water Samples from Olkiluoto - Analyzed by Quantitative PCR*. Posiva Working Report, 2008-82.

Kärki, A., Laajoki, K., and Luukas, J. (1993). Major Palaeoproterozoic shear zones of the central Fennoscandian Shield. *Precambrian Res.* 64, 207–223. doi: 10.1016/0301-9268(93)90077-F

Kellogg, C. A., and Griffin, D. W. (2006). Aerobiology and the global transport of desert dust. *Trends Ecol. Evol.* 21, 638–644. doi: 10.1016/j.tree.2006.07.004

Keppner, R. L. Jr., and Pratt, J. R. (1994). Use of fluorochromes for direct enumeration of total bacteria in environmental samples: past and present. *Microbiol. Rev.* 58, 603–615.

Kietäväinen, R., Ahonen, L., Kukkonen, I. T., Hendriksson, N., Nyyssönen, M., and Itävaara, M. (2013). Characterisation and isotopic evolution of saline waters of the Outokumpu Deep Drill Hole, Finland - implications for water origin and deep terrestrial biosphere. *Appl. Geochem.* 32, 37–51. doi: 10.1016/j.apgeochem.2012.10.013

Kietäväinen, R., Ahonen, L., Kukkonen, I. T., Niedermann, S., and Wiersberg, T. (2014). Noble gas residence times of saline waters within crystalline bedrock, Outokumpu Deep Drill Hole, Finland. *Geochim. Cosmochim. Acta* 145, 159–174. doi: 10.1016/j.gca.2014.09.012

Kita, I., Matsuo, S., and Wakita, H. (1982). H_2 generation by reaction between H_2O and crushed rock: an experimental study on H_2 degassing from the active fault zone. *J. Geophys. Res.* 87, 10789–10795. doi: 10.1029/JB087iB13p10789

Kõljalg, U., Nilsson, R. H., Abarenkov, K., Tedersoo, L., Taylor, A. F. S., Bahram, M., et al. (2013). Towards a unified paradigm for sequence-based identification of fungi. *Mol. Ecol.* 22, 5271–5277. doi: 10.1111/mec.12481

Kormas, K. A., Smith, D. C., Edgcomb, V., and Teske, A. (2003). Molecular analysis of deep subsurface microbial communities in Nankai Trough sediments (ODP Leg190, Site 1176). *FEMS Microbiol. Ecol.* 45, 115–125. doi: 10.1016/S0168-6496(03)00128-4

Kortelainen, N. (2007). *Isotopic Fingerprints in Surficial Waters: Stable Isotope Methods Applied in Hydrogeological Studies*. Geological Survey of Finland, Espoo.

Kotelnikova, S., and Pedersen, K. (1998). Distribution and activity of methanogens and homoacetogens in deep granitic aquifers at Äspö hard rock laboratory, Sweden. *FEMS Microbiol. Ecol.* 26, 121–134.

Kubo, Y., Mizuguchi, Y., Inagaki, F., and Yamamoto, K. (2014). A new hybrid pressure-coring system for the drilling vessel. Chikyu. *Sci. Dril.* 17, 37–43. doi: 10.5194/sd-17-37-2014

Kukkonen, I. (1989). *Terrestrial Heat Flow in Finland, the Central Fennoscandian Shield. Geological Survey of Finland, Nuclear Waste Disposal Research, Report YST-68*. Available online at: http://tupa.gtk.fi/julkaisu/ydinjate/yst_068.pdf

Kurakov, A. V., Lavrent'Ev, R. B., Nechitailo, T. Y., Golyshin, P. N., and Zvyagintsev, D. G. (2008). Diversity of facultatively anaerobic microscopic mycelial fungi in soils. *Microbiology* 77, 90–98. doi: 10.1134/S002626170801013X

Laine, E., Luukas, J., Mäki, T., Kousa, J., Ruotsalainen, A., Suppala, I., et al. (2015). "The Vihanti-Pyhäsalmi area," in *3d, 4d and Predictive Modelling of Mineral Belts: European Resources Under Cover*, ed P. Weihed (New York, NY: Springer), 123–144.

Lin, L., Hall, J., Lippmann-Pipke, J., Ward, J. A., Sherwood Lollar, B., DeFlaun, M., et al. (2005a). Radiolytic H_2 in continental crust: nuclear power for deep subsurface microbial communities. *Geochem. Geophys. Geosyst*. 6, Q07003. doi: 10.1016/j.gca.2004.07.032

Lin, L.-H., Slater, G. F., Sherwood Lollar, B., Lacrampe-Couloume, G., and Onstott, T. C. (2005b). The yield and isotopic composition of radiolytic H_2, a potential energy source for the deep subsurface biosphere. *Geochim. Cosmochim. Acta* 69, 893–903. doi: 10.1016/j.gca.2004.07.032

Lorenz, R., and Molitoris, H. P. (1997). Cultivation of fungi under simulated deep sea conditions. *Mycol. Res.* 101, 1355–1365.

Mayhew, L. E., Ellison, E. T., McCollom, T. M., Trainor, T. P., and Templeton, A. S. (2013). Hydrogen generation from low-temperature water-rock reactions. *Nat. Geosci.* 6, 478–484. doi: 10.1038/ngeo1825

McMahon, S., and Parnell, J. (2013). Weighing the deep continental biosphere. *FEMS Microbial. Ecol.* 87, 113–120. doi: 10.1111/1574-6941.12196

Miettinen, H., Bomberg, M., Nyyssönen, M., Salavirta, H., Sohlberg, E., Vikman, M., et al. (2015). *The Diversity Of Microbial Communities in Olkiluoto Bedrock Groundwaters 2009-2013*. Posiva Working Report, 2015-12.

Moser, D. P., Gihring, T. M., Brockman, F. J., Fredrickson, J. K., Balkwill, D. L., Dollhopf, M. E., et al. (2005). Desulfotomaculum and Methanobacterium spp. dominate a 4- to 5-kilometer-deep fault. *Appl. Environ. Microbiol.* 71, 8773–8783. doi: 10.1128/AEM.71.12.8773-8783.2005

Moser, D. P., Onstott, T. C., Fredrickson, J. K., Brockman, F. J., Balkwill, D. L., Drake, G. R., et al. (2003). Temporal shifts in microbial community structure and geochemistry of an ultradeep South African gold mine borehole. *Geomicrobiol. J.* 20, 1–32. doi: 10.1080/713851170

Muyzer, G., de Waal, E. C., and Uitterlinden, A. G. (1993). Profiling of complex microbial populations by denaturing gradient gel electrophoresis analysis of polymerase chain reaction-amplified genes coding 16S rRNA. *Appl. Environ. Microbiol.* 59, 695–700.

Nagahama, T., Hamamoto, M., and Horikoshi, K. (2006). Rhodotorula pacifica sp. nov., a novel yeast species from sediment collected on the deep-sea floor of the north-west Pacific Ocean. *Int. J. Syst. Evol. Microbiol.* 56, 295–299. doi: 10.1099/ijs.0.63584-0

Nagahama, T., Hamamoto, M., Nakase, T., Takami, H., and Horikoshi, K. (2001). Distribution and identification of red yeasts in deep-sea environments around the northwest Pacific Ocean. *Antonie Van Leeuwenhoek* 80, 101–110. doi: 10.1023/A:1012270503751

Nagano, Y., Nagahama, T., Hatada, Y., Nunoura, T., Takami, H., Miyazaki, J., et al. (2010). Fungal diversity in deep-sea sediments–the presence of novel fungal groups. *Fungal Ecol.* 3, 316–325. doi: 10.1016/j.funeco.2010.01.002

Nguyen, T. H., and Elimelech, M. (2007). Plasmid DNA adsorption on silica: kinetics and conformational changes in monovalent and divalent salts. *Biomacromolecules* 8, 24–32. doi: 10.1021/bm0603948

Nübel, U., Wngelen, B., Felske, A., Snaidr, J., Wieshuber, A., and Amann, R. I. (1996). Sequence heterogeneities of genes encoding 16S rRNAs in *Paenibacillus polymyxa* detected by temperature gradient gel electrophoresis. *J. Bacteriol.* 178, 5636–5643.

Nurmi, P. A., Kukkonen, I. T., and Lahermo, P. W. (1988). Geochemistry and origin of saline groundwaters in the Fennoscandian shield. *Appl. Geochem.* 3, 185–203. doi: 10.1016/0883-2927(88)90007-8

Nyyssönen, M., Bomberg, M., Kapanen, A., Nousiainen, A., Pitkänen, P., and Itävaara, M. (2012). Methanogenic and sulphate-reducing microbial communities in deep groundwater of crystalline rock fractures in Olkiluoto, Finland. *Geomicrobiol. J.* 29, 863–878. doi: 10.1080/01490451.2011.635759

Nyyssönen, M., Hultman, J., Ahonen, L., Kukkonen, I., Paulin, L., Laine, P., et al. (2014). Taxonomically and functionally diverse microbial communities in deep crystalline rocks of the Fennoscandian shield. *ISME J.* 8, 126–138. doi: 10.1038/ismej.2013.125

Onstott, T. C., McGown, D. J., Bakermans, C., Ruskeeniemi, T., Ahonen, L., Telling, J., et al. (2009). Microbial communities in subpermafrost saline fracture water at the Lupin Au Mine, Nunavut, Canada. *Microb. Ecol.* 58, 786–807. doi: 10.1007/s00248-009-9553-5

Orsi, W., Biddle, J. F., and Edgcomb, V. (2013). Deep sequencing of subseafloor eukaryotic rRNA reveals active fungi across marine subsurface provinces. *PLoS ONE* 8:e56335. doi: 10.1371/journal.pone.0056335

Paget, E., Monrozier, L. J., and Simonet, P. (1992). Adsorption of DNA on clay minerals: protection against DNaseI and influence on gene transfer. *FEMS Microbiol. Lett.* 97, 31–39. doi: 10.1111/j.1574-6968.1992.tb05435.x

Park, C. B., and Clark, D. S. (2002). Rupture of the cell envelope by decompression of the deep-sea methanogen *Methanococcus jannaschii*. *Appl. Environ. Microbiol.* 68, 1458–1463. doi: 10.1128/AEM.68.3.1458-1463.2002

Pedersen, K. (1987). *Preliminary Investigations of Deep Ground Water Microbiology in Swedish Granitic Rock*. SKB Technical Report 88-01, Swedish nuclear fuel and waste management Co., Stockholm.

Purkamo, L., Bomberg, M., Nyyssönen, M., Kukkonen, I., Ahonen, L., Kietäväinen, R., et al. (2013). Dissecting the deep biosphere: retrieving authentic microbial communities from packer-isolated deep crystalline bedrock fracture zones. *FEMS Microbiol. Ecol.* 85, 324–337. doi: 10.1111/1574-6941.12126

Raghukumar, C. (ed.). (2012). *Biology of Marine Fungi, Vol. 53*. Heidelberg: Springer. doi: 10.1007/978-3-642-23342-5_5

Ragon, M., Van Driessche, A. E. S., García-Ruíz, J. M., Moreira, D., and López-García, P. (2013). Microbial diversity in the deep-subsurface hydrothermal aquifer feeding the giant gypsum crystal-bearing Naica Mine, Mexico. *Front. Microbiol.* 4:37. doi: 10.3389/fmicb.2013.00037

Reed, D. W., Fujita, Y., Delwiche, M. E., Blackwelder, D. B., Sheridan, P. P., Uchida, T., et al. (2002). Microbial communities from methane hydrate-bearing deep marine sediments in a Forearc Basin. *Appl. Environ. Microbiol.* 68, 3759–3770. doi: 10.1128/AEM.68.8.3759-3770.2002

Regenspurg, S., Wiersberg, T., Brandt, W., Huenges, E., Saadat, A., Schmidt, K., et al. (2010). Geochemical properties of saline geothermal fluids from the *in-situ* geothermal laboratory GroßSchönebeck (Germany). *Chem. Erde* 70, 3–12. doi: 10.1016/j.chemer.2010.05.002

Schloss, P. D., Westcott, S. L., Ryabin, T., Hall, J. R., Hartmann, M., Hollister, E. B., et al. (2009). Introducing mothur: Open-source, platform-independent, community-supported software for describing and comparing microbial communities. *Appl. Environ. Microbiol.* 75, 7537–7541. doi: 10.1128/AEM.01541-09

Sherwood Lollar, B., Vogelsonger, K., Lin, L.-H., Lacrampe-Couloume, G., Telling, J., Abrajano, T. A., et al. (2007). Hydrogeologic controls on episodic H_2 release from Precambrian fractured rocks - Energy for deep subsurface life on Earth and Mars. *Astrobiology* 7, 971–986. doi: 10.1089/ast.2006.0096

Singh, P., Raghukumar, C., Verma, P., and Shouche, Y. (2012). Assessment of fungal diversity in deep-sea sediments by multiple primer approach. *World J. Microbiol. Biotechnol.* 28, 659–667. doi: 10.1007/s11274-011-0859-3

Sohlberg, E., Bomberg, M., Miettinen, H., Nyyssönen, M., Salavirta, H., Vikman, M., et al. (2015). Revealing the unexplored fungal communities in deep groundwater of crystalline bedrock fracture zones in Olkiluoto, Finland. *Front. Microbiol.* 6:573. doi: 10.3389/fmicb.2015.00573

Stahl, D. A., and Amann, R. (1991). "Development and application of nucleic acid probes," in *Nucleic Acid Techniques in Bacterial Systematics*, eds E. Stackebrandt and M. Goodfellow (Chichster: John Wiley & Sons), 205–248.

Stotler, R. L., Frape, S. K., Ruskeeniemi, T., Ahonen, L., Onstott, T. C., and Hobbs, M. Y. (2009). Hydrogeochemistry of groundwaters in and below the base of thick permafrost at Lupin, Nunavut, Canada. *J. Hydrol.* 373, 80–95. doi: 10.1016/j.jhydrol.2009.04.013

Takai, K., Moser, D. P., DeFlaun, M., Onstott, T. C., and Fredrickson, J. K. (2001). Archaeal diversity in waters from deep South African gold mines. *Appl. Environ. Microbiol.* 67, 5750–5760. doi: 10.1128/AEM.67.21.5750-5760.2001

Trinchero, P., Delos, A., Molinero, J., Dentz, M., and Pitkänen, P. (2014). Understanding and modelling dissolved gas transport in the bedrock of three Fennoscandian sites. *J. Hydrol.* 512, 506–517. doi: 10.1016/j.jhydrol.2014.03.011

USGS (2014). *PHREEQC*. Computer codes, United States Geological Survey. Available online at: http://wwwbrr.cr.usgs.gov/projects/GWC_coupled/phreeqc/

Wang, Q., Carrity, G. M., Tiedje, J. M., and Cole, J. R. (2007). Naïve bayesian classifier for rapid assignment of rRNA Sequences into the new bacterial taxonomy. *Appl. Environ. Microbiol.* 73, 5261. doi: 10.1128/AEM.00062-07

Weisburg, W. G., Barns, S. M., Pelletier, D. A., and Lane, D. J. (1991). 16S ribosomal DNA amplification for phylogenetic study. *J. Bacteriol.* 173, 697–703.

White, T. J., Bruns, T., Lee, S., and Taylor, J. (1990). "Amplification and direct sequencing of fungal ribosomal RNA genes for phylogenetics," in *PCR Protocols: A Guide to Methods and Applications,* ed M. Innis (San Diego, CA: Academic Press), 315–322.

Yashiro, Y., Sakai, S., Ehara, M., Miyazaki, M., Yamaguchi, T., and Imachi, H. (2011). Methanoregula formicica sp. nov., a methane-producing archaeon isolated from methanogenic sludge. *Int. J. Syst. Evol. Microbiol.* 61, 53–59. doi: 10.1099/ijs.0.014811-0

Zhou, Y., Lai, R., and Li, W.-J. (2014). "The family solimonadaceae," in *The Prokaryotes,* eds E. Rosenberg, E. F. De Long, S. Lory, E. Stackebrandt, and F. Thompson (Heidelberg; Berlin: Springer), 627–638.

Conflict of Interest Statement: The authors declare that the research was conducted in the absence of any commercial or financial relationships that could be construed as a potential conflict of interest.

frontiers in Microbiology

ORIGINAL RESEARCH
published: 24 July 2015
doi: 10.3389/fmicb.2015.00647

Microbially induced corrosion of carbon steel in deep groundwater environment

Pauliina Rajala[1], Leena Carpén[1], Mikko Vepsäläinen[2], Mari Raulio[3†], Elina Sohlberg[3] and Malin Bomberg[3]*

[1] Materials Performance, VTT Technical Research Centre of Finland, Espoo, Finland, [2] CSIRO Mineral Resources Flagship, Melbourne, VIC, Australia, [3] Geobiotechnology, VTT Technical Research Centre of Finland, Espoo, Finland

The metallic low and intermediate level radioactive waste generally consists of carbon steel and stainless steels. The corrosion rate of carbon steel in deep groundwater is typically low, unless the water is very acidic or microbial activity in the environment is high. Therefore, the assessment of microbially induced corrosion of carbon steel in deep bedrock environment has become important for evaluating the safety of disposal of radioactive waste. Here we studied the corrosion inducing ability of indigenous microbial community from a deep bedrock aquifer. Carbon steel coupons were exposed to anoxic groundwater from repository site 100 m depth (Olkiluoto, Finland) for periods of 3 and 8 months. The experiments were conducted at both *in situ* temperature and room temperature to investigate the response of microbial population to elevated temperature. Our results demonstrate that microorganisms from the deep bedrock aquifer benefit from carbon steel introduced to the nutrient poor anoxic deep groundwater environment. In the groundwater incubated with carbon steel the planktonic microbial community was more diverse and 100-fold more abundant compared to the environment without carbon steel. The betaproteobacteria were the most dominant bacterial class in all samples where carbon steel was present, whereas in groundwater incubated without carbon steel the microbial community had clearly less diversity. Microorganisms induced pitting corrosion and were found to cluster inside the corrosion pits. Temperature had an effect on the species composition of microbial community and also affected the corrosion deposits layer formed on the surface of carbon steel.

Keywords: deep biosphere, microbial corrosion, terrestrial biosphere, carbon steel, sulfate reducing bacteria

OPEN ACCESS

Edited by:
Graeme W. Nicol, L'Université de Lyon, France

Reviewed by:
Steffen Kolb, Friedrich Schiller University Jena, Germany
Md. Tanvir Rahman, Bangladesh Agricultural University, Bangladesh

****Correspondence:***
Pauliina Rajala, Materials Performance, VTT Technical Research Centre of Finland, Kemistintie 3, FI-02044 VTT, Espoo, Finland
pauliina.rajala@vtt.fi

†Present address:
Mari Raulio, Tikkurila Oyj, Vantaa, Finland

Specialty section:
This article was submitted to Terrestrial Microbiology, a section of the journal Frontiers in Microbiology

Received: *26 March 2015*
Accepted: *15 June 2015*
Published: *24 July 2015*

Citation:
Rajala P, Carpén L, Vepsäläinen M, Raulio M, Sohlberg E and Bomberg M (2015) Microbially induced corrosion of carbon steel in deep groundwater environment. Front. Microbiol. 6:647. doi: 10.3389/fmicb.2015.00647

Introduction

During the last two decades the Fennoscandian deep terrestrial biosphere has been extensively studied due to the geological repositories planned for spent nuclear fuel and radioactive decommissioning waste (Haveman and Pedersen, 2002; Itävaara et al., 2011; Purkamo et al., 2013; Bomberg et al., 2015; Rajala et al., 2015). Despite the extensive study of deep biosphere, the potential of indigenous microbial communities to induce corrosion under the prevailing environmental conditions is not well known. The assessment of microbially induced corrosion (MIC) of carbon

steel in deep bedrock environment has become important for evaluating the long-term safety of disposal of low and intermediate level radioactive (LLW/ILW) waste. Such waste is produced during the operation, maintenance, and decommissioning of nuclear power plants (NPPs). The LLW/ILW produced in Olkiluoto NPP, Finland, has since 1992 been disposed into an underground repository excavated in to bedrock to a depth of 60–100 m below sea level [Teollisuuden voima Oyj (TVO), 2015]. The metallic portion of LLW/ILW generally consists of carbon steel and stainless steels.

In oxygen-free water, the corrosion rate of carbon steel is low, unless the water is acidic or microbial activity in the environment is high. In Olkiluoto NPP the LLW/ILW is packed into concrete silos or concrete boxes. Concrete generates a high pH environment, which in turn is assumed to reduce the corrosion rate of carbon steel (Rajala et al., 2014). Nevertheless, over the time the pH decreases, for example due to the carbonization of concrete.

The groundwater at the repository depth contains large microbial populations of up to 10^5 microorganisms mL^{-1} with considerable diversity of species (Haveman and Pedersen, 2002; Nyyssönen et al., 2012). Microorganisms may significantly contribute to the corrosion of metallic waste and can accelerate corrosion rates up to 1000–10,000 fold (Videla, 1996; Carpén et al., 2013). Microorganisms are able to affect various corrosion mechanisms, such as general corrosion and localized corrosion, the latter including pitting and stress corrosion cracking (Little et al., 1992). Sulfate-reducing bacteria (SRB), in particular, are known to cause corrosion of carbon steel (Bryant et al., 1991). Carpén et al. (2012) demonstrated that the corrosion rate might be as high as 10–63 $\mu m\ a^{-1}$ in the repository environment and localized corrosion rates even higher. Such high corrosion rates in anoxic groundwater cannot occur without acceleration of the corrosion process by microbial activity. Especially microbial biofilm formed on carbon steel surface has been shown to accelerate corrosion (Little et al., 1992).

In nutrient poor conditions, such as in deep anoxic groundwater, microorganisms may significantly accelerate the corrosion rate of metals by using metallic iron as electron donor (Xu and Gu, 2011). Microorganisms are also able to produce corrosive agents, such as organic acids or sulfide, and consume hydrogen that is produced in the corrosion process (Little et al., 1992; Lee et al., 1995). As a consequence of the accelerated corrosion and increased solubility of the metal ions in acidic environments, radioactive nuclides may be released into groundwater and transferred to neighboring areas of the repository.

The aim of this study was to characterize microbial biofilms associated with corrosion, study the ability of the indigenous groundwater microbes to benefit from carbon steel, and compare the corrosion rate of carbon steel in groundwater at room temperature and *in situ* temperature. In general, elevated temperatures accelerate corrosion, but the effect of temperature on the corrosion-accelerating bacterial community is unknown. Electrochemical measurements are often conducted at room temperature instead of at *in situ* temperature. Therefore, the effect of temperature on the community composition of the biofilm formed on the surface of carbon steel was also studied.

Materials and Methods

Sample Collection

The experiment was conducted using the native groundwater from Olkiluoto VLJ-cave the geological disposal site of low and intermediate level radioactive waste (LLW/ILW) (61°14′13″N 21°26′27″E) from the drill hole located next to the repository silos. The drill hole was located at the depth of 100 m, which is the same level as the bottom of the repository silo and can be reached from the maintenance tunnel in the repository cave. Groundwater sampling was performed in June 2011. The groundwater was funneled into an anoxic glove bag (AtmosBag®, Sigma-Aldrich, St. Louis, MO, USA) without exposure to oxygen through a factory clean polyamide tube directly from the drill hole located in the cave wall. Anoxic conditions within the glove bag were maintained with constant N_2 (99.999%) flow and anaerobic generators (Anaerocult® A, Merck, Germany). In the anoxic glove bag, microbial biomass for DNA extraction was collected from three parallel 250 mL groundwater samples on 0.22 μm pore-size Sterivex- filtration units (Millipore, Billerica, MA, USA) for DNA extraction. The filtration units were frozen on dry ice immediately after sampling.

Sterile, acid washed, 250 mL boro-silicate incubation bottles (Schott, Germany) each containing one carbon steel coupon (AISI/SAE 1005, 5 mm × 80 mm × 1 mm; **Table 1**) had been prepared in advance by autoclaving. The bottles were rendered anoxic under N_2 flow inside the glove bag on site. The surface finish of carbon steel coupons was as received. The incubation bottles were filled with 250 mL groundwater and were subsequently sealed with tight fitting butyl rubber septum and open top cap within the glove bag to enable anoxic sampling from the incubation bottles. The carbon steel coupons were exposed to groundwater in the microcosms at room temperature or at 6°C, which represents *in situ* temperature of the repository cave, for 3 and 8 months. In addition, reference groundwater incubations without carbon steel coupons were prepared in order to observe the change in the microbial community during the incubation without the influence of carbon steel. Three replicate groundwater samples were prepared for microbiological analyses and corrosion analyses of each treatment, respectively.

TABLE 1 | Composition of carbon steel.

C	Si	Mn	S	P	Cr	Ni	Mo	Cu	Al	W	V	Ti	Co	B
0.03	0.009	0.21	0.007	0.007	0.04	0.05	0.01	0.02	0.048	<0.01	0.003	0.002	0.004	–

Groundwater Chemistry

The conductivity (Radiometer CDM92, Radiometer, France) and pH (HACH Sension 156, Loveland, CO, USA) of the groundwater was measured immediately on site. The chemical composition of the groundwater was analyzed at the TVO's laboratory (Eurajoki, Finland). At the end of the incubation periods (3 and 8 months) the pH, conductivity, redox-potential and oxygen content of the water in each bottle were measured inside the glove bag to protect the samples from oxygen. Conductivity was measured as above, pH using a Orion 5-star pH meter, redox with a HACH Sension 156 meter and oxygen with a dissolved oxygen test kit (CHEmetrics, 0–1 ppm, Midland, VA, USA; 3 months exposure) or HACH Sension 156 m (8 months exposure).

Nucleic Acid Extraction

After the incubation periods (3 and 8 months) the carbon steel coupons were removed from the bottles under N_2 flow inside the glove bag. Coupons for molecular biological analyses (three parallel coupons for each treatment) were stored in sterile 50 mL screw cap test tubes (Corning, Tewksbury, MA, USA) at −80°C. The microbial biomass from the water from each incubation bottle was collected on Sterivex- filtration units by filtration, and they were frozen at −80°C until DNA extraction. DNA was extracted from microbial biomass collected on filtration units from 3 replicate water samples. The biofilm DNA was extracted from the surface of the carbon steel as described by Rajala et al. (2014). Briefly, the carbon steel coupons were shaken in 10 mL sterile phosphate buffered saline (PBS) and Tween®20 (Merck, Germany; 1 μL Tween®20 1 mL^{-1} PBS) for 20 min at 150 rpm agitation followed by ultra sonication for 3 min. The removed biomass was then collected on Sterivex- filtration units. For DNA extraction, the filtration units were opened in a laminar flow hood with flame-sterilized pliers as described by Itävaara et al. (2011). DNA was extracted using the PowerWater DNA Isolation kit (MoBio Laboratories, Inc., Carlsbad, CA, USA) in accordance with the manufacturer's protocol and eluted in 50 μL elution buffer supplied by manufacturer. Possible contamination from different reagents and sample handling was determined by including DNA extraction controls. These controls comprised unused Sterivex- filtration units and the same DNA extraction protocol as used for the samples. These negative reagent control extraction were performed in parallel with the DNA extraction of the actual samples.

Quantitative PCR

Quantitative PCR (qPCR) was used to determine the abundance of bacteria and sulfate reducers based on the amount of 16S rRNA and *dsr*B gene copies in the groundwater and in the biofilm. qPCR was performed in 10 μL reaction volumes using LightCycler 480 qPCR instrument and LightCycler 480 Software 1.5.0 (Roche Applied Science, Germany). The reaction mixture contained 1 μL DNA template, standard dilution or water, 1 × KAPA SYBR® FAST Universal qPCR Master Mix (KAPA Biosystems, Wilmington, MA, USA), 2.5 μM of both forward and reverse primer and nuclease free water. The primers used for the bacterial 16S rRNA gene qPCR were fD1 (Weisburg et al., 1991) and P2 (Muyzer et al., 1993) and for *dsr*B genes primers 2060F and dsr4R (Wagner et al., 1998; Geets et al., 2006). As a standard, a plasmid dilution series containing the corresponding gene insert (10^1–10^9 copies per reaction) was used. The PCR program consisted of an initial 15 min incubation at 95°C, followed by 45 cycles of denaturation at 95°C for 10 s, annealing at 55°C for 35 s and extension 72°C for 30 s, and with final extension at 72°C for 3 min. Sample fluorescence was measured at the end of each elongation phase. Subsequently, a melting curve was recorded, to test the specificity of the qPCR, with a program consisting of 10 s of denaturation at 95°C, 1 min of annealing at 65°C, and a melting and continuous measuring step rising gradually (20°C s^{-1}) to 95°C. Three parallel qPCR reactions were performed for each extracted DNA sample, as well as for the no-template controls which were used to determine the background noise of the qPCR.

One-way analysis of variance and subsequent multiple comparisons analysis using Tuckey's variance test was performed for qPCR results using the PAST software version 3.06 (Hammer et al., 2001).

DGGE Analysis of the Bacterial and Sulfate Reducing Community

The bacterial diversity was investigated by PCR-denaturing gradient gel electrophoresis (DGGE) analysis of 16S rRNA gene fragment and SRB diversity was investigated by PCR-DGGE analysis of the dissimilatory sulphite reductase gene (*dsr*B) fragment as described in Muyzer et al. (1993) and Nyyssönen et al. (2012), respectively. For the 16S rRNA gene targeted DGGE, a 193 bp fragment covering the V3 variable region of the bacterial 16S rRNA gene was amplified with primers P2 and P3 (Muyzer et al., 1993). The amplification was performed in 50 μL reaction volumes, containing 4 μL template or nuclease free H_2O for no template controls, 1 × Dynazyme Reaction Buffer (Finnzymes, Finland), dNTP 62.5 μM each (final concentration; Finnzymes, Finland), 0.2 μM (final concentration) of both forward- and reverse primers (Eurogentec, Sweden), 1 U Dynazyme II polymerase (Finnzymes, Finland) and nuclease free H_2O (Sigma, St. Louis, MO, USA). Formamide, 0.1 μL 10^{-1} μL reaction mix, was used for amplification of the 16S rRNA gene fragments. The amplification in all PCR reactions was carried out on a thermal PCR cycler (Mastercycler gradient, Eppendorf, Germany) using the following conditions: 95°C initial denaturation for 5 min, followed by 40 cycles of 94°C for 1 min, 55°C for 1 min and 72°C for 1 min, with a final extension step at 72°C for 10 min. PCR products were visualized with agarose gel electrophoresis on a 1% agarose gel (LE-agarose, Lonza, Switzerland) in 1 × SB-buffer (Brody and Kern, 2004). The gel was stained with 1 × SyberSafe (Invitrogen, Carlsbad, CA, USA) and run at 300 V for 15 min. The 16S PCR products were resolved by DGGE on 8% acrylamide with denaturing gradient 20–65% at constant voltage of 65 V and temperature at 60°C for 18 h in 0.5 × TAE running buffer as described by Itävaara et al. (2011).

A 470 bp fragment of the *dsrB* gene was amplified with primers 2060F+GC and dsr4R (Wagner et al., 1998; Geets et al., 2006).

The PCR program and reaction mixture were as described above. The *dsr*B PCR products were resolved with a denaturing gradient of 40–70% at constant voltage of 85 V and temperature at 60°C for 20 h in 0.5 × TAE running buffer. The gels were imaged and DNA from DGGE bands was prepared for sequencing as described by Nyyssönen et al. (2012).

The DNA fragments were sequenced at Macrogen Inc. (Korea) using primer P2 and dsr4R primer for the 16S rRNA and *dsr*B gene fragments, respectively.

Analysis of DGGE Profiles and Phylogeny

The obtained DGGE profiles were normalized and analyzed with the BioNumerics software version 5.10 (Applied Maths, Kortrijk, Belgium). During this processing, the different DGGE lanes were defined, background was subtracted, differences in the intensity of the lanes were compensated by normalization, and a correlation matrix was calculated. Clustering was done with Dice's coefficient for similarity.

Sequences obtained from DGGE bands were imported into the Geneious Pro Software package (version 5.5.6, Biomatters Inc., New Zealand, Drummond et al., 2010) where they were manually checked, assembled and edited before subjecting them to phylogenetic analyses. The sequences were compared with the BLAST tool (blastn and blastx, http://blast.ncbi.nlm.nih.gov/Blast.cgi; Altschul et al., 1990) to the sequences in NCBI databases. The closest matching sequences, relevant reference sequences and sequences of type strains were included in the phylogenetic analyses. The nucleic acid sequences of the bacterial 16S rRNA gene fragments were aligned using ClustalW (Thompson et al., 1994) in Geneious Pro, and the alignment was manually edited. The *dsr*B sequences were converted to amino acid sequences and aligned using ClustalW using default parameters. The alignments were checked and manually edited. Maximum likelihood analysis was performed using PhyML (Guidon and Gascuel, 2003) with the Jukes–Cantor substitution model (Jukes and Cantor, 1969) for the nucleic acid sequence alignments, and the Whelan and Goldman (WAG) substitution model (Whelan and Goldman, 2001) for the amino acid sequence alignments. Bootstrap support for the nodes was calculated on 1000 random repeats. Due to the high number of similar 16S rRNA and *dsr*B gene sequences, the sequences were grouped into operational taxonomic units (OTUs) according to their alignment. Each OTU consisted of 16S rRNA or *dsr*B sequences sharing over 97% similarity of the nucleic acid or amino acid sequence, respectively. One representative sequences was chosen from each sample for each phylogenetic group.

Accession Numbers

The obtained sequences (16S rRNA, *dsr*B) have been submitted to European Nucleotide Archive (ENA), and are available under accession numbers LN869402–LN869518.

Corrosion

After retrieving the carbon steel coupons for corrosion analyses they were immediately rinsed with ethanol (96%) and air-dried and stored in glass desiccators until analyzed. The representative coupons from both temperature treatments (RT and 6°C) were chosen for examination with an energy-dispersive x-ray spectrometry (EDS) coupled to scanning electron microscopy (SEM). The coupons were weighed, cleaned with a brush and pickled according to the Standard Practice for Preparing, Cleaning, and Evaluating Corrosion Test Coupons (ASTM standard G 1-90, 2011). The pickling (HCl + 20 g/L Sb_2O_3 + 50 g/L $SnCl_2$, 23°C, 5 min) was performed four times. To determine the mass loss of the base metal when removing the corrosion products, a replicate uncorroded control coupon was cleaned by the same procedure as that used for the test coupons. Loss of mass of the carbon steel coupons was determined and the average corrosion rates ($\mu m\ a^{-1}$) were calculated in the following way (Equation 1):

$$\text{Corrosion rate} = (K \times W)/(A \times T \times D), \quad (1)$$

where K, constant (0.365×10^4), W, mass loss (mg), T, time of exposure (days), A, area (cm^2) of carbon steel coupon, D, density (carbon steel)(g/cm^3).

The coupons were subsequently inspected under a low magnification stereomicroscope to reveal the nature of the possible corrosion attack.

Scanning Electron Microscopy of Biofilms

Carbon steel coupons were immersed in phosphate (0.1 M, pH 7.2) buffered 2.5% glutaraldehyde, immediately after they were removed from incubation bottles, for fixation of presumed biofilm. After 2–16 h the coupons were rinsed with phosphate buffer three times. Dehydration was carried out with an ethanol series, followed by hexamethyldisilazane (Fluka, Switzerland). The membrane was coated with Au/Pd (10 nm, 208 HR High Resolution Sputter Coater, Cressington Scientific Instruments Inc., USA) and examined with Hitachi S-4800 FESEM (Japan) operated at 1–5 kV.

Results

Water Chemistry

The groundwater from 100 m depth from a borehole in the VLJ-repository in Olkiluoto was brackish and sulfate rich (**Table 2**). The water was slightly alkaline with pH of 7.8 measured on site. Conductivity (Ec) of the groundwater was 2.11 mS cm^{-1}. After the 3 months (3M) incubation period the conductivity of the water in the incubation bottles slightly decreased to 2.07 at RT (3M-RT) and 1.91 at 6°C (3M-6°C). However, after 8 months

TABLE 2 | The main chemical components in the groundwater in the beginning of the experiment.

Al $\mu g\ L^{-1}$	Br $mg\ L^{-1}$	Ca $mg\ L^{-1}$	Cl $mg\ L^{-1}$	Fe $mg\ L^{-1}$	Mg $mg\ L^{-1}$	Mn $mg\ L^{-1}$	K $mg\ L^{-1}$	SiO_2 $mg\ L^{-1}$	Na $mg\ L^{-1}$	SO_4 $mg\ L^{-1}$	pH	Ec $mS\ cm^{-1}$
4	1.4	57	430	0.08	17	0.12	7.7	14	354	123	7.8	2.11

(8M) the conductivity increased to 2.95 and 2.97 in the RT and 6°C incubations, respectively (**Table 3**). The redox potential (mV vs. standard hydrogen electrode, SHE) was −78.7 in 3M-RT and −42.8 in 3M-6°C. After 8 months the redox potential was −78.3 mV vs. SHE and −77.7 in the 8M-RT and 8M-6°C microcosms, respectively. The pH also increased during the experiment period to 8.2 and 8.4 in the microcosms at 6°C and room temperature, respectively (**Table 3**).

Microbial Community Analyses

The number of bacterial 16S rRNA genes in the groundwater was 1.69×10^6 copies mL^{-1} at the beginning of the experiment. After 3-months a 10-fold increase in the concentration of bacterial 16S rRNA genes was detected (1.95×10^7 copies mL^{-1} in 3M-6°C, and 2.23×10^7 mL^{-1} in 3M-RT, $p < 0.01$) in the groundwater exposed to carbon steel (**Figure 1A**). After 8 months the concentrations of 16S rRNA gene copies were 4.53×10^6 mL^{-1} in 8M-6°C and 2.76×10^7 mL^{-1} in 8M-RT (**Figure 1A**). The number of 16S rRNA gene copies from groundwater without carbon steel at 6°C remained at the same level as in the beginning of the experiment, i.e., 1.29×10^6 mL^{-1} in 3M-6°C and 1.43×10^6 mL^{-1} in 8M-6°C, $p < 0.01$ (**Figure 1A**). However, at room temperature the concentration of 16S rRNA gene copies had increased to 8.81×10^6 copies mL^{-1} in 3M-RT compared to that of the baseline samples but decreased again toward 8 month of incubation to 3.81×10^5 copies mL^{-1} in 8M-RT (**Figure 1A**). A denser biofilm, according to the number of 16S rRNA gene copies, was detected on RT-coupons (2.82×10^6 and 7.03×10^6 copies cm^{-2}, after 3 and 8 months, respectively, $p < 0.05$) than on 6°C-coupons (4.42×10^4 and 1.77×10^5 copies cm^{-2}, after 3 and 8 months, respectively, $p < 0.05$; **Figure 1A**).

The DGGE analysis of the bacterial community showed a distinct and diverse banding pattern in the groundwater samples at the beginning of the experiment (**Figure 2A**). The bacterial 16S rRNA gene profiles showed between 4 and 35 different bands per sample, after the 3-months incubation period (**Figure 2A**). DGGE analysis revealed between 7 and 26 bands after the 8-months incubation period (**Figure 2A**). The diversity of DGGE bands increased notably compared to the baseline samples over the 3-months incubation period (**Figure 2A**). DGGE analysis showed that the bacterial species composition of the biofilm formed on carbon steel coupons was diverse and bacterial communities of the incubation water and the biofilms of the corresponding carbon steel samples were generally similar, with exception of the water and biofilm of the microcosms at room temperature after 3-months. It was also shown that the bacterial diversity was greater in the groundwater exposed to carbon steel compared to the groundwater without carbon steel (**Figure 2A**).

The obtained 16S rRNA gene sequences fell into four different bacterial clusters in the phylogenetic analysis, Betaproteobacteria, Alphaproteobacteria, Epsilonroteobacteria, and Deltaroteobacteria (**Figure 3**). The dominating class was Betaproteobacteria (**Figure 3**). In the original groundwater, only sequences belonging to Betaproteobacteria were detected (**Figure 3**).

The Composition of the SRB Community

The number of *dsr*B gene copies mL^{-1} analyzed by qPCR was 6.3×10^4 in the original groundwater. After 3-months at 6°C the concentration increased to 2.3×10^6 copies mL^{-1} in the water ($p < 0.01$), but decreased to 8.7×10^3 copies mL^{-1} at the end of the 8 months of incubation at 6°C ($p < 0.01$; **Figure 1B**). At RT the detected amounts of *dsr*B copies were slightly higher, 3.4×10^6 and 1.5×10^4 copies mL^{-1} after 3 and 8 months incubation, respectively (**Figure 1B**). When the groundwater was exposed to carbon steel the amount of *dsr*B copies in water increased to 3.5×10^6 mL^{-1} after 3 months in both temperatures ($p < 0.01$) and decreased to the level of 2–3×10^5 copies mL^{-1} after 8 months (**Figure 1B**). The amount of *dsr*B gene copies in biofilm on the 3M-6°C-coupons and 3M-RT-coupons was 1.9×10^2 and 2.3×10^2 copies cm^{-2}, respectively (**Figure 1B**). After 8-months the amount of *dsr*B in biofilm increased to 5×10^4 and 1.9×10^3 copies cm^{-2} on 8M-6°C-coupons and 8M-RT-coupons, respectively ($p < 0.01$; **Figure 1B**).

In all samples, the PCR-DGGE profiles revealed diverse SRB communities with several different *dsrB* amplicons. In the original groundwater three DGGE bands were detected belonging to genus *Thermodesulfovibrio* (**Figure 4**). Between 7 and 13 *dsr*B-gene DGGE bands were observed per sample after 3-months and between 7 and 17 bands after 8-months of incubation (**Figure 2B**). The diversity of the SRB community had changed over the 3-months incubation at 6°C when bands belonging to families Desulfovibrionaceae, Desulfobulbaceae, and Thermodesulfovibrio were detected in the water. At RT the detected bands belonged to families Desulfobacteraceae, Desulfovibrionaceae, Desulfobulbaceae, and Thermodesulfovibrio. All *dsrB* amplicons detected belonged to Deltaproteobacteria and affiliated with the families Desulfobacteraceae, Desulfovibrionaceae, Desulfobulbaceae and Thermodesulfovibrio (**Figure 4**). Similar *dsr*B-genes were detected both from the biofilm on the carbon steel and from

TABLE 3 | Characteristics of water and surface layers.

	pH	Conductivity (mS cm^{-1})	Redox potential (mV vs. SHE)	Deposits main components (w%)	Corrosion rate μm a^{-1}
Groundwater in the beginning	7.8	2.11		–	–
3M-RT	8.2	2.07 ± 0.006	−78.7 ± 3.7	60.9 Fe, 10.4 C, 31.4 O, 0.2 S	1.4
3M-6°C	8.1	1.91 ± 0.06	−42.8 ± 0	62.7 Fe, 9.4 C, 14.9 O, 14.1 S	11.4
8M-RT	8.4	2.95 ± 0	−77.7 ± 37.6	76.5 Fe, 2.2 C, 15.6 O, 8.2 S	1.4
8M-6°C	8.2	2.97 ± 0.02	−78.3 ± 12.8	91.2 Fe, 2.2 C, 13.2 O, 0.5 S	–

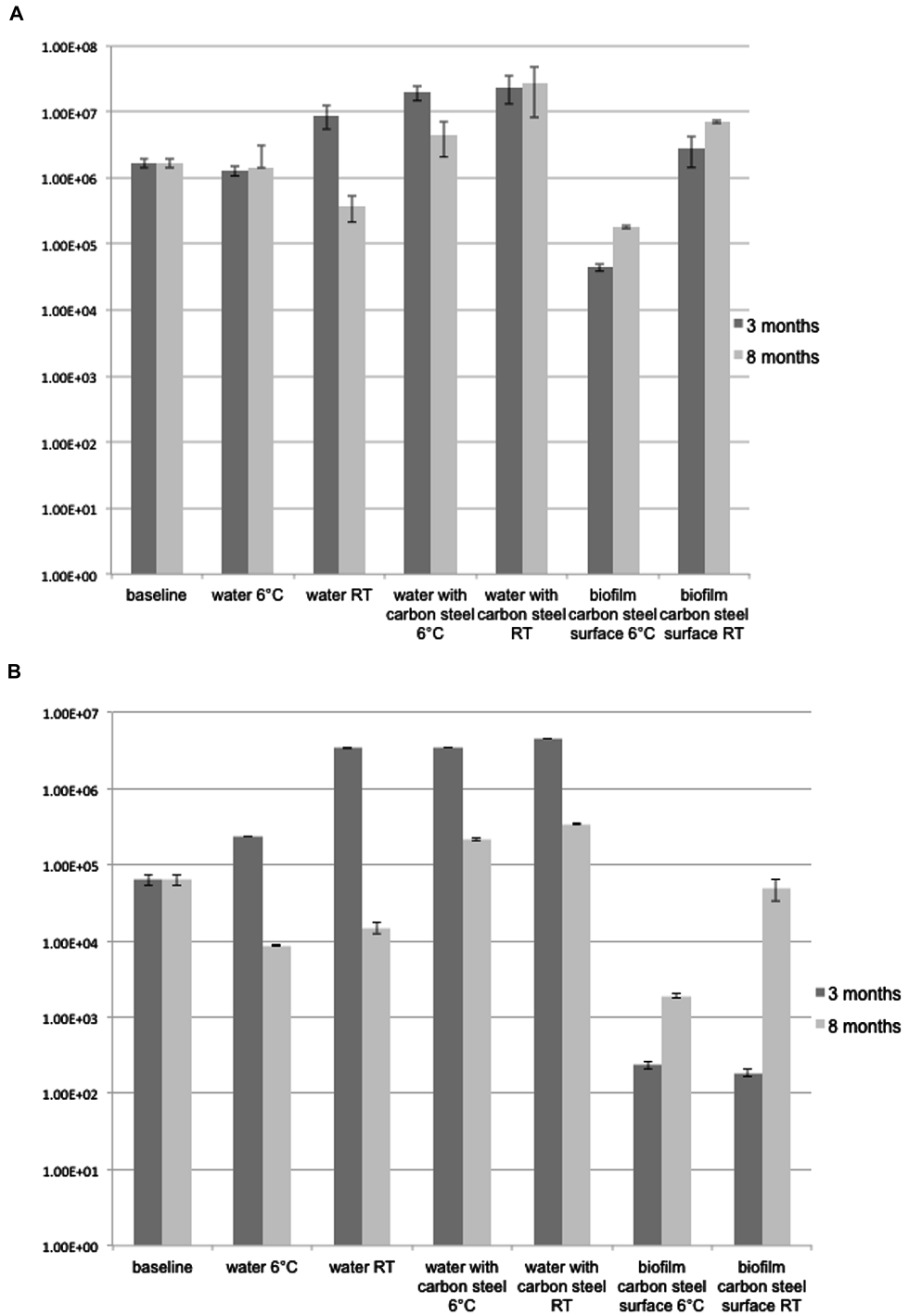

FIGURE 1 | (A) 16S rRNA gene copies ml^{-1} groundwater or carbon steel $(cm^2)^{-1}$. The error bars present SE of mean ($n = 3$). **(B)** *dsr*B gene copies ml^{-1} groundwater or carbon steel $(cm^2)^{-1}$. The error bars present SE of mean ($n = 3$).

the water (**Figures 2B** and **4**). The majority of all sequences resembled *dsrB* genes of the family Desulfobulbaceae. SRB belonging to the genus *Desulfobacula* were detected only from samples that were incubated at room temperature (**Figure 4**).

Corrosion

After 3 months of exposure to groundwater a small amount of dark deposit could be seen on the surfaces of carbon steel coupons (**Figure 5**) at both temperatures. By visual examination, the carbon steel coupons were covered by a thicker, more even

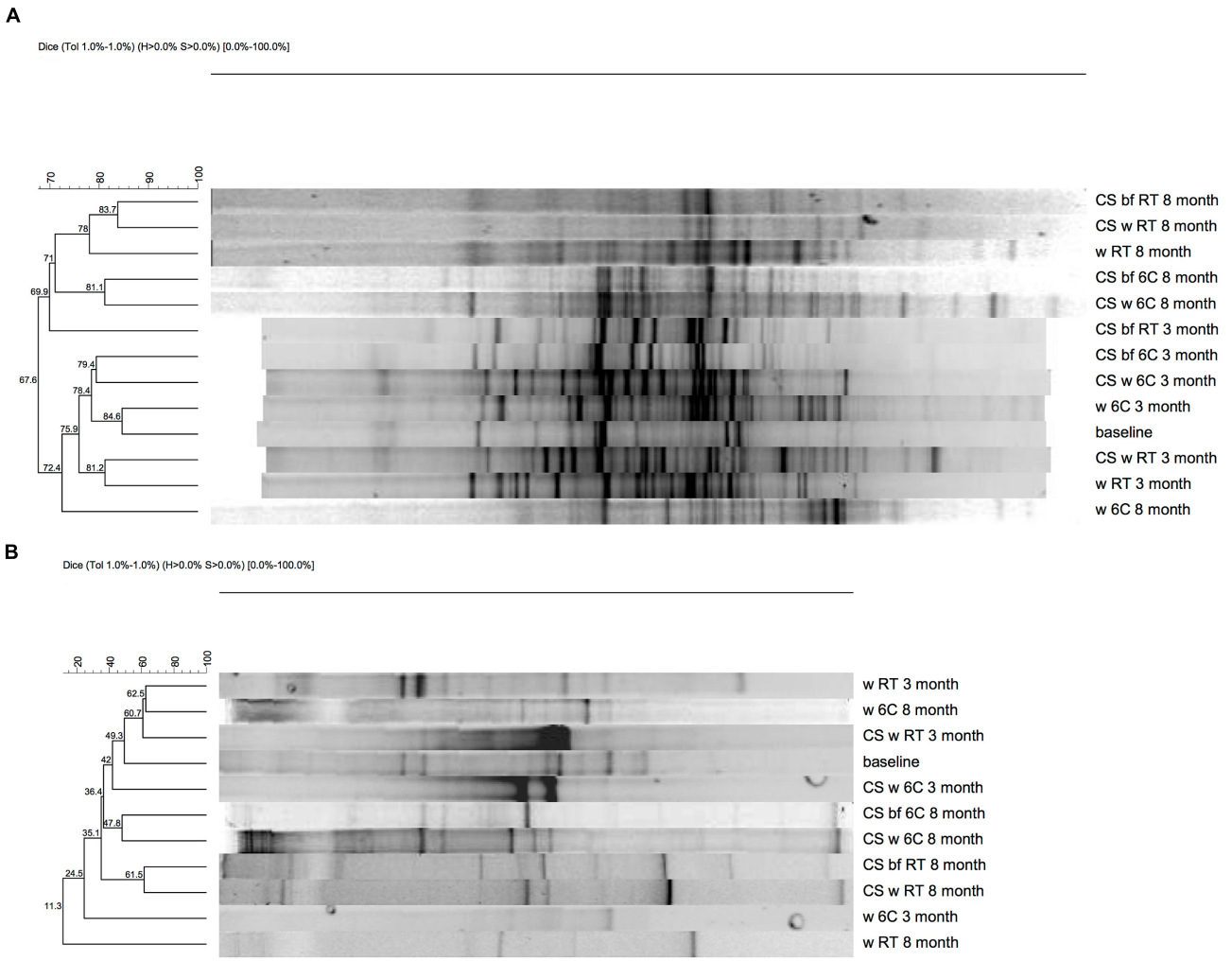

FIGURE 2 | Denaturing gradient gel electrophoresis (DGGE), (A) 16S rRNA (B) *dsr*B gene.

and darker deposit layer when incubated at room temperature (3M-RT-coupons) compared to those kept at 6°C (3M-6°C-coupons; **Figure 5**). In addition, the 3M-6°C-coupons had light brown areas on the surfaces, which were not detected on the surfaces of the 3M-RT-coupons (**Figure 5**). A higher concentration of sulfur was detected in the deposit on the 3M-RT-coupons compared to the 3M-6°C-coupons (14.1 and 0.2 w-%, respectively; **Table 3**). During 8 months (8M) the formation of the deposits became more intensive, the deposits were darker and contained more iron (w-% 76.5 RT/ 91.2 6°C) but less oxygen (w-% 15.6 RT/ 13.2 6°C) and carbon (w-% 2.2 RT/6°C) on the surfaces both 8M-6°C-coupons and 8M-RT-coupons compared to 3-months exposure (**Figure 5**; **Table 3**). In addition, the concentration of sulfur was higher on the 8M-RT-coupons compared to the 8M-6°C-coupons (8.2 w-% and 0.5 w-%, respectively).

After 3 months of exposure, measurable corrosion rates of 1.4 and 11.4 $\mu m\ a^{-1}$ were detected on 3M-RT-coupon and one 3M-6°C-coupon, respectively. After 8 months of exposure measurable corrosion of 1.35 $\mu m\ a^{-1}$ was detected in one 3M-RT-coupon. In addition, incipient localized corrosion was observed by stereomicroscope and FE-SEM examination in all coupons after pickling (**Figures 6** and **7**). The 8M-RT-coupon, having the measurable corrosion rate, also presented shallow corrosion pits with a maximum diameter of 200 μm (**Figure 7**). Also, a small number of smaller corrosion pits with a diameter of 50 μm were observed on one 8M-6°C-coupon (**Figure 6**).

Besides the corrosion pits, the FE-SEM examination revealed microorganisms adhered to the carbon steel surfaces. Microorganisms were detected on the steel surface already after 3-months but the corrosion pits evolved toward the end of the incubation period and were visible in samples incubated for 8 months (**Figures 6** and **7**). A higher number of microorganisms were detected on the surface of the 3M-RT-coupons than on the 3M-6°C-coupons. After 8 months of incubation a dense biofilm as well as a substantial number of corrosion pits had formed on the carbon steel coupons

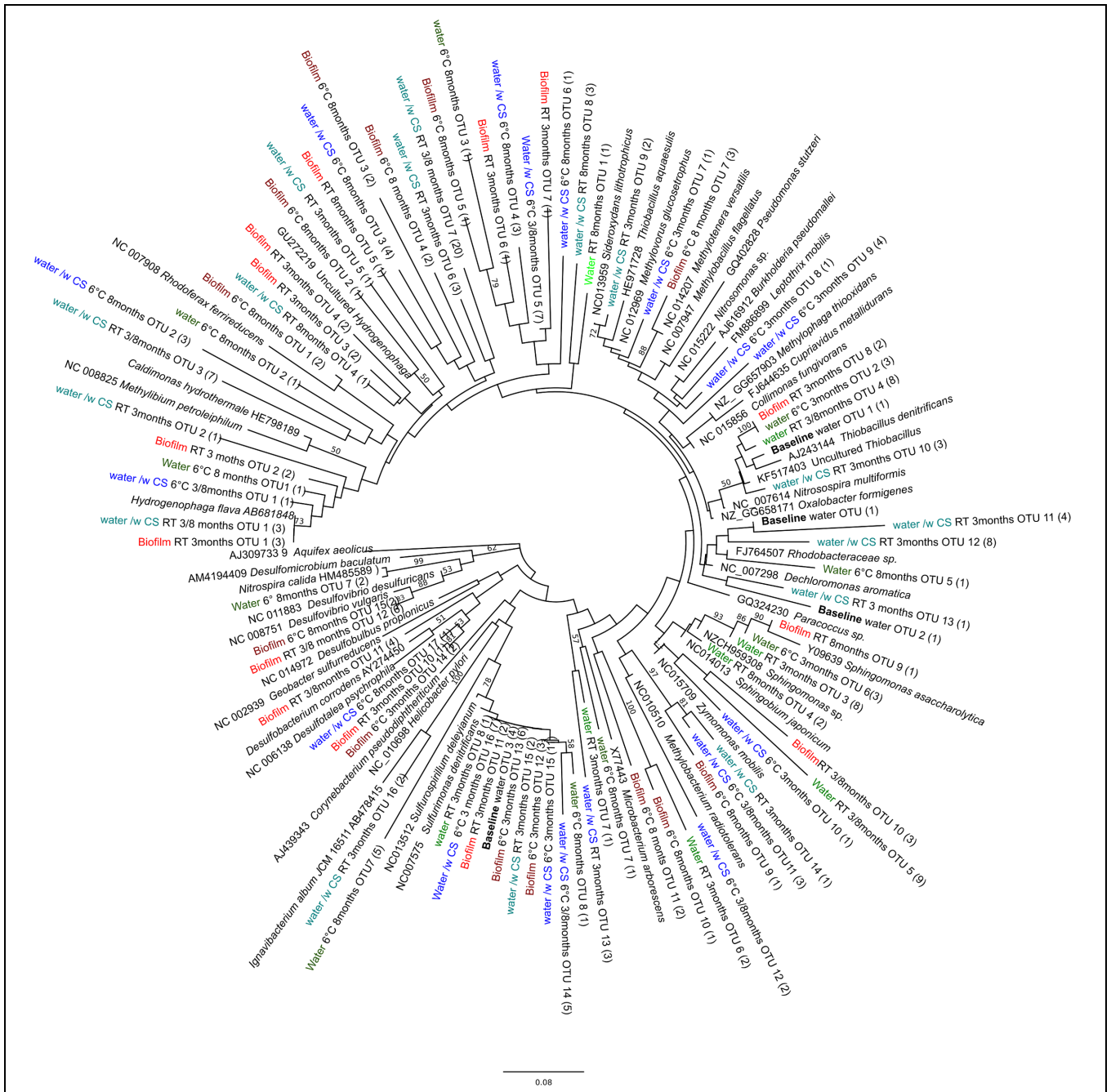

FIGURE 3 | Phylogenetic tree of bacterial diversity, based on the 16S rRNA gene sequences obtained by 16S gene-based PCR-DGGE, in relation to cultured- and the closest uncultured relatives. Parentheses indicate the number of individual sequences within the OTU. Bootstrap values, calculated from 1,000 repetitions, are shown at branch points with >50% support. The scale bar indicates 0.08 nucleic acid substitutions. The tree is rooted by *Aquifex aeolicus*.

incubated at both temperatures. Temperature also affected the type of microorganisms predominating on the carbon steel surfaces (**Figures 6** and **7**). In the pits formed at 6°C microbial cells were mostly 2 μm × 1 μm rods covered with corrosion products (**Figure 6**), whereas at RT the pits were covered with long spirilli-formed microbial cells (**Figure 7**).

Discussion

Microbially induced corrosion and its effects on metallic materials are of critical importance globally. For example, the annual cost of corrosion problems caused by MIC is estimated to be 1 trillion USD worldwide (Fleming, 1996). The biofilm formation is the key step in inducing MIC (Lee and Characklis,

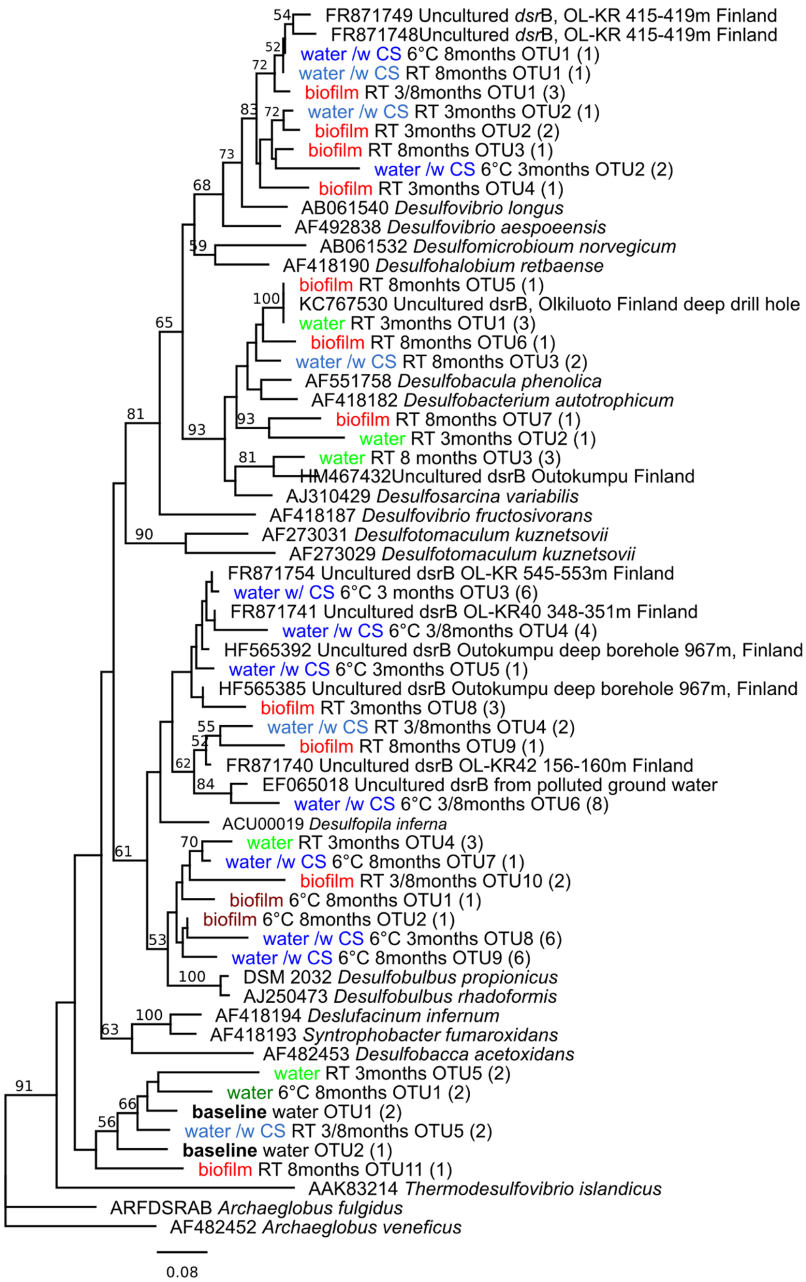

FIGURE 4 | Phylogenetic tree of sulfate reducing bacteria, based on the *dsr*B sequences (amino acid) obtained by *dsr*B gene-based PCR-DGGE, in relation to cultured SRB and the closest uncultured relatives. Parentheses indicate the number of individual sequences within the OTU. Bootstrap values, calculated from 1,000 repetitions, are shown at branch points with >50% support. The scale bar indicates 0.08 amino acid substitutions. The tree is rooted by *Archaeoglobus veneficus*.

1993). Corrosion accelerating conditions, especially localized corrosion, can evolve rapidly under the biofilm. In the present study, it was demonstrated that microorganisms in natural deep groundwater have great affinity to form biofilm on the surface of carbon steel and cause localized corrosion even when corrosion cannot be detected by gravimetric analysis. Our results indicate that deep groundwater microorganisms benefited from carbon steel. In the presence of carbon steel the planktonic microbial community in the incubation water was more diverse and 100-fold more abundant compared to the environment without carbon steel.

The Betaproteobacteria were the most dominant bacterial class in all samples where carbon steel was present, whereas in groundwater incubated without carbon steel the microbial community was less diverse and resembled more the community detected from groundwater in the beginning of

the experiment. Betaproteobacteria belonging to Burkholderiales and Hydrogenophilales are known to use hydrogen as an energy source (Willems et al., 1989; Stöhr et al., 2001). Hydrogen is released at the cathodic site, i.e., from the carbon steel, in corrosion processes and thus may attract hydrogenotrophic Betaproteobacteria (Cord-Ruwisch and Widdel, 1986). Betaproteobacteria also belonging to Burkholderiales, on the other hand, are able to oxidize iron, which has been shown to accelerate corrosion of iron (Hedrich et al., 2011; Liu et al., 2012). In our study the dominant iron oxidizing Betaproteobacteria appeared to be temperature dependent, showing *Leptothrix* species in the samples incubated at 6°C. At RT the dominant iron oxidizing Betaproteobacteria resembled most closely *Sideroxydans* species. The reddish corrosion deposit formed on surfaces of carbon steel is likely to be a result from iron oxidizing bacteria. Iron reducing Betaproteobacteria were detected in samples where carbon steel

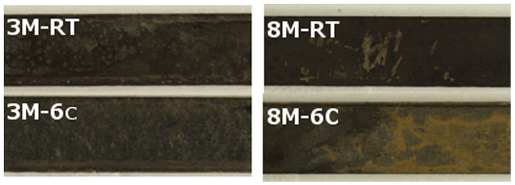

FIGURE 5 | Surface of carbon steel.

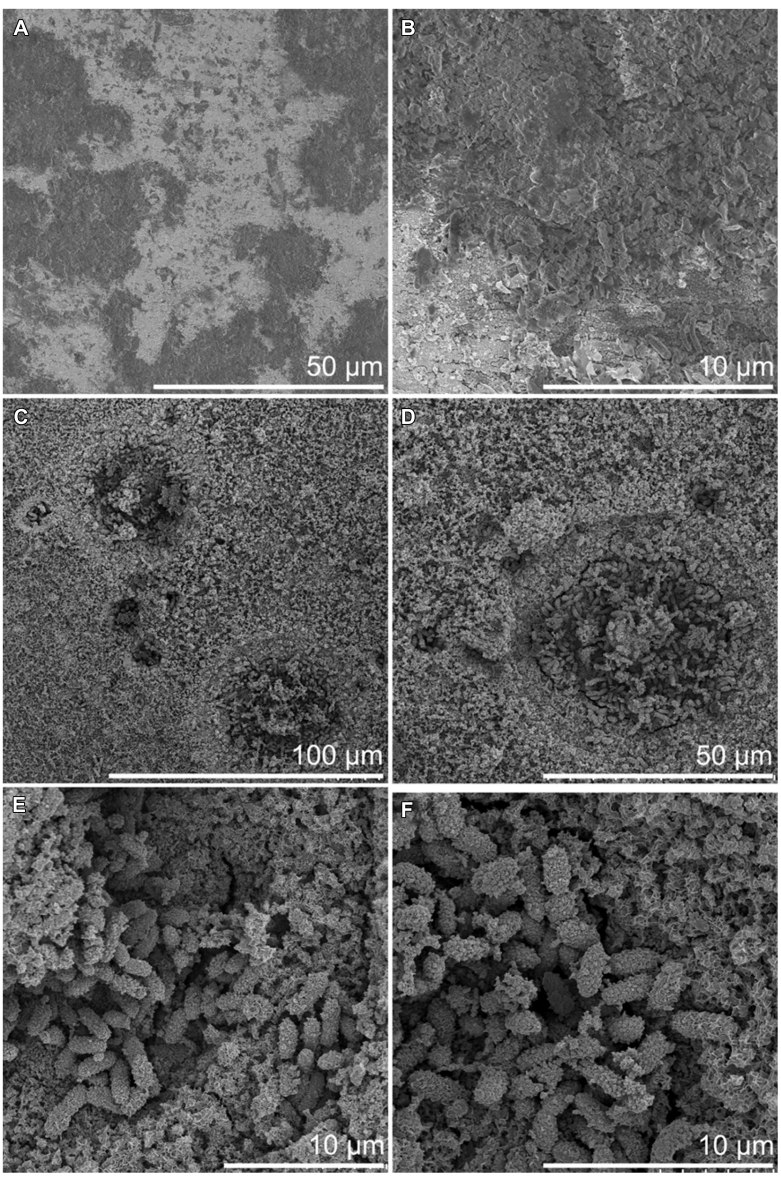

FIGURE 6 | Surface of carbon steel incubated at 6°C by FE-SEM. (A,B) After 3 months incubation. **(C–F)** After 8 month incubation.

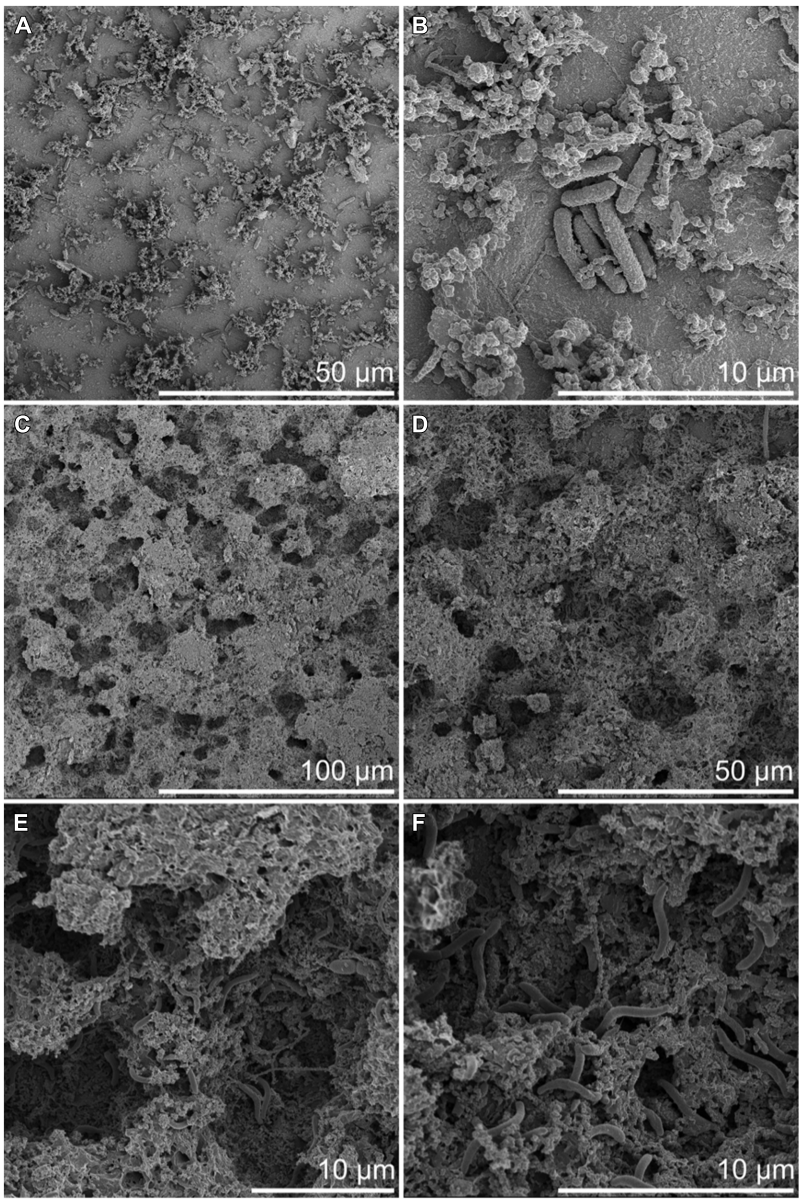

FIGURE 7 | Surface of carbon steel incubated at RT by FE-SEM. (A,B) After 3 months incubation. **(C–F)** After 8 months incubation.

was available. These iron reducers may cause corrosion by the reduction and removal of passive films of ferric compounds under anoxic conditions whereas under oxic conditions they are able to protect carbon steel from corrosion by improving the surface passivation (Herrera and Videla, 2009).

Sulfate-reducing bacteria are generally assumed to be the main bacterial group causing MIC in anoxic environments (Hamilton, 1985; Lee et al., 1995). SRB produce hydrogen sulfide, which is a corrosive agent. They are also believed to consume the excess hydrogen and thus stimulate the corrosion reaction. Nevertheless, an alternative reaction has recently been reported by which microbes can induce the corrosion of steels by using elemental iron (Fe^0) as electron source (Dinh et al., 2004). This process is used by at least some SRB and methanogenic archaea. In nutrient-poor environments, such as the deep groundwater examined in this study, the microbes may be more "aggressive" toward steels, since the concentration of organic electron donors is low (Xu and Gu, 2011). In the native groundwater at the beginning of our experiment, only *dsr*B sequences belonging to the Thermodesulfovibrio family were detected. However, in the presence of carbon steel the diversity of the SRB community was increased to comprise Deltaproteobacterial SRB. The SRB were detected from both the incubation water and as part of the biofilm attached to the surfaces of carbon steel. The planktonic and biofilm SRB communities were similar but were

affected by temperature. At RT SRB belonging to the family Desulfobacteraceae were detected whereas at 6°C the *dsr*B genes belonged to family Desulfobulbaceae. The Desulfobulbaceae include Fe^0-utilizing SRB, such as the *Desulfopila inferna.* In our experiment, this bacterium was abundant in water exposed to carbon steel, and it has been proposed that *Desulfopila inferna* is capable of using Fe^0 as electron donor for sulfate reduction (Dinh et al., 2004; Enning et al., 2012). In addition, *dsr*B sequences matching *Desulfobacterium corrodens*, another Fe^0 utilizing SRB, were found in biofilm at RT (Enning et al., 2012). Enning et al. (2012) reported that the corrosion crust observed together with these SRB consisted of Fe, S, O, and C. This is in accordance with our results, where these compounds were also detected, especially after the 3-months incubation period. Both the SRB community and the corrosion products were different depending on the temperature of incubation. At RT the amount of sulfur in deposits was 14 times higher than at 6°C while the abundance of Si was higher at 6°C than at RT. However, the amount of Fe in the deposits was not affected by temperature and was elevated in all conditions after 8-months of incubation. Microbial cells in the samples incubated at room temperature were typically long (up to 4 μm), slender (0.3 μm) and had curved or corkscrewed shape. Cells had very smooth cell envelope suggesting that they may be Gram-positive. In addition, stalk-like structures, formed customarily by iron oxidizing Proteobacteria were clearly visible at RT. At 6°C microbes were rod shaped and frequently observed as diplobacilli and had an appearance suggesting that they are Gram-negative bacteria. According to SEM images, the incubation temperature had significant effect on the morphology of the microorganisms attached on the surfaces of the samples. In conclusion, our results demonstrate that in order to obtain reliable results on MIC, the measurements should be carried under *in situ* temperature. In addition, the carbon steel had a positive effect on the bacterial community size and composition, indicating that the native groundwater bacterial communities may benefit from compounds in carbon steel and that the corrosion of carbon steel and subsequent release of these compounds may cause the number of microorganisms to increase and composition of microbial community to change.

Author Contributions

PR, LC, MV, MB conceived, designed and performed the experiments, analyzed the data and wrote the paper. MR performed the SEM analyses, analyzed the data and wrote the paper. ES analyzed the DGGE data and wrote the paper.

Acknowledgments

This work was supported by the Finnish Research Program on Nuclear Waste Management 2011–2014 (REMIC). The help of the staff in TVO Olkiluoto NPP during the samplings is gratefully acknowledged. The authors thank the skillful assistance of Taru Lehtikuusi and Seppo Peltonen in the experimental work.

References

Altschul, S., Gish, W., Miller, W., Myers, E., and Lipman, D. (1990). Basic local alignment search tool. *J. Mol. Biol.* 215, 403–410. doi: 10.1016/S0022-2836(05)80360-2

Bomberg, M., Nyyssönen, M., Pitkänen, P., Lehtinen, A., and Itävaara, M. (2015). Active microbial communities inhabit sulphate-methane interphase in deep bedrock fracture fluids in Olkiluoto, Finland. *BioMed Res. Int.* (in press). doi: 10.1155/2015/979530

Brody, J., and Kern, S. (2004). Sodium boric acid: a Tris-free, cooler conductive medium for DNA electrophoresis. *Biotechniques* 36, 214–216.

Bryant, R. D., Jansen, W., Boivin, J., Laishley, E. J., and Costerton, J. W. (1991). Effect of hydrogenase and mixed sulfate-reducing bacterial populations on the corrosion of steel. *Appl. Environ. Microbiol.* 57, 2804–2809.

Carpén, L., Maukonen, J., and Salo, S. (2012). Accelerated corrosion of carbon steel and zinc in oxygen-free groundwater - Due to the microbiological activity? *Paper Presented at the Nace International Corrosion Conference & Expo 2012,* Paper No. C2012-0001397 (Salt Lake City, UT: Nace International).

Carpén, L., Rajala, P., Vepsäläinen, M., and Bomberg, M. (2013). Corrosion behaviour and biofilm formation on carbon steel and stainless steel in simulated repository environment. *Paper Presented at the Eurocorr 2013*, Paper no. 1589, Estoril.

Cord-Ruwisch, R., and Widdel, F. (1986). Corroding iron as a hydrogen source for sulphate reduction in growing cultures of sulphate-reducing bacteria. *Appl. Microbiol. Biotechnol.* 25, 169–174. doi: 10.1007/BF00938942

Dinh, H., Kuever, J., Zligmann, M., Hasse, A., Stratmann, M., and Widdel, F. (2004). Iron corrosion by novel anaerobic microorganisms. *Nature* 427, 829–832. doi: 10.1038/nature02321

Drummond, A. J., Ashton, B., Buxton, S., Cheung, M., Cooper, A., Heled, J., et al. (2010). *Geneious v5.3*. Available at: http://www.geneious.com

Enning, D., Venzlaff, H., Garrelfs, J., Dinh, H., Meyer, V., Mayrhofer, K., et al. (2012). Marine sulfate-reducing bacteria cause serious corrosion of iron under electroconductive biogenic mineral crust. *Environ. Microbiol.* 14, 1462–2920. doi: 10.1111/j.1462-2920.2012.02778.x

Fleming, H. C. (1996). "Economical and technical overview," in *Microbially Influenced Corrosion of Materials*, eds E. Heitz, H. C. Fleming, and W. Sand (New York, NY: Springer-Verlag), 6–14.

Geets, J., Borremans, B., Diels, L., Springael, D., Vangronsveld, J., van der Lelie, D., et al. (2006). DsrB gene-based DGGE for community and diversity surveys of sulphate-reducing bacteria. *J. Microbiol. Methods* 66, 194–205. doi: 10.1016/j.mimet.2005.11.002

Guidon, S., and Gascuel, O. (2003). A simple, fast, and accurate algorithm to estimate large phylogenies by maximum likelihood. *Syst. Biol.* 52, 696–704. doi: 10.1080/10635150390235520

Hamilton, W. A. (1985). Sulphate-reducing bacteria and anaerobic corrosion. *Annu. Rev. Microbiol.* 39, 195–217. doi: 10.1146/annurev.mi.39.100185.001211

Hammer, Ø., Harper, D. A. T., and Ryan, P. D. (2001). PAST: paleontological statistics software package for education and data analysis. *Palaeontol. Electronic.* 4, 1–9.

Haveman, S., and Pedersen, K. (2002). Distribution of culturable microorganisms in Fennoscandian shield groundwaters. *FEMS Microbiol. Ecol.* 39, 129–137. doi: 10.1111/j.1574-6941.2002.tb00914.x

Hedrich, S., Schlömann, M., and Johnson, B. (2011). The iron-oxidizing proteobacteria. *Microbiology* 157, 1551–1564. doi: 10.1099/mic.0.045344-0

Herrera, L., and Videla, H. (2009). Role of iron-reducing bacteria in corrosion and protection of carbon steel. *Int. Biodeterior. Biodegradation* 63, 891–895. doi: 10.1016/j.ibiod.2009.06.003

Itävaara, M., Nyyssönen, M., Kapanen, A., Nousiainen, A., Ahonen, L., and Kukkonen, I. (2011). Characterization of bacterial diversity down to a depth of 1,500 m in the Outokumpu deep borehole, Fennoscandian shield. *FEMS Microbiol. Ecol.* 77, 295–309. doi: 10.1111/j.1574-6941.2011.01111.x

Jukes, T. H., and Cantor, C. R. (1969). *Evolution of Protein Molecules.* New York, NY: Academic Press, 21–132. doi: 10.1016/b978-1-4832-3211-9.50009-7

Lee, W., and Characklis, W. (1993). Corrosion of mild steel under anaerobic biofilm. *Corrosion* 49, 186–199. doi: 10.5006/1.3316040

Lee, W., Lewandowski, Z., Nielsen, P., and Hamilton, W. (1995). Role of sulfate-reducing bacteria in corrosion of mild steel: a review. *Biofouling* 8, 165–194. doi: 10.1080/08927019509378271

Little, B., Wagner, P., and Mansfeld, H. (1992). An overview of microbiologically influenced corrosion. *Electrochim. Acta* 37, 2185–2194. doi: 10.1016/0013-4686(92)85110-7

Liu, F., Zhang, J., Zhang, S., Li, W., Duan, J., and Hou, B. (2012). Effect of sulphate reducing bacteria on corrosion of Al Zn In Sn sacrificial anodes in marine sediment. *Mater. Corros.* 63, 1521–4176. doi: 10.1002/maco.201005955

Muyzer, G., Dewaal, E., and Uitterlinden, A. (1993). Profiling of complex microbial populations by denaturing gradient gel electroforesis (DGGE) and temperature gradient gel electroforese (TGGE) in microbial ecology. *Int. J. Gen. Mol. Microbiol.* 73, 127–141.

Nyyssönen, M., Bomberg, M., Kapanen, A., Nousiainen, A., Pitkänen, P., and Itävaara, M. (2012). Methanogenic and sulphate-reducing microbial communities in deep groundwater of crystalline rock fractures in Olkiluoto, Finland. *Geomicrobiol. J.* 29, 863–878. doi: 10.1080/01490451.2011.635759

Purkamo, L., Bomberg, M., Nyyssönen, M., Kukkonen, I., Ahonen, L., Kietäväinen, R., et al. (2013). Dissecting the deep biosphere: retrieving authentic microbial communities from packer-isolated deep crystalline bedrock fracture zones. *FEMS Microbiol. Ecol.* 85, 324–337. doi: 10.1111/1574-6941.12126

Rajala, P., Bomberg, M., Kietäväinen, R., Kukkonen, I., Ahonen, L., Nyyssönen, M., et al. (2015). Rapid reactivation of deep subsurface microbes in the presence of C-1 compounds. *Microorganisms* 3, 17–33. doi: 10.3390/microorganisms3010017

Rajala, P., Carpèn, L., Vepsäläinen, M., Raulio, M., and Bomberg, M. (2014). "Microbially induced corrosion of carbon steel and stainless steel in alkaline ground water -composition and metabolic functionality of biofilm," in *Proceedings of the Annual Waste Management Conference 2014*, Proceedings no. 14391, Phoenix, AZ.

Stöhr, R., Waberski, A., Liesack, W., Völker, H., Wehmeyer, U., and Thomm, M. (2001). *Hydrogenophilus hirschii* sp. nov., a novel thermophilic hydrogen-oxidizing beta-proteobacterium isolated from Yellowstone National Park. *Int. J. Syst. Evol. Microbiol.* 51, 481–488.

Thompson, J., Higgins, D., and Gibson, T. (1994). Clustal W: improving the sensitivity of progressive multiple sequence alignment through sequence weighting, position-specific gap penalties and weight matrix choice. *Nucleic Acids Res.* 22, 4673–4680. doi: 10.1093/nar/22.22.4673

TVO. (2015). *Teollisuuden Voima Oyj*. Available at: http://www.tvo.fi/operatingwaste (accessed March 24, 2015).

Videla, H. A. (1996). *Manual of Biocorrosion*. Boca Raton, FL: Lewis Publishers.

Wagner, M., Roger, A., Flax, J., Brusseau, G., and Stahl, D. (1998). Phylogeny of dissimilatory sulfite reductases supports an early origin of sulphate respiration. *J. Bacteriol.* 180, 2975–2982.

Weisburg, W. G., Barns, S. M., Pelletier, D. A., and Lane, D. J. (1991). 16S ribosomal DNA amplification for phylogenetic study. *J. Bacteriol.* 173, 697–703.

Whelan, S., and Goldman, N. (2001). A general empirical model of protein evolution derived from multiple protein families using a maximum-likelihood approach. *Mol. Biol. Evol.* 18, 691–669. doi: 10.1093/oxfordjournals.molbev.a003851

Willems, A., Busse, J., Goor, M., Pot, B., Falsen, E., Jantzen, E., et al. (1989). *Hydrogenophaga*, a New Genus of Hydrogen-Oxidizing Bacteria That Includes *Hydrogenophaga flava* comb. nov. (Formerly *Pseudomonas flava*), *Hydrogenophaga palleronii* (Formerly *Pseudomonas palleronii*), *Hydrogenophaga pseudoflava* (Formerly *Pseudomonas pseudoflava* and "*Pseudomonas carboxydoflava*"), and *Hydrogenophaga taeniospiralis* (Formerly *Pseudomonas taeniospiralis*). *Int. J. Syst. Bacteriol.* 39, 319–333. doi: 10.1099/00207713-39-3-319

Xu, D., and Gu, T. (2011). Bioenergetics explains when and why more severe MIC pitting by SRB can occur. *Paper Presented at the NACE Corrosion 2011*, Paper No. 11426 (Houston, TX: NACE International).

Conflict of Interest Statement: The authors declare that the research was conducted in the absence of any commercial or financial relationships that could be construed as a potential conflict of interest.

frontiers in Microbiology

ORIGINAL RESEARCH
published: 09 June 2015
doi: 10.3389/fmicb.2015.00573

Revealing the unexplored fungal communities in deep groundwater of crystalline bedrock fracture zones in Olkiluoto, Finland

*Elina Sohlberg *, Malin Bomberg, Hanna Miettinen, Mari Nyyssönen, Heikki Salavirta, Minna Vikman and Merja Itävaara*

VTT Technical Research Centre of Finland, Espoo, Finland

The diversity and functional role of fungi, one of the ecologically most important groups of eukaryotic microorganisms, remains largely unknown in deep biosphere environments. In this study we investigated fungal communities in packer-isolated bedrock fractures in Olkiluoto, Finland at depths ranging from 296 to 798 m below surface level. DNA- and cDNA-based high-throughput amplicon sequencing analysis of the fungal internal transcribed spacer (ITS) gene markers was used to examine the total fungal diversity and to identify the active members in deep fracture zones at different depths. Results showed that fungi were present in fracture zones at all depths and fungal diversity was higher than expected. Most of the observed fungal sequences belonged to the phylum Ascomycota. Phyla Basidiomycota and Chytridiomycota were only represented as a minor part of the fungal community. Dominating fungal classes in the deep bedrock aquifers were Sordariomycetes, Eurotiomycetes, and Dothideomycetes from the Ascomycota phylum and classes Microbotryomycetes and Tremellomycetes from the Basidiomycota phylum, which are the most frequently detected fungal taxa reported also from deep sea environments. In addition some fungal sequences represented potentially novel fungal species. Active fungi were detected in most of the fracture zones, which proves that fungi are able to maintain cellular activity in these oligotrophic conditions. Possible roles of fungi and their origin in deep bedrock groundwater can only be speculated in the light of current knowledge but some species may be specifically adapted to deep subsurface environment and may play important roles in the utilization and recycling of nutrients and thus sustaining the deep subsurface microbial community.

Keywords: fungal communities, high-throughput sequencing, crystalline bedrock fracture, Fennoscandian shield, deep biosphere

OPEN ACCESS

Edited by:
Paul Bodelier, Netherlands Institute of Ecology (NIOO-KNAW), Netherlands

Reviewed by:
William D. Orsi, Woods Hole Oceanographic Institution, USA
Vanessa Rédou, Université de Bretagne Occidentale, France

****Correspondence:***
Elina Sohlberg, VTT Technical Research Centre of Finland, Tietotie 2, Espoo 02150, Finland
elina.sohlberg@vtt.fi

Specialty section:
This article was submitted to Terrestrial Microbiology, a section of the journal Frontiers in Microbiology

Received: *17 April 2015*
Accepted: *25 May 2015*
Published: *09 June 2015*

Citation:
Sohlberg E, Bomberg M, Miettinen H, Nyyssönen M, Salavirta H, Vikman M and Itävaara M (2015) Revealing the unexplored fungal communities in deep groundwater of crystalline bedrock fracture zones in Olkiluoto, Finland. Front. Microbiol. 6:573. doi: 10.3389/fmicb.2015.00573

Introduction

Fungi are mainly decomposers that play a major role in the biodegradation of plant materials in terrestrial ecosystems. In deep biosphere environments, however, fungal diversity, and their role in ecosystem functioning remains largely unknown. According to the small number of studies conducted thus far viable fungi have been detected in different sub-seafloor and subterranean environments, such as groundwater aquifers, continental sedimentary and hard rocks, and deep

subseafloor sediments (Sinclair and Ghiorse, 1989; Madsen and Ghiorse, 1993; Fredrickson and Onstott, 1996; Palumbo et al., 1996; Raghukumar and Raghukumar, 1998; Ludvigsen et al., 1999). Based on a recent review by Nagano and Nagahama (2012) deep sea extreme environments harbor diverse fungal communities. These fungi represent mainly Ascomycota phyla with Eurotiomycetes, Dothideomycetes, Sordariomycetes, and Saccharomycetes being the most abundant fungal classes but also fungi belonging to Basidiomycota and Chytridiomycota have been detected with culture-independed methods. The first viable fungi isolated from deep continental hard rock environments originated from deep crystalline bedrock aquifers in Äspö, Sweden (Pedersen, 1987) and later several yeast species were detected also with DNA-based methods (Pedersen et al., 1996).

Physiological properties of fungi isolated with traditional cultivation-based methods from deep crystalline bedrock fractures indicate that they are adapted to and capable of growing in the subterranean environment (Ekendahl et al., 2003). Identification of facultative anaerobic or strictly anaerobic fungi from deep sea environments indicates that anaerobic conditions are not a limiting factor for fungal growth (Cathrine and Raghukumar, 2009; Jebaraj et al., 2010; Raghukumar, 2012). Remains of bacterial biofilms in these environments also suggest that the biofilms may have supported the nutritious demands of the fungal cells in otherwise extremely oligotrophic environments (Gadd, 2006). Fungi generally prefer mono- or polysaccharides as carbon and energy sources, which would have been provided by the bacterial biofilms. In addition, fungi may be involved in the formation of humic aggregates and carbon contribution by fungal biomass as well as production of extracellular enzymes involved in the cycling of nutrients, as suggested by Raghukumar et al. (2010).

Cultivation-based techniques reveal only a small part of the fungal communities in any environment and with these methods activity of fungi in deep subsurface environments cannot be determined. Novel sequencing technologies would have great potential for obtaining new information on the diversity and ecological role of fungi in the deep geosphere. However, in contrast to the characterization of the bacterial and archaeal communities of deep subsurface habitats, the fungal communities in deep crystalline bedrock fractures have not been characterized by modern culture-independent methods, such as high throughput amplicon sequencing. In this study DNA- and cDNA-based high-throughput amplicon sequencing analysis of the fungal internal transcribed spacer (ITS) gene markers was used to examine the total fungal diversity and to identify the active members of the fungal communities in deep bedrock fracture zones at different depths in Olkiluoto, Finland. The results reveal previously unexplored fungal communities in deep groundwater of crystalline rock fracture zones.

Materials and Methods

Site Description and Sampling

Olkiluoto is an island situated in the western coast of Finland. The bedrock of Olkiluoto belongs to the Fennoscandian Shield and consists mostly of Precambrian highly deformed and metamorphosed migmatitic mica gneisses. The characteristics of the site have been described in more detail by Pitkänen et al. (2004), Posiva (2013), Nyyssönen et al. (2012) and Bomberg et al. (2015). In brief, the groundwater in Olkiluoto is anaerobic and saline and salinity increases with depth from 0.1 g L^{-1} at ground level to 100 g L^{-1} at 900 m. The temperature of the groundwater varies from ca. 7°C at 50 m to 20°C at 1000 m and pH is slightly alkaline in all fracture zones. Sulfate is enriched in the upper 300 m and beneath this depth zone, only traces of sulfate are observed. The concentration of methane increases with depth from 300 m.

Altogether, deep groundwater samples from 17 different boreholes at depths ranging from 296 to 798 m were collected between December 14th, 2009 and August 21st, 2013 from the Olkiluoto island in Finland (**Table 1**). Sampling was done as described in Bomberg et al. (2015). In short, the samples were collected from multi-packered boreholes as well as from open boreholes where the sampling section was packered-off in order to seal off a specific water-conducting fracture zone from the rest of the borehole. This isolated fracture zone was purged by pumping out the water collected between the packers and allowing water from the isolated fracture zone to run into the packered off section of the borehole. In order to assure that sample water was coming only from fracture zones, the packer-sealed fracture zones were pumped for at least 4 weeks before sampling. The conductivity and pH of the pumped water was followed, and when the values settled, it was assumed that the water represents the endemic fracture zone water. Microbial biomass for nucleic acid analyses was concentrated from 500 to 1000 mL samples by filtration on cellulose acetate filters (0.2 μm pore size, Corning) by vacuum suction in the anaerobic chamber. The filters were immediately cut out from the filtration funnels with sterile scalpels and frozen on dry ice.

Geochemical Analyses of the Groundwater

Conductivity, pH, total dissolved solids (TDS), alkalinity, total organic, and dissolved inorganic carbon and different cations and anions were analyzed from the sampled groundwater. Analysis methods are described before (Posiva, 2013; Bomberg et al., 2015). All analyses were conducted by Posiva Oy (Olkiluoto, Finland).

Nucleic Acid Isolation

Total DNA was isolated directly from the frozen cellulose-acetate filters. The filters were cut to pieces with sterile scalpels in a laminar flow hood, and the DNA was extracted and purified with the PowerSoil DNA extraction kit (MoBio Laboratories, Inc., Solana Beach, CA). The isolation was performed according to the instructions of the manufacturer. The isolated and purified DNA was then stored frozen at −80°C until use. Total RNA was isolated directly from the frozen cellulose-acetate filter with the PowerWater RNA isolation kit (MoBio Laboratories, Inc., Solana Beach, CA). The filters were thawed on ice and care was taken to minimize the time of thawing. The intact filters were inserted into the bead tubes with flame-sterilized forceps and the RNA extraction was performed according to the manufacturer's instructions. Negative DNA and RNA isolation controls were

TABLE 1 | Selected hydrogeochemical characteristics of the Olkiluoto fracture zones investigated in this study.

Sample*	Ec (ms/m)	pH	TDS (mg L^{-1})	N tot (mg L^{-1})	NPOC (mgC L^{-1})	DIC (mgC L^{-1})	HCO_3(mg L^{-1})
OL-KR13/296m_10	897	7.9	4994	0.71	10	27	134
OL-KR13/296m_12	807	7.8	4481	4.4	38	28	116
OL-KR3/303m_12	987	8	5378	0.6	7.8	4.3	26
OL-KR20/323m_13	1116	7.7	6242	0.91	11	13	67
OL-KR6/328m_10	1832	7.9	10670	<0.05	<2.40	4.1	22.6
OL-KR6/330m_13	1800	8	10590	0.051	<2.40	4.6	27
OL-KR25/330m_11	642	7.9	3502	0.96	13	33	171
OL-KR3/340m_11	1012	8.3	5656	1.1	12	4.1	25
OL-KR23/347m_09	2190	7.5	12710	0.42	5.1	3.9	17.1
OL-KR46/372m_13	1778	7.7	10460	1.5	18	5.9	32
OL-KR46/390m_13	1701	7.7	10370	0.86	4.7	18	98
OL-KR5/405m_12	2170	8.1	12880	1.2	19	<3	16
OL-KR49/415m_09	2670	8.1	15900	0.16	<3	<3	9.8
OL-KR9/423m_11	2300	7.5	13430	0.38	5.1	3	11.6
OL-KR9/510m_11	2960	8.1	18580	0.66	6.6	<3	7.3
OL-KR2/559m_10	4110	8.6	25500	1.1	11	<3.75	17.7
OL-KR1/572m_10	3770	7.8	23260	0.41	5	<3.75	14
OL-KR44/693m_13	5520	7.3	37410	10	110	6.5	30
OL-KR29/798m_10	7820	7.3	53210	3.1	<12	<12	7.9

**Vertical depth and sampling year are presented in the sample name.*

also included. DNA contamination of the RNA extracts was checked by PCR with bacterial 16S rRNA gene specific primers 8F (Edwards et al., 1989) and P2 (Muyzer et al., 1993). If no PCR product was obtained, sample was assumed uncontaminated and the RNA extract was submitted to cDNA synthesis. If a PCR product was obtained, the RNA extract was first treated with DNase (Promega, Madison, WI) according to the manufacturer's instructions before cDNA synthesis. Aliquots of 11.5 μL of RNA was incubated together with 250 ng random hexamers (Promega, Madison, WI) and 0.83 mM final concentration dNTP (Thermo Fisher Scientific, Vantaa, Finland) at 65°C for 5 min and cooled on ice for 1 min. The cDNA was synthesized with the Superscript III kit (Invitrogen), by adding 4 μL 5 × First strand buffer, 40 U DTT and 200 U Superscript III to the cooled reactions. To protect the RNA template from degradation, 40 U recombinant RNase inhibitor, RNaseOut (Promega, Madison, WI), was used. The reactions were incubated at 25°C for 5 min, at 50°C for 1 h and at 70°C for 15 min. Two to four parallel reactions per sample as well as no template controls were performed. The parallel reactions were subsequently pooled. RT-PCR was also performed on the negative RNA extraction controls as well as negative reagent RT-PCR controls.

Amplification Library Preparation

The amplification libraries for 454 high throughput sequencing were prepared by PCR from the DNA and cDNA samples. Fungal ITS fragments were amplified in a two-step PCR. First, a 420–825 bp long fragment was amplified with primers ITS1F and ITS4 (White et al., 1990; Gardes and Bruns, 1993). Length of the ITS region varies between species (Manter and Vivanco, 2007). The product of this PCR was used as template in a secondary PCR with tagged primers ITS1F and ITS2 (Buée et al., 2009) generating a ca. 400 bp product. First step of PCR amplification was performed in 10 μL and second step in 50 μL reactions containing 1x KAPA Fidelity buffer (Kapa Biosystems, Cape Town, South Africa) (2 mM $MgCl_2$), 0.3 mM final concentration of dNTP, 6 pmol of each primer in 10 μL reaction and 25 pmol in 50 μL reaction, 1 unit of KAPA Hifi polyeraze enzyme (Kapa Biosystems, Cape Town, South Africa) and 1 μL of template. The PCR program for both PCR steps consisted of an initial denaturation step at 98°C for 5 min, 39 cycles of 20 s at 98°C, 50 s at 50°C, and 30 s at 72°C. A final elongation step of 5 min was performed at 72°C. In addition negative reagent PCR controls with only PCR-grade water as template were performed to rule out possible contamination. PCR products were confirmed in 1 × SYBR safe-stained 1% agarose gel electrophoresis. The pyrotag libraries were sent for sequencing to Beckman Coulter Genomics (Danvers, MA, USA) where amplicon libraries were purified and smallest and largest fragments were removed based on fragment analysis. Pyrotaq libraries were run on a Genome Sequencer FLX 454 System according to manufacturer's protocol (454 Life Sciences/Roche Applied Biosystems, Branford, CT, USA).

Sequence Processing and Analysis

The sequence reads obtained from the 454 high-throughput sequencing were partly processed with in-house pipeline (Salavirta et al., in press). First, sequences were subjected to quality control using the MOTHUR software version v.1.31.2 (Schloss et al., 2009). During this step, adapters, barcodes, and primers were removed from the sequence reads, and the quality of base-calls was assessed in order to remove erroneous reads from the data set. Subsequently, chimeric sequence reads were removed from the data set with the USEARCH algorithm version 5.2.236 (Edgar, 2010) by *de novo* detection and through similarity

searches against the 97% representative OTU set of the UNITE reference database (Kõljalg et al., 2013).

Groups of similar sequences, i.e., Operational Taxonomic Units (OTUs), were selected from the chimera-filtered sequence data set following open-reference OTU-picking protocol of QIIME v. 1.7.0 (Caporaso et al., 2010) against the 97% identity UNITE database OTU sets (Kõljalg et al., 2013). OTU clustering was performed with UCLUST v. 1.2.22q (Edgar, 2010) and the seed sequences were selected as the representative OTU sequences. Only few fungal sequences were amplified from negative control. This is possibly due to two-step PCR and these OTUs based on these sequences were removed from the entire sequence data set. All reads that failed to hit the UNITE reference database with a minimum of 60% identity threshold were discarded as sequencing error. Next, singleton OTUs, i.e., OTUs that were represented by a single sequence, were filtered from the data set. Finally, taxonomy from domain to species-level was assigned to OTUs via representative OTU sequences with BLASTN with a maximum *E*-value of 0.001 (Altschul et al., 1990). Alpha diversity indexes chao1 (Chao, 1984) and Shannon diversity index (Shannon, 1948) were calculated from normalized sequence data where sequence data was subsampled to 1500 sequences to adjust for sequencing coverage. Heatmaps of the fungal communities were generated in the R environment (R Development Core Team, 2008) utilizing the reshape2 (Wickham, 2007), grid (Murrell, 2005), and ggplot2 (Wickham, 2009) packages.

Statistical Analysis

Non-metric multidimensional scaling analyses (NMDS) for comparing the similarity of the fungal communities at class level between the different samples and the effect of chemical parameters on the microbial communities was performed using the PAleontological STatistics (PAST) program (Hammer et al., 2001). Non-Euclidean Bray-Curtis distance matrix was generated with PAST and correlation coefficient values of the matrix was calculated with 1000 permutations with R. In addition Pearson's correlation between total (DNA fraction) and active (RNA fraction) fungal communities was calculated at genus level with compare_taxa_summaries.py command within QIIME. Venn diagrams of each sample were calculated with MOTHUR showing shared OTUs between DNA and RNA fraction.

Accession Numbers

The fungal ITS gene region sequences have been submitted to the European Nucleotide Archive (ENA, https://www.ebi.ac.uk/ena/) under accession numbers ERS706390- ERS706426.

Results

Fungal Diversity and Community Structure in Different Bore Holes

Fungal sequences were detected in the DNA fraction of all of the 19 analyzed fracture water samples and in 18 samples of the RNA fraction. In total 378,831 quality-filtered fungal ITS sequences were obtained from the different fracture zones. The number of obtained sequences ranged from 306 to 24,616 in different samples with a median of 10,941 sequences per sample (Table S1). When comparing the Chao1 OTU richness estimate values to true detected OTU numbers, 22–100% of estimated fungal OTUs were obtained from the subsampled sequence data meaning that sequencing depth was sufficient enough to fully characterize the fungal communities in most of the samples. Altogether, 965 fungal OTUs ranging from 33 OTUs at 328 m in OL-KR6 to 163 OTUs in OL-KR9 at 423 m in DNA fraction and 7 OTUs in OL-KR3 at 303 m to 69 OTUs at 330 m and 405 m in RNA fraction were detected in the total sequence data (Table S1). Fungal diversity based on subsampled OTU richness in the DNA samples originating from the fracture waters peaked at 347 m in OL-KR23 (79 OTUs) and was lowest at 328 m in OL-KR6 (19 OTUs) (**Figure 1**). In RNA fraction highest OTU richness was detected at 390 m in OL-KR46. However, no clear connection between sampling depth and fungal OTU numbers was detected. In the DNA fraction highest Shannon diversity index ($H' = 4.3$), which indicates the abundance and evenness of the species present, was obtained at 423 m depth in sample OL-KR9 and lowest at 330 m depth in sample collected from OL-KR6 ($H' = 1.0$). In the active fungal community highest diversity was observed at 510 m in OL-KR9 ($H' = 3.5$). No fungi were detected in OL-KR44 at 693 m in the active fungal community.

Most of the observed fungal sequences belonged to the phylum Ascomycota (63.9%). Phylum Basidiomycota was represented by 8.9% of all the sequences. Other fungal phyla detected were Chytridiomycota, Glomeromycota, and Zygomycota, which were represented as a minor (0.1–2.1%) part of the whole fungal community. Altogether approximately 25% of the fungal sequences obtained were identified as fungal according to UNITE database but a more specific classification remained unknown. This can be due to insufficient representation of fungal sequences in the sequence databases or these species have not been characterized before and could be considered as novel.

Structure of the fungal communities varied between different fracture zones and sampling times (**Figure 2**). Sequences affiliating with Ascomycota dominated fungal community in both DNA and RNA fraction in most of the fracture zones. However, Basidiomycota was the dominating phylum in OL-KR2 at 559 m (58%) in the total fungal community and in OL-KR9 at 423 m (98.5%) and OL-KR29 at 798 m in the active fungal communities. In addition, Chytridiomycota was the dominating phylum in OL-KR44 at 693 m (66%) in the total fungal community.

Sordariomycetes from the Ascomycota phylum was the major active fungal class (47–100% of all the sequences) in most of the boreholes and also the dominating fungal class in the total fungal community in OL-KR13 at 296 m, OL-KR3 at 303 m, OL-KR25 at 330 m, OL-KR3 at 340 m, OL-KR49 at 415 m and OL-KR29 at 798 m (39–65%) (**Figure 2**). OTUs belonging to Sordariomycetes were mostly related to *Nectria* genus and minority to *Fusarium*, *Pochonia, Pseudallescheria*, and unidentified Hypocreales groups (Figure S1). Fungal class Eurotiomycetes was identified as dominating fungal class in total fungal community of OL-KR20 at 323 m (84%) and OL-KR6 at 330m (2013) (95%) and in active fungal community of OL-KR25 at 330 m (94%). The majority

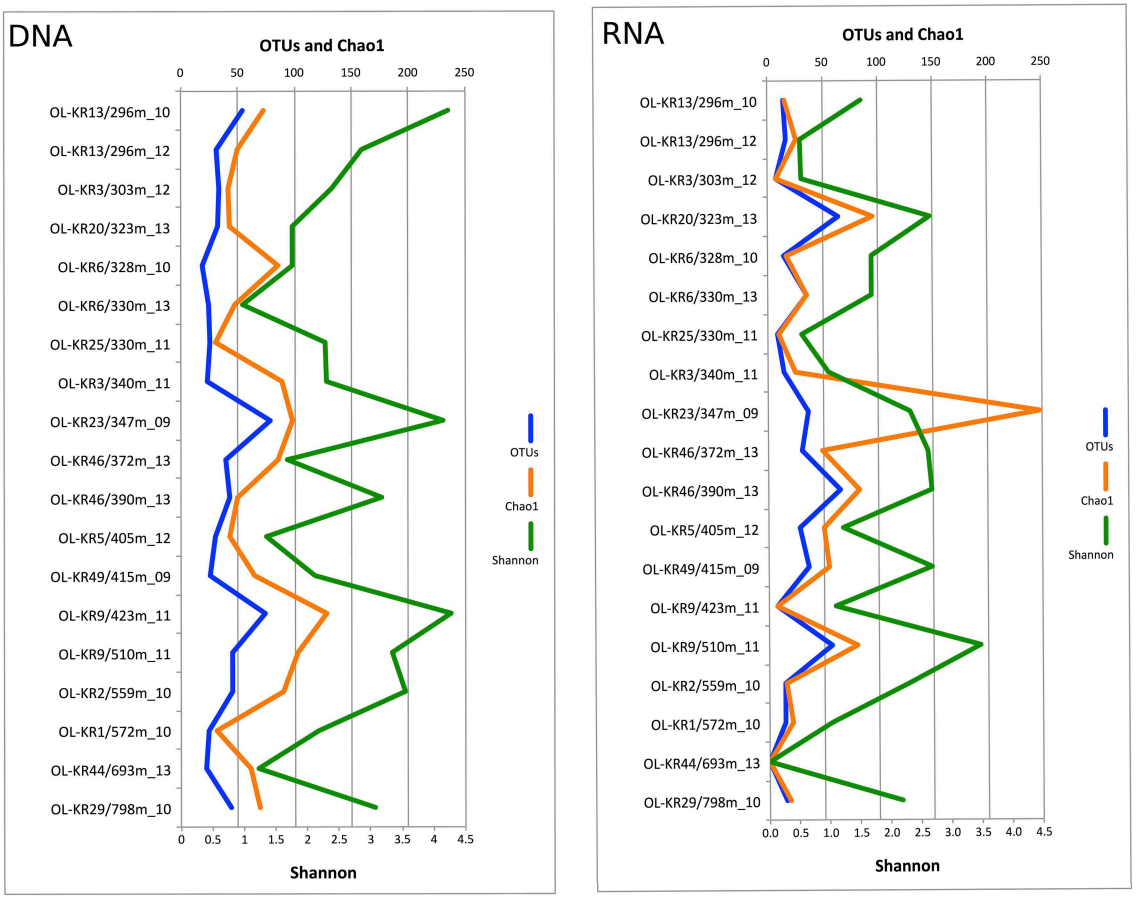

FIGURE 1 | Fungal diversity in deep groundwater of crystalline bedrock fracture zones in Olkiluoto, Finland. Number of observed taxonomic units (OTUs), estimated number of OTUs (Chao1) and Shannon diversity index achieved from the sequence data subsampled to 1500 sequences are presented.

of the sequences belonging to the class Eurotiomycetes were members of the *Penicillium* genus. In addition sequences most closely related to genus *Aspergillus* were found from OL-KR46 at 390 m and OL-KR2 at 559 m as a minor group. Other detected Ascomycota fungal classes in Olkiluoto groundwater samples were Dothideomycetes that dominated the active community in OL-KR6 at 328 m (2010) (40,5%), Leotimycetes that dominated the active fungal community in OL-KR49 at 415 m (47%) and total identified fungal community in OL-KR6 at 328 m (2010) (26%) and OL-KR1 at 572 m (23%) and Saccharomycetes in OL-KR25 at 330 m (19%) and OL-KR6 at 328 m (2010) (5%) total community (**Figure 2**). In addition sequences belonging to class Orbilliomycetes was only found in OL-KR13 at 296 m (2012), but they contributed only as a minor (1.2%) part of the fungal community.

In OL-KR2 at 559 m in the total fungal community and OL-KR29 at 798 m in the active community where Basidiomycota was the dominating identified phylum most of the sequences were closely related to class Microbotryomycetes (37–39%) and more closely to Sporodiobolales order and *Sporobolomyces* and *Rhodotorula* genera (Figure S2). In addition in OL-KR2 at 559 m Tremellomycetes and more specifically *Cryptococcus*-like yeast sequences were detected in total community and Malasseziales order in active community. Other identified Basidiomycota classes in Olkiluoto boreholes were Agaricomycetes in OL-KR13 at 296 m and in OL-KR49 at 415 m in the active community (**Figure 2**). Pucciniomycetes was detected in OL-KR46 at 390 m as a minor part of the total community (0.2%). The Chytridiomycota phylum dominated the total fungal community in OL-KR44 at 693 m (66%) and was also present in OL-KR29 at 798 m. Chytridiomycota sequences from these boreholes were most similar with order Rhizophydiales. No Chytridiomycota sequences were detected in the active fungal community.

Statistical Analysis of Fungal Diversity and Correlation to Geochemistry

Non-metric multidimensional scaling analysis of fungal communities and environmental parameters grouped the samples into four clusters in both DNA and RNA fractures (**Figure 3** and Table S2). The deepest samples (693 and 798 m) clustered together in the DNA fraction that indicates that depth has an influence in the fungal community structure and fungal communities in the deepest communities are most similar. In addition, at greater depth higher salinity also affect the communities and slightly lower pH was observed to significantly correlate with fungal community structure ($p < 0.05$). At depths

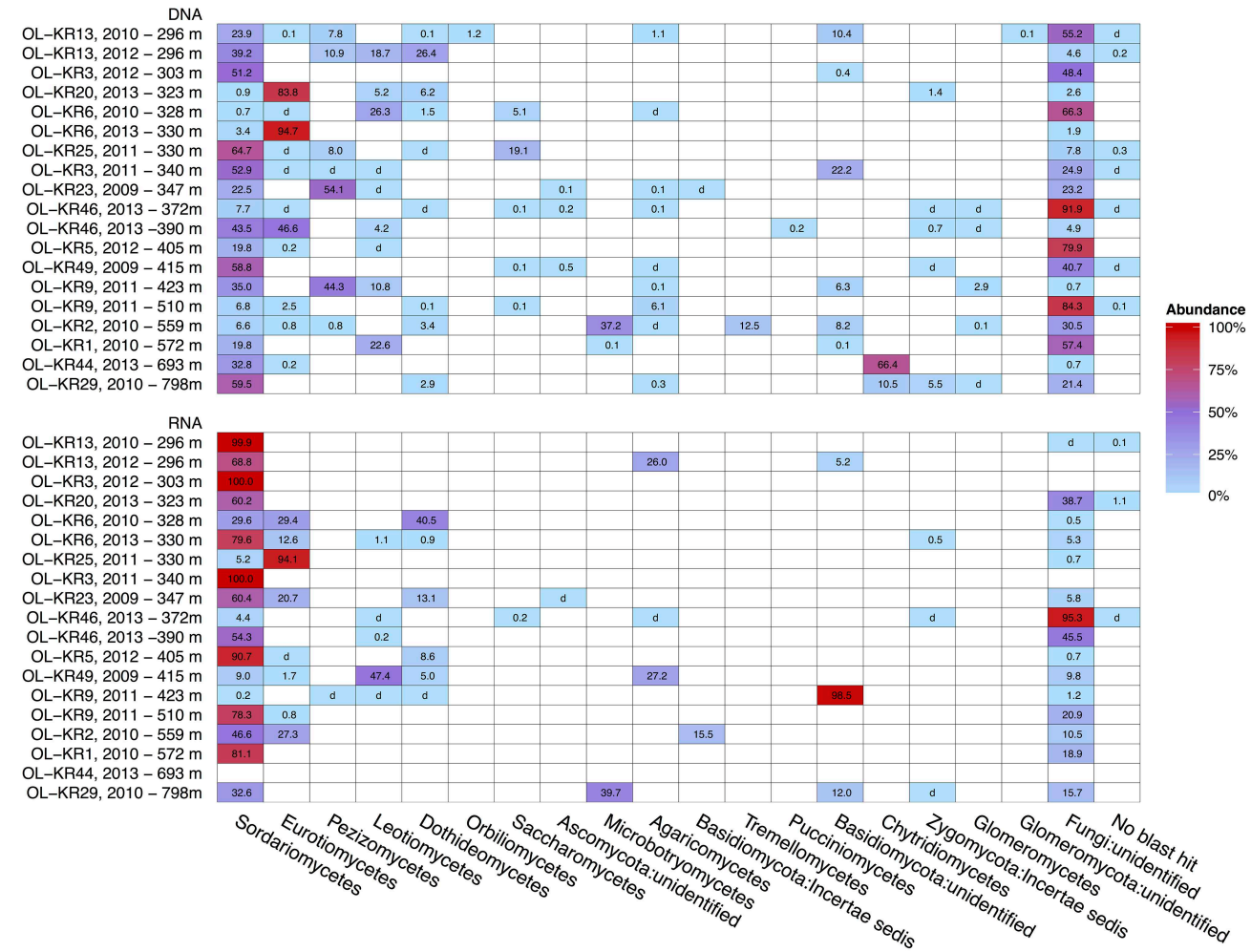

FIGURE 2 | Heatmap of fungal taxonomy in deep groundwater of crystalline bedrock fracture zones in Olkiluoto, Finland. Taxonomic classification of the fungal sequence reads obtained by high throughput sequencing of the total (DNA) and active (RNA) fungal communities presented at the class-level. The samples are arranged by true vertical depth from the surface down. d, detected; but relative abundance less than 0.1%.

from 296 to 340 m carbon availability (DIC, HCO_3) affected the fungal communities in both DNA and RNA fractions and these samples grouped together. In those fracture zones concentrations of DIC and HCO_3 were higher than in deeper fracture zones ranging from 4.1 to 33 mgC L^{-1} of DIC and 25 to 134 mg L^{-1} of HCO_3 (**Table 1** and Table S3). Amount of total organic carbon was highest at 693 m in OL-KR44 where concentration of NPOC was 110 mgC L^{-1}. However, in the NMDS analysis organic carbon concentration did not significantly affect the fungal community structure ($p > 0.1$). Ammonium, nitrate, nitrite, magnesium, and sulfate concentrations were associated with the changes in fungal community profiles especially in OL-KR46 at 372 and 390 m and OL-KR6 at 328 and 330 m in both RNA and DNA fraction that grouped together (**Figure 3**). Especially nitrite and nitrate had a significant effect on the fungal communities in the DNA fraction ($p < 0.001$), but concentrations are very low.

The similarities of fungal communities between DNA and RNA fractions were assessed at genus level by Pearson's one-sided t-distribution tests, with the hypothesis that positive correlation would be detected between total and active communities. In the total dataset Pearson's correlation was 0.33 (± 0.3 95% CI, $p < 0.001$) between the total and active fungal communities. When we compared specific samples, statistically significant correlation ($p < 0.05$) was found in 10 of the 18 fracture zones (Table S4). Statistically significant Pearson's correlations varied between 0.20 and 0.99 with highest correlation found at 372 m in OL-KR46 and weakest at 303 m OL-KR3. Moderate or strong correlation was found in seven of the fracture zones (0.32–0.99). The number of shared OTUs between DNA and RNA fraction was 0–23% (Figure S3).

Discussion

Terrestrial deep subsurface mycology is still an unexplored research field as the major research done until now has been focusing on the diversity and functional studies of bacteria and archaea. To our knowledge this is the first study where fungal communities in deep groundwater of crystalline bedrock fracture

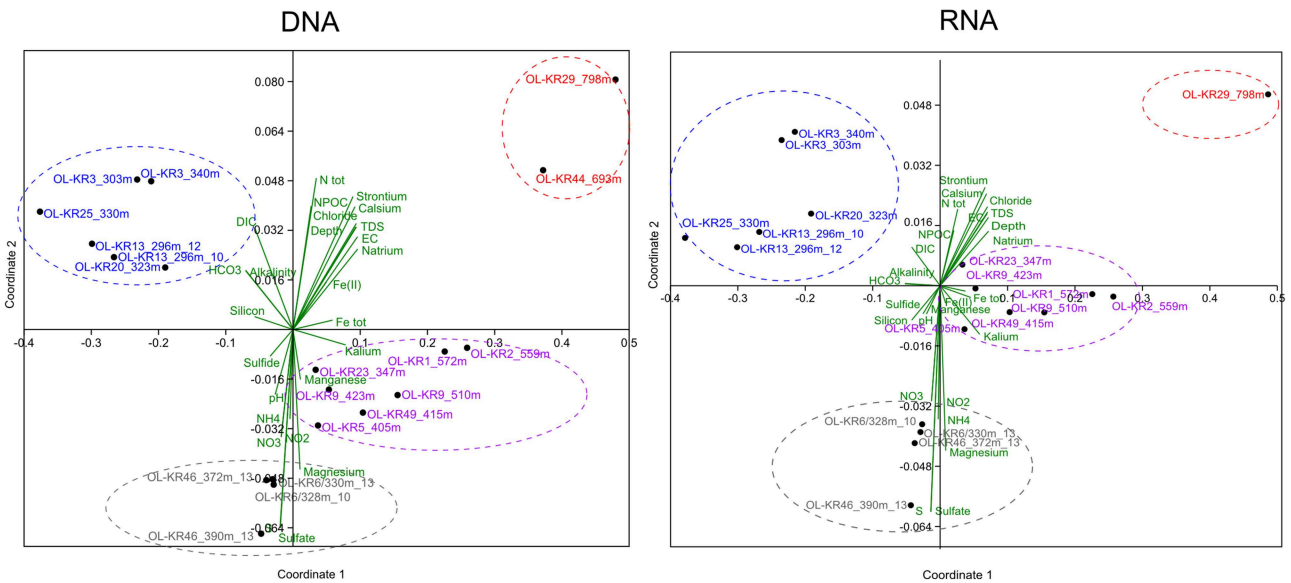

FIGURE 3 | Fungal community structure in relation to sample depth and its associated environmental factors in the groundwater of Olkiluoto fracture zones. A non-metric multidimensional scaling analysis of Bray–Curtis distances was performed to examine the relative abundance of fungal OTUs clustering at the class level.

zones were studied using high-throughput amplicon sequencing. Our results show that diverse and active fungal communities exist in the deep subsurface in Olkiluoto, Finland. Actually, in most of the studied fracture zones the fungal diversity was higher than what has been detected so far in deep sea environment. Deep sea studies have reported up to 43 fungal OTUs with >99% sequence similarity by using fungal ITS region cloning and sequencing (Lai et al., 2007; Nagano et al., 2010; Singh et al., 2012) and Orsi et al. (2013a) detected up to 26 fungal OTUs with 454 pyrosequencing of the eukaryotic 18S rRNA region, whereas we detected up to 163 OTUs in different fracture zones and depths. In our study fungal ITS1 region was chosen over ribosomal genes because it is highly variable and can separate fungi even at species level (Lindahl et al., 2013). ITS2 is considered generally less variable in length than ITS1 and is somewhat better represented in sequence databases. However, ITS1 and ITS2 share many properties, and similar results can be obtained with these two marker genes (Bazzicalupo et al., 2013). With cultivation-based methods five *Rhodotorula* and *Cryptococcus* yeast species and 17 molds have been detected in Fennoscandian rock aquifers in Äspö, Sweden (Ekendahl et al., 2003). Fungi belonging to the Ascomycota phylum were the most abundant in Olkiluoto fracture zones and this is in good agreement with findings from deep sea environments (Nagano and Nagahama, 2012). The deepest fracture zones with higher salinity and temperature and lower pH, were the only ones where fungi belonging to the Chytridiomycota phylum were detected. In addition, the number of basidiomycete species also increased with depth (**Figure 2**). Altogether 25% of the fungal sequences remained unidentified and some of these OTUs could be potentially novel species that have not been characterized before.

Fungal diversity in the deep crystalline fracture water in Olkiluoto was surprisingly high. Unexpectedly no fungal OTUs were detected in the RNA fraction at 693 m depth, where the highest concentration of total organic carbon that fungi could easily use in their metabolism was detected. Although no clear connection between fungal diversity and some of the geochemical parameters were detected, NMDS analysis showed that salinity, which increases with depth, had an influence on the fungal community structure in deeper fracture zones and also nitrogen compounds, sulfate, and inorganic carbon were associated with the changes in the fungal communities at more shallow depths. Fungi are involved in many biogeochemical cycles such as nitrogen and sulfur cycles and fungi are for example able to solubilize minerals, dissolute, and precipitate metal ions, degrade silicates and dissolve rock phosphates in oxygen-limited environments (Gadd, 2006; Sterflinger, 2010). Some filamentous fungi and yeast species are able to oxidase sulfur and sulfur compounds and release sulfate to environment (Wainwright and Grayston, 1989; Reitner et al., 2006; Sterflinger, 2010). Thus, fungi could provide sulfate to sulfate-reducing bacteria and could potentially be involved in the sulfur cycle in subsurface environment. Although fungi and bacteria are competing for the same low amounts of nutrients in subsurface oligotrophic conditions, they can also benefit from each other. For example, Fournier et al. (1998) found that the yeast *Rhodotorula rubra* has a stimulating effect on the growth of the iron sulfide-oxidizing bacterium *Thiobacillus ferrooxidans*. Similar cooperation between fungi and bacteria could potentially occur also in Olkiluoto deep fracture zones.

Members of the Sordariomycetes were the most commonly observed fungi from Olkiluoto fracture waters. These fungi are ubiquitous and cosmopolitan and function in virtually all

ecosystems (Zhang et al., 2006). The group includes pathogens, endophytes of plants, mycoparasites and saprobes involved in decomposition and nutrient cycling but their role in deep biosphere ecosystems is not studied. Sordariomycetes are together with Eurotiomycetes, Saccharomycetes and Dothideomycetes one of the most frequently detected fungal taxa in deep sea environments where living conditions resemble the ones of subterranean deep fracture zones (Nagano and Nagahama, 2012). However, phylotypes within the class Sordariomycetes are few and unique to the studied deep sea areas and their role and functions are still unknown. The fungal sequences obtained from Olkiluoto fracture waters belonging to the Sordariomycetes class were closely related to members of the Nectriaceae family and *Nectria* and *Fusarium* genera. The family Nectriceae includes, e.g., facultative anaerobic microscopic fungi capable of using nitrate or nitrite as alternative terminal electron acceptor in their respiration in the absence of oxygen (Kurakov et al., 2008). Fungal species belonging to *Nectria* have been detected in deep sea sediments (Singh et al., 2012). Some species belonging to genus *Fusarium* that are capable of denitrification have been found in deep sea environments, especially from oxygen-depleted regions (Jebaraj et al., 2010).

NMDS analysis showed correlation between fungal community in OL-KR6 at 330 m, where the most *Penicillium* -sequences were detected, and ammonium, nitrate and nitrite concentrations. This indicates that these species might be involved in nitrogen cycle also in the deep fracture zones in Olkiluoto. Strong correlation between fungal diversity and nitrate has been found also from deep marine sediments (Orsi et al., 2013b) *Penicillium* and *Aspergillus* species are common in outdoor air and terrestrial environments but they are also frequently detected in deep sea environments (Nagano and Nagahama, 2012; Raghukumar, 2012). Deep sea species differed from terrestrial species by their physiological properties and that they were adapted to an aqueous environment (Raghukumar and Raghukumar, 1998; Damare et al., 2006; Damare and Raghukumar, 2008). Salt-tolerant *Penicillium* and *Aspergillus* species have also been identified from oxygen-deficient environments (Raghukumar, 2012) and from anaerobic marine sediments where they were reported to play on important role in the denitrification process (Jebaraj et al., 2010). This suggests a possible versatile role of fungi in major ecological processes in extreme nutrient-poor environments, such as Olkiluoto deep fracture zone fluid. *Aureobasidium* and *Cladosporium* genera found especially in OL-KR6 at 328 m from the RNA-fraction and OL-KR13 at 296 m from the DNA-fraction are reported in many deep sea environment studies (Damare et al., 2008). Common characteristics of these fungal groups are resistance or adaptation to high osmotic pressure that is essential for survival in extreme conditions such as the ones in deep subsurface environments.

The most common classes of the Basidiomycota phylum detected in Olkiluoto groundwater were Microbotryomycetes, Tremellomycetes, and order Malasseziales. These fungal groups are common in deep sea environments (Nagano and Nagahama, 2012) and RNA transcripts from active species within these phyla have been detected in deep marine sediments (Orsi et al., 2013a). Yeast genera within class Microbotryomycetes detected from Olkiluoto were *Rhodotorula* and *Sporobolomycetes* related species. The *Rhodotorula* strain isolated from Fennoscandian rock aquifers in Äspö was able to grow in a wide range of NaCl concentrations (0–100 g L^{-1}) and pH interval of 4–10 at temperatures ranging from 4 to 30°C (Ekendahl et al., 2003). Salinity, pH and temperature in Olkiluoto are also within these limits. This indicates that these yeast species are adapted to conditions in the deep subsurface environment. In Olkiluoto *Sporobolomycetes* related species were also detected in the RNA-fraction, which proves that these species were active in these conditions. *Cryptococcus*-like yeasts from class Tremellomycetes that were identified from Olkiluoto have also been detected from other deep igneous rock aquifers sites on the Fennoscandian shield (Ekendahl et al., 2003) and deep sea environments like deep sea methane seeps (Takishita et al., 2006, 2007). *Cryptococcus*-like yeasts were identified from the active community in OL-KR2 at 559 m where also high methane concentration (386 ml L^{-1}) was detected (Bomberg et al., 2012) that fungi could potentially use in their metabolism. Yeast genera within the order Malasseziales observed in Olkiluoto fracture zone water were closely related to cultured *Malassezia* sp. LCP-2008 and uncultured *Malassezia* from deep sea sediments (Singh et al., 2012). Phylotypes belonging to *Malassezia* sp. have also been recovered from methane hydrate-bearing deep sea sediments (Lai et al., 2007). These yeast species could potentially be methylotrophic and could play a crucial role in converting methane into more accessible carbon and energy substrates for the use of the microbial community (Lai et al., 2007; Raghukumar et al., 2010). In addition, fungi have been found to be involved in methane release in a coal mine (Beckmann et al., 2011). In the coal mine, weathering of coal, and timber were initiated by fungi and in the lower, oxygen depleted regions fungi were observed to perform incomplete oxidation of coal and wood substrates and release reduced carbon substrates, which can be channeled into methanogenesis.

Chytridiomycota that dominated in DNA-fraction of OL-KR44 at 693 m were most similar to the order Rhizophydiales that also have been found in oxygen-deficient marine environments (Raghukumar, 2012). Chytridiomycota are the earliest diverging lineage of fungi and produces zoospores, which indicates adaptation to aquatic environments (Nagano and Nagahama, 2012; Raghukumar, 2012). Chytridiomycota was not detected in RNA fraction. However, statistically significant correlation of fungal taxonomy profiles between total and active communities was found in majority of the fracture zones, which suggests that fungal communities were similar in both DNA and RNA fraction. In three of these samples only weak correlation and in eight of the fracture zones no significance correlation was found, which indicates that total and active communities in these fracture zones were different. In half of samples with no significant correlation insufficient sampling depth of the RNA fraction may have affected the result. In OL-KR6 at 328 m, OL-KR9 at 423 m, OL-KR49 at 415 m and OL-KR25 at 330 m total and active communities appear to be truly different, suggesting that different species are active in these fracture zones compared to total community.

The universal distribution of the many fungal species detected also in deep subsurface environments raises the question about possible contamination. It is known that controlling contamination during drilling in hard rock is more difficult than for example sedimentary rock and life dwelling in fracture zones is exposed to drill water during drilling. Origin of the fungi in Olkiluoto fracture zones is unknown and possible runoff from the surface or contamination during drilling cannot be ruled out based on this study. On the other hand, fungi can be authentic members of the microbial community in the different fracture zones. In this study water from the drill hole was purged for a long time after drilling and by using packers only water originating from the specific fracture zone was collected. Hydrogeochemical characteristics of the fracture fluids also indicates that the chemical parameters were stabilized confirming that water from specific fracture zone was collected. Most importantly, active fungi were found from Olkiluoto groundwater and this indicates that fungi have adapted to deep biosphere conditions and are able to maintain cellular activity.

The metabolic activities of fungi in deep terrestrial environment remain still unknown. However, the first fungal metabolic transcriptomics study from sub-seafloor environment confirms the previous suggestions of living fungi and active fungal metabolism in the deep marine biosphere (Orsi et al., 2013b). The authors showed that 5% of the obtained transcripts were involved in carbohydrate, amino acid, and lipid metabolism suggesting that fungi have a role in organic carbon cycling in sub-seafloor sediment. Fungal expression of transcripts encoding hydrolases involved in protein, carbohydrate, and lipid degradation suggests that they degrade a variety of organic substrates. Fungal dissimilatory nitrate reductase (nar) transcripts involved in energy production were found, which indicate that fungi are involved in nitrogen cycle, probably reducing nitrate and nitrite resulting from nitrate reduction performed by bacteria.

In our study surprisingly high diversity of active fungi were detected for the first time in deep groundwater of crystalline rock fractures. Unlike bacterial 16S rRNA gene, the RNA fraction of fungal ITS is only present in the cell when the genomic copy is being actively transcribed and thus is a true evidence that fungi are active in the deep fracture waters (Blazewicz et al., 2013). The most interesting question now is what are these fungi doing in the deep fracture zones in Olkiluoto and in deep terrestrial environment in general and what is their role in the whole microbial community? Metatranscriptomic studies could be the answer and next step in understanding the functionality of the fungal communities in deep subterranean environments. Interesting was that the amount of organic carbon did not correlate with fungal diversity and activity in deep fracture zones suggesting that fungi may have some other functions in deep subterranean environments than degradation of organic materials.

Acknowledgments

The research project was funded by Posiva Oy and Finnish Research Programme on Nuclear Waste Management (KYT) 2011–2014. Tiina Lamminmäki and Petteri Pitkänen from Posiva Oy are thanked for access to the samples, sample metadata, and fruitful discussions. Mirva Pyrhönen is acknowledged for skillful technical assistance in the laboratory.

Supplementary Material

The Supplementary Material for this article can be found online at: http://journal.frontiersin.org/article/10.3389/fmicb.2015.00573/abstract

References

Altschul, S. F., Gish, W., Miller, W., Myers, E. W., and Lipman, D. J. (1990). Basic local alignment search tool. *J. Mol. Biol.* 215, 403–410. doi: 10.1016/S0022-2836(05)80360-2

Bazzicalupo, A. L., Bálint, M., and Schmitt, I. (2013). Comparison of ITS1 and ITS2 rDNA in 454 sequencing of hyperdiverse fungal communities. *Fungal Ecol.* 6, 102–109. doi: 10.1016/j.funeco.2012.09.003

Beckmann, S., Krüger, M., Engelen, B., Gorbushina, A. A., and Cypionka, H. (2011). Role of bacteria, archaea and fungi involved in methane release in abandoned coal mines. *Geomicrobiol. J.* 28, 347–358. doi: 10.1080/01490451.2010.503258

Blazewicz, S. J., Barnard, R. L., Daly, R. A., and Firestone, M. K. (2013). Evaluating rRNA as an indicator of microbial activity in environmental communities: limitations and uses. *ISME J.* 7, 2061–2068. doi: 10.1038/ismej.2013.102

Bomberg, M., Nyyssönen, M., and Itävaara, M. (2012). Characterization of Olkiluoto Bacterial and Archaeal Communities by 454 Pyrosequencing. Working Report 2011-31. Olkiluoto, Posiva.

Bomberg, M., Nyyssönen, M., Pitkänen, P., Lehtinen, A., and Itävaara, M. (2015). Active microbial communities inhabit sulphate-methane interphase in deep bedrock fracture fluids in Olkiluoto, Finland. *BMRI* 979530.

Buée, M., Reich, M., Murat, C., Morin, E., Nilsson, R. H., Uroz, S., et al. (2009). 454 Pyrosequencing analyses of forest soils reveal an unexpectedly high fungal diversity. *New Phytol.* 184, 449–456. doi: 10.1111/j.1469-8137.2009.03003.x

Caporaso, J. G., Kuczynski, J., Stombaugh, J., Bittinger, K., Bushman, F. D., Costello, E. K., et al (2010). QIIME allows analysis of high-throughput community sequencing data. *Nat. Methods* 7, 335–336. doi: 10.1038/nmeth.f.303

Cathrine, S. J., and Raghukumar, C. (2009). Anaerobic denitrification in fungi from the coastal marine sediments off Goa, India. *Mycol. Res.* 113, 100–109. doi: 10.1016/j.mycres.2008.08.009

Chao, A. (1984). Non-parametric estimation of the number of classes in a population. *Scandinavian J. Stat.* 11, 265–270.

Damare, S., and Raghukumar, C. (2008). Fungi and macroaggregation in deep-sea sediments. *Microb. Ecol.* 56, 168–177. doi: 10.1007/s00248-007-9334-y

Damare, S., Raghukumar, C., and Raghukumar, S. (2006). Fungi in deep-sea sediments of the Central Indian Basin. *Deep Sea Res. P. I* 53, 14, e27. doi: 10.1016/j.dsr.2005.09.005

Damare, S. R., Nagarajan, M., and Raghukumar, C. (2008). Spore germination of fungi belonging to *Aspergillus* species under deep sea conditions. *Deep Sea Res. P. I* 55, 670–678. doi: 10.1016/j.dsr.2008.02.004

Edgar, R., C. (2010). Search and clustering orders of magnitude faster than BLAST. *Bioinformatics* 26, 2460–2461. doi: 10.1093/bioinformatics/btq461

Edwards, U., Rogall, T., Blöcker, H., Emde, M., and Böttger, E. C. (1989). Isolation and direct complete nucleotide determination of entire genes. Characterization of a gene coding for 16S ribosomal RNA. *Nuc. Aci. Res.* 17, 7843–7853. doi: 10.1093/nar/17.19.7843

Ekendahl, S., O'Neill, A. H., Thomsson, E., and Pedersen, K. (2003). Characterisation of yeasts isolated from deep igneous rock aquifers of the Fennoscandian Shield. *Microb. Ecol.* 46, 416–428. doi: 10.1007/s00248-003-2008-5

Fournier, D., Lemieux, R., and Couillard, D. (1998). Essential interactions between Thiobacillus ferrooxidans and heterotrophic microorganisms during a wastewater sludge bioleaching process. *Env. Pol.* 101, 303–309. doi: 10.1016/S0269-7491(98)00035-9

Fredrickson, J. K., and Onstott, T. C. (1996). Microbes deep inside the earth. *Sci. Am.* 8, 42–47. doi: 10.1038/scientificamerican1096-68

Gadd, G. M. (2006). *Fungi in Biochemical Cycles*. New York, NY: Cambridge University Press.

Gardes, M., and Bruns, T. D. (1993). ITS primers with enhanced specificity for basidiomycetes - application to the identification of mycorrhizae and rusts. *Mol. Ecol.* 2, 113–118. doi: 10.1111/j.1365-294X.1993.tb00005.x

Hammer, Ø., Harper, D. A. T., and Ryan, P. D. (2001). PAST: paleontological statistics software package for education and data analysis. *Palaeontol. Elect.* 4:1.

Jebaraj, C. S., Raghukumar, C., Behnke, A., and Stoeck, T. (2010). Fungal diversity in oxygen-depleted regions of the Arabian Sea revealed by targeted environmental sequencing combined with cultivation. *FEMS Microbiol. Ecol.* 71, 399–412. doi: 10.1111/j.1574-6941.2009.00804.x

Kõljalg, U., Nilsson, R. H., Abarenkov, K., Tedersoo, L., Taylor, A. F. S., Bahram, M., et al. (2013). Towards a unified paradigm for sequence-based identification of fungi. *Mol. Ecol.* 22, 5271–5277. doi: 10.1111/mec.12481

Kurakov, A. V., Lavrent'Ev, R. B., Nechitailo, T. Y., Golyshin, P. N., and Zvyagintsev, D. G. (2008). Diversity of facultatively anaerobic microscopic mycelial fungi in soils. *Mikrobiologiia* 77, 90–98. doi: 10.1134/S002626170801013X

Lai, X., Cao, L., Tan, H., Fang, S., Huang, Y., and Zhou, S. (2007). Fungal communities from methane hydrate-bearing deep sea marine sediments in South China Sea. *ISME J.* 1, 756–762. doi: 10.1038/ismej.2007.51

Lindahl, B. D., Nilsson, R. H., Tedersoo, L., Abarenkov, K., Carlsen, T., Kjøller, R., et al. (2013). Fungal community analysis by high−throughput sequencing of amplified markers–a user's guide. *New Phyt.* 199, 288–299. doi: 10.1111/nph.12243

Ludvigsen, L., Albrechtsen, H. J., Ringelberg, D. B., Ekelund, F., and Christensen, T. H. (1999). Distribution and composition of microbial populations in landfill leachate contaminated aquifer (Grindsted, Denmark). *Microb. Ecol.* 37, 197–207. doi: 10.1007/s002489900143

Madsen, E. L., and Ghiorse, W. C. (1993). "Groundwater microbiology: subsurface ecosystem processes," in *Aquatic Microbiology*, ed T. E. Ford (London: Blackwell Scientific Publications), 167–213.

Manter, D. K., and Vivanco, J. M. (2007). Use of the ITS primers, ITS1F and ITS4, to characterize fungal abundance and diversity in mixed-template samples by qPCR and length heterogeneity analysis. *J. Microbiol. Meth.* 71, 7–14. doi: 10.1016/j.mimet.2007.06.016

Murrell, P. (2005). R Graphics. *WIREs Comp Stat.* 1, 216–220. doi: 10.1002/wics.22

Muyzer, G., de Wall, E., and Uitterlinden, A. (1993). Profiling of complex microbial populations by denaturing gradient gel electrophoresis analysis of polymerase chain reaction-amplified genes coding 16S rRNA. *Appl. Environ. Microbiol.* 59, 695–700.

Nagano, Y., and Nagahama, T. (2012). Fungal diversity in deep sea extreme environments. *Fung. Egol.* 5, 463–471. doi: 10.1016/j.funeco.2012.01.004

Nagano, Y., Nagahama, T., Hatada, Y., Nunoura, T., Takami, H., Miyazaki, J., et al. (2010). Fungal diversity in deep sea sediments–the presence of novel fungal groups. *Fung. Ecol.* 3, 316–325. doi: 10.1016/j.funeco.2010.01.002

Nyyssönen, M., Bomberg, M., Kapanen, A., Nousiainen, A., Pitkänen, P., and Itävaara, M. (2012). Methanogenic and sulphate-reducing microbial communities in deep groundwater of crystalline rock fractures in Olkiluoto, Finland. *Geomicrobiol. J.* 29, 863–878. doi: 10.1080/01490451.2011.635759

Orsi, W., Biddle, J. F., and Edgcomb, V. (2013b). Deep sequencing of subseafloor eukaryotic rRNA reveals active fungi across marine subsurface provinces. *PLoS ONE* 8:e56335. doi: 10.1371/journal.pone.0056335

Orsi, W. D., Edgcomb, V. P., Christman, G. D., and Biddle, J. F. (2013a). Gene expresssion in the deep biosphere. *Nature* 499, 205–208. doi: 10.1038/nature12230

Palumbo, A. V., Zhang, C., Liu, S., Scarborough, S. P., Pfiffner, S. M., and Phelps, T. J. (1996). "Influence of media on measurement of bacterial populations in the subsurface," in *Seventeenth Symposium on Biotechnology for Fuels and Chemicals*, eds C. E. Wyman and B. H. Davison (Totowa, NJ: Humana Press), 905–914.

Pedersen, K. (1987). *Preliminary Investigations of Deep Groundwater Microbiology in Swedish Granitic Rock*. SKB Technical report 88-01. Stockholm: Swedish Nuclear Fuel and Waste Management Co.

Pedersen, K., Arlinger, J., Ekendahl, S., and Hallbeck, L. (1996). 16S rRNA gene diversity of attached and unattached bacteria in boreholes along the access tunnel to the Äspö Hard Rock Laboratory. *FEMS Microbiol. Ecol.* 19, 249–262. doi: 10.1016/0168-6496(96)00017-7

Pitkänen, P., Partamies, S., and Luukkonen, A. (2004). *Hydrogeochemical Interpretation of Baseline Groundwater Conditions at the Olkiluoto Site*. Olkiluoto; Posiva.

Posiva. (2013). *Olkiluoto Site Description 2011*. Eurajoki: POSIVA 2011-02.

Raghukumar, C. (2012). *Biology of Marine Fungi*. Heidelberg: Springer.

Raghukumar, C., Damare, S. R., and Singh, P. (2010). A review on deep-sea fungi: occurrence, diversity and adaptations. *Botan. Mar.* 53, 479–492. doi: 10.1515/bot.2010.076

Raghukumar, C., and Raghukumar, S. (1998). Barotolerance of fungi isolated from deep sea sediments of the Indian Ocean. *Aquat. Microb. Ecol.* 15, 153–163. doi: 10.3354/ame015153

R Development Core Team. (2008). *R: A Language and Environment for Statistical Computing*. Vienna: R Foundation for statistical Computing. Available online at: http://www.R-project.org

Reitner, J., Schumann, G., and Pedersen, K. (2006). "Fungi in subterranean environments," in *The Fungi in Biogeochemical Cycles*, ed G. M. Gadd (Cambridge: Cambridge University Press), 377–403.

Salavirta, H., Bomberg, M., Nyyssönen, M., Miettinen, H., Sohlberg, E., Vikman, M., et al. (in press). Archaea have thrived and diversified in deep subsurface Fennoscandian aquifers. *Front. Microbiol.*

Schloss, P. D., Westcott, S. L., Ryabin, T., Hall, J. R., Hartmann, M., Hollister, E. B., et al. (2009). Introducing mothur: open- source, platform-independent, community-supported software for describing and comparing microbial communities. *Appl. Env. Microbiol.* 75, 7537–7541. doi: 10.1128/AEM.01541-09

Shannon, C. E. (1948). A mathematical theory of communication. *Bell Syst. Tech. J.* 27, 379–423, 623–656. doi: 10.1002/j.1538-7305.1948.tb01338.x

Sinclair, J. L., and Ghiorse, W. C. (1989). Distribution of aerobic bacteria, protozoa, algae, and fungi in deep subsurface sediments. *Geomicrobiol. J.* 7, 15–31. doi: 10.1080/01490458909377847

Singh, P., Raghukumar, C., Verma, P., and Shouche, Y. (2012). Assessment of fungal diversity in deep sea sediments by multiple primer approach. *World J. Microbiol. Biotechnol.* 28, 659–667. doi: 10.1007/s11274-011-0859-3

Sterflinger, K. (2010). Fungi as geologic agents. *Geomicrobiol. J.* 17, 97–124. doi: 10.1080/01490450050023791

Takishita, K., Tsuchiya, M., Reimer, J. D., and Maruyama, T. (2006). Molecular evidence demonstrating the basidiomycetous fungus Cryptococcus curvatus is the dominant microbial eukaryote in sediment at the Kuroshima Knoll methane seep. *Extremophiles* 10, 165–169. doi: 10.1007/s00792-005-0495-7

Takishita, K., Yubuki, N., Kakizoe, N., Inagaki, Y., and Maruyama, T. (2007). Diversity of microbial eukaryotes in sediment at a deep sea methane cold seep: surveys of ribosomal DNA libraries from raw sediment samples and two enrichment cultures. *Extremophiles* 11, 563–576. doi: 10.1007/s00792-007-0068-z

Wainwright, M., and Grayston, S. J. (1989). "Accumulation and oxidation of metal sulphides by fungi," in *Metal–Microbe Interactions*, ed K. Sterflinger (Oxford: IRL press), 119–131.

White, T. J., Bruns, T., Lee, S. J. W. T., and Taylor, J. W. (1990). Amplification and direct sequencing of fungal ribosomal RNA genes for phylogenetics. *PCR Protoc.* 18, 315–322. doi: 10.1016/b978-0-12-372180-8.50042-1

Wickham, H. (2007). Reshaping Data with the reshape Package. *J. Stat. Soft*. 21, 1–20.

Wickham, H. (2009). *Ggplot2: Elegant Graphics for Data Analysis*. New York, NY; Springer. doi: 10.1007/978-0-387-98141-3-2

Zhang, N., Castlebury, L. A., Miller, A. N., Huhndorf, S. M., Schoch, C. L., Seifert, K. A., et al. (2006). An overview of the systematics of the Sordariomycetes based on a four- gene phylogeny. *Mycologia* 98, 1076–1087. doi: 10.3852/mycologia.98.6.1076

Conflict of Interest Statement: Posiva Oy funded this research. The authors declare that the research was conducted in the absence of any commercial or financial relationships that could be construed as a potential conflict of interest.

frontiers in Microbiology

ORIGINAL RESEARCH
published: 11 August 2015
doi: 10.3389/fmicb.2015.00833

Deep subsurface mine stalactites trap endemic fissure fluid Archaea, Bacteria, and Nematoda possibly originating from ancient seas

Gaëtan Borgonie[1,2], Borja Linage-Alvarez[2], Abidemi Ojo[2], Steven Shivambu[3], Olukayode Kuloyo[2†], Errol D. Cason[2], Sihle Maphanga[3], Jan-G Vermeulen[2], Derek Litthauer[2], Colin D. Ralston[4], Tullis C. Onstott[5], Barbara Sherwood-Lollar[6] and Esta Van Heerden[2]*

[1] Extreme Life Isyensya, Gentbrugge, Belgium, [2] Department of Biotechnology, University of the Free State, Bloemfontein, South Africa, [3] Geology, Beatrix Gold Mine, Theunissen, South Africa, [4] Bergville Retirement Village, George, South Africa, [5] Department of Geosciences, Princeton University, Princeton, NJ, USA, [6] Department of Earth Sciences, University of Toronto, Toronto, ON, Canada

OPEN ACCESS

Edited by:
Malin Bomberg,
VTT Technical Research Centre of Finland, Finland

Reviewed by:
Lotta Purkamo,
VTT Technical Research Centre of Finland, Finland
Cassandra Marnocha,
University of Delaware, USA

***Correspondence:**
Gaëtan Borgonie,
Extreme Life Isyensya, PB 65, 9050 Gentbrugge, Belgium
gaebor@eli-deeplife.be

† Present Address:
Olukayode Kuloyo,
Department of Geoscience, University of Calgary, Calgary, AB, Canada

Specialty section:
This article was submitted to Terrestrial Microbiology, a section of the journal Frontiers in Microbiology

Received: 30 April 2015
Accepted: 28 July 2015
Published: 11 August 2015

Citation:
Borgonie G, Linage-Alvarez B, Ojo A, Shivambu S, Kuloyo O, Cason ED, Maphanga S, Vermeulen J-G, Litthauer D, Ralston CD, Onstott TC, Sherwood-Lollar B and Van Heerden E (2015) Deep subsurface mine stalactites trap endemic fissure fluid Archaea, Bacteria, and Nematoda possibly originating from ancient seas. Front. Microbiol. 6:833. doi: 10.3389/fmicb.2015.00833

Stalactites ($CaCO_3$ and salt) from water seeps are frequently encountered in ceilings of mine tunnels whenever they intersect water-bearing faults or fractures. To determine whether stalactites could be mineralized traps for indigenous fracture water microorganisms, we analyzed stalactites collected from three different mines ranging in depth from 1.3 to 3.1 km. During sampling in Beatrix gold mine (1.4 km beneath the surface), central South Africa, $CaCO_3$ stalactites growing on the mine tunnel ceiling were collected and observed, in two cases, to contain a living obligate brackish water/marine nematode species, *Monhystrella parvella*. After sterilization of the outer surface, mineral layers were physically removed from the outside to the interior, and DNA extracted. Based upon 16S and 18S rRNA gene sequencing, Archaea, Bacteria, and Eukarya in different combinations were detected for each layer. Using CT scan and electron microscopy the inner structure of $CaCO_3$ and salt stalactites were analyzed. $CaCO_3$ stalactites show a complex pattern of lamellae carrying bacterially precipitated mineral structures. Nematoda were clearly identified between these layers confirming that bacteria and nematodes live inside the stalactites and not only in the central straw. Salt stalactites exhibit a more uniform internal structure. Surprisingly, several Bacteria showing highest sequence identities to marine species were identified. This, together with the observation that the nematode *M. parvella* recovered from Beatrix gold mine stalactite can only survive in a salty environment makes the origin of the deep subsurface colonization enigmatic. The possibility of a Permian origin of fracture fluids is discussed. Our results indicate stalactites are suitable for biodiversity recovery and act as natural traps for microorganisms in the fissure water long after the water that formed the stalactite stopped flowing.

Keywords: subsurface sea, stalactites, diversity, *Monhystrella parvella*

Introduction

Studying deep subsurface terrestrial biodiversity can only be achieved through deep drilling and mining or exploration of caverns. In deep mining, access to fracture water is unpredictable, irregular and the volume available for collection may be too limited. The latter is important as cell counts of bacteria in deep subsurface fracture water is typically low, requiring large volumes for deriving sufficient DNA for characterization of the taxonomic diversity. During deep mine sampling, we have encountered on several occasions stalactites on the corridor or tunnel ceilings.

In many caverns a large variety of communities comprised of Algae, Bacteria, and Fungi are found embedded in stalactites and in some cases, these microorganisms have been implicated in the precipitation of carbonate soda-straw ("straws") stalactites in caves. This occurs through a number of processes that include ammonification, denitrification, sulfate reduction and anaerobic sulfide oxidation (Danielli and Edington, 1983; Cox et al., 1989; Castanier et al., 1999, 2000; Riding, 2000; Desmarchelier et al., 2006). Thus, underground mine stalactites raised the possibility that they may act as natural traps for microorganisms in the fissure water. More importantly they could serve as enrichment sites allowing sampling drip waters that defy more traditional sampling methods due to the low water volume. Arguing against such an approach is the contamination issue of a stalactite hanging free in a strongly ventilated mine corridor where anthropogenic contamination is a daily possibility. Previous research on fungal spores in mine air (Pohl et al., 2007) justified this concern and biofilms growing on tunnels walls below a fissure water outlet from a fracture or a borehole is generally considered not to be representative of the microbial community with the fracture zone that is supplying the water. Furthermore, the small size of the stalactites and the enrichment potential would only allow studying partial biological/chemical content.

During routine sampling at a depth of −1.4 km in Beatrix gold mine, South Africa, several stalactites were collected and stored in Ziplock sample bags. Upon examination with a stereomicroscope we identified a nematode in the fluid that came out of these stalactites. In the course of the following days, a total of eight nematodes were observed in the sampling bag. This puzzling observation led us to examine several stalactites from three different mines to test the hypothesis that stalactites in mines may serve as useful natural (enrichment) traps for Archaea, Bacteria, and Eukarya. Additionally we wanted to establish the origin of the nematodes that occurred within the stalactites, as they are not known to be tube builders compared to other Animalia.

Materials and Methods

Origin of the Stalactites

The Republic of South Africa hosts some of the world's deepest mines, some of which exceed 4 km below land surface (kmbls). These, deep gold, platinum and diamond mines and their network of tunnels and crosscuts, allow exceptional access to the deep subsurface. During the course of normal mining operations, the advancing tunnels or exploratory boreholes intersect water-bearing fractures. Stalactites occur associated with water-weeping fractures intersected by the tunnel. Since the presence of stalactites in the mines is haphazard, stalactites were collected from mines when and where available. Samples were taken at Beatrix gold mine, Moab Khotsong gold mine, Evander gold mine and Tau Tona gold mine.

Beatrix Gold Mine (Sibanye Gold, Ltd.) 28°14′24.37″S/26°47′49.30″E

Beatrix gold mine is located near the towns of Welkom and Virginia, some 240 km southwest of Johannesburg in the Free State Province of South Africa. Geologically the mine is located along the southern margin of the Witwatersrand Basin. Twelve carbonate stalactites were collected in the same tunnel at two different locations approximately 100–200 m apart on level 26 of #3 shaft, 1.4 km below the surface. The stalactites were collected in 2009–2010 and 2013. During the 2010 collection campaign, five soil samples were taken from the tunnel floor to look for nematodes. This tunnel is located in the Witwatersrand Supergroup, which at this location is directly overlain by 400–800 m of Carboniferous Karoo sediments. The age of the carbonate stalactites is unknown but cannot be older than 2–3 years since the tunnel was excavated in 2007.

Moab Khotsong, (Anglogold Ashanti Ltd.) 26°59′14.20″S/26°48′5.01″E

Moab Khotsong is the newest deep-level gold mine in South Africa and is situated near Orkney, Klerksdorp, and Viljoenskroon in North West Province, about 180 km southwest of Johannesburg. The principal reef is the Vaal Reef of which the gold grade and morphology are considered to be a down-dip extension to the south and southeast of Kopanang and Great Noligwa mines. The reef is comprised of an oligomictic conglomerate, where gold is associated with carbon at the base. Stalactite samples some as large as 3 m were collected in December 2012 growing on the rim of a man-made ventilation shaft at level 120, which is at a depth of −3.1 km. The age of these stalactites can be no more than 5 years for the smallest used for DNA analysis, and up to 10 years for the largest specimen used in the CT scan.

Evander Gold Mine (Harmony Gold Mining Company Ltd.) 26°27′20.57″S/29°4′15.76″E

Evander gold mine is situated 8 km northwest from Secunda in the Mpumalanga Province. The Evander Basin is a tectonically preserved sub-basin outside the main Witwatersrand Basin and forms an asymmetric syncline, plunging north-east. It is structurally complex with a series of east-north-east striking normal faults. At the southeast margin of the basin, vertically to locally overturned reef is present. The only economic reef horizon exploited in the Evander Basin is the Kimberley Reef. The Intermediate Reef is generally poorly mineralized, except where it erodes the sub-cropping Kimberley Reef to the south and west of the basin. Several small dried out stalactites were collected in 2007 at shaft #8, level 13 at a depth of ∼1.4 km. One of these was kept in a closed tube from 2007 until 2012 when it was used for the present analysis. The age of the stalactite is unknown.

Tau Tona Gold Mine (Anglo Gold Ashanti Ltd.) 26°21′21.29″S/27°24′10′12″E

Tau Tona gold mine is located south of Carletonville in the Gauteng Province and about 70 km southwest of Johannesburg. The sampling site was a nearly horizontal borehole located on level 118 at a depth of 3.4 km in the Witwatersrand Supergroup and intersected the Pretorious fault zone. The borehole was not sealed and flowed intermittently. This borehole was the site of the deepest metazoan ever found in 2011, a monhysterid nematode of which only a DNA sequence was known to date. The fissure water was sampled again in 2012–2013 in an attempt to recapture the nematode previously found there because of its relevance to the DNA results from the Beatrix gold mine subsurface nematode.

Stalactites Used for Analysis

Twelve $CaCO_3$ stalactites were collected in Beatrix gold mine of which two contained a total of 20 nematodes. Of those 12 stalactites, two containing nematodes and one devoid of nematodes was used for micro-CT scan, XRD and DNA analysis. Only one still intact stalactite from Evander mine was used for XRD and DNA analysis. One small stalactite from Moab Khotsong was used for XRD analysis. One very large salt stalactite from Moab Khotsong was used for macro CT scan and DNA analysis. The different stalactite layers are designated as NSX.Y where N is the first letter of the mine from which the stalactite (S) was collected, X is the number identifying the collection order of the stalactite in a given mine, Y refers to the peeled or dissolved layer in question counting from the outside toward the center. For example, ES1.4 means the first collected stalactite from Evander mine, layer number 4.

Micro-CT Scan

Micro-CT is a non-destructive 3D imaging technique for studying the internal structure of an object. Setup and conditions are described in detail in Borgonie et al. (2010). Volume rendering and segmentation was performed using VGStudio Max (Volume Graphics). In an attempt to visualize the nematodes, the bulk was rendered transparent. Three stalactites were scanned. One yielded nematodes while the other two did not.

Macro-CT Scan

Larger stalactites were CT scanned at the UFS Campus Netcare Hospital using a General Electric HD 750 (Milwaukee, USA) with following settings: KvP 140, MA 450 helical with 0.625 mm slices with a 0.312 interval.

Scanning Electron Microscopy

Pieces of stalactite were mounted on a specimen stub and sputter coated with gold using a BIO-RAD (Microscience Division) Coating System (London, UK) and observed with a Jeol JSM 8440 SEM microscope. For fixation of the $CaCO_3$ containing nematodes, 70°C 30% formaldehyde was used followed longitudinal cutting with a sterile scalpel, then dehydration, critical point drying, coating and mounting. SEM pictures were assembled in plates using Adobe Photoshop (Adobe Systems Inc., San Jose, CA, USA) and where relevant colored using Smart Photo editor (Anthropics Technology, Ltd., London, UK).

X-Ray Diffraction (XRD)

Before melting the different stalactites a small piece was removed and homogenized from each for XRD analysis. The samples were ground to a grain size of $<50\,\mu m$ using a carbon steel ring and agate mortar and pestle. The loose powder samples were then mounted into steel ring sample holders, and slightly compressed to give a smooth surface. XRD measurements were performed using a Panalytical Empyrean X-ray diffractometer, with the following con urations: The samples are irradiated with CuKα-radiation generated at 40 mA and 45 kV. No monochromator was inserted while a fixed divergence slit of 0.2177° was part of incoming beam optics. Scanning was continuous starting at 5° 2θ and ending at 70° 2θ, with step size 0.017 2θ for 15.875 s per step. Measurements were carried out on a stationary sample without spinning of the sample holder. The identification of minerals was carried out using Panalytical Highscore software with the PDF-2 (2009) powder diffraction file database, and estimates of relative abundances were made based on semi-quantitative data associated with the files in this database.

Dissolving Salt Stalactites/Dissecting Carbonate Stalactite

The outer surface of salt/carbonate stalactites was sterilized by immersion in 100% ethanol and set alight allowing the ethanol to burn off. Three small pieces were subsequently chipped off and inoculated onto three different media namely, Luria Bertani (LB), nutrient agar (NA), and Potato dextrose Agar (PDA) to confirm the effectiveness of sterilization. The individual layers within the stalactite in the case of carbonate were carefully dissected using sterilized tweezers; pieces were collected in 1.5 mL Eppendorf tubes for DNA extraction. For the salt stalactites sterile deionized water was sprayed on the layers to dissolve the stalactite carefully. Cross contamination through dripping from the ends of the sample was prevented by holding the stalactite horizontally along its longest axis and spraying carefully from beneath.

Nematode Culture/Halotolerance Test

Collection and identification of nematodes from fluids that leached out of the Beatrix gold mine carbonate stalactite was done aseptically. Twelve nematodes were recovered in the course of 7 days in 2010, and the second stalactite collected in 2013 yielded eight nematodes. Culturing was attempted by placing the nematodes on a 3% salt-agar plate covered with the saline (14 g/L) water that oozed out of the stalactite. Halotolerance by the nematodes was performed in artificial salt agar. Due to the low number of nematodes available, the test was performed twice using 12 nematodes in total. The initial salt concentration was 14 g/L; nematodes were transferred to a different concentration every 24 h. The nematodes died quickly when the salt concentration was too high/low acting as a suitable marker for tolerance. Control nematodes: *Halicephalobus mephisto* collected previously from the same mine but from a borehole (Borgonie et al., 2011) and *Poikilolaimus oxycercus* a surface collected nematode. For both *P. oxycercus* and *H. mephisto* thirty worms were used and were directly placed on agar plates with different salt concentrations. In an attempt to identify Bacteria used as food by *M. hystrella* one

specimen was slowly dissolved in a 1% NaOCl solution until the outer cuticle had dissolved as observed under a stereomicroscope. The specimen was then washed three times in deionized water and DNA extracted.

DNA Analysis

DNA Extraction

Nucleic Acid Extraction from the Stalactite Layers

$CaCO_3$stalactite layers were pulverized in an Eppendorf tube using a sterile pestle. The dissolved halite stalactite layers were collected in 50 mL Falcon tubes and then filtered using a 0.22 μm filter membrane (MIS). DNA was extracted from the pulverized $CaCO_3$ and filter using the InstaGene Matrix kit (BIO-RAD 732-6030). Quality and concentration of DNA was determined using ND-1000 Spectrophotometer (NanoDrop).

Nucleic Acid Extraction from Nematodes

Nematodes were collected from the petri dish with a sterile platinum needle and transferred into sterile deionized water in a 1.5 mL Eppendorf tube. DNA was extracted directly using the InstaGene Matrix kit (BIO-RAD 732-6030). Quality and concentration of DNA was determined using ND-1000 Spectrophotometer (NanoDrop).

PCR Amplification

PCR Amplification from Stalactites

Fragments of 16S and 18S rDNA suitable for DGGE analysis were obtained by using different primer sets for different domains, (Muyzer et al., 1993; Casamayor et al., 2002; Mühling et al., 2008; Stomeo et al., 2012), Bacteria: 27F, 341FGC, 908R, and 1492R; Archaea: 934R and 344FGC; Eukarya: 516R and 1AFGC. The primer sets and the PCR conditions were modified from protocols described by Casamayor et al. (2002). Due to the small size of the stalactites, an initial PCR was performed using 27F and 1492R primers followed by *nested* PCR using 341F with GC clamp and 908R. PCR conditions for the two steps were: initial denaturation at 94°C for 3 min; 29 cycles (94°C, for 30 s; 55°C for 30 s; 72°C for 1 min); and a final extension at 72°C for 5 min. For the Archaeal 16S rDNA fragments, we used an initial denaturation step at 94°C for 2 min followed by 30 PCR cycles with annealing at 61°C and a final 10 min. extension step at 72°C. The eukaryal 18S rDNA fragments were amplified using: initial denaturation at 94°C for 130 s; 35 cycles (94°C for 30 s; 57°C for 30 s; 72°C for 7 min); and a final extension at 72°C for 5 min.

PCR Amplification of 18S rRNA Gene from Nematodes in Culture

PCR amplification of 18S rDNA fragments was performed using primer setsEukA [AACCTGGTTGATCCTGCCAGT] and EukB [TGATCCTTCTGCAGGTTCACCTAC] (Diez et al., 2001), and Nem18S(F) [CGCGAATRGCTCATTACAACAGC] and Nem18S(R) [GGGCGGTATCTGATCGCC] (Floyd et al., 2005). A standard reaction volume was 25 μL containing: 1x concentration of Standard *Taq* buffer (New England BioLab), (including 1.5 mM $MgCl_2$), 0.5 μM of each primer, dNTPs at a concentration of 0.2 mM for each nucleotide, 0.025 units/μL *Taq* DNA polymerase and 10 ng of extracted DNA template was added to each reaction. The thermocycling conditions used for eukaryal and nematode PCR reactions are: an initial denaturation at 94°C for 5 min; 35 cycles (94°C for 30 s; 54°C for 30 s; 72°C for 1 min); and a final extension at 72°C for 10 min (Floyd et al., 2005) in a PXE 0.2 Thermal Cycler (Thermo Electron Corporation).

PCR Amplification of the Nematode Mitochondrial COI Gene

A portion of the mitochondrial cytochrome oxidase c subunit 1 (COI) gene was amplified with the primer sets COI1F (5′-GGT CAA CAA ATC ATA AAG ATA TTG G-3′) and COI1R (5′-TAA ACT TCA GGC TGA CCA AAA AAT CA-3′) (Valenzuela et al., 2007); and JB3F (5′-TTT TTT GGG CAT CCT GAG GTT TAT-3′) and JB4.5R (5′-TAA AGA AAG AAC ATA ATG AAA ATG-3′) (Derycke et al., 2005). Amplification was conducted for 35 cycles, each consisting of a 30 s denaturation at 94°C, 30 s annealing at 54°C, and 30 s extension at 72°C, with an initial denaturation step of 5 min at 94°C and a final extension step of 10 min at 72°C.

DGGE Analysis

DGGE Analysis of PCR Products of Ribosomal DNA Fragments from Stalactites

The amplified 16S/18S rRNA gene fragments (600–800 ng) were separated on 7% (w/v) polyacrylamide gel with a urea/formamide denaturing gradient ranging from 40 to 60%. Electrophoresis was performed in 1X TAE buffer (40 mM Tris, 20 mM acetic acid, 1 mM EDTA; pH 8.3) at a constant voltage of 100 V at 60°C and run for 16 h. Gels were stained for 40 min in 1X TAE buffer containing Sybr SYBR® Gold Nucleic acid stain (Molecular Probes, Invitrogen) and visualized with UV radiation by using a Gel doc XR and the Quantity one 4.6.7 imaging software (Bio-Rad).

Sequencing of DNA Fragments

Sequencing of Stalactites DNA Fragments

DNA was recovered from each excised band reamplified using the same set of primers mentioned above, without the GC clamp. The PCR products were then purified using Exonuclease I (Exo I) Thermo Scientific FastAP and Thermosensitive Alkaline Phosphatase (#EF0651, Werle et al., 1994). Sequencing reactions were performed with the ABI Prism™Big Dye terminator™V3.1 cycle sequencing ready reaction kit and data collected on an ABI 3130*XL* genetic analyzer (Applied biosystems). The sequences were checked for chimeras using Bellerophon (Huber et al., 2004) and then compared to the GenBank nucleotide database [National Center for Biotechnology Information, (NCBI)] using BLAST. Neighbor-joining phylogenetic trees were generated using reference sequences from the RDP (Maidak et al., 1997) and using Geneious 4.8.5.

Sequencing of Nematode DNA Fragments

The amplified DNA fragments were sequenced using the ABI Prism™BigDye terminator™V3.1 cycle sequencing kit and data collected on an ABI 3130*XL* genetic analyzer (Applied

biosystems). The quality of ABI files retrieved using FinchTV software was evaluated and the sequence reads were assembled using CodonCode Aligner software (CodonCode Corporation, Dedham, MA, USA). Overlapping reads or contigs thar represented the consensus regions of DNA were aligned using ClustalW (http://www.ebi.ac.uk/Tools/msa/clustalw2/). The alignment was examined for conserved regions so as to provide sufficient information that reveals any similarity between the two isolated organisms. BLASTN analysis of DNA database was used. Sequences were compared to the Nucleotide collection (nr/nt) database and optimized for highly similar sequences (Megablast).

Genbank Submissions

All sequences were deposited in Genbank with accession numbers: Bacteria KJ546057-KJ546071, Archaea KJ546072-KJ546075, Eukarya: KJ546076-KJ546081.

Microscopy

The low number of nematodes available made a tradeoff necessary between retaining enough specimens to measure for taxonomic purposes and retaining enough for attempted culturing. To avoid losing too many nematodes to the attempted culture only three adult nematodes were used for taking microscopic measurements. These nematodes were anesthetized by a brief slide heating. A Zeiss Axioskop Microscope was used. This approach had the disadvantage that not all small details could be measured but left enough valid measurements for proper identification of the nematode species. These selected nematodes were returned to the culture but were not used for the salt tolerance experiment.

Results

XRD analysis of the carbonate stalactites from Beatrix and Evander showed its composition to be mixture of calcite and aragonite. The XRD analysis of the Moab Khotsong salt stalactite determined the composition as ∼98% halite + ∼1% sylvite + ∼1% quartz.

The $CaCO_3$ stalactites each yielded 3–4 layers when peeled, whereas the salt stalactite from Moab Khotsong was dissolved in four layers (**Table 1**). After sterilization none of the outer layers that were tested on PDA, LB or NA agar showed any growth indicating that sterilization worked satisfactorily.

DNA extraction was successful for all layers and resulted in archaeal, bacterial and/or eukaryal DNA (**Table 1**). A difference is noted between salt and $CaCO_3$ stalactites where the salt stalactite show a more uniform yield of archaeal, bacterial or eukaryote DNA in all layers of the same stalactite, whereas the $CaCO_3$ stalactites showed a more variable pattern with not all layers of the same stalactite having the same DNA content. Sequencing of extracted DNA was not always successful (**Table 1**). Salt stalactites consistently yielded a higher number DNA bands on DGGE than $CaCO_3$ stalactites, but yielded poorer sequencing results (**Table 1**).

Eukaryal sequences revealed one Fungus (Ordo *Saccharomycetales Candida* sp., Berkh, 1923) and a protozoan, *Acanthamoeba* sp. Castellani, 1930 and a ciliate, *Colpoda* sp. Müller, 1773 No nematode DNA was identified in the stalactite layers (**Table 1**).

Identification of the nematode species that flowed out of the stalactites was done using light microscopy of three adult individuals (**Table 2**). Notwithstanding the limitations in usable specimen (see Materials and Methods) the nematode species recovered from the two stalactites belong to the genus *Monhystrella* Cobb, 1918 based on the cephalic setae, small body length, and fovea position, presence of a pharyngeal bulbus, a prominent progaster, and vulva at midbody. Measurements were compared with known populations from Ethiopia, Namibia and Bulgaria and confirm the identity as *Monhystrella parvella* (Filipjev, 1931; Jacobs, 1987) a brackish water/marine nematode. The measurements agree with the Namibian population more than the Ethiopian/Bulgarian populations (**Table 2**). An 18S rRNA gene sequence for *M. parvella* was obtained but could not be compared with the Ethiopian, Namibian or Bulgarian population as no DNA of those samples has been analyzed. Similarity searches using BLASTN algorithm (NCBI database) revealed a 91% similarity to the next closest surface nematode *Diplolamelloides* sp., which is a marine nematode. This indicates that the Beatrix stalactite nematode species has not yet been barcoded on the surface to date. Similarity searches also revealed a 96% identity with a previously collected subsurface nematode DNA at Tau Tona mine in fissure water of 48°C, salinity 14g/L at −3.4 km, 230 km to the North of Beatrix gold mine (Borgonie et al., 2011). An attempt was made to recapture the Tau Tona nematode in 2013, which resulted in two nematode specimens being collected. DNA analysis only was hence possible and revealed a 100% match of the 18S rRNA gene sequence and of the COI mitochondrial gene sequence between Beatrix gold mine *M. parvella* and the newly collected Tau Tona Monhysterid. Sequence comparison between the Tau Tona 2011 and 2013 sequences confirmed the 96% identity of the 18s rRNA gene sequence.

Only the salt stalactite of Moab Khotsong contained 16S rRNA gene sequences belonging to the *Euryarchaeota (Halobacteriales)*, in all 4 dissolved layers (**Table 1**, **Figure 1**). NCBI BLAST results of those four sequences showed 99% of identity to one uncultured archaeon clone (EV818CFSSAHH131—*Halobacteriales*) previously detected in a calcitic mineral fracture of a drill core collected from Evander mine level 18 of #8 shaft at a depth of 2 km (Davidson et al., 2011).

The bacterial phylogenetic diversity is represented by seven orders (**Figure 2**). Sphingobacteriales, Thermales, Burkholderiales, Alteromonadales, Enterobacteriales, Oceanospirillales, Bacillales. The largest represented groups were from the Orders Enterobacteriales, Burkholderiales, and Oceanospirillales. Significant was the identification of most likely marine Bacteria. The Order Oceanospirillales included one sequence that shared the closest identity 92% to one uncultured bacterium (SGUS738) identified from coral fragments taken in Panama. Two additional sequences clearly linked to Gamma-proteobacteria and Alcanivorax sp. In the Order Alteromonadales the sequence was closely related to Bowmanella as well as an uncultured marine bacterium.

TABLE 1 | Archaeal, Bacterial, and Eukaryal DNA results from the stalactite extractions.

Layer	# DGGE bands	DNA (ng/μl)/260/280 ratio	Closest relative/Taxonomic position	Acc. number	% Identity	Source
ARCHAEA/BACTERIA						
E S1.1	2	7.43/1.74	*Ureibacillus*	JQ734423	100	Oil-water mixture
E S1.2	1	8.23/1.61	*Klebsiella*	KC907123.1	100	Soil
	1		*Uncultured Citrobacter*	GQ416126	100	Biological degreasing systems
E S1.3	2	5.82/1.54	*Pantoea*	AJ002811	100	Gut
E S1.4	2	5.62/1.80	*Thermus*	AB661716	100	Deep mine, Beatrix
B S2.1	2	147.13/1.70	*Bowmanella*	GQ246642	99	Ocean water
B S2.2	2	41.02/1.74	*Klebsiella*	HE716897	100	Host leaves
B S2.3	1	13.45/2.22	*Uncultured SGUS738 (Oceanospirillales)*	FJ202645	91	Caribbean coral
	1		*Staphylococcus* sp.	EF419336	100	Soil
B S5.1	0	19.99/1.80				
B S5.2	1	10.04/1.98	Could not be sequenced			
B S5.3	0	6.54/1.79				
B S6.1	1	13.36/1.57				
B S6.2	1	28.25/1.54	*Cupriavidus*	DQ777727	100	Soil
B S6.3	1	16.79/1.85	*Cupriavidus*	DQ777727	100	Soil
M S3.1	1	10.0/2.04	*Archaeon clone (Halobacteriales)*	DQ336966.1	99	Deep mine Evander
	3		*Alcanivorax* sp.	HQ662960	99	Sea water
M S3.2	1	7.74/1.70	*Archaeon clone (Halobacteriales)*	DQ336966.1	99	Deep mine Evander
	1		*Alcanivorax* sp.	HQ662960	100	Sea water
	1		*Uncultured Bacteroidetes*	JF421218	98	Saline-alkali soil
M S3.3	1	3.63/1.97	*Archaeon clone (Halobacteriales)*	DQ336966.1	99	Deep mine Evander
	1		*Pantoea* sp.	AF394539	100	Grass
M S3.4	1	3.72/1.94	*Archaeon clone (Halobacteriales)*	DQ336966.1	99	Deep mine Evander

Layer	# DGGE bands	Closest relative/Taxonomic position	Acc. number	% Identity	Source
EUKARYA					
E S1.1	2	Could not be sequenced			
E S1.2	3	*Acanthamoeba (Protozoa)*	GQ397466.1	99	Fresh water
	1	*Candida (Fungi)*	HM161746.1	92	Human associated
E S1.3	2	*Uncultured eucarya*	FN394866.1	92	
E S1.4	4	Could not be sequenced			
B S2.1	2	Could not be sequenced			
B S2.2	0				
B S2.3	2	Could not be sequenced			
B S5.1	2	Could not be sequenced			
B S5.2	4	*Colpoda (Protozoa)*	JN251157.1	100	Freshwater
		Uncultured eucarya	AY905498.1	100	
B S5.3	4	Could not be sequenced			
B S6.1	0				
B S6.2	0				
B S6.3	1	Could not be sequenced			
M S3.1	9	Could not be sequenced			
M S3.2	9	Could not be sequenced			
M S3.3	4	Could not be sequenced			
M S3.4	7	Could not be sequenced			
B S2&5*		*Monhystrella parvella (Nematoda)*			Brackish water/thermal springs

Name of the mine is referred as E (Evander), B (Beatrix), and M (Moab Khotsong). Beatrix stalactite BS 1 and BS2 contained nematodes, BS 3 did not. The listed 260/280 ratio is used to assees purity of the extracted DNA using a Nanodrop® spectrophotometer. A value of ∼1.80 is generally accepted as "pure" for DNA.
**Isolated by capturing the fluid flowing out of the collected stalactite.*

TABLE 2 | Measurements of *M. parvella* from Beatrix stalactites compared with the population from Ethiopia, Namibia, and Bulgaria.

	Filipjev's specimen from Ethiopia 1926				Gerlach's specimen from Bulgaria 1951			Beatrix gold mine republic of South Africa 2013				Namibia 1986				
												Ai-Ais			Namutoni	
	n	Mean	Min-max	*s*	*n*	Mean	Min-max	*n*	Mean	Min-max	*s*	*n*	Mean	Min-max	*n*	Mean	Min-max
L	11	445.0	396.0–486.0	26.8	7	420.0	380.0–460.0	3	449.6	401.0–493.0	6.2	10	438	427–478	6	472	406–505
v.b.w	11	24.0	21.0–31.0	3.3	7	17.5		3	27.6	22.0–33.0	5.5	10	15.9	14.9–17.0	6	17.1	15–17
ph.l	12	88.0	76.0–101.0	7.0	7	68.9		3	91.3	81.0–103.0	11.0	10	79	72–83	6	91	80–99
t.l.	11	96.0	80.0–117.0	10.5	7	101.2		3	102.6	88.0–120.0	16.1	10	106	94–112	6	112	101–120
v	11	249.0	224.0–271.0	15.8	7	220.5		3	252.6	228.0–276.0	24.0						
Ph.v.l.	11	148.0	133.0–162.0	10.4	7	151.6		3	150.0	134.0–164.0	15.0						
v.a.l	11	100.0	82.0–124.0	10.9	7	98.3		3	109.0	97.0–119.0	11.1	10	106	93–113	6	115	94–123
h.d	12	8.5	7.6–9.3	0.5				3	8.6	8.0–9.4	0.7	10	5.3	5–6	6	5.8	5.5–6.0
f.d.	12	2.9	2.2–3.3	0.3				3	2.6	2.5–2.7	0.1	10		2.4–2.6	6		2.4–2.6
a.f.b.l.	12	9.2	7.5–11.4	1.1				3	9.5	9.2–10.0	0.4						
c.b.w.	12	21.1	19.0–25.0 1.7					3	22.6	20.0–25.0	2.5						
r.l.	11	10.4	7.7–13.2	1.7				3	10.3	8.0–11.0	4.3	10	10.9	10–11.5	6	12.6	11.5–13.5
a	11	18.2	15.0–20.0 1.7		7	24.0	21.0–27.0	3	18.3	16.0–21.0	2.5	10	27.5	23.8–29.5	6	27.6	27.1–28.9
b	11	5.1	4.6–5.4	0.3	7	6.1	5.4–6.8	3	4.8	4.7–4.9	0.1	10	5.5	5.2–6.0	6	5.2	5.1–5.4
c	11	4.7	4.0–5.3	0.4	7	4.2	3.9–4.4	3	4.4	4.1–4.6	0.3	10	4.2	4.0–4.4	6	4.2	4.0–4.4
V	11	55.9	51.0–59.0 2.0		7	52.3	50.0–55.0	3	55.3	55.0–56.0	0.6						
G	7	21.1	17.0–29.0 5.1					1	30.0								
n.r.	11	57.1	51–62.0	3.6				3	57.0	55.0–60.0	2.6						
ph.v.l./ph.l.	11	1.7	1.5–1.9	0.1	7	2.2		3	1.64	1.6–1.7	0.1						
v.a.l./ph.l.	11	1.1	0.9–1.3	0.1	7	1.4		3	1.2	1.1–1.2	0.1						
t.l./ph.l.	11	1.1	0.9–1.3	0.1	7	1.5		3	1.1	1.0–1.2	0.1						
t.l./v.a.l.	11	1.0	0.7–1.2	0.1	7	1.0		3	1.0	1.0	0.0						
C'	11	5.9	5.0–7.5	0.7	1	10.0		3	6.3	5.8–6.7	0.5						
v.a.l./an.b.w.	11	6.1	4.6–7.3	0.7	7	9.7		3	6.6	6.3–6.9	0.3						

Measurements from Ethiopia, Bulgaria, and Namibia were from Jacobs (1987), Gerlach (1951), and Heyns and Coomans (1989), respectively.

A, body length divided by largest body width; a.f.b.l., distance between anterior body end and anterior margin of fovea apertures, measured along the central body axis, an.b.w., anal body width; b, body length divided by pharynx length; c, body length divided by tail length; C', tail length divided by anal body length; c.b.w., body width at pharyngo-cardial junction; f.d., outer fovea aperture diameter measured parallel to body axis; G, distance between ovarium tip and vulva as percentage of body length; h.d., head diameter = body width at the cephalic setae measured perpendicular to central body axis; L, body length measured along central body axis; n, number of specimens measured; n.r., distance between anterior body end and nerve ring as percentage of pharynx length; ph.l., pharynx length; ph.v.l., distance between pharynx and vulva; r.l., rectum length; s, standard deviation; t.l., tail length; v, distance between anterior body end and vulva; V, distance of vulva from anterior body end as percentage of body length; v.a.l., distance between vulva and anus; v.b.w., body width at vulva.

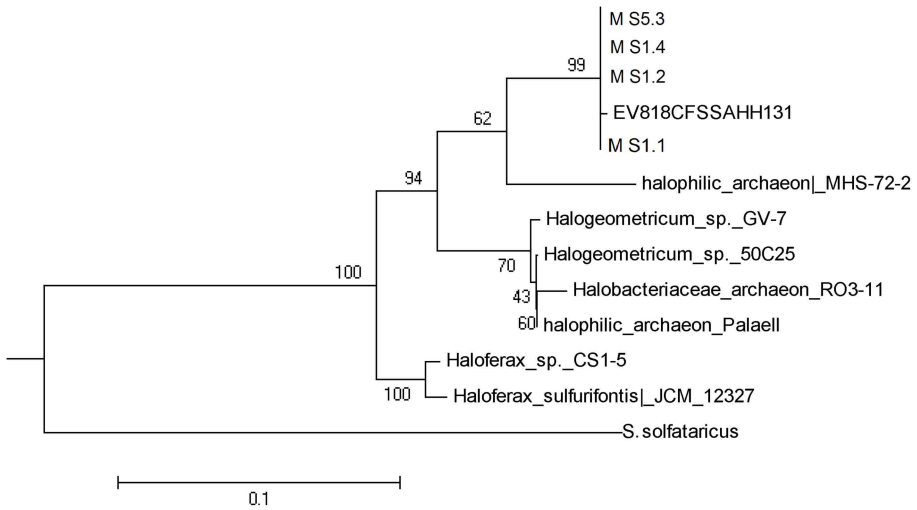

FIGURE 1 | Phylogenetic tree of the Archaea extracted from the salt stalactites.

Attempts to culture Archaea and Bacteria from the layered extracts failed on three attempts.

Culture Tests

To support the potential for a marine origin for and to determine the degree of obligatory salt requirement of *M. parvella* we tested the culture in a salt gradient. The salt tolerance test clearly showed a salinity requirement range of 9–14 g/L for *M. parvella* whereas the control species clearly showed very little tolerance for any salt (**Table 3**). *M. parvella* was difficult to keep in culture since the nematodes were not producing offspring and becoming immobile. In an attempt to halt the decline of the culture an attempt was made to identify the Bacteria associated with the nematodes. One nematode specimen from the culture was sacrificed and DNA sequencing identified the presence of *Alicyclobacillus* sp. (99% identity). This is a spore-forming, aerobic sulfur and ferrous iron oxidizer (*Firmicutes*) (Wisotzkey et al., 1992). Subsequent addition of sulfate (1 mM $MgSO_4$ final concentration) to the nematode culture led to a marked rebound of nematode activity however the effect could not be sustained and the nematode culture died out eventually.

CT Scanning

Micro CT scanning and SEM of the $CaCO_3$ stalactites that yielded nematodes failed to reveal any apertures in the outermost $CaCO_3$ layer. Micro CT scanning revealed a circular layered internal stalactite structure, laminae, with cavities between the layers themselves populated with several type of different shaped outgrowths mainly, although not always, pointed toward the center (**Figures 3A–C**, **Video 1**). All $CaCO_3$ stalactites scanned showed turning laminae more numerous closer to the ceiling than at the bottom. Using CT scan the highest number of laminae counted was 16 layers of partial or complete laminae in the stalactite part near the ceiling, diminishing to a minimum of 8 near the exit of the straw. Four morphologically different outgrowths were identified; the "coralloid," the "pine," the "amphora" and the "Chinese fan" (**Figures 3D**, **4A–F**). Nematodes were identified using SEM between these calcified layers (**Figures 5A,B**) thereby confirming the nematodes also live inside the stalactite and not only in the central tube of the stalactite.

Macro CT scan of the salt stalactites showed no organized internal structure was evident as in the $CaCO_3$ stalactites. To ascertain that this was not due to resolution problems a CT scan of a large salt stalactite from the same sampling site at Moab Khotsong (23 cm length, largest width 8.5 cm weight 2.0 kg) was scanned under a hospital CT-scanner (**Videos 2**, **3**). The scans did not reveal an organized internal structure but a random sponge-like structure punctuated by a considerable number of air/water vacuoles (**Videos 2**, **3**).

Discussion

Using ethanol-flame sterilized stalactites, extraction of archaeal, bacterial and eukaryotic DNA from salt and $CaCO_3$ stalactites is possible. Salt has been shown to be a very effective preservative for DNA (Frantzen et al., 1998) and probably explains the higher diversity yield in salt stalactites. Because the $CaCO_3$ stalactites were dry at the moment of sterilization it may explain the less consistent and lower yield which probably originates from organisms in survival stages hence yielding more sequenceable DNA. The drying out would explain the absence of nematode DNA as *M. parvella* does not have a survival stage.

Eumetazoa have been reported inhabiting stalactite like structures (so called biostalactites) (Sanfilippo et al., 2014). But these biostalactites consist of crusts produced by (among others) the Eumetazoa themselves. Generally these are a few centimeters thick and consist of small serpulids and other Eumetazoa. The larger ones often include a nucleus of serpulid tubes. The metazoans include mainly serpuloideans, sponges, bryozoans and foraminifers (Sanfilippo et al., 2014). Nematodes

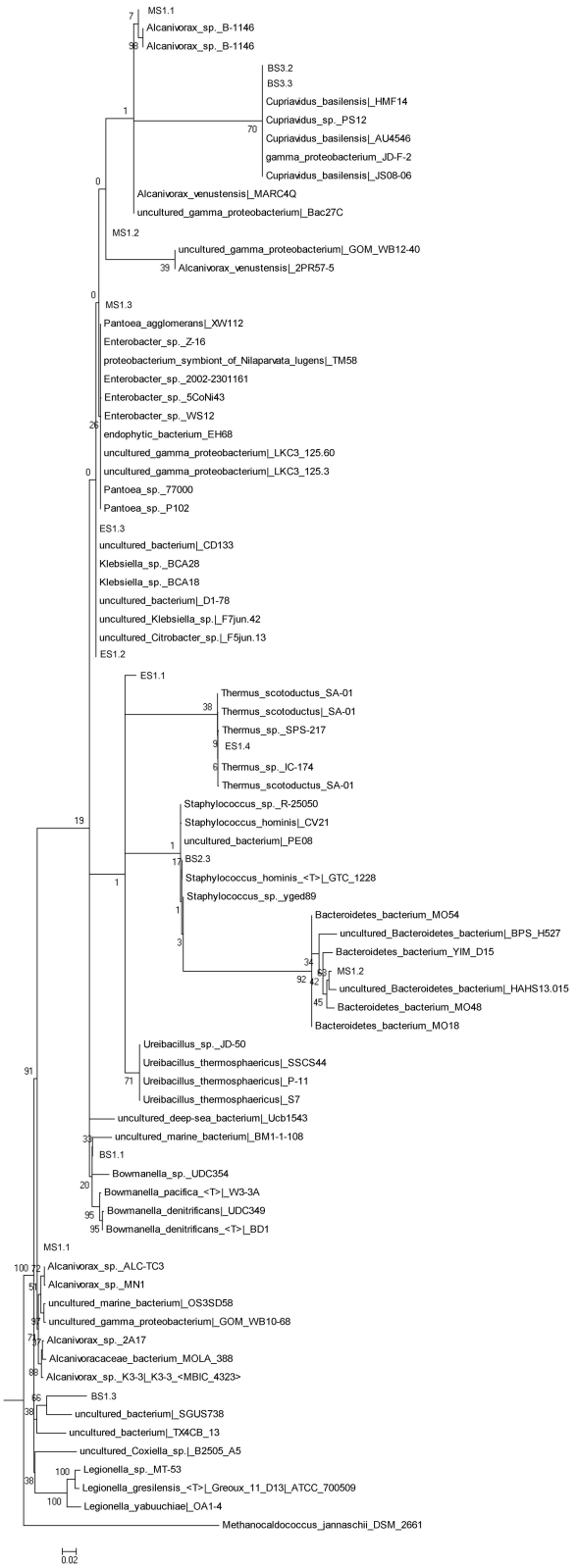

FIGURE 2 | Phylogenetic tree of the Bacteria extracted from the salt stalactites.

TABLE 3 | Salt requirement experiment.

Salt g/l	0	2	3	5	8	9	10	14	15	16
Poikilolaimus oxycercus	+	+	−	−	−	−	−	−	−	−
Monhystrella parvella	−	−	−	−	−	+	+	+	−	−
Halicephalobus mephisto	+	+	+	−	−	−	−	−	−	−

Poiukilolaimus oxycercus is a nematode from the surface, Halicephalobus mephisto a deep subsurface collected species. All are bacteriophagous nematodes.

have never been reported living inside stalactites before. Additionally nematodes are not tube building Eumetazoa like e.g., some Annelida. The discovery cannot be compared to the aforementioned biostalactites as it concerns Eumetazoa effectively "trapped" and surviving inside a solid stalactite. The nematodes themselves do not excrete stalactite material or otherwise contribute directly to the stalactite formation.

Puzzling findings were one Archaea and two stalactite Bacteria with a high identity to marine species. MS1.1–1.4 all contained a species with closest identity to *Halobacteriales*. These organisms are the dominant taxa in hypersaline ecosystems, such as salterns, salt and soda lakes and coastal areas, in which NaCl concentrations can reach 150–350 g/L (Andam et al., 2012). However, *Halobacteriales* strains from ecosystems with low salinities (1–3.5% NaCl) have been reported, where they appear to possess exceptional survival capabilities and/or are capable of exploiting niches of relatively higher salinities created due to temporal and spatial variations in geochemical conditions in such ecosystems (Youssef et al., 2012). BS2.1 closest identity to *Bowmanella* sp. is only known from marine habitats. BS2.3 was identified as an uncultured bacterium showing highest similarity again to the marine group *Oceanospirillales*. MS3.1 shared closest identity to *Alcanivorax* sp. also of marine origin (Yakimov et al., 1998). Although the DNA results of the Bacteria are not extensive enough to state as a certainty that these are marine Bacteria, the discovery of *M. parvella* that cannot survive outside a salty environment however does point strongly to a marine fingerprint. Since none of the Bacteria from the stalactites could be cultured the evidence rests on the nematode. Although *M. parvella* resulting from human contamination is difficult to fathom for an organism that requires a salty environment, it is essential to establish that *M. parvella* is indigenous to the stalactite as a result of fissure water. Three major questions are important to determine whether the nematode *M. parvella* recovered is indigenous to the carbonate stalactite: (1) are there apertures in the stalactite that would explain entry in the stalactite by nematodes other than the fissure water?, (2) Is there evidence of bacterial growth serving as a food source for the nematode inside the stalactites?, (3) The high salt tolerance of the nematode species might support indigenous origin, but to what extent is the salt tolerance of the nematode species restrictive?

Apertures Other than the Soda Straw in the Carbonate Stalactites

An alternative way of nematode entry would be that a nematode either from the mine tunnel or flowing out of a fissure and into

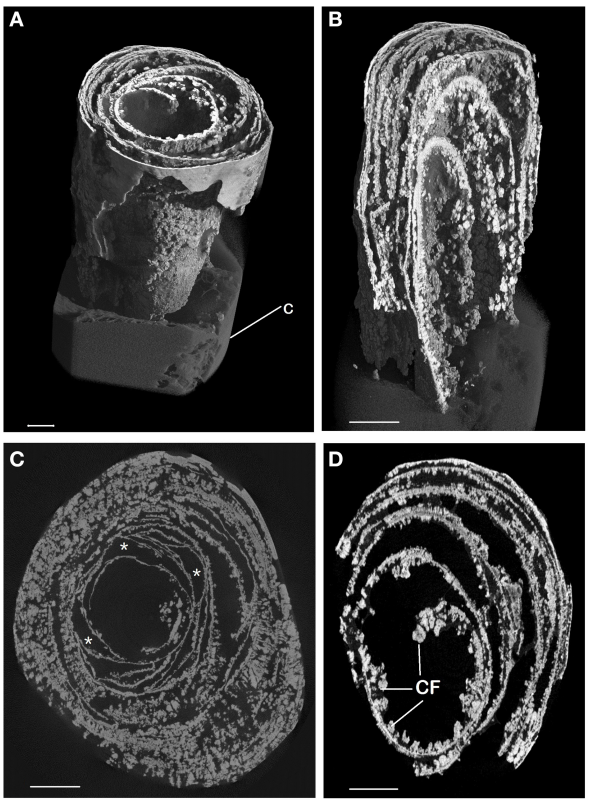

FIGURE 3 | Micro CT scan of $CaCO_3$ stalactite. (A) General habitus of CT scan of $CaCO_3$ stalactite that contained nematodes. The area shown is near the tip of the soda straw at the bottom of the stalactite away from the ceiling. The bent laminae are clearly visible as is the knob like outgrowths on them. Cotton (C) was used to stabilize the stalactite for scanning. **(B)** Longitudinal section inside the lower part of image **(A)**. The lamellar built of the stalactite and the outgrowths are plainly visible. **(C,D)** Cross sections of the stalactite in an area close to the ceiling **(C)** and near the end **(D)**. Outgrowths can become very dominant and the laminae can form complete or partially enclosed spaces (*) within the inner stalactite. Scale bars: **(A)** 4 cm, **(B)**: 0.1 cm, **(C)**: 7cm, **(D)**: 5 cm.

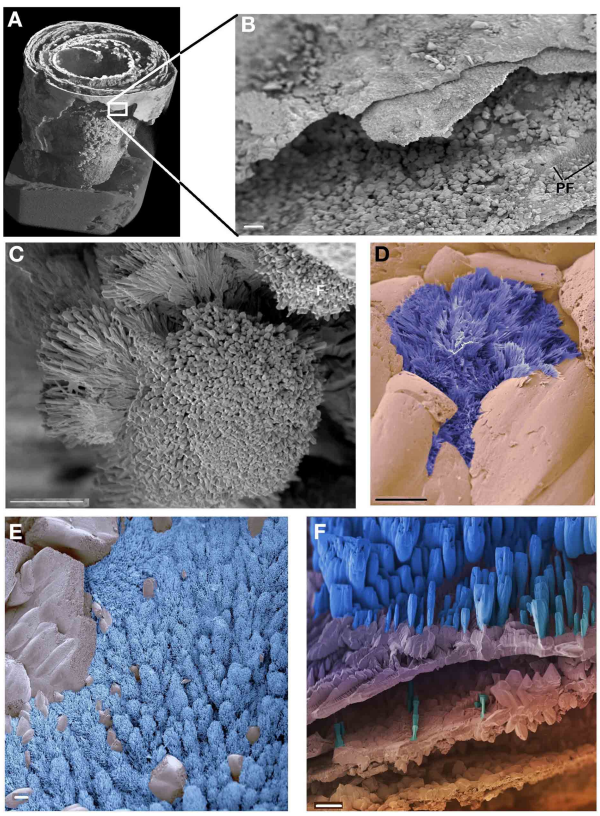

FIGURE 4 | SEM of the $CaCO_3$ stalactite. (A) General built. Image identical to **Figure 3A** but non-linearly compacted as it only serves to highlight the position of image **(B)**. **(B)** Detail of the outer, smooth surface of the stalactite showing the much coarser built of the more interior layers inside. Low resolution of an area covered in the shrub called "pine forest." **(C–F)** The different types of shrubs identified in the $CaCO_3$ stalactite. **(C)** The "cauliflower" the most dominantly present. **(D)** The "Chinese fan" (dark blue) **(E)** the "pine forest" (light blue). **(F)** The "amphora" (blue). No logical pattern of presence could be deduced for any of these shrubs. Scale bars **(B)** and **(F)**: 100 μm, **(C–E)**: 10 μm.

the mine tunnel floor crawls all the way up the wall, on the ceiling where it has to withstand the water flow forming the stalactite and crawl into the stalactite. (Micro)-CT scan and SEM did not reveal any apertures in the carbonate stalactites that could explain an alternative pathway of entry for the nematodes than transport via the fissure water that built the stalactite. Although the absence of apertures does not rule out the gradual "incorporation" of the nematodes as the stalactite grows and nematodes crawl their way up and move against the water drip into the soda straw. Using the Andrassy formula (Andrassy, 1956) and a density of 1.13 g cm^{-3}, the estimated dry weight mass of *M. parvella* is 2.03×10^{-8} g, which makes it highly unlikely it would be able to move against the water drip on the ceiling. No nematodes were found immediately beneath or in the vicinity of the stalactite drip on the second stalactite collection trip in 2010 or anywhere in the tunnel thus weakening the alternative theory of nematodes crawling up the wall but supporting an indigenous origin of the nematodes.

Bacteria Growth inside Carbonate Stalactites

If, as we contend, the nematodes become trapped inside the stalactite with the water that forms the stalactite, the nematodes can only survive if they have a ready supply of bacterial food inside the stalactite. Although a number of Bacteria have been identified in the stalactite layers the presence of Bacteria in itself does not constitute evidence that these Bacteria are available as a food source for the nematodes. SEM was used to identify structures that are bacterially induced and support Bacteria were effectively growing inside the $CaCO_3$ stalactites. We had therefore, we had to rely on secondary structures indicating the presence of Bacteria the so-called bacterial deposited "shrubs" as described and experimentally grown and proven to be Bacteria induced by Sánchez-Navas et al. (2013). The SEM revealed, based on their morphology, four types of shrubs of which one was very similar to the experimentally induced ones (Figure 14 in Sánchez-Navas et al., 2013). Since we based the types of shrubs on morphology and cannot link a specific type of shrub to a specific

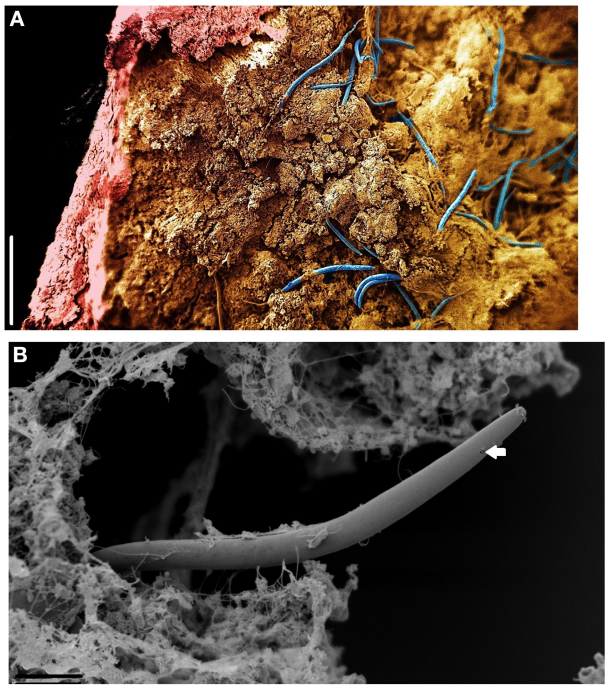

FIGURE 5 | SEM of *Monhystrella parvella* inside a $CaCO_3$ stalactite after longitudinal sections with a scalpel. (A) Composite image made of four images taken at different focal points and assembled using Adobe Photoshop. Nematodes (blue) reside in the amorph mass within the confines of the $CaCO_3$ outer stalactite wall (pink). **(B)** Detail of *M. parvella*, arrow highlights the fovea. Scale bars: **(A,B)**: 200 μm.

Bacteria species. We cannot determine whether the different types of shrubs are just different stages of the same bacterial species or represent different morphologies caused by the growth of different species of Bacteria. Morphologically the large number of "coralloid" shrubs observed, which resemble most closely those experimentally grown and (Sánchez-Navas et al., 2013), indicates a high bacterial growth within the carbonate stalactites and thus food support for nematodes.

High Salt Requirement of *M. parvella* Supports an Indigenous Origin

Salt requirement tests showed *M. parvella* could not survive longer than 2 h when salinity in the medium dropped below 9 g/L and did not tolerate salinity higher than 14 g/L. The inability to survive in a salt-less environment in a terrestrial environment is surprising. This test effectively rules out the possibility of *M. parvella* crawling up to the ceiling to the stalactite as none of the water tested in the tunnel has enough salinity to let it survive, besides the observation that it was not found in control samples. The only saline water anywhere near the sampling site where this *M. parvella* could survive is the fissure water that forms the stalactite. These facts strongly support an indigenous origin of the nematode in the stalactite and effectively rule out other possibilities (e.g., contamination, anthropogenic or otherwise). Nematodes have been discovered at 1–3.8 km below the surface in fissure water before (Borgonie et al., 2011), but these were terrestrial/freshwater species. The discovery that brackish water/marine nematode species are surviving in deep underground stalactites in a terrestrial area deep inland is a novelty.

There was initial apprehension that DNA isolated from stalactites in mines would be all "contamination" from mine operations. Specifically an earlier study in a mine environment had indicated a high level of fungal spores in mine air (Pohl et al., 2007). Results of bacterial diversity analysis allow us to broadly distinguish between organisms that can be considered originating from deep mine fissure water and organisms originating from anthropogenic influences. Examples of confirmed deep fissure Archaea/Bacteria are MS3.1 with closest identity to a *Halobacteriales* previously recovered from Evander mine. ES1.4 with closest identity to *Thermus* sp. (Kieft et al., 1999). BS2.1 with closest identity to *Bowmanella* sp. is only known from 40 marine habitats, is Gram-negative, heterotrophic sulfate reducer (Klepac-Ceraj et al., 2004) and very probably also deep fissure water related rather than anthropogenic. Similarly, some Bacteria are clearly not originating from the deep subsurface but are most likely anthropogenic in origin mediated by high moisture, heat and ventilation in the mine tunnels; ES1.2 and BS2.2 showed closest homology to *Klebsiella* sp. and BS2.3 *Staphylococcus* sp. The *Alicyclobacillus* sp. identified with *M. parvella* was not recovered in any of the stalactite layers, which may be due to a nematode linked enrichment phenomenon rather than the absence in the stalactite.

Table 1 lists where the Archaea/Bacteria isolated from the stalactites have been observed in other deep subsurface settings. The bacterial content in the stalactite compared with that of fissure water from Beatrix gold mine could only be done using data from a borehole (Be326) approximately 100 m away from the stalactite collection site. In 2011, a new nematode species, *H. mephisto* that was not marine linked was found in fissure water from this borehole (Borgonie et al., 2011). This species, which was used as a control organism for the halotolerance test in this study (**Table 3**) could not survive even moderate salt concentrations. Thus, the fissure water at the time was at least chemically different from the fissure water that supported *M. parvella*. The bacterial composition analyzed in 2011 revealed none of the Bacteria found in the stalactite (*Thermus, Bowmanella, Cupriavidus, Oceanospirillales*).

Surprisingly only one fungus (*Candida* sp.) was found and three protozoa (*Acanthamoeba*, *Colpoda*, and an unknown species). Pohl et al. (2007) had already shown in a previous study the abundance of fungi spores in mine air, which can then easily account for the presence of *Candida* sp. in the stalactites. Similarly for *Acanthamoeba* sp. (Khan, 2009) and *Colpoda* sp. (Finlay et al., 2001), which are both ubiquitously distributed in the environment and are known to develop resistant stages in adverse conditions. If in the future these Eukarya would be confirmed originating from the fissure water it would be the first report of Fungi and Protozoa at this depth in the subsurface of South Africa.

The micro CT scan revealed a highly unusual inner structure of the $CaCO_3$ stalactites consisting of numerous laminae with spaces in between and is identical to the structure reported by

Martinez-Martinez et al. (2010) for similar stalactites. However, no information as to its genesis was offered nor can we propose one based on our results. SEM analysis (**Figure 5**) clearly shows that the space between the lamellae is the nematode residing space. This geometry additionally explains the different DNA extracted patterns observed between $CaCO_3$ and salt stalactites; salt stalactites form a continuous unit while $CaCO_3$ stalactites are divided through laminae.

The current recharge source for Beatrix gold mine is impossible to trace with certainty. Data from the closest borehole (Be326) sampled approximately 100 m away from the stalactites in Beatrix gold mine yields $\delta^{18}O$ and $\delta^{2}H$ values (residence time >40–80 kyr) for the fissure water samples that are similar to those previously reported from the Welkom mining region. Although these values are also on the Global Meteoric Water Line (Lau et al., 2014), they are distinct from those lying on the meteoric waterline from the northern and eastern margins of the Witwatersrand Basin (Ward et al., 2004; Onstott et al., 2006). Only two regions exist in South Africa with predicted $\delta^{2}H$-values for precipitation that coincide with the very light −40 to −47‰ range observed for the Welkom fracture water samples, the Kalahari Desert and the Lesotho highlands (West et al., 2014). Given that the Welkom mining district lies south of the Vaal River at an elevation of 1370 m, it is more likely that groundwater recharge for this mining district occurs 150 km to the southeast in the mountains of Lesotho (at an elevation of ∼2500 m), than from the Kalahari Desert (across the Vaal River to the north and at a lower elevation). The long flow path from the Lesotho highlands could explain the age for the Welkom fracture water (Lau et al., 2014). It is obvious that neither of these freshwater sources can be the source of a salt requiring nematode, Bacteria and/or Archaea species.

The Origin of *M. parvella*

The origin of *M. parvella* is thus enigmatic. The possibility that *M. parvella* was originally a freshwater nematode is unlikely as it would imply that evolution toward obligate brackish water conditions for survival occurred several times independently from each other (Ethiopia (18,g/L), Namibia (salinity not reported, Bulgaria/Black Sea 18 g/L and in the mines (14 g/L). This focuses the origin on marine/brackish water related source on the surface. The geological history of Southern Africa indicates two large windows of opportunity; one 350–250 myr ago during the initial existence stage of the inland Karoo Sea (McCarthy and Rubidge, 2005) and a second geological more recent period linked to the origin of the salt pans in South Africa (Roelofse, 2010). In the event of the Karoo Sea origin, the nematodes could have traveled to the deep subsurface from brackish coastal waters. From the nematode evolutionary timeline there is no conflict; the line that led to the Nematoda split off from the branch to man about 1.1 billion years ago based on histone and cytochrome c sequences (Vanfleteren et al., 1990). The most recent common ancestor to the extant nematode species *Caenorhabditis elegans, Trichostrongylus colubriformis, Nippostrongylus brasiliensis, Ascaris suum,* and *Pseudaterranova decipiens* lived about 550 myr ago based on cytochrome c and globin amino acid sequences (Vanfleteren et al., 1994). Thus, the Precambrium origin of nematodes predates the Karoo Sea by some 200 myr. This, however, does not prove that *M. parvella* as a species already existed at the time of the Karoo Sea and in absence of any decent fossil record, this point remains unsolvable. We were also unable to identify clearly marine sediments (carbonate deposits) overlying the Witwatersrand basin in support of this possibility.

South Africa has a very high number of salt pans per area (Allan et al., 1995). Salt pans are regularly visited by large flocks of birds and this constitutes a way *M. parvella* could have been transported from coastal areas to the inland after the disappearance of the Karoo Sea, as nematode transport by birds has been documented (Frisch et al., 2007). The oldest date for a salt pan known to us in South Africa was cited by Roelofse (2010) as 100 kyr. It is doubtful that this is the upper limit for the presence of salt pans in South Africa but in the absence of more rigid age data on salt pans, this second window of opportunity cannot be more exactly defined other than at least 100 kyr.

Although the possibility of a descent to the deep subsurface by *M. parvella* during the Permian must seem preposterous, there are two arguments in its favor. Firstly, to date and to our knowledge no *M. parvella* has been recovered from the ocean coast but has only been recovered from terrestrial thermal springs (Gerlach, 1951; Jacobs, 1987; Heyns and Coomans, 1989). This argues against the salt pan theory. Second, during the mixed stage culture attempt of *M. parvella*, it became obvious that no survival stage (dauer) was formed. This indicates this species does not have a way to survive unfavorable conditions. Furthermore, the culture of *M. parvella* showed an absolute requirement of salinity for its survival. This means that *M. parvella* must have been in continuous salty water during its entire descent to the deep subsurface. Any mixing with fresh water that diluted the salt too much would have been deadly. Therefore, if the area of descent is covered by a sea, as it was during the Permian/Triassic, groundwater would have been salty and offers a higher probability for *M. parvella* to remain in suitable brackish water. If the area of descent is pockmarked by salt pans as a source of salty groundwater but the majority of the area yields fresh groundwater the chances for continuous suitable salty conditions are less.

Unfortunately we only have DNA sequences of the subsurface populations of *M. parvella*, none from the known surface populations. Therefore, we cannot use DNA, for now, as a marker to determine to what extent both populations have diverged and hence support either window of opportunity.

Conclusion

This study has demonstrated that stalactites can be used to extract valuable information on Archaea, Bacteria, and Eukarya even after the water flow that formed the stalactites has ceased. This trapping/concentrating function is all the more evident if one compares the DNA yield/number of individual species extracted from the small pieces of stalactite vs. the huge amounts of fissure water that is normally filtered to obtain bio signatures (e.g., Lau et al., 2014). It is unclear how long the environment inside the stalactite remains viable for eumetazoa once the fissure flow

stops. If the species have a survival stage in their life cycle then renewed flow at a later date could reactivate them. The stalactites used in this study were small and were uniform in morphology. Future research may determine whether it would be possible to distinguish if the characteristics of different water flows over time can be determined from individual stalactite layers. Contamination due to anthropogenic activity is present but offers in itself new possibilities for archeologists as an additional tool to study human inhabited caves.

Acknowledgments

GB is grateful for financial support from DCO, TIA, KIC. We would like to thank M. Dierick for the CT scan and management at Beatrix, Evander, Tau Tona and Moab Khotsong mines for granting access and assistance to the sampling sites.

Supplementary Material

The Supplementary Material for this article can be found online at: http://journal.frontiersin.org/article/10.3389/fmicb.2015.00833

Video 1 | Micro CT scan of $CaCO_3$ stalactite.

Video 2 | Macro CT scan of large salt stalactite from Moab Khotsong showing the many randomly dispersed vacuoles (black) inside.

Video 3 | CT scan cross sections of the salt stalactite from Moab Khotsong. Several vacuoles can be followed along the reconstruction, clearly showing the enclosed nature of several of these.

References

Allan, D. G., Seaman, M. T., and Kaletja, B. (1995). "The endorheic pans of South Africa," in *Wetlands of South Africa,* ed G. I. Cowan (Pretoria: Department of Environmental Affairs and Tourism), 75–110.

Andam, C. P., Harlow, T. J., Papke, R. T., and Gogarten, J. P. (2012). Ancient origin of the divergent forms of leucyl-tRNA synthetases in the Halobacteriales. *BMC Evol. Biol.* 12:85. doi: 10.1186/1471-2148-12-85

Andrassy, I. (1956). Die rauminhalts- und gewichtsbestimmung der fadenwürmer (Nematoden). *Acta Zoo Hung.* 2, 1–15.

Borgonie, G., Dierick, M., Houthoofd, W., Willems, M., Jacobs, P., and Bert, W. (2010). Refuge from predation, the benefit of living in an extreme acidic environment? *Biol. Bull.* 219, 268–276.

Borgonie, G., García-Moyano, A., Litthauer, D., Bert, W., Bester, A., van Heerden, E., et al. (2011). Nematoda from the terrestrial deep subsurface of South Africa. *Nature* 474, 79–82. doi: 10.1038/nature09974

Casamayor, E. O., Massana, S., Benlloch, R., Øvreås, L., Díez, B., Goddard, V. J., et al. (2002). Changes in archaeal, bacterial and eukaryal assemblages along a salinity gradient by comparison of genetic fingerprinting methods in a multipond solar saltern. *Environ. Microbiol.* 4, 338–348. doi: 10.1046/j.1462-2920.2002.00297.x

Castanier, S., Le Metayer-Levrel, G., and Perthuisot, J. P. (1999). Ca-carbonate precipitation and limestone genesis – the microbiologist point of view. *Sediment. Geol.* 126, 9–23.

Castanier, S., Le Metayer-Levrel, G., and Perthuisot, J. P. (2000). "Bacterial roles in the precipitation of carbonate minerals," in *Microbial Sediments,* eds R. E. Riding and S. M. Awramik (Heidelberg: Springer-Verlag), 32–39. doi: 10.1007/978-3-662-04036-2_5

Cox, G., James, J. M., Leggett, K. E. A., and Osborne, R. A. L. (1989). Cyanobacterially deposited speleothems: subaerial stromatolites. *Geomicrobiol. J.* 7, 245–252. doi: 10.1080/01490458909377870

Danielli, H. M. C., and Edington, M. A. (1983). Bacterial calcification in limestone caves. *Geomicrobiol. J.* 3, 1–16. doi: 10.1080/01490458309377780

Davidson, M., Silver, B., Onstott, T., Moser, D., Pratt, L., Boice, E., et al. (2011). Capture of planktonic microbial diversity in fractures by long term monitoring of flowing boreholes, evander basin, south africa. *Geomicrobiol. J.* 28, 275–300. doi: 10.1080/01490451.2010.499928

Derycke, S., Remerie, T., Vierstraete, A., Backeljau, T., Vanfleteren, J., Vincx, M., et al. (2005). Mitochondrial DNA variation and cryptic speciation within the free-living marine nematode *Pellioditis marina*. *Mar. Ecol. Prog. Ser.* 300, 91–103. doi: 10.3354/meps300091

Desmarchelier, J., Hellstrom, J., and McCulloch, M. (2006). Rapid trace element analysis of speleothems by ELISA-ICP-MS. *Chem. Geol.* 231, 102–117. doi: 10.1016/j.chemgeo.2006.01.002

Díez, B., Pedros-Alio, C., Marsh, T. L., and Massana, R. (2001). Application of denaturing gradient gel electrophoresis (DGGE) to study the diversity of marine picoeukaryotic assemblages and comparison of DGGE with other molecular techniques. *Appl. Environ. Microbiol.* 67, 2942–2951. doi: 10.1128/AEM.67.7.2942-2951.2001

Filipjev, I. (1931). Report on freshwater Nematoda: Mr Omer-Cooper's investigation of the Abyssinian freshwaters (Hugh Scott Expedition). *Proc. Zool. Soc. Lond.* 2, 429–443. doi: 10.1111/j.1096-3642.1931.tb01021.x

Finlay, B. J., Esteban, G. F., Clarke, K. J., and Olmo, J. L. (2001). Biodiversity of terrestrial protozoa appears homogeneous across local and global spatial scales. *Protist* 152, 355–366. doi: 10.1078/1434-4610-00073

Floyd, R. M., Rogers, A. D., Lambshead, P. J. D., and Smith, C. R. (2005). Nematode-specific PCR primers for the 18S small subunit rRNA gene. *Mol. Ecol. Note* 5, 611–612. doi: 10.1111/j.1471-8286.2005.01009.x

Frantzen, M. A. J., Silk, J. B., Ferguson, J. W. H., Wayne, R. K., and Kohn, M. H. (1998). Empirical evaluation of preservation methods for faecal DNA. *Mol. Ecol.* 7, 1423–1428. doi: 10.1046/j.1365-294x.1998.00449.x

Frisch, D., Green, A. J., and Figuerola, J. (2007). High dispersal capacity of a broad spectrum of aquatic invertebrates via waterbirds. *Aquat. Sci.* 69, 568–574. doi: 10.1007/s00027-007-0915-0

Gerlach, S. A. (1951). Freilebende nematoden aus vanna an der bulgarischen küstedes schwarzen meeres. *Archiv. Hydrobiol.* 45, 193–212.

Heyns, J., and Coomans, A. (1989). Three *Monhystrella* species from inland waters in south west Africa-Namibia (Nematoda: Monhysteridae). *Nematologica* 35, 1–14. doi: 10.1163/002825989X00016

Huber, T., Faulkner, G., and Hugenholtz, P. (2004). Bellerophon; a program to detect chimeric sequences in multiple sequence alignments. *Bioinformatics* 20, 2317–2319. doi: 10.1093/bioinformatics/bth226

Jacobs, L. (1987). Redescription of *Monhystrella parvella* (Filipjev) comb. N. (Nemata, Monhysteridae). *Biol. Scr.* 16, 117–124. doi: 10.1111/j.1463-6409.1987.tb00059.x

Khan, N. (2009). *Acanthamoeba: Biology and Pathogenesis*. Norfolk, UK: Caister Academic Press.

Kieft, T. L., Fredrickson, J. K., Onstott, T. C., Gorby, Y. A., Kostandarithes, H. M., Bailey, T. J., et al. (1999). Dissimilatory reduction of Fe(III) and other electron acceptors by a *Thermus* isolate. *Appl. Environ. Microbiol.* 65, 1214–1221.

Klepac-Ceraj, V., Bahr, M., Crump, B. C., Teske, A. P., Hobbie, J. E., and Polz, M. F. (2004). High overall diversity and dominance of microdiverse relationships in salt marsh sulphate-reducing bacteria. *Environ. Microbiol.* 6, 686–698. doi: 10.1111/j.1462-2920.2004.00600.x

Lau, M. C., Cameron, C., Magnabosco, C., Brown, C. T., Schilkey, F., Grim, S., et al. (2014). Phylogeny and phylogeography of functional genes shared among seven terrestrial subsurface metagenomes reveal N-cycling and microbial evolutionary relationships. *Front. Microbiol.* 5:531. doi: 10.3389/fmicb.2014.00531

Maidak, B. L., Olsen, G. J., Larsen, N., Overbeek, R., McCaughey, M. J., and Woese, C. R. (1997). The RDP ribosomal database project. *Nucleic Acids Res.* 25, 109–110. doi: 10.1093/nar/25.1.109

Martinez-Martinez, J., Fusi, N., Barberini, V., Canaveras, J. C., and Crosta, G. B. (2010). X-Ray Microtomography for Studying 3D Textures of Speleotherms Developed inside Historic Walls. *Rev. Soc. Esp. mineralogía* 13, 145–146.

McCarthy, T., and Rubidge, B. (eds.). (2005). "The rocks of Gondwana," in *The Story of Earth and Life: a Southern African Perspective on a 4.6 Billion Year Journey* (Cape Town: Struik Nature publishers), 185–211.

Mühling, M., Wolven-Allen, J., Murrell, J. C., and Joint, I. (2008). Improved group-specific PCR primers for denaturing gradient gel electrophoresis analysis of the genetic diversity of complex microbial communities. *ISME J.* 2, 379–392. doi: 10.1038/ismej.2007.97

Muyzer, G., de Waal, E. C., and Uitterlinden, A. G. (1993). Profiling of complex microbial populations by denaturing gradient gel electrophoresis analysis of polymerase chain reaction amplified genes coding for 16S rRNA. *Appl. Environ. Microbiol.* 59, 695–700.

Onstott, T. C., Lin, L.-H., Davidson, M., Mislowack, B., Borcsik, M., Hall, J., et al. (2006). The origin and age of biogeochemical trends in deep fracture water of the Witwatersrand Basin, South Africa. *Geomicrobiol. J.* 23, 369–414. doi: 10.1080/01490450600875688

Pohl, C. H., Kriel, W., Venter, P., van Heerden, E., and Albertyn, J. (2007). The diversity of culturable airborne fungi in an active South African gold mine. *S. Afr. J. Sci.* 103, 7–8.

Riding, R. (2000). Microbial carbonates: the geological record of calcified bacterial-algal mats and biofilms. *Sedimentology* 47, 179–214. doi: 10.1046/j.1365-3091.2000.00003.x

Roelofse, T. (2010). *Mineralogy and Geochemistry of Clay Sediments in Pans of the Northern Cape Province, South Africa*. M.Sc. thesis, University of Kwazulu-Natal.

Sanfilippo, R., Rosso, A., Guido, A., Mastandrea, A., Russo, F., Riding, R., et al. (2014). Metazoan/microbial biostalactites from present-day submarine caves in the Mediterranean Sea. *Mar. Ecol.* doi: 10.1111/maec.12229. (in press).

Sánchez-Navas, A., Martín-Algarra, A., Sánchez-Román, M., Jiménez-López, C., Nieto, F., and Ruiz-Bustos, A. (2013). "Crystal growth of inorganic and biomediated carbonates and phosphates," in *Advanced Topics on Crystal Growth,* ed S. O. Ferreira (InTech). doi: 10.5772/52062

Stomeo, F., Makhalanyane, T. P., Valverde, A., Pointing, S. B., Stevens, M. I., Cary, C. S., et al. (2012). Abiotic factors influence microbial diversity in permanently cold soil horizons of a maritime-associated Antarctic Dry Valley. *FEMS Microbiol. Ecol.* 82, 326–340. doi: 10.1111/j.1574-6941.2012.01360.x

Valenzuela, I., Hoffmann, A. A., Malipatil, M. B., Ridland, P. M., and Weeks, A. R. (2007). Identification of aphid species (Hemiptera: Aphididae: Aphidinae) using a rapid polymerase chain reaction restriction fragment length polymorphism method based on the *cytochrome oxidase* subunit I gene. *Aust. J. Entomol.* 46, 305–312. doi: 10.1111/j.1440-6055.2007.00615.x

Vanfleteren, J. R., Evers, E. A., van de Werken, G., and van Beeumen, J. J. (1990). The primary structure of cytochrome c from the nematode *Caenorhabditis elegans*. *Biochem J.* 271, 613–620.

Vanfleteren, J. R., Van de Peer, Y., Blaxter, M. L., Tweede, S. A., Trotman, C., Lu, L., et al. (1994). Molecular genealogy of some nematode taxa as based on cytochrome c and globin amino acid sequences. *Mol. Phylogenet. Evol.* 3, 92–101. doi: 10.1006/mpev.1994.1012

Ward, J. A., Slater, G. F., Moser, D. P., Lin, L.-H., and Lacrampe-Couloume, G., Bonin, A. P., et al. (2004). Microbial hydrocarbon gases in the Witwatersrand Basin, South Africa: implications for the deep biosphere. *Geochim. Cosmochim. Acta* 68, 3239–3250. doi: 10.1016/j.gca.2004.02.020

Werle, E., Schneider, C., Renner, M., Völker, M., and Fiehn, W. (1994). Convenient single-step, one tube purification of PCR products for direct sequencing. *Nucleic Acids Res.* 22, 4354–4355. doi: 10.1093/nar/22.20.4354

West, A. G., February, E. C., and and Bowen, G. J. (2014). Spatial analysis of hydrogen and oxygen stable isotopes ("isoscapes")in groundwater and tapwater across South Africa. *J. Geochem. Explor.* 145, 213–222. doi: 10.1016/j.gexplo.2014.06.009

Wisotzkey, J. D., Jurtshuk, P. Jr., Fox, G. E., Deinvird, G., and Poralla, K. (1992). Comparative Sequence Analyses on the 16s rRNA (rDNA) of *Bacillus acidocaldarius, Bacillus acidotenestris,* and *Bacillus cycloheptanicus* and proposal for creation of a new genus, *Alicyclobacillus* gen. nov. *Int. J. Syst. Bacteriol.* 42, 263–269. doi: 10.1099/00207713-42-2-263

Yakimov, M. M., Golyshin, P. N., Lang, S., Moore, E. R., Abraham, W. R., Lunsdorf, H., et al. (1998). *Alcanivorax borkumensis* gen., nov., sp., nov., a new hydrocarbon-degrading and surfactant-producing marine bacterium. *Int. J. Syst. Bacteriol.* 48, 339–348. doi: 10.1099/00207713-48-2-339

Youssef, N. H., Ashlock-Savage, K. N., and Elsahed, M. S. (2012). Phylogenetic diversities and community structure of members of the extremely halophilic archaea (Order Halobacteriales) in multiple saline sediment habitats. *Appl. Environ. Microbiol.* 78, 1332–1344. doi: 10.1128/AEM.07420-11

Conflict of Interest Statement: The authors declare that the research was conducted in the absence of any commercial or financial relationships that could be construed as a potential conflict of interest.

Advantages of publishing in Frontiers

OPEN ACCESS
Articles are free to read, for greatest visibility

COLLABORATIVE PEER-REVIEW
Designed to be rigorous – yet also collaborative, fair and constructive

FAST PUBLICATION
Average 85 days from submission to publication (across all journals)

COPYRIGHT TO AUTHORS
No limit to article distribution and re-use

TRANSPARENT
Editors and reviewers acknowledged by name on published articles

SUPPORT
By our Swiss-based editorial team

IMPACT METRICS
Advanced metrics track your article's impact

GLOBAL SPREAD
5'100'000+ monthly article views and downloads

LOOP RESEARCH NETWORK
Our network increases readership for your article

Frontiers
EPFL Innovation Park, Building I • 1015 Lausanne • Switzerland
Tel +41 21 510 17 00 • Fax +41 21 510 17 01 • info@frontiersin.org
www.frontiersin.org

Find us on